Author:
Foster, Rebecca Rachael

Title:
The effects of vascular endothelial growth factor on podocyte biology

The effects of vascular endothelial growth factor (VEGF) on podocyte biology

Rebecca Rachael Foster

Department of Physiology

June 2004

A dissertation submitted to the University of Bristol in accordance with requirements of the degree of PhD in the faculty of Science.

Word count: 59,064

Abstract

Aims: Mature podocytes are terminally differentiated and their turnover is very low under physiological conditions. This suggests that they are maintained by an endogenous survival signal. Vascular endothelial growth factor (VEGF) is known to promote survival in endothelial cells via activation of the PI3-Kinase/AKT survival pathway. VEGF is highly expressed by podocytes, which are known to express a co-receptor for VEGF-receptor 2. The aim of this thesis was to investigate if VEGF could promote survival in cultured podocytes.

Results and conclusions: Exogenous and endogenous VEGF significantly reduced cytotoxicity in cultured podocytes in an autocrine manner via a reduction in apoptosis. The reduction in cytotoxicity was dependent on VEGF-R1 (and possibly VEGF-R3) and PI3-Kinase activation. $VEGF_{165}$ also induced the phosphorylation of nephrin, a cell adhesion molecule associated with the slit diaphragm of podocytes and linked to survival signalling in podocytes. The reduction in apoptosis induced by VEGF in podocytes was also shown to be dependent on normal nephrin expression. This was demonstrated with the use of two podocyte cell lines, one with a mutation in the extracellular domain of nephrin, the other which was nephrin deficient. VEGF-C, expressed by podocytes, also significantly reduced cytotoxicity in cultured podocytes and was shown to induce the phosphorylation of VEGF-receptor 3 and nephrin. $VEGF_{165}b$, a novel VEGF isoform shown to be anti-angiogenic by its action on endothelial cells, dose dependently reduced cytotoxicity in cultured podocytes, but in the presence of VEGF dose dependently increased cytotoxicity. In conclusion members of the VEGF family are expressed in podocytes and play a role in promoting their survival, yet they may also antagonise each other under pathological conditions.

Acknowledgements

I would like to give my wholehearted thanks to my supervisors Dr Dave Bates and Dr Steve Harper. Without their continued support and encouragement I would not have even considered undertaking a PhD. Together they have made this a challenging yet enjoyable experience.

I would also like to acknowledge J. Yem and A. Nishiwaki, who undertook their undergraduate projects in this laboratory under my direct supervision. I have used their work in chapter 10 (figures 10.2-10.4).

I would like to acknowledge Dr Y. Qiu for the development of the anti-$VEGF_{xxx}b$ antibody, used in chapter 10 and also Dr J. Woolard for the $VEGF_{165}b$ protein producing CHO cells ($VEGF_{165}b$ and pcDNA3 transfected) also used in chapter 10.

I wish to thank Sam Baldwin and Rachel Perrin for their technical support and lab management.

I would like to acknowledge everyone at the Microvascular Research Laboratories for their training, support and most of all for making it such an enjoyable environment to work in.

Finally I would like to acknowledge the bodies that provided funding throughout the three years: The National Kidney Research Foundation, The Showering Fund and The Prostate Research Campaign.

Authors Declaration

I declare that the work in this dissertation was carried out in accordance with the Regulations of the University of Bristol. The work is original except where indicated by special reference in the text and no part of the dissertation has been submitted for any other degree.

Any views expressed in the dissertation are those of the author and in no way represent those of the University of Bristol.

The dissertation has not been presented to any other University for examination either in the United Kingdom or overseas.

SIGNED: Rebecca Foster DATE: 1/11/09

Table of contents

List of tables and illustrative material

Abbreviations

ABC	Avidin biotin complex
Ang 1	Angiopoietin 1
ANOVA	Analysis of Variance
AT1	Angiotensin receptor 1
AV	Annexin V
bp	Base pair
BSA	Bovine serum albumin
$CaCl_2$	Calcium chloride
CAD	Caspase activated DNAse
CD2AP	CD2 associated protein
CDK	Cyclic dependent kinase
CDKI	Cyclic dependent kinase inhibitors
CHO cells	Chinese hamster ovary cells
CM	Conditioned media
DAG	Diacylglycerol
DDT	Dithiothreitol
Dep. H_2O	DiEthylPyroCarbonate treated water
DG	Dystroglycan
DISC	Death inducing signalling complex
DMEM	Dulbecco's modified eagles medium
DMSO	Dimethyl sulphoxide
DNA	Deoxyribonucleic acid
EGF	Epidermal growth factor
EGFR	EGF receptor
EGTA	Tetra(acetoxymethyl ester)
EM	Electron microscopy
ER	Endoplasmic reticulum

F-actin	Filamentous actin
FADD	Fas associated death domain
FasL	Fas ligand
FBS	Fetal bovine serum
FEC	Fenestrated endothelial cells
FITC	Fluorescein isothiocyanate
FLIP	(FADD) inhibiting protein
FSGS	Focal and segmental glomerulosclerosis
Fura-2 AM	Fura-2 Acetoxymethyl ester
GAPDH	Glyceraldehyde-3-phosphate dehydrogenase
GBM	Glomerular basement membrane
HBSS	Hanks balanced salt solution
hCIPs	Human conditionally immortalised podocytes
HEK293 cells	Human embryonic kidney 293 cells
HGF	Hepatocyte growth factor
HMVECS	Human microvascular endothelial cells
HRP	Horseradish peroxidase
HUVECs	Human umbilical vein endothelial cells
IAP	Inhibitor of apoptotic proteins
Ig	Immunoglobulin
INT	Iodotetrazolium chloride
JNK	c-jun n-terminal protein kinase
Kd	Dissociation constant
LDH	Lactate dehydrogenase
MAPK	Mitogen activated protein kinase
MEKK3	MAPK kinase kinase 3
mRNA	Messenger RNA
NaCl	Sodium chloride
NAD	Nicotine adenine dinucleotide

NaOH	Sodium hydroxide
NDhCIPs	Nephrin deficient hCIPs
NF-kB	Nuclear factor Kappa B
NMhCIPs	Nephrin mutated hCIPs
Np	Neuropilin
p-Y	Phospho-tyrosine
PAN	Puromycin aminonucleoside
PBS	Phosphate buffered saline
PCPs	Primary culture podocytes
PCR	Polymerase chain reaction
PDGF	Platelet derived growth factor
PDGF-R	PDGF receptor
PECAM-1	Pan endothelial cell adhesion molecule
PECs	Parietal epithelial cells
PH	Pleckstrin homology
PI	Propidium iodide
PIGF	Placental growth factor
PKC	Protein kinase C
PLC	Phospholipase C
PMA	Plasma membrane ATPase
PMT	Photomultiplier tube
PS	Phosphatidyl serine
PTK	Protein tyrosine kinase
PVDF	Polyvinylidine fluoride
RAFTK	Activated related focal adhesion kinase
RNA	Ribonucleic acid
RPMI	Roswell park Memorial Institute (media)
RT-PCR	Reverse transcription-PCR
SDS	Sodium dodecyl sulphate

SDS PAGE	SDS polyacrylamide gel electrophoresis
SEM	Standard error of the mean
Sema-3A	Semaphorin 3-A
SERCA	Sarco-endoplasmic reticulum calcium ATPase
SH	Src homology
siRNA	Short interfering RNA
SV40	Simian virus 40
TEMED	Tetramethylethylene diamine
TGF-B	Transforming growth factor-B
TNF	Tumor necrosis factor
TNF-R1	TNF-receptor 1
TRAIL	Tumor related apoptosis inducing ligand
TRP	Transient receptor potential
VEGF	Vascular endothelial growth factor
VEGF-Mab	Neutralising monoclonal antibody to VEGF
VEGF-R	VEGF receptor
vWF	Von Willebrand Factor
WT-1	Wilms tumor-1
ZO-1	Zonula occludin-1
$[Ca^{2+}]_i$	Intracellular calcium
$[Ca^{2+}]_o$	Extracellular calcium

Chapter 1

The effects of VEGF on podocyte biology

Introduction

1.1 Renal Disease

Renal disease is relatively uncommon in the general population (Feest et al., 1990). Despite its relative rarity however, it is a very significant health care problem. Approximately 30% of all cases of glomerular disease progress to end stage renal failure and renal replacement therapy (long term dialysis or renal transplantation). Renal replacement therapy is associated with significant increased mortality – a 5 year survival rate of 50% (2001). This equates to the survival figures for grade II stomach cancer. In addition, renal replacement therapy costs the NHS approximately £30,000 per patient/per year (2001) and most centres have in the region of 400 such patients.

A greater understanding of glomerular function in health and disease is therefore warranted since any potential therapeutic interventions that result would have profound clinical and financial implications.

1.2 Podocytes

The glomerulus is a unique ultra filtration unit (Berne and Levy, 1992). It is a network of capillaries supplied by the afferent arteriole and drained by the efferent arteriole. These capillaries are covered by a basement membrane, which in turn is covered by epithelial cells or podocytes (Berne and Levy, 1992) (figure1.1). Mesangial cells sit between the capillaries and provide them with structural support, secrete extracellular matrix, and exhibit phagocytic activity (Berne and Levy, 1992). Three clearly defined barriers are believed to determine permeability in the glomerulus; the basement membrane, endothelial and epithelial cells. These are highly permeable to water, small solutes and small proteins, however large proteins

are generally retained. These layers are collectively known as the glomerular filtration barrier (Berne and Levy, 1992) (figure 1.1).

Permeability is partly determined by the presence of 700 Å fenestrations in the endothelium (EC) of the capillary (Pavenstadt, 2000), which selects for molecular size.

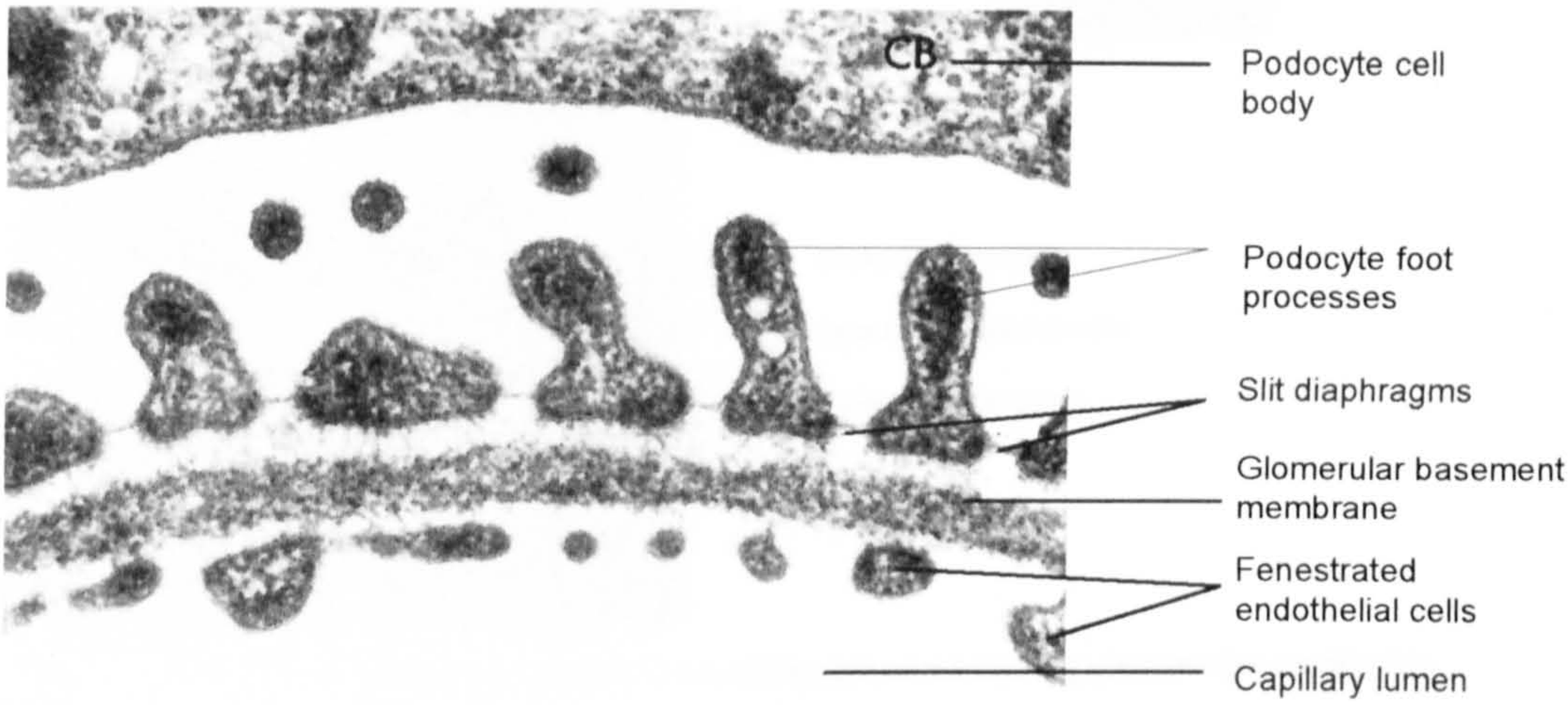

Figure 1.1. A transmission electron micrograph of the glomerular filtration barrier.

The glomerular filtration barrier consists of fenestrated endothelial cells (FEC) which lack diaphragms, a glomerular basement membrane (GBM) and podocytes, with interdigitating foot processes, which together regulate permeability (Berne and Levy, 1992).

The GBM is a heteropolymetric network, composed of type IV collagen, laminin and fibronectin (Pavenstadt, 2000). This network creates a negative charge of matrix proteins (Deen et al., 2001), which act to repel positively charged molecules. It is the podocytes (figure1.1), however that account for ~40% of hydraulic resistance of the filtration barrier (Deen et al., 2001). They differ from normal vascular epithelial cells (pericytes) because they cease to proliferate and differentiate to form foot processes when they reach maturity. The foot processes are separated by slit diaphragms that contain pores of dimensions 40 x 140Å (Berne and Levy, 1992). The foot processes interdigitate around the GBM surrounding the capillaries (Berne and Levy, 1992) as shown in figure 1.2. Together the basement membrane

and the podocytes effectively retain molecules over 36Å through size selectivity, and even smaller anionic molecules through charge selectivity (Berne and Levy, 1992).

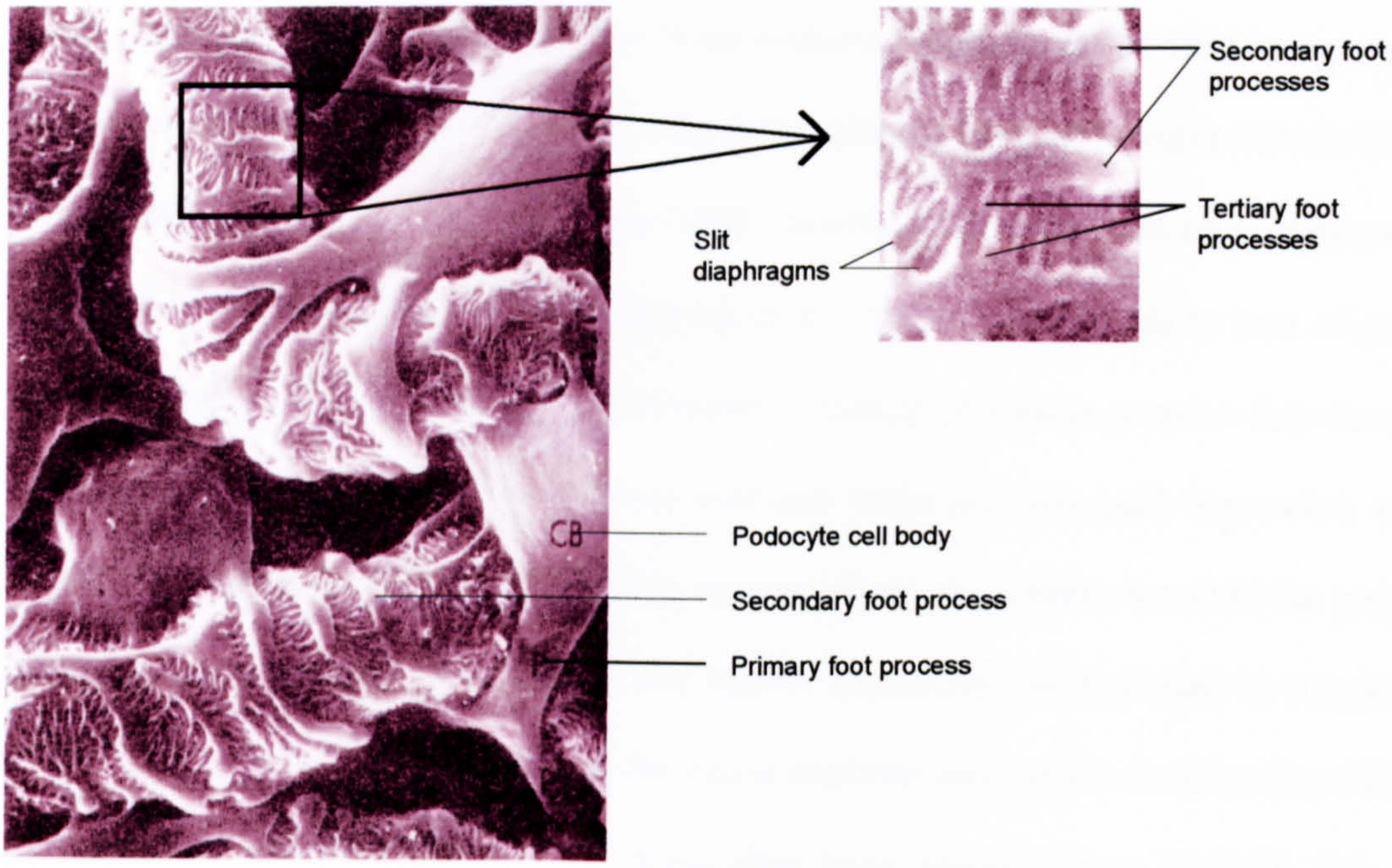

Figure 1.2. Scanning electron micrograph of podocytes surrounding glomerular capillaries.

Primary podocyte foot process extend from the podocyte cell body, branch into secondary foot processes and finally into tertiary foot processes (enlarged area). The tertiary foot processes interdigitate with tertiary foot processes of the same cell or of neighbouring podocytes (Berne and Levy, 1992).

Podocytes are the last line of defence against macromolecular leakage, and therefore disruption of podocytes for example through disease, would have profound consequences on filtration control. Many types of glomerular disease are characterised by podocyte injury (Gassler et al., 2001), but humans do not usually present until glomerular disease is well established. The pathological characteristics of glomerular disease with time are unknown, therefore the following sequence for progressive renal disease was attempted using a fa/fa Zucker rat model, originally a rat model for non-insulin-dependent diabetes mellitus. The authors described the sequence of podocyte injury (Gassler et al., 2001). Firstly, there is foot process effacement defined as retraction of foot processes and loss of foot process and slit

diaphragm organisation, a process that can be reversed if the cause of injury is acute rather than chronic (Schwartz, 2000). Secondly, lipid droplets and lysosomal elements accumulate in the podocyte cytoplasm presumably from podocyte endocytosis of GBM macromolecules. Thirdly, podocytes are lost, which has a direct correlation with glomerulosclerosis (Kim et al., 2001) resulting in denuded areas of the GBM. Fourthly, tuft adhesions form at denuded areas of GBM to the Bowman's capsule (Gassler et al., 2001), which leads to loss of glomerular filtration capacity (Schwartz, 2000). Excessive leakage of plasma proteins into the proximal tubule follows and the proximal tubules reabsorb these proteins until they reach saturation levels. In response to this mediators are released from the tubules towards the interstitium, giving rise to interstitial proliferation and matrix deposition (as discussed in (Gassler et al., 2001)). This leads to the sclerosis of the entire nephron unit, which is often situated in close proximity to healthy nephrons, or those that have already gone through this process independently (Gassler et al., 2001). Such a sequence of putative events in humans would be one explanation of primary podocyte injury progressing to end stage renal disease. A greater understanding of the factors that influence podocyte maintenance and survival may provide novel therapeutic avenues designed to enhance podocyte survival and minimise subsequent nephron loss and reduction of GFR. The terminally differentiated, growth arrested phenotype, of the podocyte may provide a clue to the susceptibility of podocytes to injury.

1.2.1 Podocyte differentiation

Cell cycle completion (cytokinesis) is controlled by cyclin activation of partner cyclin dependent kinases (CDKs). Cell cycle arrest is controlled by cycle dependent kinase inhibitors (CDKIs) (Barisoni et al., 2000), which bind to specific cyclin complexes (Petermann et al., 2002) (figure 1.3). During human glomerulogenesis immature podocytes are proliferative, but from the capillary loop stage of glomerulogenesis expression of cyclins

change from that of cyclin A to cyclin D and there is upregulation of CDKIs p57 and p27. The podocytes then exit the cell cycle, become terminally differentiated and quiescent (Barisoni et al., 2000).

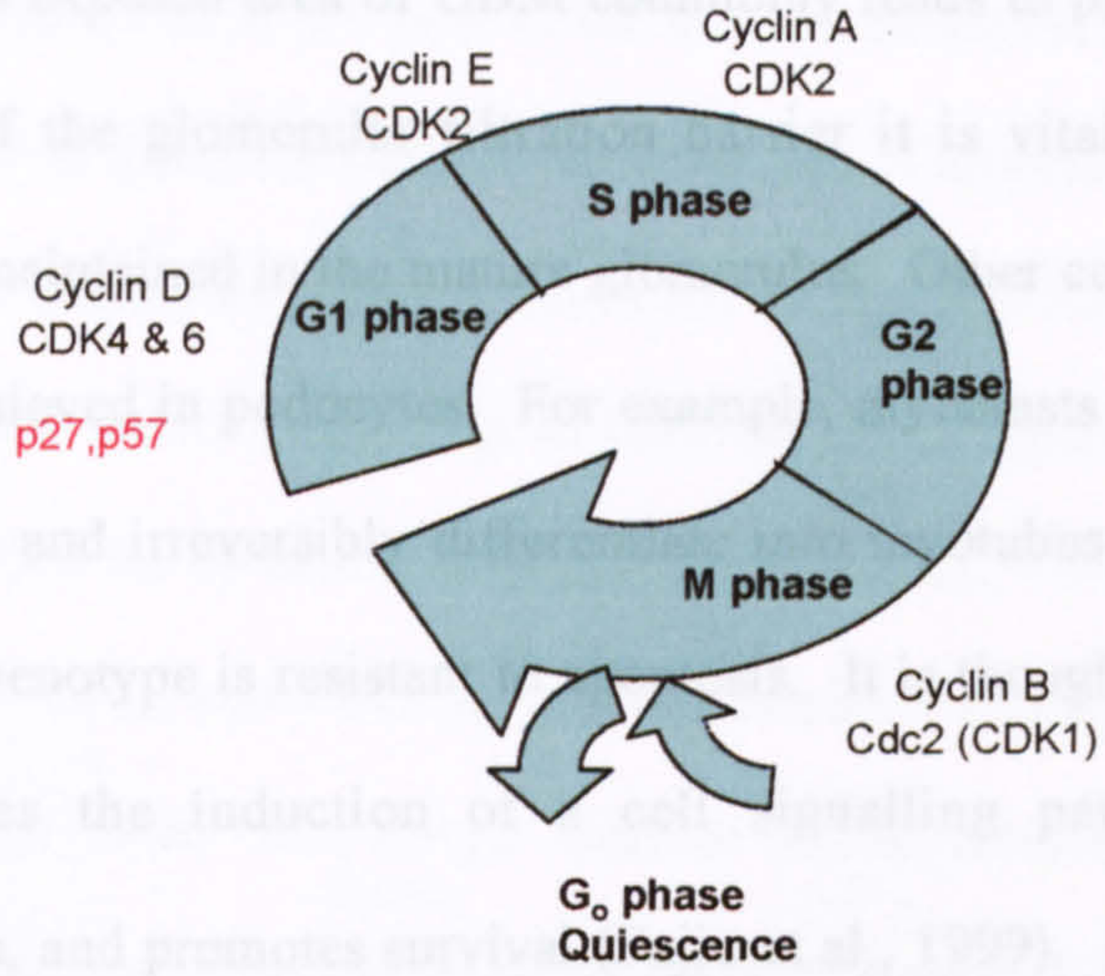

Figure 1.3. The cell cycle.

Each phase of the cell cycle is controlled by specific cyclin/CDK complexes. Upregulation of the CDK inhibitors, p27 and p57, prevent cyclin activation by CDKs at the G1 phase of the cell cycle. This is the stage of the cell cycle in which podocytes are held at differentiation (Nagata et al., 1998).

A natural response of cells to injury is to proliferate and recover but this is rarely the case with podocytes (Shankland et al., 2000). In fact it is thought that this may underlie the development of glomerulosclerosis (Griffin et al., 2003). It is widely accepted that the expression of p27 and p57 ensures that the podocyte does not re-enter the mitotic phase of the cell cycle (Barisoni et al., 2000). However Bailey et al (Bailey et al., 1998) demonstrated that human podocytes can enter S-phase using in situ hybridisation for histone mRNA, (a reliable marker of S phase of the cell cycle). This leads to podocytes undergoing DNA synthesis, but not cytokinesis and therefore it is not uncommon to find podocytes with polyploid nuclei. One of the few times podocyte proliferation is evident is in collapsing glomerulosclerosis, where it

is an early feature of the disease: Podocytes become hypertrophic and hyperplastic due to a loss of CDKIs and cyclin A is re-expressed (Barisoni et al., 2000). For the most part, however, if podocytes are lost then the neighbouring podocytes have a limited capacity to cover the area of denuded basement membrane (Nagata et al., 2003a) and it has been suggested, as discussed earlier, that this exposed area of GBM commonly leads to proteinuria. Therefore, to ensure the integrity of the glomerular filtration barrier it is vital that terminally differentiated podocytes are maintained in the mature glomerulus. Other cell types provide clues as to how this may be achieved in podocytes. For example, myoblasts are similar to podocytes in that they terminally and irreversibly differentiate into myotubes and some also have polyploid nuclei. This phenotype is resistant to apoptosis. It is thought that withdrawal from the cell cycle facilitates the induction of a cell signalling pathway, which involves AKT phosphorylation, and promotes survival (Fujio et al., 1999). It has also been considered that Insulin-like growth factors may activate AKT phosphorylation through activation of phosphatidylinositol 3-kinase (PI3 Kinase) in an autocrine manner (Fujio et al., 1999). *In vitro* assays using sense oligonucleotides to p21 CDKI mRNA showed that endogenous AKT induction is p21 dependent. Human podocytes do not express p21 (Griffin et al., 2003), however this same paper has shown that forced expression of p27 (expressed in podocytes) can compensate for p21. The link in this cell type between mitotic activity and apoptosis provides a clue to prolonged survival of podocytes. It may be possible that growth factors, expressed by podocytes, also play a role in maintenance of differentiated podocytes. One paradox of podocyte biology is that podocytes appear to express a high level of vascular endothelial growth factor (VEGF) mRNA and protein.

1.3 VEGF in endothelial cells

VEGF is a powerful endothelial cell migration, vasodilator, mitogen, angiogenic and permeability factor and has permeability properties more potent than histamine (Aiello and Wong, 2000). The importance of this molecule was outlined by Ferrara et al, who demonstrated that a loss of just one VEGF allele is embryonically lethal in mice (Ferrara et al., 1996). The VEGF gene has eight exons from which alternate splicing can form a number of different active disulphide linked homodimer isoforms (Ferrara, 2001, Neufeld et al., 1999).

The isoforms are named according to their length of amino acids; they all have different properties encoded for by different exons (Neufeld et al., 1999). The most common isoforms are $VEGF_{189}$, $VEGF_{165}$ and $VEGF_{121}$, all of which have different binding affinities for heparin-sulphate proteoglycans. The longer isoform is cell associated due to its high affinity for proteoglycans and may be activated by protease activation and cleavage (Ferrara, 2001), while the two shorter isoforms are secreted. $VEGF_{165}$ binds heparin and therefore can bind to the cell surface or the extracellular matrix, but $VEGF_{121}$ has no heparin binding ability and therefore is freely diffusible (Ferrara, 2001, Simon et al., 1995). Due to its widespread expression $VEGF_{165}$ is the most studied of the VEGF isoforms. VEGF-C, which will be discussed later in detail, is a member of the VEGF family of growth factors and has an N terminal and a C-terminal extension flanking a VEGF homology domain (Joukov et al., 1997). It is a ligand for both VEGF-R2 (with a lower binding affinity than VEGF) and VEGF-R3 (see figure 1.4), is pre-dominantly expressed in the lymphatic system and is thought to function in lymphangiogenesis (Joukov et al., 1997) as oppose to VEGF in angiogenesis.

The VEGFs act through three class III tyrosine kinase receptors: VEGF receptor 1 (VEGF-R1), VEGF receptor 2 (VEGF-R2) and VEGF receptor 3 (VEGF-R3) all of which have seven extracellular immunoglobulin-like domains (Neufeld et al., 1999), a single transmembrane

domain and an intracellular tyrosine kinase domain (figure 1.4). VEGF binds to both VEGF-R1 and VEGF-R2 causing dimerization and auto-phosphorylation. There is, however, no evidence to suggest that it can directly bind to VEGF-R3: a receptor expressed on lymphatic endothelial cells, which is known to bind VEGF-C (Jussila and Alitalo, 2002). VEGF-R1 binds $VEGF_{165}$ with a greater affinity than VEGF-R2, although it has been suggested that it acts mainly as a decoy receptor by competitively binding VEGF (Neufeld et al., 1999). Various studies have suggested it is likely that VEGF-R2 is the sole mediator of VEGF-induced migration, angiogenesis and permeability in endothelial cells (Gille et al., 2001).

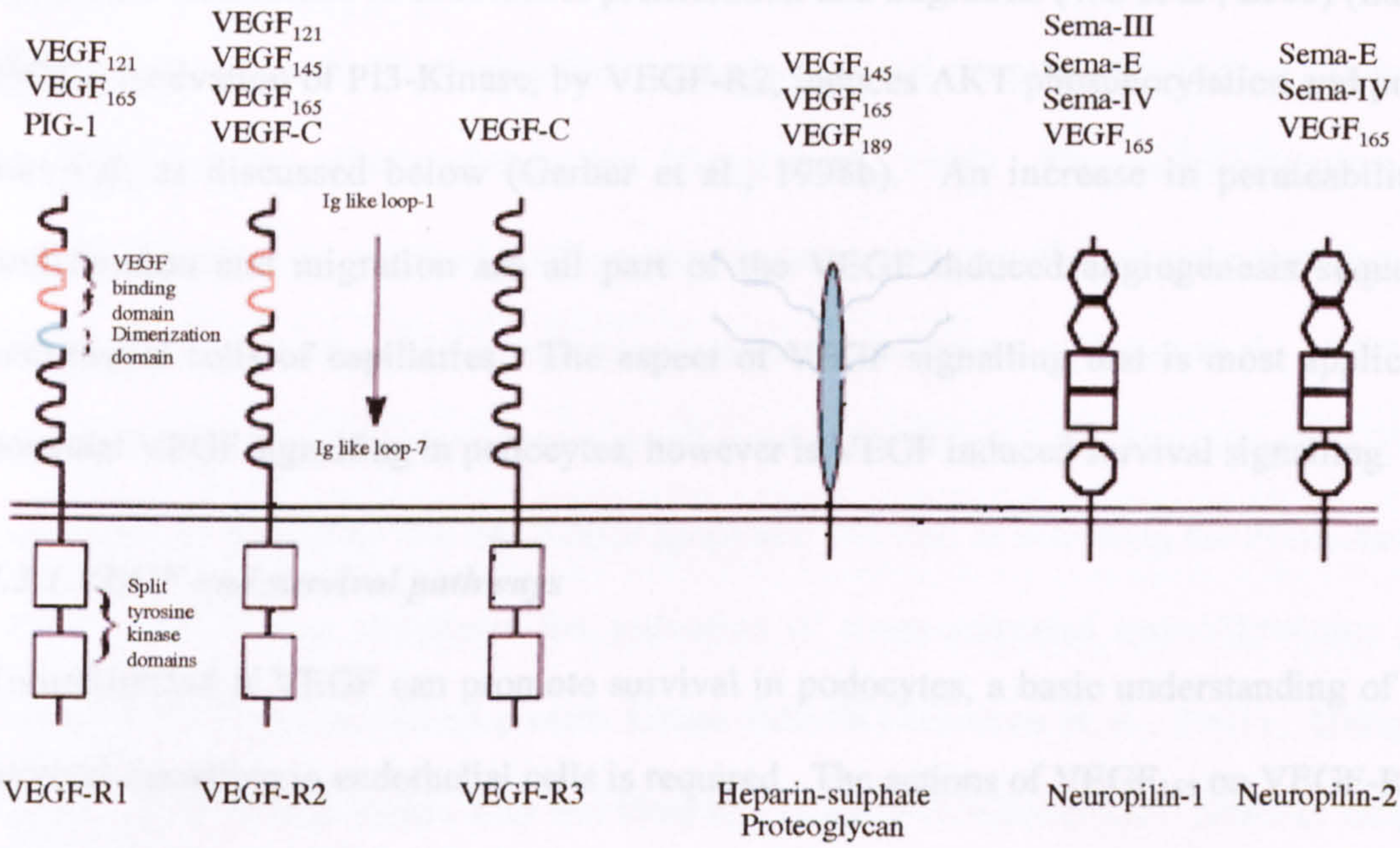

Figure 1.4. Growth factors and receptors of the VEGF family.

The three signalling class III tyrosine-kinase receptors of the VEGF family (VEGF-R1, VEGF-R2 and VEGF-R3), the accessory isofrom specific receptors neuropilin-1 and neuropilin-2, and VEGF binding heparin-sulphate proteoglycans are displayed with general structural features. $VEGF_{165}$ is able to bind to every receptor except VEGF-R3 (adapted from figure 1, (Neufeld et al., 1999)).

VEGF activates a diverse range of signalling pathways in endothelial cells via VEGF-R2. For example auto-phosphorylation of VEGF-R2 by VEGF activates phospholipase C γ (PLC), which leads to diacylglycerol (DAG) generation and consequently an increase in $[Ca^{2+}]_i$, probably due to an external influx via transient receptor potential (TRP) channels in the plasma membrane, resulting in an increase in vessel permeability (Bates and Curry, 1997) (Pocock et al., 2000). An increase in $[Ca^{2+}]_i$ also leads to nitric oxide activation by nitric oxide synthase, resulting in vessel vasodilatation (as reviewed in (Bates et al., 1999)). VEGF-R2 auto-phosphorylation also activates a PLCγ, PKC, Raf, mitogen activated protein kinase kinase (MEK), p42/44 mitogen activated protein kinase (MAPK), dependent signalling cascade, which results in endothelial proliferation and migration (Wu et al., 2000) (Ilan et al., 1998). Activation of PI3-Kinase, by VEGF-R2, induces AKT phosphorylation and promotes survival, as discussed below (Gerber et al., 1998b). An increase in permeability, cell proliferation and migration are all part of the VEGF induced angiogenesis sequence in endothelial cells of capillaries. The aspect of VEGF signalling that is most applicable to potential VEGF signalling in podocytes, however is VEGF induced survival signalling.

1.3.1 VEGF and survival pathways

To understand if VEGF can promote survival in podocytes, a basic understanding of VEGF survival signalling in endothelial cells is required. The actions of $VEGF_{165}$ on VEGF-R2 have been well documented, mostly in vascular endothelial cells due to the original, but erroneous concept that VEGF was endothelial cell specific. VEGF has been shown to act as a survival factor in these cells via a pathway well recognised in a variety of cell types, which is independent of VEGF mediated vasodilatation, permeability and migration pathways. VEGF, via VEGF-R2, induces the phosphorylation of PI3-Kinase by binding the SH2-domain of the PI3-Kinase p85 regulatory subunit. This is probably via an adapter molecule, because the

motif to bind the SH2 domain is not present on VEGF-R2 (Gerber et al., 1998b). This increases intracellular levels of phosphatidylinositol-3,4,5 bisphosphate ($PI(4,5)P_2$) and phosphatidylinositol-3,4,5 trisphosphate ($PI(3,4,5)P_3$). These positively regulate the serine-threonine protein kinase AKT by binding to its pleckstrin homology (PH) domain (Gerber et al., 1998b) (figure 1.5). The VEGF survival pathway is PI3-kinase/AKT dependent (Gerber et al., 1998a, Gerber et al., 1998b) and has been associated with increased levels of two anti-apoptotic proteins: Bcl-2 and A1 (Gerber et al., 1998a). The Bcl-2 family of proteins consists of both pro- and anti-apoptotic proteins. Examples of pro-apoptotic proteins are BAX, BAK and Bcl-X_s. Examples of anti-apoptotic molecules are Bcl-2, Bcl-X_L and A1 (Oltvai et al., 1993). These proteins have the ability to form homo- and heterodimers with each other and, depending on the ratio of proteins from each pro- and anti-apoptotic family, can compete with and neutralise the effects of the other (Gross et al., 1999). The phosphorylation of pro-apoptotic proteins by activated AKT proteins sequesters them to the cytosol where they cannot insert into the mitochondrial membrane to release cytochrome c (Gross et al., 1999), which would result in apoptosis (programmed cell death) (see figure 1.5). Surprisingly, VEGF can also stimulate a pathway that can induce apoptosis. As well as activating the PI3-Kinase/AKT pathway VEGF also stimulates the activation of stress-activated serine/threonine protein kinase p38 mitogen activated protein kinase (MAPK) (Gratton et al., 2001). Using a cell culture model it was shown that the blockade of the PI3-Kinase/AKT pathway attenuated VEGF stimulated MAPK kinase kinase 3 (MEKK3) phosphorylation thereby increasing Src dependent (McMullen et al., 2004) p38 signalling.

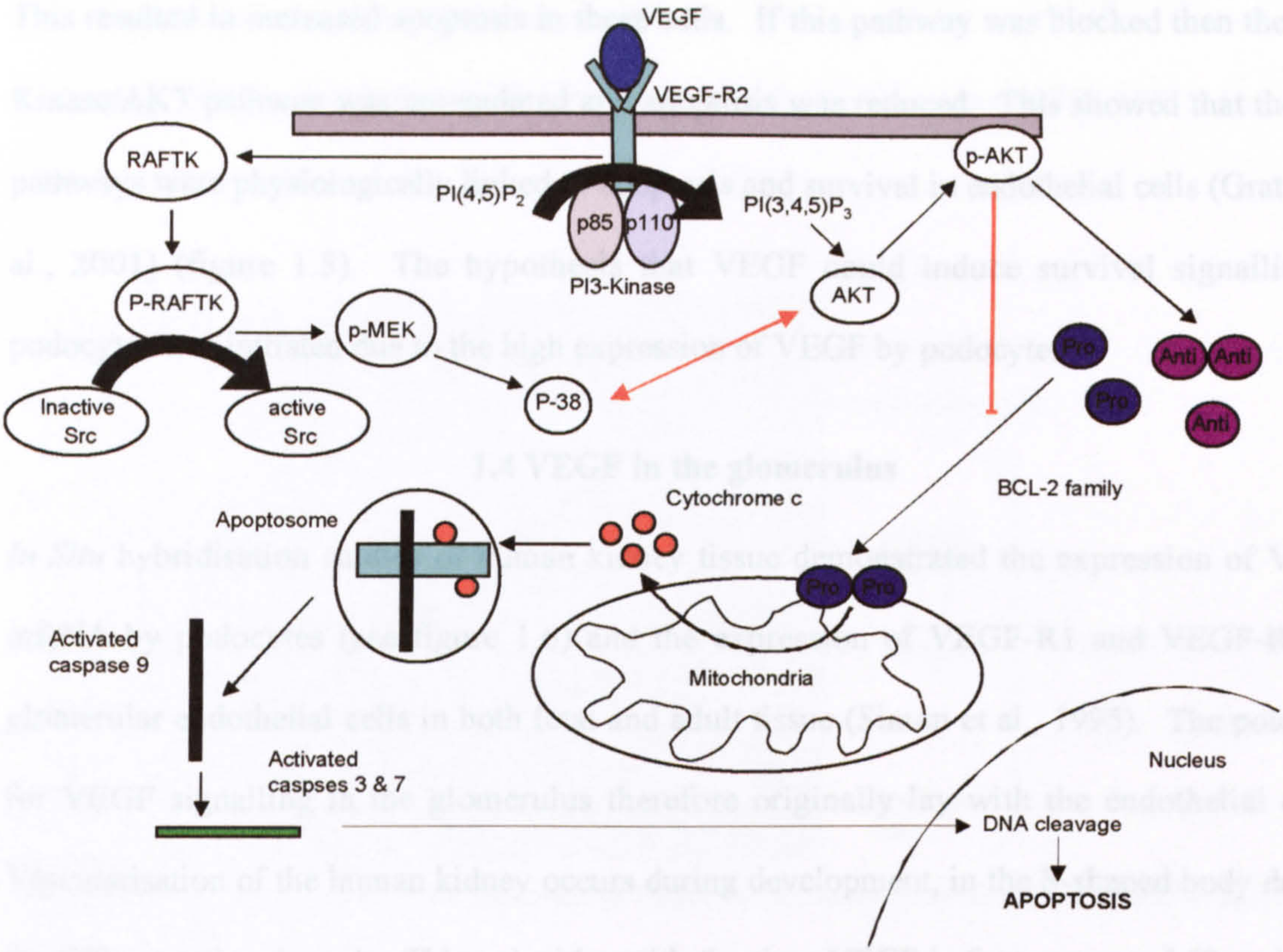

Figure 1.5. Schematic of VEGF survival signalling in endothelial cells.

Activation of VEGF-R2 by its ligand, VEGF, induces its autophosphorylation, which activates PI3-Kinase. This converts $PI(4,5)_2$ to $PI(3,4,5)P_3$, which induces the translocation of AKT to the plasma membrane where it is phosphorylated. Phospho-AKT induces the phosphorylation of members of the pro-apoptotic proteins, which inactivates them. If these proteins are not inactivated then they insert into the mitochondrial membrane and induce the release of cytochrome c, which forms an apoptosome with caspase 9 and Apaf 1 (apoptotic protease activating factor, a caspase recruitment domain). This cleaves and activates caspase 9, which cleaves and activates the effector caspases, 3 and 6. These cleave nucleases, which translocate to the nucleus and induce DNA fragmentation and death due to apoptosis. There is cross-talk between two VEGF signalling pathways, which balances pro- and anti-apoptotic signalling in endothelial cells. Activated related focal adhesion tyrosine kinase (RAFTK), by VEGF-R2, activates Src, which results in the phosphorylation of MEK (p-MEK), which then phosphorylates p38 MAPK. This is linked to an increase in apoptosis, but can be inhibited by phosphorylated AKT. Thus, phosphorylated AKT is anti-apoptotic through two separate pathways.

This resulted in increased apoptosis in these cells. If this pathway was blocked then the PI3-Kinase/AKT pathway was upregulated and apoptosis was reduced. This showed that the two pathways were physiologically linked to apoptosis and survival in endothelial cells (Gratton et al., 2001) (figure 1.5). The hypothesis that VEGF could induce survival signalling in podocytes was initiated due to the high expression of VEGF by podocytes.

1.4 VEGF in the glomerulus

In Situ hybridisation studies of human kidney tissue demonstrated the expression of VEGF mRNA by podocytes (see figure 1.6) and the expression of VEGF-R1 and VEGF-R2 on glomerular endothelial cells in both fetal and adult tissue (Simon et al., 1995). The potential for VEGF signalling in the glomerulus therefore originally lay with the endothelial cells. Vascularisation of the human kidney occurs during development, in the S-shaped body during the fifth gestational week. This coincides with the time VEGF is first expressed (Eremina et al., 2003), and also the time endothelial cells migrate into the developing glomerulus (Simon et al., 1995). It is thought that the VEGF expressing, de-differentiated podocytes situated next to the endothelial cells during the development of the vascular cleft provide the migratory cues to the endothelial cells to establish the glomerular vascular structure (Saxen and Sariola, 1987, Simon et al., 1995). VEGF therefore plays a specific paracrine role in angiogenesis during human kidney organogenesis (Simon et al., 1995). At maturity, it is thought that VEGF expression ensures the maintenance of the fenestrated endothelium (Simon et al., 1995) and also plays a role in maintaining the filtration barrier (Eremina et al., 2003). This was supported by Eremina et al using a Cre-*lox*P system, which allows switching on and off of specific genes, whereby the VEGF gene was switched off at various stages of murine development. It was shown that a reduction in VEGF at establishment of the vascular beds led to a loss of endothelial fenestrations (Eremina et al., 2003). Four isoforms of VEGF mRNA

are expressed in the cortex of the human kidney: $VEGF_{121}$, $VEGF_{165}$ $VEGF_{189}$ (Simon et al., 1995) and $VEGF_{148}$ (Whittle et al., 1999), of which $VEGF_{165}$ is predominantly expressed (Simon et al., 1995).

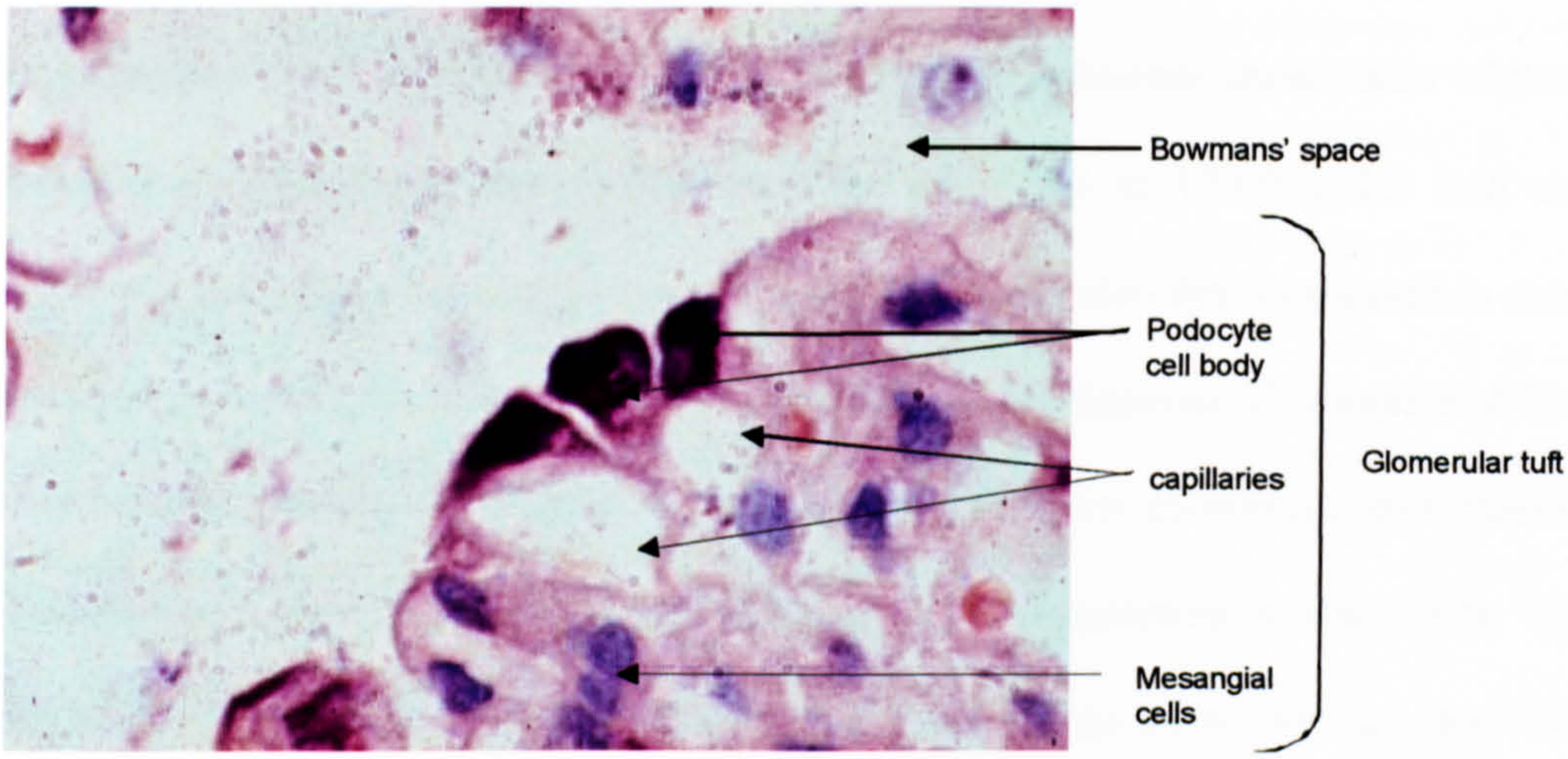

Figure 1.6. Non-isotopic, *in situ* hybridisation for VEGF mRNA in the glomerular tuft (Bailey et al., 1999).

Human renal cortex sections were probed with labelled VEGF mRNA. This section demonstrates that, within the glomerulus, dark staining for labelled VEGF mRNA was detected in cells at the periphery of the glomerular tuft, which, because of their micro-anatomy are known to be podocytes. Hence podocytes are the site of VEGF production in the healthy, mature human glomerulus. (Bailey et al., 1999).

The same pattern of isoform expression has been seen in the mouse kidney, although each of these lack one amino acid compared to the human isoforms (Kretzler et al., 1998). Mouse and rat glomerular endothelial cells express VEGF-R1 and VEGF-R2 and have also been shown to express neuropilin-1 (Np-1) (Robert et al., 2000) (Villegas and Tufro, 2002). Np-1 is a co-receptor for receptors of the plexin family (Neufeld et al., 2002). Together these bind the ligand Sema-3A, a member of the class III semaphorin subfamily (Neufeld et al., 2002), which stimulates collapse of neural growth curves and repels axons (Neufeld et al., 2002). Np-1 is also a co-receptor for VEGF-R2 and binds $VEGF_{165}$ at the protein sequence encoded by exon 7 (Soker et al., 1998). It was first described as $VEGF_{165}R$ (Soker et al., 1997) in relation to

VEGF signalling until Soker et al discovered that it was identical to Np-1 (Soker et al., 1998). Over expression of Np-1 can cause abnormalities in the development of both the vascular and nervous system (Neufeld et al., 2002) and Np-1 knock out mice do not survive past embryonic day 12.5 (Takashima et al., 2002). Np-1 enhances the binding of $VEGF_{165}$ to VEGF-R2 4 to 6 fold compared to VEGF-R2 expression alone, it also enhances chemotaxis of porcine aortic endothelial (PAE) cells expressing VEGF-R2 and Np-1 to $VEGF_{165}$ 2.5 fold compared to VEGF-R2 expression alone (Soker et al., 1998). Np-1 is also first expressed in mouse and rat glomerular endothelial cells at the S-shaped body of development (Villegas and Tufro, 2002). This indicates that co-expression of Np-1 and VEGF-R2 on glomerular endothelial cells aids glomerular vascular development and enhances VEGF signalling in these cells. Np-2 is also expressed on glomerular endothelial cells at the same time point (Villegas and Tufro, 2002) and can bind both $VEGF_{165}$ and $VEGF_{145}$ (a rarer isoform) (Gluzman-Poltorak et al., 2001). Little is known about its function in the vascular system although it is thought to form complexes with Np-1 and VEGF-R1 (as reviewed in (Neufeld et al., 2002)).

Recently, it has been shown that human podocytes express mRNA and protein for Np-1 and mRNA for Np-2 (Harper et al., 2001), which gave rise to the potential for VEGF signalling in podocytes. Neuropilins lack a cytoplasmic signalling domain (Soker et al., 2001) (Harper et al., 2001) and were not thought to be able to signal independently, but by associating with tyrosine kinase receptors it is thought they could function as signalling complexes (Gluzman-Poltorak et al., 2001). It is therefore surprising that there is no evidence to date to suggest that podocytes express VEGF-R1 or VEGF-R2. In mice heterozygous for VEGF there was a dramatic loss of podocytes by week nine of development following endotheliosis and proteinuria (Eremina et al., 2003). The authors have suggested endothelial cells signal back to

podocytes to maintain them. Another interpretation is that VEGF signals directly to the podocytes, epithelial in origin, to maintain their survival.

1.5 VEGF signalling in non-endothelial cells

Work in recent years has uncovered a role for VEGF in cell types other then endothelial cells, despite the fact that it was thought to be endothelial specific, and these studies provide clues to potential VEGF signalling pathways in podocytes. Haematopoietic stem cells express VEGF, VEGF-R1 and VEGF-R2 (Gerber et al., 2002). Using a cre-*lox*P system in mice to knock down VEGF Gerber et al elucidated that VEGF regulated haematopoietic stem cell survival through an internal autocrine loop, not generally seen to operate in endothelial cells (Gerber et al., 2002). This was demonstrated by the lack of effect of external acting inhibitors, although VEGF-R2 still plays a role in internal VEGF signalling. A similar mechanism was seen in VEGF expressing leukaemia cell lines. Although they express and signal through VEGF-R2 there appear to be two independent autocrine VEGF signalling pathways: an external and an internal (Rosa Santos and Dias, 2004). Interestingly it appears that the internal autocrine pathway has a greater effect on cell survival. They suggest that VEGF-R2 is not exclusively membrane bound although it is still constitutively activated. This provides an interesting insight to the expanding signalling potential of VEGF. Taking this novel concept a step further Bachelder et al demonstrated, using anti-sense VEGF oligonucleotides in metastatic breast carcinoma cell lines, that VEGF promotes survival in a PI3-kinase/AKT dependent manner (Bachelder et al., 2001). Not only are these cells not endothelial but they do not express VEGF-R1 or VEGF-R2. They do however express Np-1, as do podocytes, and the authors have shown that Np-1 is associated with elevated levels of survival. It is not known how VEGF can signal independently through Np-1, but this is not an isolated case. Miao et al have shown that overexpression of Np-1 in rat prostate carcinoma AT2.1 cells, which express

VEGF but not VEGF-R1 and VEGF-R2, led to an increase in tumour angiogenesis and reduced apoptosis (Miao et al., 2000). These authors have also postulated that $VEGF_{165}$ may stimulate cells directly via Np-1 binding, which would have relevance to VEGF signalling in podocytes independently of other VEGF receptors. This contradicts previous workers, who postulated that the intracellular domain of Np-1 does not contain a signalling domain. Recent work by Wang et al, however, indicates that Np-1 may be able to signal independently. They created a chimeric receptor by fusing the extracellular domain of epidermal growth factor receptor (EGFR) to the transmembrane and intracellular domains of Np-1 (Wang et al., 2003). This was then transduced into human umbilical vein endothelial cells (HUVECs) using a retroviral expression vector. It was shown that epidermal growth factor (EGF) stimulated Np-1 dependent migration of HUVECs via a PI3-kinase dependent pathway (Wang et al., 2003). From this they deduced that Np-1 alone could mediate VEGF induced endothelial cell migration via activation of the intracellular domain of Np-1. This research encourages the theory that VEGF may signal in podocytes, despite VEGF receptor expression limited to Np-1, although conclusions drawn from the work done by Wang et al may be premature. HUVECs express VEGF-R1, VEGF-R2 and Np-1, so the signalling pathway studied may not have been isolated to the chimeric receptor. Also, the 3-dimensional conformation of EGF bound to its extracellular domain would probably be completely different to that of VEGF binding to the extracellular domain of Np-1. This may affect the conformational change of the intracellular domain of Np-1 and therefore its auto-phosphorylation sites. Therefore, it seems that the intracellular domain of Np-1 may be capable of signalling independently, but not necessarily in response to VEGF in a non-artificial system. The literature on the effects of VEGF on non-endothelial cells is growing fast, however, and apart from podocytes examples of cell lines expressing VEGF and Np-1, but not VEGF-R1 and VEGF-R2 seems limited to carcinoma cell lines. The function of isolated Np-1 expression may be to sequester $VEGF_{165}$,

or to enhance actions of VEGF through some unknown mechanism (Soker et al., 1998). This could potentially allow VEGF signalling in podocytes to promote survival, but in order to understand the potential of VEGF survival signalling in podocytes, current understanding of survival signalling in podocytes should be examined.

1.6 Podocyte maintenance

1.6.1 External factors

Despite the obvious importance of differentiated podocyte survival and maintenance, the literature on it is very limited. There is a lot of information in the literature on the causes of pathological apoptosis, and effacement of podocytes, but an understanding of what makes podocytes so robust *in vivo* and *in vitro* is warranted. Many types of cells receive external survival stimuli from various growth factors or cytokines. Work by Fornoni et al has shown that cultured podocytes are protected from cyclosporin A induced apoptosis by hepatocyte growth factor. This was dependent on Bcl-X_L regulation and is postulated to be PI3-kinase dependent (Fornoni et al., 2001). Despite the similarities seen between this pathway and the apoptosis pathway described earlier these authors believe that the same growth factors may stimulate different apoptosis pathways in podocytes. Indeed, they show that DNA fragmentation is an early event in podocytes (Fornoni et al., 2001), detectable before a decrease in cell number. Apart from this piece of work there is little to link other growth factors with survival in podocytes.

1.6.2 Internal factors

Much of the evidence for podocyte survival in the literature is based on intracellular observations. There is growing evidence linking podocyte survival with its actin cytoskeleton, found in the podocyte foot processes (figure 1.7). Reorganisation of the podocyte actin

cytoskeleton leads to retraction and effacement of foot processes (Reiser et al., 2000b), which invariably leads to proteinuria; the hallmark of many glomerular diseases (Huh et al., 2002). The link between podocyte survival and its cytoskeleton has been outlined by work done by Smoyer et al. Heat shock protein 27 (hsp27), a low molecular weight, rapidly phosphorylated protein that is upregulated in response to exposure to toxicants and oxidative stress (Jia et al., 2001), has been associated with increased cell survival and recovery (Jia et al., 2001). Hsp27 was shown to inhibit actin polymerisation in podocytes (Smoyer and Ransom, 2002); transfection of an immortalised mouse podocyte cell line with hsp27 sense DNA caused cell retraction, detachment and death (Smoyer and Ransom, 2002). Podocyte hsp27 levels also correlated with resistance to puromycin aminonucleoside (PAN) induced cell death (Smoyer and Ransom, 2002). This indicates that podocyte survival is maintained if the actin cytoskeleton is not disrupted. Therefore, an understanding of the podocyte cytoskeleton is critical to the elucidation of how the cytoskeletal structure affects podocyte survival.

1.6.2.1 Organisation of podocyte cytoskeleton

The podocyte is composed of three compartments, consisting of the cell body, the major processes and the foot processes (Ichimura et al., 2003) (figure 1.2). Both the cell body and the major processes contain cytoplasmic microtubules and intermediate filaments (vimentin and tubulin), but the foot processes only contain microfilaments (Vasmant et al., 1984), namely actin and α actinin (Drenckhahn and Franke, 1988) (figure 1.7). These proteins generate the contractile force that resists the high intraluminal hydrostatic pressure from the capillaries, and it has been speculated that they actively modify their surface area for filtration (Drenckhahn and Franke, 1988). The podocyte actin cytoskeleton appears to be associated with the plasma membrane, and can communicate externally via numerous contact proteins,

associated with transmembrane proteins of the slit diaphragm, GBM and apical membrane (figure 1.7).

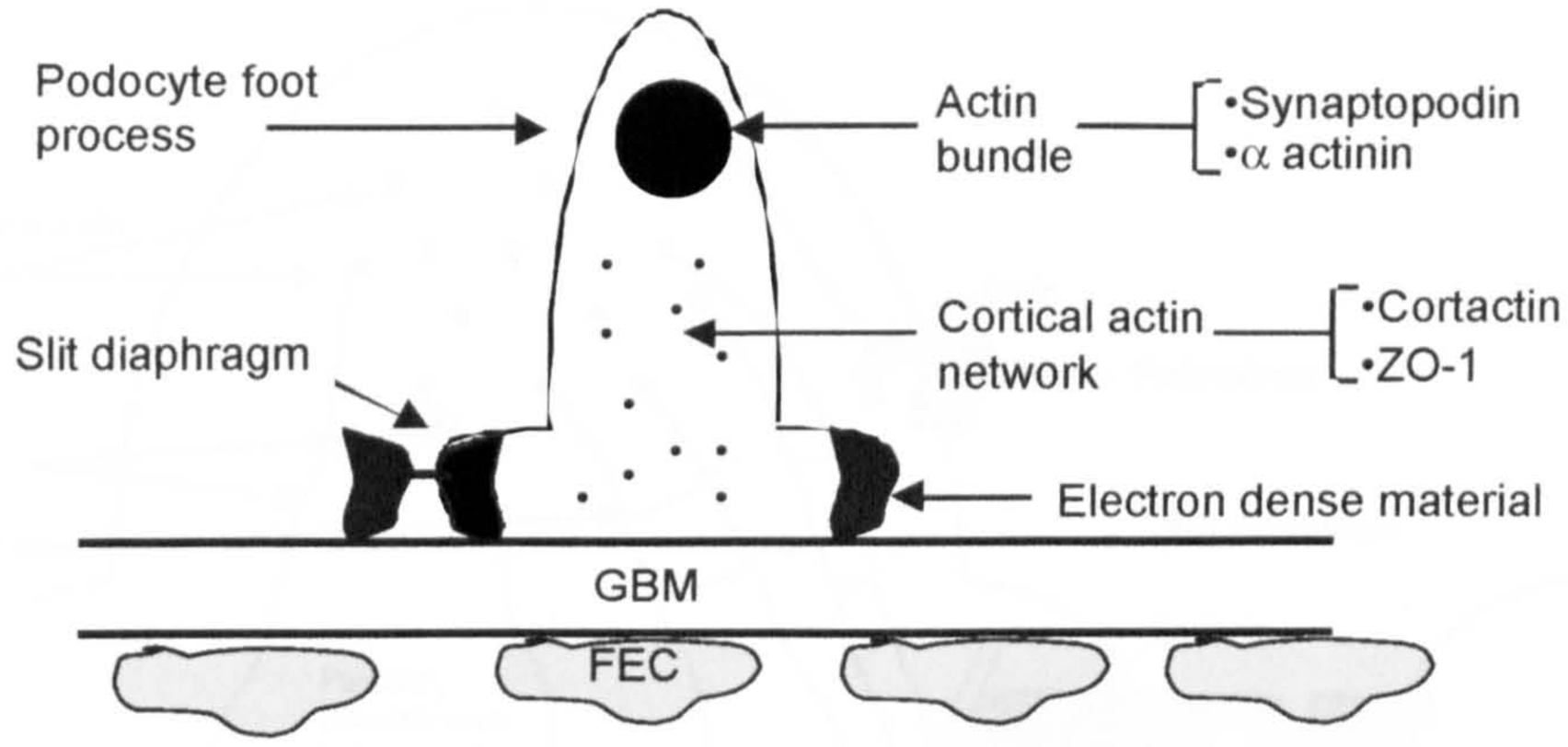

Figure 1.7. A schematic representation of actin filament organisation in the podocyte foot process.

There are two distinct sub populations of actin filaments in the foot processes; the actin bundle, concentrated in the apical region of the foot processes, which includes proteins such as α-actinin and synaptopodin and the cortical actin network spread throughout the cytoplasm, which contains proteins such as cortactin and ZO-1. Adapted from (Ichimura et al., 2003). GBM= glomerular basement membrane, FEC = fenestrated endothelial cells.

1.6.3 Podocalyxin

Podocalyxin is a sialylated transmembrane protein found in the podocyte cell body and in the apical plasma membrane of the foot processes. It carries a highly negative charge and is thought to prevent normal cell-cell aggregation in culture by charge repulsion (Takeda et al., 2000). Similarly, when podocyte tight junctions transform into slit diaphragms during the S-shaped body stage of glomerulogenesis it is thought to be due to the charge repulsion of proteins such as podocalyxin. This maintains the open slits between neighbouring foot processes (Takeda et al., 2000). Podocalyxin has been shown to form complexes with ezrin (Orlando et al., 2001) (figure 1.8). This is a phospho-tyrosine protein localised to the apical membrane region of the cytosol (Kurihara et al., 1995), which is known to bind to the actin cytoskeleton (Tsukita and Yonemura, 1997). Any stimuli that modify podocalyxin expression

may therefore influence its intracellular interactions with cytosolic proteins (Orlando et al., 2001) and are likely to affect the morphology of the foot processes.

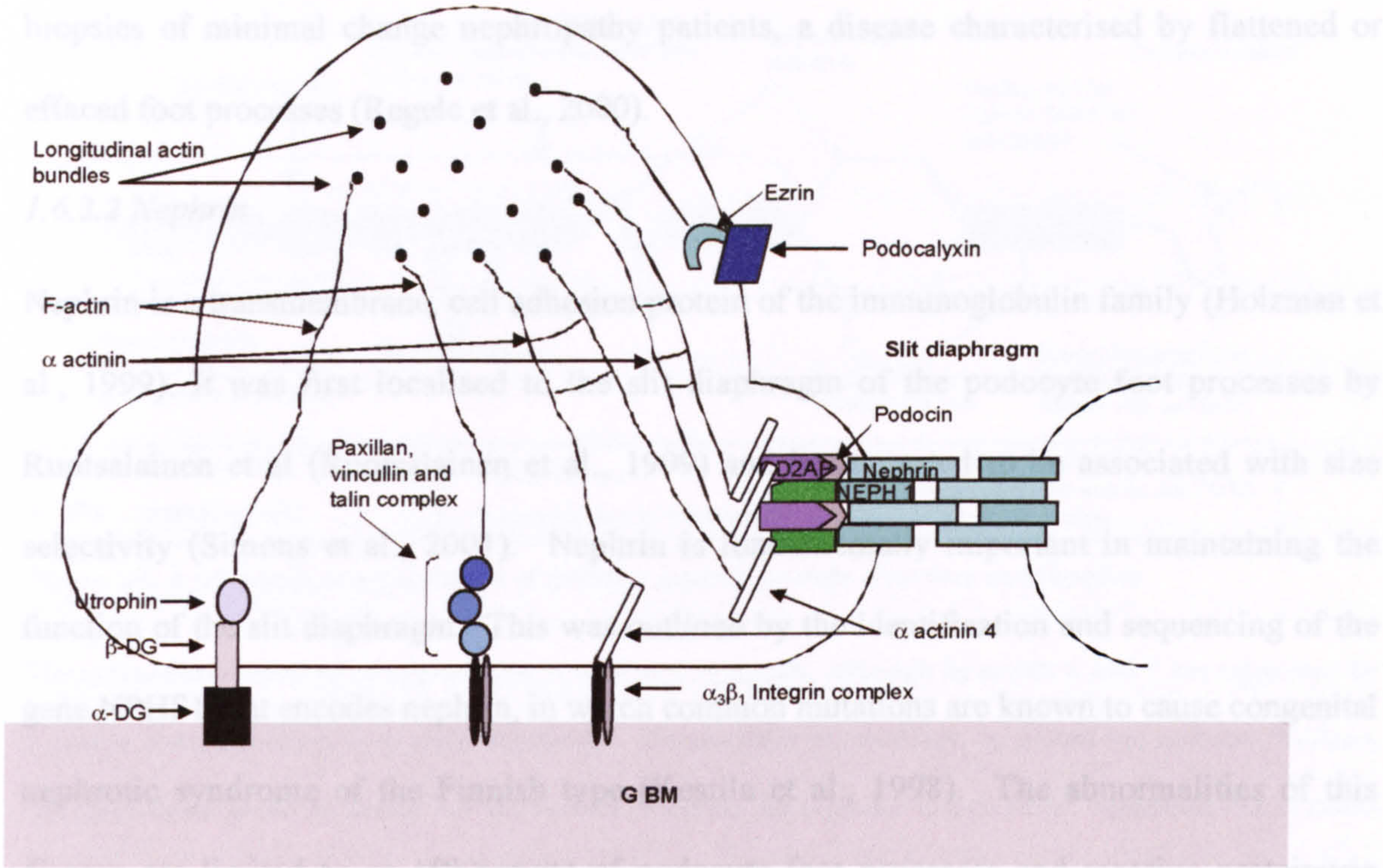

Figure 1.8. A schematic representation of the anatomy of the actin cytoskeleton in the podocyte.

The morphology of the podocyte is maintained via communications between the plasma membrane and actin cytoskeleton. Communicative proteins, such as nephrin, podocalyxin and dystroglycan provide a link from the outside of the cell to the actin cytoskeleton via actin binding proteins, such as α actinin 4, utrophin and ezrin. In some instances a large complex is formed, such as at the slit diaphragm, which provides an indirect link between the communicative proteins and the actin binding proteins.

1.6.3.1 Dystroglycans

The podocytes govern the topography of the GBM matrix proteins using actin-guided dystroglycan (DG) complexes (Regele et al., 2000) (figure 1.8). Dystroglycan α and β are expressed in the basal cell membranes of the podocyte foot processes (Regele et al., 2000). It has been postulated that they provide a link with the cytoskeleton of the podocytes (via utrophin, an intracellular binding partner of DGs (Regele et al., 2000)) and the GBM to help to

stabilise the podocytes to the GBM (Regele et al., 2000); thus they oppose podocyte detachment and may contribute to function. Expression of dystroglycans is reduced in renal biopsies of minimal change nephropathy patients, a disease characterised by flattened or effaced foot processes (Regele et al., 2000).

1.6.3.2 Nephrin

Nephrin is a transmembrane, cell adhesion protein of the immunoglobulin family (Holzman et al., 1999). It was first localised to the slit diaphragm of the podocyte foot processes by Ruotsalainen et al (Ruotsalainen et al., 1999) and is suggested to be associated with size selectivity (Simons et al., 2001). Nephrin is fundamentally important in maintaining the function of the slit diaphragm. This was outlined by the identification and sequencing of the gene NPHS1 that encodes nephrin, in which common mutations are known to cause congenital nephrotic syndrome of the Finnish type (Kestila et al., 1998). The abnormalities of this disease are limited to an effacement of podocyte foot processes and massive proteinuria resulting in death within the first two years of life unless a kidney transplant is received (Kestila et al., 1998). An alteration of nephrin expression is not just isolated to genetic mutations-it can also be acquired and is associated with many other types of renal disease. A reduction in nephrin expression was noted in areas of effaced foot processes in human renal biopsies of various chronic glomerulonephritides (Huh et al., 2002), membranous glomerulonephritis, minimal change glomerulonephritus and focal and segmental glomerulosclerosis (Doublier et al., 2001). It is interesting to note that there was no change in nephrin expression in biopsies from patients with IgA nephropathy, which is a disease in which proteinuria tends to be a less prominent feature. This indicates that nephrin expression is related to the proteinuric state rather than the specific disease (Doublier et al., 2001). Nephrin has an extracellular domain probably involved in cell adhesion, a transmembrane domain and an intracellular domain with nine putative tyrosine phosphorylation sites (Kestila

et al., 1998), which suggests that nephrin may function as a signalling molecule (Doublier et al., 2001, Simons et al., 2001) (figure 1.9).

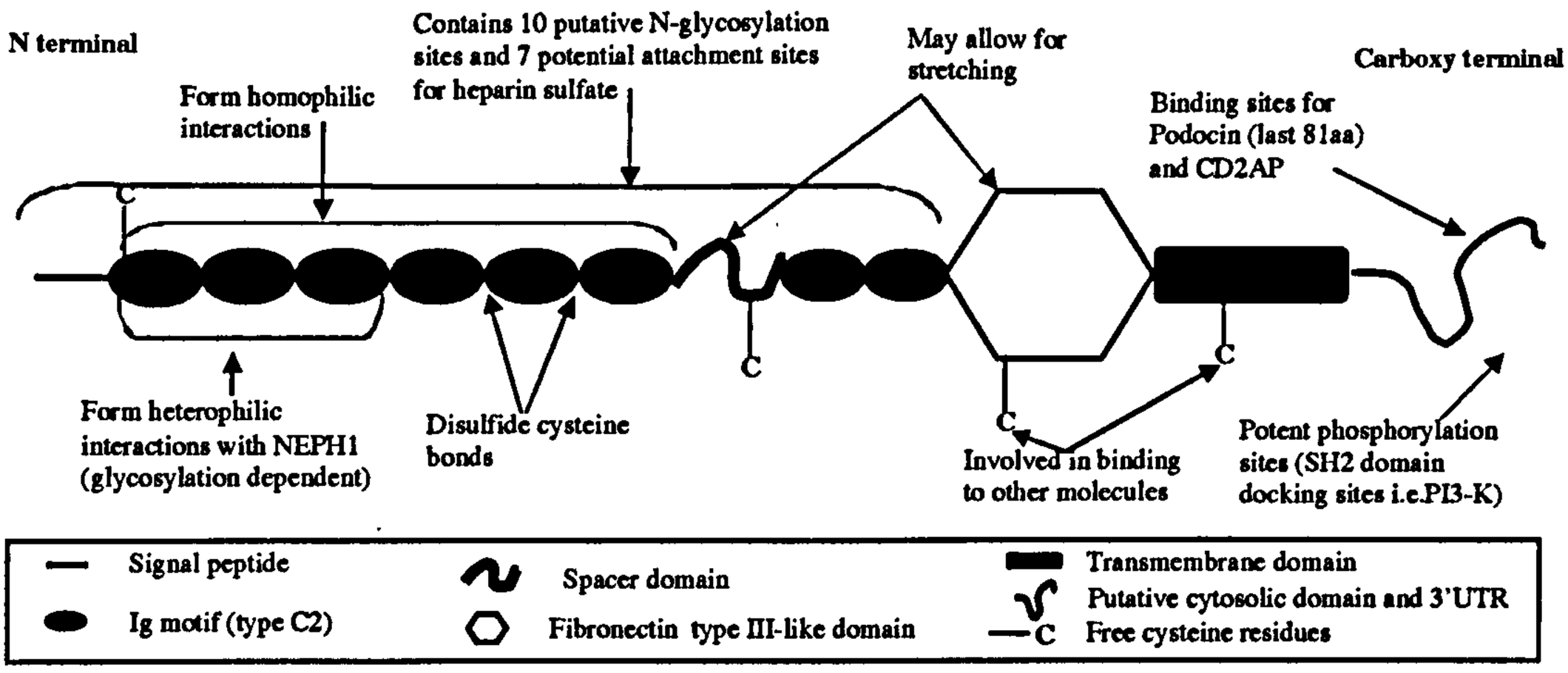

Figure 1.9. A schematic representation of putative nephrin protein structure and function

The extracellular domain of nephrin has a total of 8 Ig motifs, although Ig motifs 6 and 7 are separated by a spacer domain, which may allow flexibility. Heterophilic interactions, mediated via cysteine residues, are postulated to be Ig motif 1-3 dependent, whereas homophilic interactions, mediated via cysteine residues, are postulated to be Ig motif 1-6 dependent. There is a fibronectin type III-like domain and a transmembrane domain. The cytoplasmic domain contains 9 putative tyrosine residues, which are implicated in nephrin signalling.

During podocyte development, apical tight junctions migrate down the lateral aspect of the plasma membrane and are eventually replaced by the slit diaphragm. These earliest slit pore regions were often densely labelled with anti-nephrin antibodies in electron microscopy studies (Holzman et al., 1999), which demonstrates that nephrin complexes associate when podocytes transdifferentiate into mature cells and this is thought to be aided by lipid rafts (Simons et al., 2001). Lipid rafts are regions of the plasma membrane enriched in glycosphingolipids and cholesterol. They organise the cell membrane into different compartments and function in a variety of cell biological processes such as cell adhesion and signal transduction (Simons et al., 2001) and are highly concentrated in transduction molecules (Huber et al., 2003b). The oligomerized form of nephrin has been shown to

associate with these lipid rafts and is redistributed via the cytoskeleton to the slit diaphragm (Simons et al., 2001). These lipid rafts may also be important in the conversion of the apical tight junctions to slit diaphragms (Simons et al., 2001).

It is possible that nephrin can induce a change in the cytoskeleton and also that the cytoskeleton can induce a change in nephrin distribution. For example it has been shown that angiotensin-II can induce redistribution of nephrin from the slit diaphragm and also induce the shedding of nephrin (Doublier et al., 2003). This occurred on a time course of just 30 minutes, which suggests that this is independent of mRNA expression. On the contrary it has been shown that angiotensin-II directly stimulates the F-actin cytoskeleton. This nephrin redistribution and shedding is thought to be an early effect of type 1 and type 2 diabetes in diabetic nephropathy (Doublier et al., 2003). Angiotensin-II has been shown to depolarise the podocyte in intact glomeruli via its receptor (AT_1). This results in an increase in $[Ca^{2+}]_i$ (Nitschke et al., 2000) (which causes the cytoskeleton to contract) and ultimately stimulates an increase in extracellular matrix production, which determines matrix deposition in glomerular disease (Candiano et al., 2001). Other studies investigating the effect of angiotensin-II on glomerulonephropathies have shown that there is a time dependent reduction in nephrin mRNA in chronic injury correlated with increased proteinuria. Histological sections from a rat model of human membranous nephropathy (passive Heymann nephritis) showed reduced glomerular expression of nephrin mRNA (using *in situ* hybridisation) and also nephrin protein. The effects on nephrin expression and distribution could be fully blocked using inhibitors to angiotensin-II converting enzyme and the receptor of angiotensin-II (Losartan), which also blocked chronic injury (Benigni et al., 2001). This indicates, at least in this rat model, that angiotensin-II dependent chronic renal injury is dependent on changing expression and

distribution of nephrin, in addition to any haemodynamically-dependent angiotensin-II induced changes in single nephron glomerular filtration rate (Durvasula et al., 2004).

1.6.3.3 Podocin

Podocin is an integral membrane hairpin protein of the raft-associated stomatin family with a short N-terminal domain, a transmembrane region and a C-terminal domain (Huber et al., 2001, Huber et al., 2003b). It is encoded by the gene NPHS2, mutations in which cause a subset of childhood steroid-resistant nephrotic syndrome with focal and segmental glomerulosclerosis (Boute et al., 2000). This disease follows a milder clinical course than that caused by mutations in the NPHS1 gene (Huber et al., 2001). It is localised to the slit diaphragm (Simons et al., 2001) in mature podocytes (Huber et al., 2001) and forms homo-oligomers involving the amino and carboxy-terminal domains (Huber et al., 2003b) to form a widespread structure (Boute et al., 2000, Huber et al., 2003b). Podocin binds to the cytoplasmic tail of nephrin by forming oligomers (Huber et al., 2001) (figure 1.8) and immunoprecipitation studies on transfected human embryonic kidney (HEK) 293T cells involving podocin mutants show that it plays a role in recruiting nephrin into the lipid raft microdomains (Huber et al., 2003b).

1.6.3.4. CD2AP

Another molecule shown to play a vital role in the slit diaphragm is CD2 associated protein (CD2AP). CD2AP is an adapter protein containing three SH3 domains and multiple polyproline motifs that was originally shown to bind to the cytoplasmic domain of CD2 (which is a transmembrane protein of an immunoglobulin family expressed on T-cells) (Dustin et al., 1998). CD2AP supports a role as molecular scaffolding and may polarise the cytoskeleton (Dustin et al., 1998). Homozygous CD2AP knock out mice died by weeks 6 or 7, and surprisingly, one symptom revealed by histological examination was severe kidney

pathology (Shih et al., 1999). The initial defect was isolated to the podocytes using electron microscopy showing obliterated slit diaphragms. CD2AP was also shown to be co-immunoprecipitated with a nephrin fusion protein and was localised in the lipid rafts by the slit diaphragm along with podocin and nephrin (Schwarz et al., 2001, Shih et al., 1999). This study and others demonstrate that foot processes can develop in the absence of CD2AP and that CD2AP-nephrin interactions are not necessary for the accumulation of nephrin, therefore it may function to anchor nephrin to the cytoskeleton (Li et al., 2000, Shih et al., 1999). Nephrin and CD2AP develop together in the capillary loop stage of kidney development and CD2AP binds to the cytoplasmic tail of nephrin (Li et al., 2000). The interaction of podocin with CD2AP and nephrin independently of each other via the COOH-terminus of podocin has also been shown (Schwarz et al., 2001). CD2AP is co-localised with F-actin of the cortical actin network and cytochalasin D studies demonstrated that the two are physically associated (Welsch et al., 2001). It appears that both CD2AP and podocin play a role in clustering nephrin-containing rafts; providing a secure scaffolding for the slit diaphragm, and anchoring the complex to the actin cytoskeleton (Schwarz et al., 2001)[Dustin, 1998 #345 (figure 1.8).

1.6.3.5. α-Actinin-4

α-Actinin-4 is an F-actin cross linking protein, which has been localised to the podocyte foot processes within the glomerulus where it is highly expressed (Kaplan et al., 2000). ACTN4 is the gene that encodes it and mutations in this gene are the cause of an autosomal dominant form of focal and segmental glomerulosclerosis (Kaplan et al., 2000), originally mapped to a region of chromosome 19q13 (Mathis et al., 1998). The disease is defined by a mild onset of proteinuria in the teenage years with slow but progressive loss of renal function and the development of end stage renal failure in later life (Michaud et al., 2003). FSGS associated mutations in ACTN4 are associated with a greater binding affinity of α-Actinin-4 to actin

filaments (Kaplan et al., 2000). This leads to the development of sclerotic lesions as a result of the dysregulation of the actin cytoskeleton (Michaud et al., 2003). Using a mouse model with a high affinity mutated form of α-Actinin-4 expressed specifically in the podocytes Michaud et al found that by 10 weeks 3/8 mice developed proteinuria and had reduced renal function. These mice had reduced nephrin mRNA expression suggesting a cause and effect relationship between dysregulation of the actin cytoskeleton by α-Actinin-4 and the deterioration of the slit diaphragm complex (Michaud et al., 2003).

1.6.3.6. ZO-1

Zonula occludin-1 (ZO-1) is a membrane associated multi-adapter polypeptide whose expression was thought to be restricted to tight junctions (Huber et al., 2003a). There is growing evidence, however, that it is involved in the slit diaphragm complex. ZO-1 is present early in podocyte development at the time when they express tight junctions (Schnabel et al., 1990). In fact ZO-1 is involved in the conversion of the slit diaphragms back to tight junctions seen in podocyte effacement (Schnabel et al., 1990). The function of ZO-1 at podocyte differentiation has remained elusive until recently. ZO-1 contains three PSD95/Dlg/ZO-1 (PDZ) domains, which are protein-binding modules that recognise short peptide PDZ domain binding motifs within their protein targets (Huber et al., 2003a). In the slit diaphragm region ZO-1 is the only protein to express these PDZ domains, which provides the clue to its function (Huber et al., 2003a). It binds to an isoform of a recently discovered family of proteins related to nephrin named Neph1, which contains a putative PDZ domain binding motif (Huber et al., 2003a). Neph1 is a member of three structurally related proteins: Neph1, Neph2 and Neph3, all of which consist of five immunoglobulin-like repeats, a transmembrane domain and a cytoplasmic domain (Sellin et al., 2003). The cytoplasmic domain of Neph1 has been shown to bind the carboxy-terminus of podocin, which it is co-localised with in the podocyte foot

processes (Sellin et al., 2003). Neph1 and nephrin also interact via their cytoplasmic domains in a cis-interacting hetero-oligomeric complex (Barletta et al., 2003). Nephrin is shown to form heterodimers, as is Neph1, in promiscuous interactions (Gerke et al., 2003). Furthermore, Neph1 and nephrin have also been shown to interact via their extracellular domains in an *in vivo* mouse model, although murine Neph1 only has four immunoglobulin-like domains and lacks a transmembrane domain (Liu et al., 2003) (figure 1.9). A head to head assembly of human nephrin has been postulated using the first six Ig domains of opposing nephrin molecules (Gerke et al., 2003) (Figure 1.9). A combination of antibodies to Neph1 and nephrin injected into mice also resulted in a dramatic reduction in expression of ZO-1 (Liu et al., 2003). As with other components of the slit diaphragm Neph1 plays a pivotal role: Neph1-/- mice died between 3 and 8 weeks of age and electron microscopy revealed effacement of foot processes (Donoviel et al., 2001). The clinical phenotype is similar to that of mutated podocin but not as severe as that of mutated nephrin.

Hence, there are many proteins that link the transmembrane integrins to the actin cytoskeleton in podocytes. Disruption of any one of these complexes would have a similar effect on morphological changes in podocytes leading to proteinuria and foot process effacement. The slit diaphragm complex is the area most targeted in human glomerular disease. It plays a vital role in maintaining a physical barrier to filtrate, but there is growing evidence to suggest that this is also the site of signal transduction. Evidence to support this latter function was first presented in 1995 with the observation that there were increased levels of tyrosine phosphorylation of proteins at newly formed tight junctions of the foot processes and also at the induction of foot process effacement (Kurihara et al., 1995).

1.6.4. Signalling at the slit diaphragm complex

1.6.4.1. Nephrin

It has been shown that nephrin mRNA expression can be upregulated in HEK A293 cells, which constitutively express nephrin, by protein kinase C (PKC) (Wang et al., 2001). PKC is a large family of serine/threonine kinases involved in the phosphorylation of a variety of intracellular proteins (Wang et al., 2001). It was suggested that PKC phosphorylated the intracellular domain of nephrin either directly or indirectly. Nephrin also mediates signalling pathways including those of p38 protein kinase and c-Jun N-terminal protein kinase (JNK). Podocin was shown to synergistically augment this activation almost 40 fold more than nephrin alone (Huber et al., 2001). Recently, members of the Src family kinases have been implicated in nephrin signalling. Src family kinases are regulated by their SH3 and SH2 domains, which repress kinase activity by interacting with amino acids within the catalytic domain. The kinase is activated when a protein phosphatase dephosphorylates the COOH-terminal tyrosine (as reviewed in (Thomas and Brugge, 1997)). These were initially implicated in kidney damage and loss of renal filtration barrier in a study done by Yu et al. Homozygous knock out mice for Fyn, Lyn (Src family kinase members) and both together were developed. Fyn-/- and Lyn-/- mice excreted moderate levels of albumin, but Fyn-/- Lyn-/- mice suffered from chronic kidney damage and a high death rate (Yu et al., 2001a). It was shown that Fyn can bind directly to nephrin both *in vitro* and *in vivo* via its SH3 domain (Verma et al., 2003). This induced the phosphorylation of nephrin. Deletion of Fyn in a knockout mouse model resulted in attenuated nephrin phosphorylation and coarsening of the foot processes (Verma et al., 2003). Nephrin was also shown to interact with Yes, another member of the Src family kinases but the consequences of this are not yet clear (Verma et al., 2003). The nephrin signalling pathway was further clarified by work done by Huber et al.

Co-immunoprecipitation studies showed that the carboxy-terminal cytoplasmic tail of both nephrin and CD2AP interact with the p85 regulatory subunit of PI3-kinase (Huber et al., 2003c). This interaction was inhibited by incubation with genistein; a broad-spectrum tyrosine kinase inhibitor with some preference for members of the Src family kinases. PI3-kinase activation by nephrin and CD2AP was associated with a strong activation of AKT and phosphorylation of the anti-apoptotic protein Bad, correlated with reduced apoptosis (Huber et al., 2003c). The phosphorylation of nephrin induced by Src can activate the PI3-kinase/AKT pathway resulting in inhibition of apoptosis, shown in three independent cell models including differentiated podocytes; HEK 293 cells, canine kidney epithelial cells and differentiated mouse podocytes (Huber et al., 2003c). Clustering of nephrin on the surface of transfected HEK293 cells (that express the same Src family kinases as podocytes) by anti-nephrin antibodies induced auto-phosphorylation of nephrin (Lahdenpera et al., 2003). Inhibition by PP2, a Src inhibitor, showed that nephrin phosphorylation was Src family kinase dependent and more than one was involved: Fyn, Src, Yes and possibly Lyn. Tyrosine phosphorylation of nephrin is thought to create binding sites for other signalling proteins stimulating a signal cascade (Lahdenpera et al., 2003). Clustering of nephrin on the cell surface mimics clustering at the slit diaphragm and this is shown to be a very dynamic process, suggesting that podocytes have an ability to rapidly rearrange the actin cytoskeleton in the foot process (Lahdenpera et al., 2003). This is potentially possible if the tyrosine phosphorylation induced by Src is multiple and processive (i.e. the enzyme remains bound to the peptide substrate during multiple phosphorylation events) (Scott and Miller, 2000). This theory was tested by Scott et al using a synthetic peptide system and found that Src remained bound to its substrate until it completed all its phosphorylations, so only one Src/substrate collision was necessary (Scott and Miller, 2000). The affinity of Src to its substrate increased with multiple interactions via SH2 and SH3 and the catalytic domains. This ensures that there is rapid

multiple phosphorylation, which is needed *in vivo* for the slit diaphragm to be so dynamic. Although the signalling dynamics of nephrin are still under investigation it is clear that the intracellular domain of nephrin can be phosphorylated (i.e. by PKC and Src family members), which induces various signalling pathways such as PI3-Kinase and p38/c-Jun.

1.6.4.2 Neph1

Neph1 contains a SH2 binding site and is also thought to be a signalling protein. Incubation with v-Src (a viral form of Src) reduced the interaction between Neph1 and podocin at the carboxy-terminal domain, indicating that tyrosine phosphorylation of the Neph1 podocin binding motif regulates the interaction between the two proteins (Sellin et al., 2003). This could potentially disrupt the slit diaphragm complex. Itk, a member of the Tec kinase family, resulted in a four-fold increase in Neph1 mediated AP-1 activation (a transcription factor complex that modulates a variety of signalling pathways such as survival and apoptosis (Eferl and Wagner, 2003)), demonstrating downstream signalling of Neph1. Tec kinases are present in the lipid rafts of the podocyte foot processes (Sellin et al., 2003) and are the second largest family of cytoplasmic protein tyrosine kinases after Src (Smith et al., 2001). They contain a pleckstrin homology (PH) domain and Src homology 3 (SH3), SH2 and SH1 domains and lack a C-terminal tyrosine, so have an auto-inhibitory function in their phosphorylated state (Smith et al., 2001). Activation of PI3-kinase generates PIP_3, which recognises proteins with PH domains such as AKT (figure 1.5). It can also bind to and activate Tec kinases and these have been linked to the transcriptional control of complex survival and differentiation events (as reviewed in (Smith et al., 2001)).

1.6.4.3. ZO-1

ZO-1 was the first molecule shown to be tyrosine phosphorylated at the slit diaphragm region of the rat kidney (Kurihara et al., 1995). In fact, tyrosine phosphorylated proteins were not

detected in normal rat podocytes, but two tyrosine phosphorylated protein bands were detected in Western blots for protamine sulphate treated rat glomeruli. Protamine sulphate neutralises the negative charges between podocytes and is thought to induce tight (occluding) junction formation, which eventually leads to denuded areas of basement membrane (Caulfield et al., 1976). Two bands were detected, one at 225kDa, which was found to be ZO-1, and one at 180kDa, which was co-immunoprecipitated with ZO-1 (Kurihara et al., 1995) (although this was not shown in the blot probed with anti-ZO-1). This protein was not identified, however it is the same MW as nephrin. The reason that no phospho-tyrosine proteins were detected in normal rat podocytes may have been because the expression levels of the proteins concerned were too low to be picked up by the antibody or enhanced chemiluminescence kit used. The tyrosine phosphorylation occurred only 15 minutes after the initiating the perfusion of protamine sulphate, which demonstrates the speed at which the podocyte can rearrange its cytoskeleton (Kurihara et al., 1995). ZO-1 can also induce the tyrosine (and serine) phosphorylation of Neph1 and accelerate Neph1-mediated AP-1 activity (Huber et al., 2003a). The function of this may be to induce the clustering of Neph1 into homo/heterodimers. Tyrosine phosphorylation at the slit diaphragm has been associated with podocyte dysfunction (i.e. transition of slit diaphragms to tight junctions) and also with podocyte function (i.e. clustering of the slit diaphragm proteins and survival pathways). Therefore, it is wise to study each tyrosine phosphorylation pathway separately, not associate it with one consequence.

1.6.5. Summary of survival mechanisms in podocytes

There appear to be three potential mechanisms by which podocytes can maintain their survival:

1. Upregulation of cyclic dependent kinase inhibitors such as p27 and p57 at the point of differentiation onwards, which may upregulate the PI3-Kinase/AKT survival pathway.

2. Maintenance of the actin cytoskeleton within the foot processes through cell-cell contact and adherence to the glomerular basement membrane.
3. Activation of signalling complexes at the slit diaphragm or glomerular basement membrane.

1.7 Potential of VEGF-nephrin signalling

VEGF has been shown to increase phosphorylation of tight junctions in bovine retinal epithelial cell (BREC) cultures and in an *in vivo* model in the rat eye vitreous cavity (Antonetti et al., 1999). Of the seven tight junction proteins both occludin and ZO-1 were phosphorylated by VEGF; occludin by serine/threonine phosphorylation and ZO-1 by tyrosine phosphorylation. These changes were rapid (15 minutes post injection of VEGF into the vitreous cavity) (Antonetti et al., 1999) and in a time frame consistent with a VEGF induced increase in the microvascular permeability barrier *in vivo* (Pocock et al., 2000). It is known that: 1) VEGF is expressed in differentiated podocytes as is its co-receptor Np-1; 2) the slit diaphragm contains ZO-1; a protein associated with tight junctions and indeed slit diaphragms are thought to transform from them (Reiser et al., 2000a); 3) VEGF can induce the phosphorylation of proteins at tight junctions; 4) the slit diaphragm contains proteins that can be phosphorylated; and 5) podocytes are terminally differentiated and have prolonged survival. Therefore, it is possible that the role of VEGF in the podocyte may, at least in part, be to act in an autocrine manner in podocytes to positively maintain the slit diaphragm, and cell survival.

In endothelial cells VEGF-R2 is highly enriched in caveolae, where VEGF signalling is initiated (Labrecque et al., 2003). Caveolae are defined as specialised membrane microdomains that appear as flask shaped invaginations (Feng et al., 1999). In fact they could

be described as vesicular lipid rafts. They are found in many cell types, particularly in terminally differentiated cells (Labrecque et al., 2003). Caveolae are expressed in the podocyte foot processes (Sorensson et al., 2002): Caveolin-1, the protein that defines caveolae, was co-immunoprecipitated along with CD2AP and nephrin in mouse glomerular lysates suggesting that caveolae are localised to the slit diaphragm. Surprisingly, caveolin-1 deficient mice showed normal podocyte foot process ultrastructure (Sorensson et al., 2002). Interestingly, both caveolae and CD2AP have been implicated in internalisation of ligand/receptor complexes by endocytosis. VEGF stimulation of the caveolin/VEGF-R2 complex, which contains many types of signalling proteins, caused the translocation of the caveolin complex to the nucleus (Feng et al., 1999). Similarly epidermal growth factor (EGF) stimulation of EGF receptor induced cortactin recruitment (an actin linking protein) to CD2AP and led to epidermal growth factor receptor endocytosis and trafficking (Lynch et al., 2003). This suggests that the dynamic slit diaphragm is also capable of endocytosis of growth factors, although none have yet been implicated in signalling at the slit diaphragm. Localisation of VEGF-R2 to caveolae in endothelial cells also implies the localisation of Np-1 because it acts as a co-receptor for VEGF-R2, however there is no evidence yet to show this. It is known that; 1) caveolae are localised to the slit diaphragm; 2) nephrin is localised to the slit diaphragm; 3) caveolae express VEGF-R2 in endothelial cells; 4) nephrin and VEGF are implicated in cell survival; 5) VEGF induces the phosphorylation of Src family kinases in endothelial cells and 6) Src family kinases induce the phosphorylation of nephrin. Therefore, it is possible that VEGF can signal at the slit diaphragm to phosphorylate nephrin and promote survival in differentiated podocytes. To investigate these effects, human cultured podocytes were used as experimental models.

1.8. Experimental Podocyte models

There are many animal models of renal disease, however although these models can provide valuable insight into podocyte pathology they bear limited resemblance to human kidney diseases. Animal renal disease tends to be acute, overwhelming and fulminant whereas most human renal diseases are chronic, modest and intermittent. Therefore animal models have limited uses, which is why cell culture of human podocytes is becoming more attractive.

Using primary culture podocytes (PCPs) can present their own difficulties. Major criticisms of the isolation technique used are that the resulting cells (podocytes) isolated from the glomeruli almost never form pure populations and may also change phenotype in culture (Yaoita et al., 2001). To overcome difficulties related to primary culture of podocytes different groups have tried to develop conditionally immortalised podocyte cell lines. This was first successfully described in 1996 by Mundel et al using podocytes originally isolated from mouse glomeruli. A transgenic mouse cell line, H-2K^{b}-tsA58, was developed that carries a thermolabile mutant of the SV40 large T antigen-tsA58 under the control of a γ-interferon inducible promoter, H-2K^{b} (Mundel et al., 1997b). This allowed the cells to be proliferative when incubated at 33°C with γ-interferon and growth arrested and differentiated when incubated at 37°C without γ-interferon, to inactivate the immortalising SV40 Tag. This development changed the dynamics of podocyte investigations. Despite this advancement a human model of cell culture was still needed because rat and mouse podocytes, although very similar to human podocytes, do express some different proteins (e.g. megalin is expressed in rats but not human podocytes), therefore podocyte functions may differ between species. Saleem et al developed the first temperature sensitive SV40 human conditionally transformed podocyte cell line in 2002. Similarly to the mouse podocyte cell line the human podocytes

were infected with an SV40 large T-antigen gene containing tsA58/U19 mutations. They are therefore also temperature sensitive, and when incubated at the permissive temperature of 33°C are proliferative and de-differentiated, but when incubated at the non-permissive temperature of 37°C for a fortnight they became non-proliferative and differentiated (Saleem et al., 2002). These cells have been fully characterised and at differentiation express the podocyte specific markers of maturity nephrin, podocin and synaptopodin amongst others. Of note, these cells were originally cloned from podocytes isolated in the same way as primary cultured podocytes. Although primary culture podocytes (PCPs) were initially used, their use in this investigation was limited to assays where the specific quality of these cells was needed, such as the ability to proliferate. Otherwise, once it was established that the two types of cultured podocytes responded in a similar manner, human conditionally immortalised podocyte cell lines were used as models to investigate the effects of VEGF on podocyte biology.

1.9 Hypotheses and Aims

This study will test the hypotheses that; 1) VEGF can act in an autocrine manner in podocytes; 2) VEGF promotes survival in differentiated podocytes; 3) VEGF can signal at the slit diaphragm; 4) VEGF directly or indirectly induces the phosphorylation of nephrin; 5) VEGF and nephrin interact synergistically to protect differentiated podocytes.

Using various human podocyte cell lines, both primary and conditionally immortalised, I will investigate:

1. If VEGF can stimulate a change in intracellular calcium in podocytes, a common signal transduction pathway of VEGF;
2. The possible effects of VEGF on podocytes via established mechanisms already known in endothelial cells such as proliferation, cytotoxicity and apoptosis;
3. The ability of nephrin to promote podocyte survival using nephrin deficient and nephrin mutated cell lines;
4. The ability of VEGF to induce phosphorylation of nephrin and the consequences on podocyte cell survival.

Chapter 2

Methods

2.1 Chemicals

All chemicals are from Sigma-Aldrich (Ayreshire, UK) unless otherwise stated.

2.2 Solutions

10 x Phosphate buffered saline solution (PBS): 1.37M NaCl, 27mM KCl, 100mM Na_2HPO_4 and 30mM KH_2PO_4, pH 7.4 (autoclaved).

1 x PBS: 1:10 dilution 10 X PBS in de-ionised water

All others are as described in the text.

2.3 Cell culture

All tissue culture was carried out in a sterile laminar flow hood. All human tissue was taken with ethical committee approval (see appendix).

2.3.1 Primary culture podocytes (PCPs) (as described by (Mundel et al., 1997a))

A section of renal cortex was taken from the unaffected pole of a human nephrectomy specimen with renal carcinoma. The tissue was macroscopically normal and such tissue has been shown to be microscopically normal on previous preliminary studies (Whittle et al., 1999). The tissue was transported in sterile 1xPBS on ice for a maximum of 30 minutes. Instruments and solutions used were sterilised either by autoclaving or using 70% ethanol (Fisher Scientific, Leicestershire, UK). Scissors and forceps were used to remove the kidney capsule and the cortex was chopped finely. Three brass sieves with mesh sizes of 425µm, 180µm and 125µm (Endecotts, London, UK) were stacked on top of each other. The cortex was placed in the top sieve and gently but firmly pressed through using a sterile syringe plunger. Sterile room temperature 1xPBS was used intermittently to wash the tissue through. The 180µm mesh sieve retained some glomeruli and tubules whilst the 125µm mesh sieve retained glomeruli and debris. The glomeruli from the 125µm mesh sieve were washed three

times with complete RPMI (Roswell Park Memorial Institute) media (containing inorganic salts; 1g/L $Ca(NO_3)_2 \cdot 4H_2O$, 0.049 g/L $MgSO_4$, 0.4g/L $NaHCO_3$, 6g/L NaCl and 0.8g/L Na_2HPO_4 with additional 0.1% insulin transferrin selenite, and 10% fetal bovine serum (FBS)) in a 50ml Falcon tube (Fisher Scientific, leicestershire, UK): glomeruli were centrifuged at 1000rpm, the supernatant was aspirated off, resuspended in complete RPMI and repeated twice more. The glomeruli were resuspended again in complete RPMI and transferred to a vented $75cm^3$ tissue culture flask (Greiner, Fickenhausen, Germany) and placed in an incubator at 37°C with 5% CO_2 (Sanyo, Bensenville, USA), for 14 days allowing the primary cultured podocytes, which are proliferative to grow out from the glomeruli. The glomeruli were then washed away using sterile 1xPBS and the media replaced three times a week. Cells were passaged when they achieved 100% confluency and were only used for a maximum of four passages as the cells become senescent.

2.3.2 Human conditionally immortalised podocytes (hCIPs)

Two hCIP cell lines were developed and characterised by Dr M. Saleem, at the Academic Renal Unit, Southmead Hospital, Bristol. Nephrectomy specimens were taken from a three-year old child with hydronephrosis (hCIPa) (Saleem et al., 2002) and a four year old child with a Wilms Tumor (Saleem et al, unpublished). Glomeruli were isolated and primary culture podocytes grown out as above. The cells were passaged after 14 days once they had reached confluency (Saleem et al., 2002). Saleem et al then transfected the cells with a retroviral construct consisting of an SV40 large T antigen gene containing containing the temperature sensitive A58 (tsA58) mutation. The use of hCIPs, kept at 33°C, ensures a uniform population of de-differentiated podocytes. After infection with the retrovirus containing the SV40 T antigen, the virions translocate to the nucleus where they are uncovered and the viral chromatin is released (Pipas and Levine, 2001). The cells enter S phase a few hours after

infection and the large T antigen initiates viral DNA replication by binding to its origin and recruiting cell replication apparatus. The large T antigen contributes to cell transformation in a number of ways. For example it binds to and stabilises (and therefore inactivates) p53 by blocking the ability of p53 to bind to its DNA consensus sequence, thereby blocking its ability to act as a transcription factor (Pipas and Levine, 2001). p53 transactivates genes that lead to growth arrest, therefore inactivation of p53 allows proliferation. The replication of the retrovirus, containing the SV40 T antigen, is impaired at high temperature by the tsA58 mutant (Sompayrac and Danna, 1983). This ensures that, at the tsA58 permissive temperature of 33°C the hCIPs remain proliferative and de-differentiated, but at the tsA58 non-permissive temperature of 37°C, p53 is activated and hCIPs become differentiated. Infection, selection and continuous culture were carried out in an incubator kept at 33°C. Cells were subcloned by seeding at increasing densities in the presense of irradiated NIH 3T3 mouse fibroblast cells, provided as nondividing feeder cells. Cells were then selected using plastic cloning rings (Saleem et al., 2002). Differentiation was induced by thermoswitching the cells from the permissive temperature of 33°C to the non-permissive temperature of 37°C, for 14 days to inactivate the SV40 T antigen. These cells stained positively for WT-1 at both de-differentiation and differentiation and stained for synaptopodin, P-cadherin, nephrin and podocin at differentiation (Saleem et al., 2002). Cells were used between passages 10 and 20.

2.3.3 Nephrin mutated conditionally immortalised podocytes (NMhCIPs)

These cells were developed and characterised as above by Saleem et al (unpublished) except that the cells were isolated from a nephrectomy specimen taken from a patient with a homozygous R460Q mutation at nucleotide 1379 in exon 11 of the NPHS1 gene that encodes nephrin (Figure 2.1). This mutation leads to a missense reading in the part of the nephrin protein that corresponds to immunoglobulin (Ig) 5 of the extracellular domain, where arginine

is replaced by glutamine (Koziell et al., 2002). This protein is expressed at the slit diaphragm but still causes a classically severe congenital nephrotic syndrome (Koziell et al., 2002).

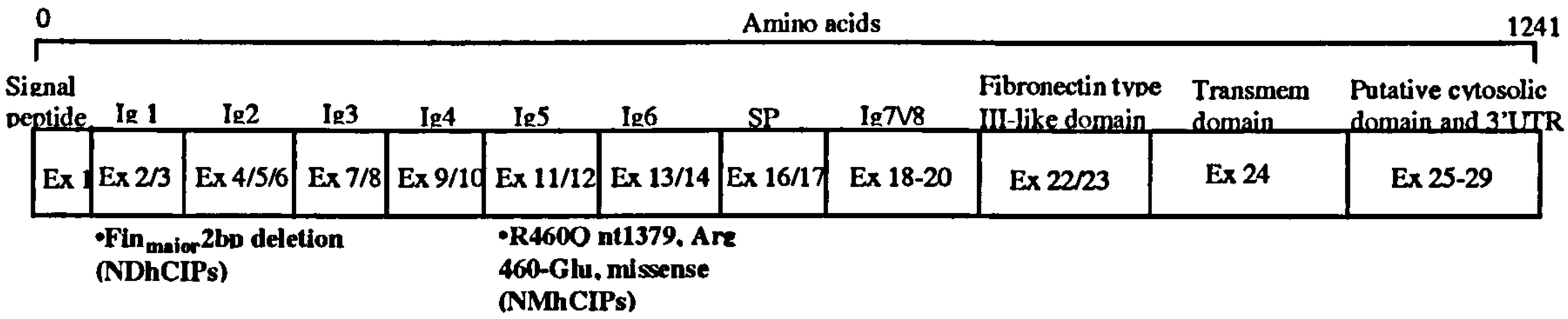

Figure 2.1. A schematic of the putative NPHS1 gene structure.

The location of the mutations that define the NMhCIP and the NDhCIP cell lines are indicated in the nephrin gene, and the corresponding putative amino acid sequences of the protein, encoded by each exon (Ex) are also indicated.

2.3.4 Nephrin deficient human conditionally immortalised podocytes (NDhCIPs)

These cells were developed and characterised by Saleem et al (unpublished) as above except that the cells were isolated from a nephrectomy specimen taken from a patient with a Fin_{major} mutation in the NHPS1 gene. This is a two base pair deletion in exon 2 at nucleotide 121 (figure 2.1), which results in a truncated protein of 90 amino acids and a complete absence of protein expression (Patrakka et al., 2000). This also leads to a severe congenital nephrotic syndrome.

2.3.5 Passaging cells (adapted from (Saleem et al., 2002))

Both primary culture podocytes and conditionally immortal podocyte cell lines were passaged using the same protocol as follows. At 100% confluency serum was washed from the cells using sterile 1xPBS then incubated for 5 minutes at 37°C with 3ml 1x trypsin. 7ml of complete RPMI media was added to stop the reaction and pipetted over the flask surface to wash off the cells. Cells were then centrifuged at approximately 3000rpm for 5 minutes, the supernatant aspirated off and the cell pellet resuspended in complete RPMI media. Cells were divided 1:4 (primary culture podocytes) into new $75cm^3$ tissue culture flasks or 1:5 (podocyte

cell lines) to freeze down a cryovial of cells (see below). 10ml media was also added to the flasks of podocyte cell lines that were split even though there were few cells remaining, this was kept as the stock flask and achieved 100% confluency weekly. The cell lines were kept at 33°C for 2-3 days until they achieved 100% confluency and then transferred to 37°C to differentiate. The primary culture cells were kept at 37°C constantly and were slow to proliferate. They achieved confluency once every one or two weeks depending on the age of kidney they were isolated from.

2.3.6 Freezing down and bringing up cells

Cell lines were frozen down at every passage up to passage 18 to keep stocks replenished. Freezing media consisted of 20% DMSO (a cryoagent) and 80% FBS. 500µl of this was added to 500µl of podocyte cell suspension (of trypsinised cells) in complete RPMI (see passaging above). This was transferred to cryovials (Simport plastics, Quebec, Canada), which were frozen down in the -80°C freezer. To thaw, the cryovials were taken out and run under warm water to avoid formation of crystals in the cells. The cells were quickly transferred to a 75cm^3 flask containing 9.5mls of complete RPMI to prevent cytotoxicity due to the high DMSO concentration. The cells were mixed into the media and were then grown in the same way as passaged cells.

2.4 Immunohistochemistry

2.4.1 Tissue processing and fixation

Whole rat kidneys were dissected from Male Wistar rats (200-300g), anaesthetised by inhalation of 5% halothane and maintained on 3% halothane (Merial, animal health ltd, Essex, UK). Kidney tissue was fixed in 10% buffered formalin at room temperature overnight. Tissue was then processed-each step included gentle agitation of samples in each solution for

four hours. Tissue was first dehydrated in 70%, 90% and 100% Methanol and two steps of 100% Ethanol. The alcohol was then displaced with xylene (x3) and then embedded in melted paraffin wax at ~40°C in three separate steps, the last one in a vacuum. Wax blocks were then placed into cassettes and kept in the fridge ready for cutting. Blocks were cut on the microtome (Leica, Milton Keynes, UK) in 7μm sections and flattened using warm water and 100% ethanol onto gelatin/poly-L-lysine coated glass slides to ensure tissue adherence (see below). Tissue and slides were then left to dry in a slide rack and then baked overnight at 37°C to further ensure that the tissue had firmly adhered.

2.4.2 Slide preparation

2g gelatin (BDH, Pool, UK) was dissolved in 400ml (1:200 dilution) heated distilled water and 0.2g of chromium potassium sulphate then dissolved into it. Racks containing clean slides were dipped into this solution for five minutes and then dried overnight in an incubator at 37°C. 10mM Tris-HCl was made up in water and adjusted to pH 7.6. 25mg of Poly-L-lysine was dissolved in a small amount of 10mM Tris-HCl and then added to the rest of the solution. The gelatin-coated slides were then placed in the solution as before and again left to dry overnight at 37°C.

2.4.3 Cell fixation (adapted from (Harlow and Lane, 1998))

Primary culture podocytes were grown to confluency on 10% collagen (Autogen Bioclear, Wiltshire, UK)/PBS coated 22mm diameter glass coverslips (BDH, Pool, UK) in a six well plate (Corning, Birmingham, UK). They were then washed twice with 1xPBS and fixed in 1ml 10% formaldehyde (Fisher Scientific, Leicestershire, UK) for 10 minutes. The formaldehyde was washed off twice with 1xPBS and the cells then permeabilised in 0.2% Triton X/PBS for 15 minutes. This was washed off again four times with 1xPBS.

2.4.4 Immunohistochemistry (adapted from (Harlow and Lane, 1998))

Microscope slides with tissue sections on them were dewaxed in histoclear for 5 minutes and rehydrated in graded ethanol: 100, 95 and 70% (Fisher Scientific, Leicestershire, UK) for 2 minutes each. They were then washed twice in distilled water for 5 minutes each and washed once in 1xPBS for another 5 minutes. Half of the slides were microwaved in 100mM Tris-HCl/2mM ethylenediaminetetraacetic acid (EDTA) buffer for 2x4 minutes at full power to promote antigen retrieval, then left to cool for 20 minutes. The non-microwaved slides were left in 1xPBS and used to compare efficiency of immuno-staining. All slides were treated with 3% hydrogen peroxide (BDH, Pool, UK) for 5 minutes to block endogenous peroxidases and then washed twice for 5 minutes with 1xPBS. Slides were then incubated with a 1.5% normal serum (Vecta, California, USA)/PBS blocking solution from the animal in which the secondary antibody was raised for 30 minutes in a humid chamber to block non-specific binding sites. Slides were split into microwaved and non-microwaved groups and treatment in one group was paired with treatment in the other. They were then incubated with 40µl of an optimised dilution of primary antibody (when using an antibody for the first time it was used in various concentrations, as was the secondary antibody). Each primary antibody treatment had a matched IgG control of the same concentration (an isotype control) diluted in the blocking solution described above. The tissue was protected from drying out by covering with a glass coverslip and was incubated in a humid chamber at 4°C overnight. The following day the coverslips were removed in 0.1% PBS/Tween and washed twice in 1xPBS. Slides were treated for a second time with 1.5% normal serum/PBS blocking solution for 30 minutes in a humid chamber. All slides, including the controls, were treated with 5µg/ml biotinylated secondary antibody (Vecta, California, USA)/blocking solution to the species in which the primary was raised for 30 minutes in a humid chamber. They were then washed twice in 0.1% PBS/Tween (a more stringent wash solution than 1xPBS) and then incubated in a pre-prepared

HRP conjugated avidin-biotin complex (ABC) solution (Vecta, California, USA) for 30 minutes in a humid chamber. This bound to the biotinylated secondary antibodies. The slides were washed twice for 5 minutes in 0.1% PBS/Tween and were then incubated with diaminobezidine (Vecta, California, USA), which provided the substrate for the HRP conjugated to the ABC, until brown colour was visualised. The reaction was stopped by washing twice in distilled water for 5 minutes and counter-stained with haematoxylin (a nuclear dye) for 5 minutes before leaving in gently running tap water (to aid the "bluing") for 5 minutes. The tissue was then dehydrated in 70, 90 and 100% ethanol for 2 minutes each, cleared in xylene for 10 minutes and finally mounted with DPX, glass coverslips and nail varnish. Immunostaining was visualised using a light microscope and images were captured using a digital camera (Leica, Milton Keynes, UK), downloaded and saved as an AdobePhotoshop file.

2.4.5 Immunocytochemistry (adapted from (Harlow and Lane, 1998))

Fixed cells on coverslips were treated in a similar manner as tissue on slides except that they were not rehydrated as they were not dehydrated or wax embedded. They were treated for endogenous peroxidase and from that stage forward, the methodology was the same (although they were covered with a slide overnight) until the last stages where they were not dehydrated and cleared.

2.5 PCR

2.5.1 Ribonucleic acid (RNA) extraction (as described by Gibco BRL Life Technologies TRIzol Data sheet)

Cells were grown to confluency in a 75cm^3 tissue culture flask. Media was aspirated off and the cells were lysed with 0.3ml TRIzol (Invitrogen Life Technologies, California, USA)

/10cm^2 surface area, which was washed over the cells then left at room temperature for 5 minutes. This lysate was transferred to a 15ml Falcon tube, 0.2ml chloroform (BDH, Pool, UK) /0.75mlTrizol added and the tube shaken vigorously. This was left at room temperature for 2-15 minutes and then centrifuged at 12,000g (Annita IIR, ISTCP, New Jersey, USA) for 15minutes at 4°C. This separated the solution into an aqueous phase, which contained the RNA and an organic phase. The top aqueous phase was transferred to a clean tube and 0.5ml isopropanol/0.75ml TRIzol was added and left at room temperature for 10 minutes to precipitate the RNA. This was centrifuged at 12,000g for 10 minutes at 4°C, the supernatant removed and washed once with 1ml/0.75ml TRIzol 75% ethanol/ Dep. H_2O (RNAse treated). The solution was vortexed (Jencons, Leighton Buzzard, UK) and then centrifuged at 7,500g for 5 minutes at 4°C. The supernatant was removed and the RNA pellet air dried for 5 minutes (but not completely). Subsequently it was dissolved by adding 50µl DiEthylPyroCarbonate water (Dep. H_2O) (RNAse free treated water) and incubated at 60°C for 10 minutes. RNA was only briefly kept on ice otherwise kept in the -80°C freezer to prevent the breakdown by RNAses (New Brunswick Scientific, Hertforshire, UK).

2.5.2 Quantifying RNA

RNA was diluted in 1ml Dep. H_2O at various dilutions, starting at 1:200 and mixed well before being transferred to a quartz cuvette (Fisher Scientific, Leicestershire, UK). 1ml Dep. H_2O was used to calibrate the spectrophotometer (Shimadzu, Duisburg, Germany) and RNA was quantified at 260nm, protein was also quantified simultaneously at 280nm, so that the ratio of the two measurements could be used. If the ratio was over 1.5 then there was little protein contamination so the quality was deemed adequate. It was assumed that one optical density (OD) unit read by the spectrophotometer was equivalent to 40µg/ml RNA (Sambrook

and Russell, 2001a). Therefore to find the volume of starting solution needed to yield 1µg of RNA the following equations were used:

$$((OD_{260} \times 40\mu g/ml)\ D)/1000 = X\mu g/\mu l\ RNA$$

$$1\mu l\ /(X\mu g/\mu l)\ RNA = \text{volume containing } 1\mu g\ RNA$$

Where D is the dilution factor used and X is the unknown quantity. Of note, this can only provide overall RNA concentration, not just mRNA concentration.

2.5.3 Reverse transcription - polymerase chain reaction (RT-PCR)(adapted from (Sambrook and Russell, 2001a))

1µg of RNA from each sample was added to 1µl 50µM Oligo (dT) (Promega, Wisconsin, USA) (a universal primer, which anneals to the 3' poly A tail of mammalian mRNA) and Dep. H_2O to bring the volume to 10µl. This was incubated at 65°C for 5 minutes to denature the RNA, followed by rapid chilling on ice. To this, 10µl of solution was added containing: 2µl Dep. H_2O; 4µl 5x first strand synthesis buffer (Roche, Mannheim, Germany) (a buffer for reverse transcriptase); 1µl 0.1M dithiothreotol (DTT) (Roche, Wisconsin, USA) (a reducing agent that prevents secondary folding of RNA); 1µl 25mM dNTPs (nucleotides for the reaction); 1µl RNA guard (Roche, Wisconsin, USA) (an RNAse inhibitor) and 1µl 50u/µl expand reverse transcriptase (Roche, Wisconsin, USA) (RNA dependent DNA polymerase to catalyse the synthesis of complementary DNA). This reaction was incubated for 60 minutes at 42°C. The first strand synthesis of cDNA from mRNA was primed by the Oligo (dT), which creates a DNA:RNA hybrid.

2.5.4 PCR

Complementary DNA (or cDNA) was amplified at this stage. 1µl cDNA (made above) was added to a solution containing: 13.5µl Dep. H_2O; 2µl 10x amplification buffer (Abgene, Surry, UK); 1µl 25mM $MgCl_2$ (Abgene, Surry, UK) (to control the pH of the solution); 0.3µl 25mM dNTPs; 1µl sense primer, 1µl antisense primer (Invitrogen Life Technologies, California, USA) and 0.2µl Taq (Abgene, Surry, UK) (a thermostable DNA polymerase enzyme to amplify the cDNA). Each reaction had a positive cDNA control (i.e. tissue cDNA or a plasmid containing the cDNA in question), a positive primer control (i.e. GAPDH) and a negative primer control (i.e. Dep. H_2O). These reactions were run in a PCR thermal cycler (Hybaid, Thermo-Electron, Basingstoke, UK) on a standard cycle: 35 cycles of 94°C for 3 minutes; 55°C for 30 seconds; 72°C for 1 minute; 94°C for 30 seconds then one cycle of 72°C for 3 minutes, then held at 4°C . This cycle of temperature change induced denaturation of the double stranded cDNA template (high temperatures), primer annealing to the single stranded DNA and extension of the desired portion of cDNA (dictated by the sense and antisense primers used) by the DNA polymerase, which was again denatured in the next cycle.

2.5.5 Primer design (Sambrook and Russell, 2001a)

Primer sequences were either taken from the literature or designed. Primers were designed with the following criteria: a G-C content of 50-55%, G-C base pairs have three bonds whereas A-T base pairs only have two so the G-C content ensures that the sequence is not bound too tightly or too loosely during the amplification cycles. Triplicates and quadruples were avoided for the same reason; the primer sequence was required to end in GC, CG, CC or GG to secure the binding. The amplicon length of 250-500 base pairs (bp) was required and the length of the primer was 18-25 nucleotides. Members of primer pairs did not differ in

number by more then 3 bp. The melting temperature of the primers was above 72°C, for the Taq to work optimally and was calculated using the following equation:

$$2(A+T)+4(G+C)$$

The primers were designed in such a way that the 3' sequence of one primer could not bind to a site on the other primer. All primer sequences were checked for specificty using BLAST in PubMed.

2.5.6 Agarose gel (Sambrook and Russell, 2001b)

2% agarose (Roche) was added to 40mM Tris-acetate/1mM EDTA (BDH, Pool, UK) (TAE) buffer. This was heated in a conical flask in the microwave for 20 seconds at a time until the powder dissolved. It was left to cool, then 5% ethidium bromide (Invitrogen Life Technologies, California, USA) was added to decrease the negative charge of the double stranded DNA, increase its stiffness and length and allow visualisation under UV light. The solution was poured into a cast with a comb (BioRad, Hertforshire, UK) and left to set. 5µl of Dep. H_2O was added to 5µl of PCR reaction with 2µl of 6x loading buffer (0.25% bromophenol blue, 0.25% xylene cyanol FF and 30% glycerol/dep. water). This increased the density of the samples, allowed visualisation of the samples and migrated through the gel at a predictable rate. Once the combs were removed and the cast put in the gel tank with a good covering of 1x TAE buffer a 100 base pair ladder was loaded into the gel so that the size of the cDNA bands could be assessed accurately. The PCR reaction samples with loading buffer were loaded into the gel. The gel then had 70 volts applied through it, which caused the proportional migration of the linear DNA. The size of DNA was inversely proportional to the rate of migration therefore the length of time the gel ran for depended on the size of DNA band expected. A 2% agarose gel was chosen because the molecular size of the cDNA used was relatively small (150-500 base pairs).

2.5.7 Visualisation

Bands were visualised on an UV transilluminator (Gibco Life Technologies, Maryland, USA) with 100% UV light applied. A Polaroid picture was taken using a Polaroid gel cam and hood (Fisher scientific, Leicestershire, UK) using black and white film.

2.6 Intracellular calcium ($[Ca^{2+}]_i$) measurements

2.6.1 Calcium Rig set up (adapted from methods used in (Pocock et al., 2000) and (Glass, 2003))

A calcium rig has been set up in this laboratory to measure $[Ca^{2+}]_i$ changes in *in vitro* and in *in vivo* models. A schematic of the *in vitro* set-up is shown in figure 2.2. A glass coverslip with a monolayer of cells sits in a coverslip holder on an epifluorescence microscope (Leica, Milton Keynes, UK). The cells, loaded with Fura 2AM (see below) are excited by three different wavelengths of light emitted from a xenon light source via a filter wheel containing 340, 360 and 380nm filters that spins at 50 Hz, controlled by the filter wheel controller. Each filter position is synchronised to channels 1-4 respectively on the spectrophotometer (Cairn, Kent, UK). The filtered light passes through a 400nm dichroic mirror, which reflects light below 400nm and allows greater wavelengths to pass through. The mirror is set at 45° to the light path, so it reflects light up to the specimen. This light excites the Fura 2 in the cells. When bound to calcium this emits a wavelength of 510±35nm. The 510nm emitted light passes through the 400nm dichroic mirror and the light can then be guided down one of two pathways by an adjustable prism. In one position it allows the light to be viewed through the eyepiece, to visualise the cells, in the other position the light is directed to the photomultiplier tube (PMT). Readings can only be taken when the light is guided to the PMT.

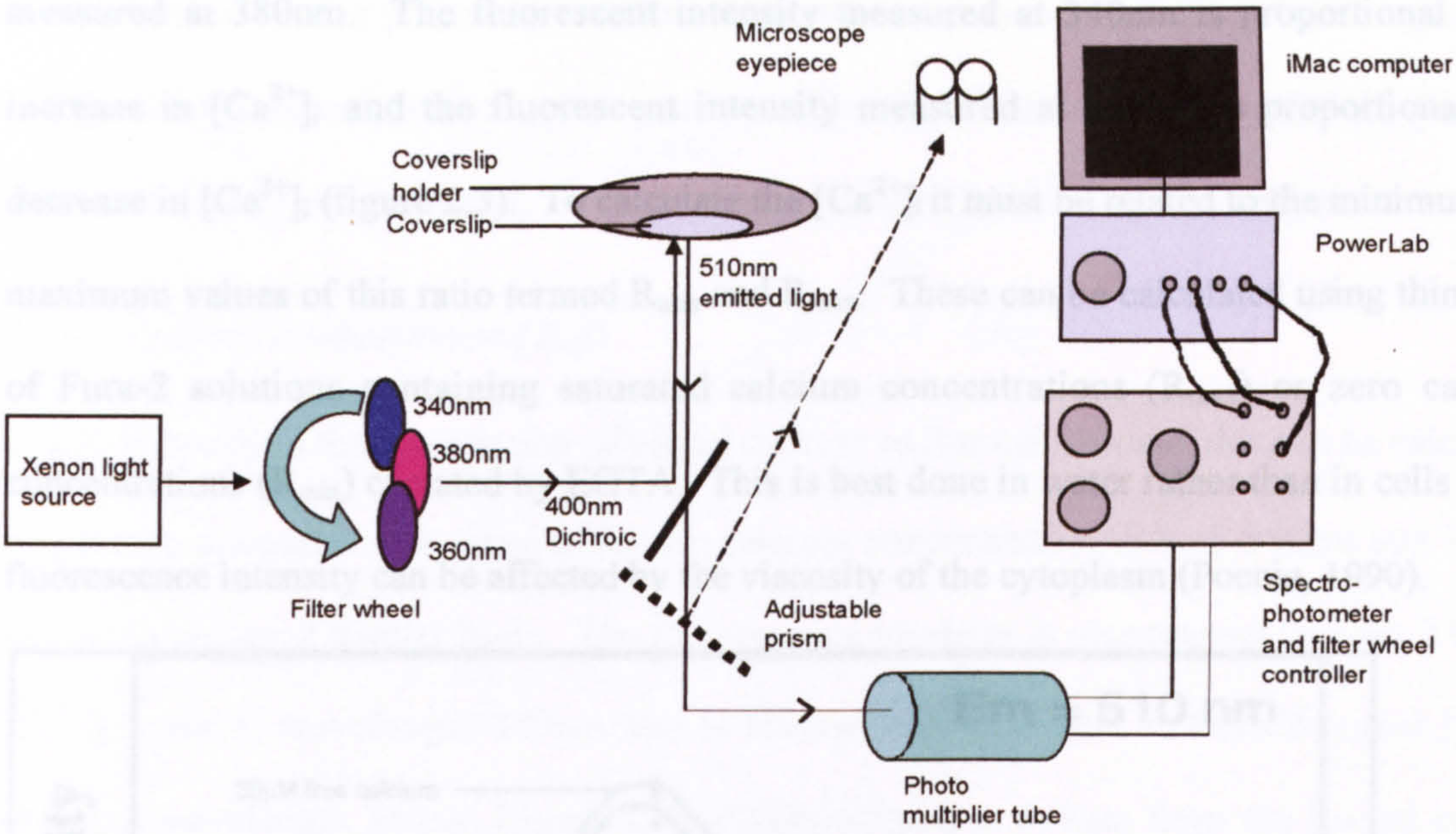

Figure 2.2. *In vitro* schematic of the calcium rig

White light is filtered through 340, 360 and 380nm filters and passes through a dichroic mirror that reflects light <400nm up to the Fura-2 loaded cells. The $[Ca^{2+}]_i$ bound Fura-2 is exited by light at 340, 360 and 380nm and emits light at 510nm. This light passes through the 400nm dichroic and is either visualised in the microscope eyepiece, or is directed, by the adjustable prism, to the PMT, where the signal is amplified. The signal is then converted by the spectrophotometer and is recorded by PowerLab/4sp, which synchronises emitted light to the wavelength of light it was excited by, i.e. 340, 360, or 380nm.

The PMT amplifies the signal and relays this to the spectrophotometer, which converts the light signal to voltage. This unit also controls the PMT output and gain (amplitude). The fluorescence intensity for each filter is displayed and recorded by the PowerLab/4sp (AD Instruments, Oxfordshire, UK) software on the computer.

2.6.2 Fura 2-AM

Fluorescence intensity is measured using the fluorescence calcium indicator Fura 2, which forms a 1:1 complex with calcium. Both free and bound forms of the dye fluoresce but when bound to calcium the fluorescence has a shorter excitation wavelength (Poenie, 1990). $[Ca^{2+}]_i$ can be calculated from the ratio of the fluorescent intensity measured at 340nm to that

measured at 380nm. The fluorescent intensity measured at 340nm is proportional to an increase in $[Ca^{2+}]_i$ and the fluorescent intensity measured at 380nm is proportional to a decrease in $[Ca^{2+}]_i$ (figure 2.3). To calculate the $[Ca^{2+}]_i$ it must be related to the minimum and maximum values of this ratio termed R_{min} and R_{max}. These can be calculated using thin films of Fura-2 solutions containing saturated calcium concentrations (R_{max}) or zero calcium concentrations (R_{min}) chelated by EGTA. This is best done in water rather than in cells as the fluorescence intensity can be affected by the viscosity of the cytoplasm (Poenie, 1990).

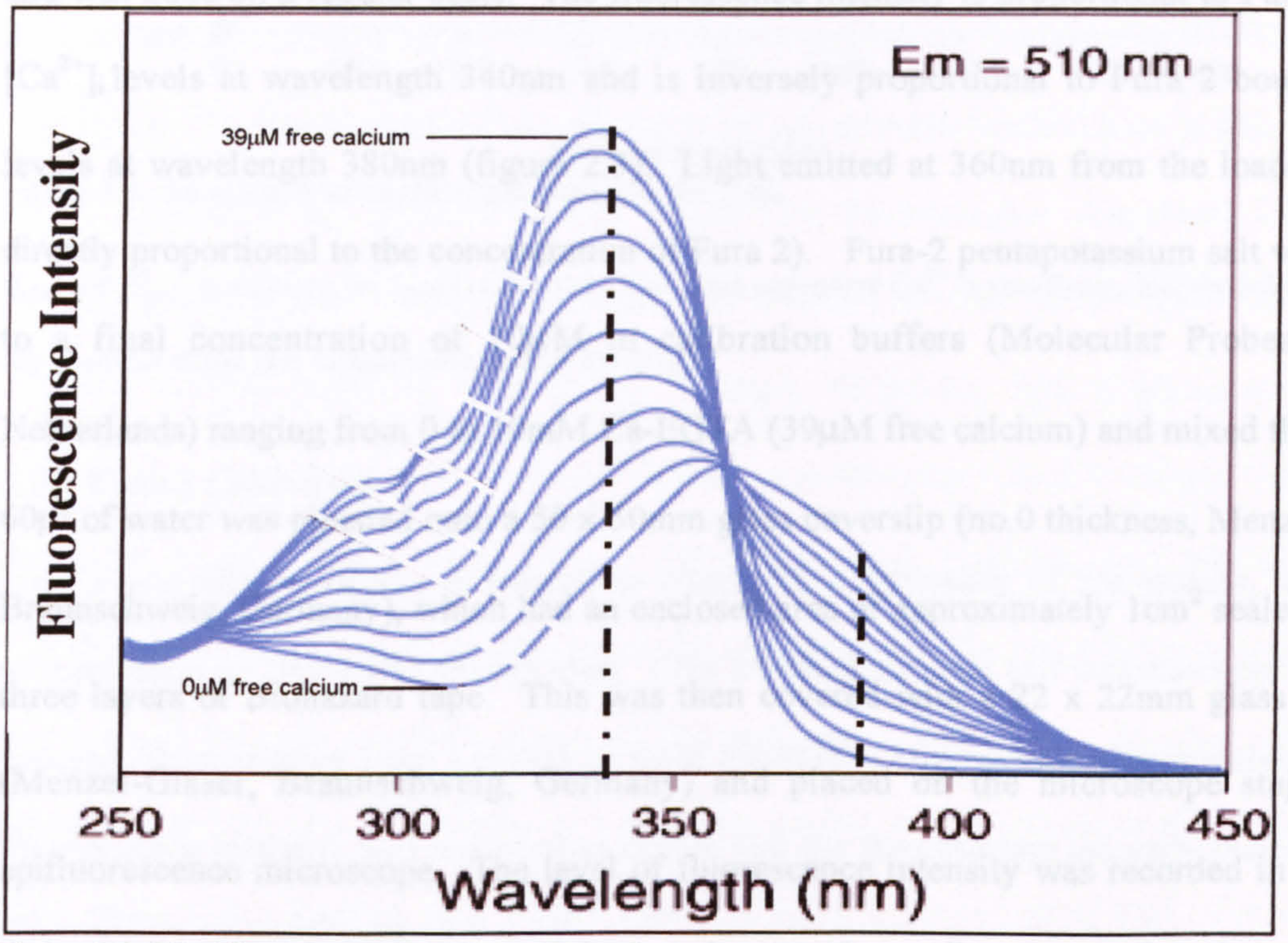

Figure 2.3. The Fluorescence intensity of Fura-2.

The fluorescence intensity of Fura-2 is proportional to an increase in calcium when excited at wavelength 340nm and is inversely proportional to an increase in calcium when excited at wavelength 380nm. Emission (EM) is at wavelength 510nm. Adapted from Molecular Probes' calcium calibration buffer kits data sheet.

Fura-2 is used in this project in two forms, pentapotassium salt and Fura-2 acetoxymethyl (AM). Fura 2 pentapotassium salt is used to calibrate the dissociation co-efficient (K_d) (see below) and is not cell permeant. Fura 2 AM is an ester of Fura 2 and is cell permeant.

2.6.2.1 Calcium calibration and $K_d\beta$

The $K_d\beta$ describes the dissociation of bound calcium to free calcium and this can be calculated by plotting emissions of a range of known calcium concentrations at both 340nm and 380nm and was done on a regular basis. The fluorescence intensity is proportional to Fura 2 bound $[Ca^{2+}]_i$ levels at wavelength 340nm and is inversely proportional to Fura 2 bound $[Ca^{2+}]_i$ levels at wavelength 380nm (figure 2.3). Light emitted at 360nm from the loaded cells is directly proportional to the concentration of Fura 2). Fura-2 pentapotassium salt was diluted to a final concentration of 10μM in calibration buffers (Molecular Probes, Leiden, Netherlands) ranging from 0 to 10mM Ca-EGTA (39μM free calcium) and mixed thoroughly. 60μl of water was pipetted onto a 50 x 50mm glass coverslip (no.0 thickness, Menzel-Glaser, Braunschweig, Germany), which had an enclosed area of approximately $1cm^2$ sealed off with three layers of Biohazard tape. This was then covered with a 22 x 22mm glass coverslip (Menzel-Glaser, Braunschweig, Germany) and placed on the microscope stage of the epifluorescence microscope. The level of fluorescence intensity was recorded in complete darkness for approximately 10 seconds to make sure the reading was unchanging. This was then repeated with 60μl from all 10 calcium buffer solutions. The data was analysed (see below) and the $K_d\beta$ plotted as the fluorescence intensity ratio against free calcium concentration (see figure 2.4). The $K_d\beta$ is defined as the calcium concentration at which it reaches the half saturation point.

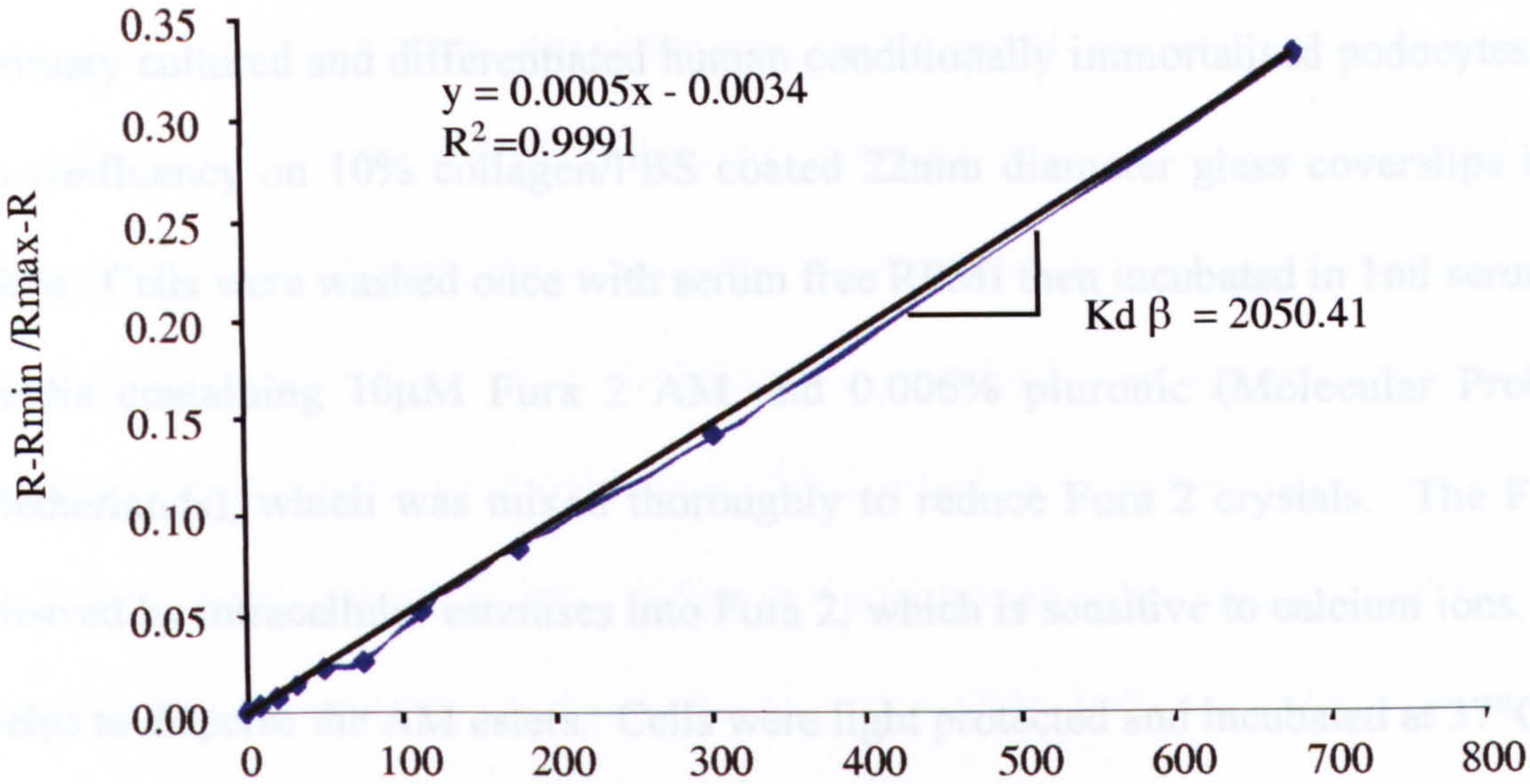

Figure 2.4. An example of a calibration curve for the Kdβ.

R_{min} and R_{max} are the ratios I_{f340}/I_{f380} for zero Ca^{2+} and saturated Ca^{2+} respectively. Kdβ is calculated from the gradient of the line as demonstrated on the graph.

2.6.3 Fura 2 Calibration

Fura 2 was also optimally calibrated to check the consistancy of the system, although a concentration of 10μM was always used. Fura 2 pentapotassium salt was dissolved at various concentrations ranging from 1-20μM in 5mM Ca-EDTA calibration buffer (number 5 of 11). Fluorescence intensity was recorded as before and the fluorescence intensity plotted against the concentration of Fura 2.

2.6.4 R_{min} and R_{max} calibration

At the beginning of each day the system was calibrated using 0mM calcium and 10mM Ca-EGTA calibration buffers. This was necessary to work out the R_{min} and R_{max} for each set of experiments (see analysis below). The fluorescence intensity of water, R_{min} and R_{max} were measured in the same way as above.

2.6.5 Loading the cells

Primary cultured and differentiated human conditionally immortalised podocytes were grown to confluency on 10% collagen/PBS coated 22mm diameter glass coverslips in a six well plate. Cells were washed once with serum free RPMI then incubated in 1ml serum free RPMI media containing 10μM Fura 2 AM and 0.006% pluronic (Molecular Probes, Leiden, Netherlands), which was mixed thoroughly to reduce Fura 2 crystals. The Fura 2 AM is cleaved by intracellular esterases into Fura 2, which is sensitive to calcium ions, and pluronic helps to disperse the AM esters. Cells were light protected and incubated at 37°C for between 1 and 2hrs. The Fura 2 solution was aspirated off and the cells washed once in phenol red free Hanks' Balanced Salt Solution (HBSS, Gibco Life Technologies, Maryland, USA). The HBSS contained either minimal (approximately 200μM) calcium (with 0.4g/L KCL, 0.06g/L KH_2PO_4, 0.35g/L $NaHCO_3$, 8g/L NaCL, 0.048g/L Na2HPO_4, 1g/L D-glucose) or 1.3mM calcium (i.e. physiological extracellular calcium concentration) (with 0.185g/L $CaCl_2 \cdot 2H_2O$, 0.098 g/L $MgSO_4$, 0.4g/L KCL, 0.06g/L KH_2PO_4, 0.35g/L $NaHCO_3$, 8g/L NaCL, 0.048g/L Na2HPO_4, 1g/L D-glucose) depending on the experiment. The coverslip was handled with forceps and the cells carefully wiped off the underside using tissue. Surplus solution was drawn off and the coverslip placed in a coverslip holder, which was covered in a thin film of silica paste with a Perspex plate placed firmly on top to achieve a good seal. The area above the coverslip was exposed and 1ml HBSS was pipetted into a lip that allows gradual spill-over onto the coverslip. The coverslip was slotted into a Perspex tray on the epifluorescence microscope. The cells were brought into focus in the light and then the Fura 2 loaded cells were fine focussed in complete darkness. An appropriate view was found with confluent cells, high fluorescence intensity and minimal Fura 2 background. A stable baseline was established over a minimum of 2 minutes and in most cases recordings were taken for approximately 1 minute prior to treatment. If fluorescence intensity was too low or the recordings not regular

then another view was found. To add the treatment to the cells the PMT was closed to protect it from white light, a torch was shone over the coverslip, the treatment was pipetted carefully into the HBSS without disturbing the cells, the torch was turned off and the PMT reopened. In this manner recording could continue and changes in $[Ca^{2+}]_i$ could be detected as soon as the PMT was turned back on. $[Ca^{2+}]_i$ changes were recorded for approximately 5. At the end of each experiment 10μM ionomycin was added, which is a calcium ionophore that perforates all cell membranes causing a heavy influx of calcium both extracellularly and from intracellular stores. This was used as a positive control followed by 5mM Manganese chloride ($MnCl_2$) to quench the Fura 2 bound calcium. This last reading was used as the R_{min} to calculate actual calcium concentrations (see analysis below).

2.6.6 Data analysis

Voltage readings for all three wavelengths plus the time since the start of the experiment were recorded using the Chart V3.6 MacLab system. This was opened in Excel as a .txt document and was converted into individual data points. Actual calcium was calculated using the following equation:

$$[Ca^{2+}]_i = K_d\,[(Rnorm - 0.85) / (0.85 \times R_{max}norm) - Rnorm])$$

Where 0.85 represents the correction value to account for cytoplasm viscosity (Poenie, 1990), R is the normalised ratio of fluorescence intensity (I_f) calculated as:

$$R = R_{exp} / R_{min}$$

Where $R_{exp} = (I_{f340}-B_{340})/(I_{f380}-B_{380})$. I_{f340} is the I_f measured during excitation at 340nm, I_{f380} is the I_f measured during excitation at 380nm and B_{340} and B_{380} are the background I_f values measured during excitations at 340nm and 380nm respectively (measured as the I_f after Mn^{2+} quenching). R_{min} is the *in vitro* ratio for zero $[Ca^{2+}]_i$ concentration calculated where $R_{min} = (I_{f340}-W_{340})/(I_{f380}-W_{380})$. W_{340} and W_{380} are the background I_f values during excitations at 340nm and 380nm of water. R_{max} norm is the ratio of R_{max}/R_{min} and R_{max} is the *in vitro* ratio for saturated $[Ca^{2+}]_i$ and is calculated by $R_{max}=(I_{f340}-S_{340})/(I_{f380}-S_{380})$, where S_{340} and S_{380} are the I_f values of saturated $[Ca^{2+}]_i$. Rnorm is the Ratio normalised to R_{min}. Actual calcium was used as well as the Rnorm. This was to compare between sets of experiments where the calcium levels were variable. $[Ca^{2+}]_i$ was plotted against time of treatment introduction. Changes in $[Ca^{2+}]_i$ were measured by taking the average of select data points representative of a baseline reading and a peak or trough reading after treatment. To look for significance within an experiment these were compared using a paired *t*-test. To check for significance between experiments the ratio of the experimental over baseline reading was taken and the averages of these compared using an unpaired *t* -test. $P<0.05$ was accepted as statistically significant.

2.7 Proliferation

This assay was adapted from the one described in (Bates et al., 2002). It uses the principle that DNA replicates during proliferation and if Methyl-^{3}H labelled thymidine is present it will be incorporated into the DNA. Therefore the radioactive signal will be directly proportional to DNA replication. Only primary culture podocytes were used in this assay because they are proliferative. 200µl of a podocyte cell suspension was seeded onto a 24 well plate (Nunc, Fisher Scientific, Leicestershire, UK) with 800µl complete RPMI. Cells were left for 48 hrs or until 70% confluent then media was removed and replaced with serum free RPMI media. Treatment was added to half the cells and half were left untreated. 24hrs later 1µCi/ml

Methyl-^{3}H thymidine (Amersham Pharmacia, Buckinghamshire, UK) was added to each well and mixed. After just 4 hrs the wells were washed once with 1xPBS and then 0.2ml 1x trypsin was added to each well and left for 5 minutes. 0.2mls complete RPMI was added to each well to stop the reaction and remaining cells were pipetted into 1.5ml tubes (Eppendorf, Hamburg, Germany) from which a cell count was taken using a students' haemocytometer (Neubeaur, Weber, UK). The samples were spun at 300g for 10mins (Biofuge, Hereaus, Hanu, Germany). The supernatant was removed and 0.2ml NaOH was added to lyse the cells at room temperature for 30 minutes. Cells were then pipetted into scintillation vials (Fisher Scientific, Leicestershire, UK) and 5ml of biodegradable scintillation fluid (Amersham Pharmacia, Buckinghamshire, UK) was added before counts per minute (cpm) were read by a scintillation counter (1217 Rackbeta, Perkin Elmer, Boston, USA). Data was expressed as cpm/treatment and ^{3}H thymidine incorporation/cell for each treatment. A paired *t*-test was used to test for significance.

2.8 Cytotoxicity (adapted from LDH kit instruction manual, Roche)

2.8.1 Principles

Percentage cell death (cytotoxicity) was measured using a colourimetric assay to detect lactate dehydrogenase (LDH) activity released from the cytosol of damaged cells into the supernatant (Roche). Released LDH reduces nicotine adenine dinucleotide (NAD+), a coenzyme for oxidation, to NADH/H+ by the oxidation of lactate to pyruvate. Then a second catalyst (diaphorase) transfers two hydrogen ions from NADH/H+ to the yellow iodotetrazolium chloride (INT), which forms red formazan as shown in figure 2.5. Therefore the amount of LDH produced was directly proportional to the colour produced by the assay.

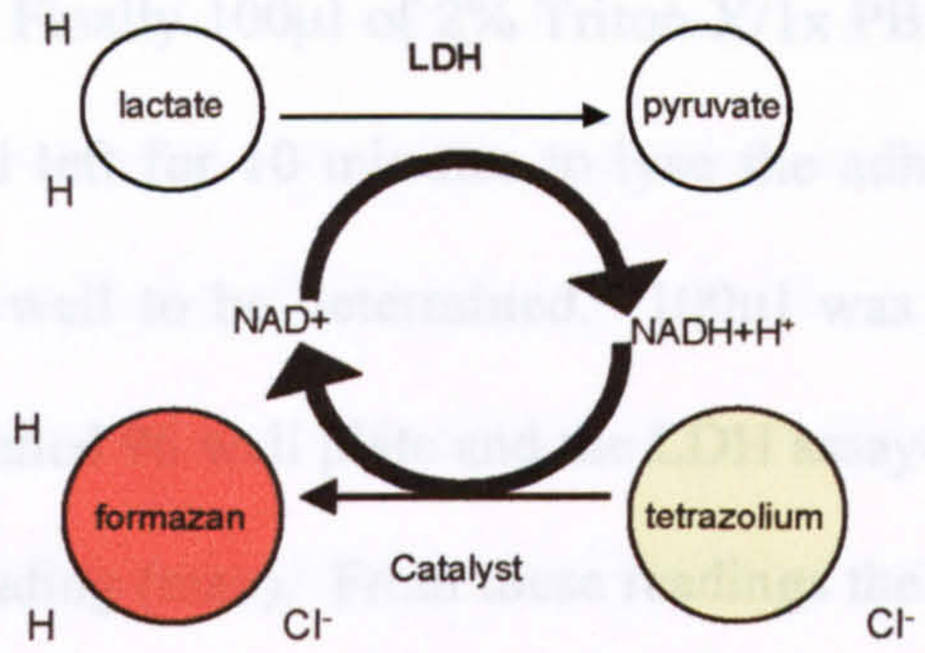

Figure 2.5. Principle of LDH assay

LDH release induces the reduction of NAD+ to NADH/H+. This allows the transfer of two hydrogen ions from NADH/H+ to iodotetrazolium chloride (yellow) to form formazan (red). The colour of the media is therefore directly proportional to the amount of LDH release and the percentage of cytotoxicity can be calculated from this.

2.8.2 Protocol

On day one a 96 well plate (Corning, Birmingham, UK) was seeded with 200µl/well primary culture or conditionally immortal podocyte cell suspensions in complete RPMI media and left for 48hrs or until confluent. On day three the media was removed using a multichannel pipettor, washed once with sterile 1xPBS and 200µl serum free RPMI added. On day 4 100µl from each well was transferred to a similarly labelled 96 well plate. For a full 96 well plate 11.25ml of solution containing diaphorase/NAD^+ from the LDH kit (Roche, Manheim, Germany) was mixed with 250µl of solution containing INT and sodium lactate. 100µl of this solution was added to each well and light protected for 30 minutes at room temperature. It was then quantified using a Bichrometric Multiscan plate reader (Bioscan, Washington, USA), using an absorbance spectra at wavelength 492nm. This was the low control reading (min). The test 96 well plate was divided into non-treatment and treatment(s) and 100µl of serum free RPMI containing either treatment (double final concentration) or not was added to the 100µl media left in the 96 well plate. On day 5 100µl of the 200µl from each well was transferred to a similarly labelled 96 well plate and the LDH assayed and quantified as above. This was the

experimental reading (exp). Finally 100µl of 2% Triton X/1x PBS (final concentration 1%) was added to each well and left for 10 minutes to lyse the adherent cells and enable the maximum LDH from each well to be determined. 100µl was removed from each well, transferred to a similarly labelled 96 well plate and the LDH assayed and quantified as above. This was the high control reading (max). From these readings the % cytotoxicity (T_x) can be calculated:

$$T_x = (exp-(min/2^A))/(max + ((exp/2^B)-(min/4^C))) \times 100$$

A. Min values are divided by 2 because the control media still left in the 96 well plate was diluted twice by day two. B. Exp values are divided by 2 because the exp media in the plate was diluted twice by day three. C. By the third day the low control was diluted twice more and therefore was a quarter of the original reading. The max and exp readings were combined to allow for differences between treatments in the high control readings. Data were expressed as changes in % cytotoxicity and significance was tested within experiments using a paired *t*-test and between experiments using an unpaired *t*-test (two samples) or unpaired ANOVA (more than two samples).

2.9 Apoptosis Assay

2.9.1 Principles

Apoptosis is programmed cell death that can be initiated through a number of different stimuli via a number of different pathways. This assay uses the principle that the plasma membrane fatty acid residues are normally polarised with phosphatidylserine (PS) residues on the cytoplasmic side. During apoptosis this polarity is lost and the PS residues are exposed to the extracellular fluid. This is just one of the cell surface residues that are recognised by phagocytotic cells. Annexin V is a member of a family of calcium dependent phospholipid-

binding proteins involved in cytoplasmic signal transductions, whose preferential cytosol-binding partner is PS. FITC conjugated recombinant annexin V protein has been developed to bind to PS residues of apoptotic cells. This assay also uses the principle that during necrosis (pathological cell death) the plasma membrane loses its integrity allowing propidium iodide, which is a hydrophilic polar nuclear binding dye and therefore not normally able to cross the plasma membrane, entry into the cell, which is taken up by the nucleus. Necrotic cells have very low cell surface exposure of annexin V. Apoptotic cells do not lose their membrane integrity until late in the process when apoptotic bodies are formed, just before phagocytosis.

2.9.2 Protocol

Confluent conditionally immortal podocyte cell lines in 75cm^3 tissue culture flasks were serum starved for 4,16 or 48hrs to induce growth factor withdrawal induced apoptosis, then treated or left untreated for a further 4hrs. Cells were then scraped into suspension using cell scrapers (Nalge Nunc, Fisher Scientific, Leicestershire, UK) and left in a 15ml falcon tube on a roller (Stuart Scientific, Watford, UK) for 4 hrs more to ensure cells did not re-adhere. This was also to promote anoikis, which is apoptosis induced by disturbance of cell surface integrins. Cells were then spun for 5 minutes at approximately 3000rpm, the supernatant discarded and each pellet resuspended in 1ml 1x binding buffer (Bender Medsystems, Vienna, Austria) (final concentration 10mM Hepes/NaOH, pH 7.4, 140mM NaCL, 2.5 mM $CaCl_2$). Each ml was divided four ways into: 1) a background sample; 2) an annexin V only treated sample; 3) a propidium iodide (PI) only treated sample and 4) a sample treated with a combination of annexin V and PI. 10 µl of FITC conjugated recombinant (rh) annexin V protein was added to the annexin V sample (sample 2) and the combination sample (sample 4). All samples were protected from light and incubated at room temperature for 15 minutes on a roller to mix and stop cell re-adherence. The unbound annexin V was washed away by

centrifuging at 600g for 5 minutes, discarding the supernatant, adding 250µl 1xPBS, resuspending the cell pellet and centrifuging again at 600g for 5 minutes. 5µl of 20µl/ml PI was added to the PI only (sample 3) and the combination sample (sample 4) and mixed. Samples were then immediately assayed using a flow cytometer. Samples not immediately used were kept in the fridge under gentle agitation until ready for use. Samples were used in no specific order.

2.9.3 Flow cytometer

The cell suspension sample was taken up into the flow cell of the flow cytometer (Beckman Coulter, Buckinghamshire, UK) where hydrodynamics focused the cells into a single stream. An argon laser emitted light at 488nm, which excited the samples in the flow cell. Light was scattered from the sample and captured at 90°, termed the forward scatter and at 45°, termed the side scatter (figure 2.6).

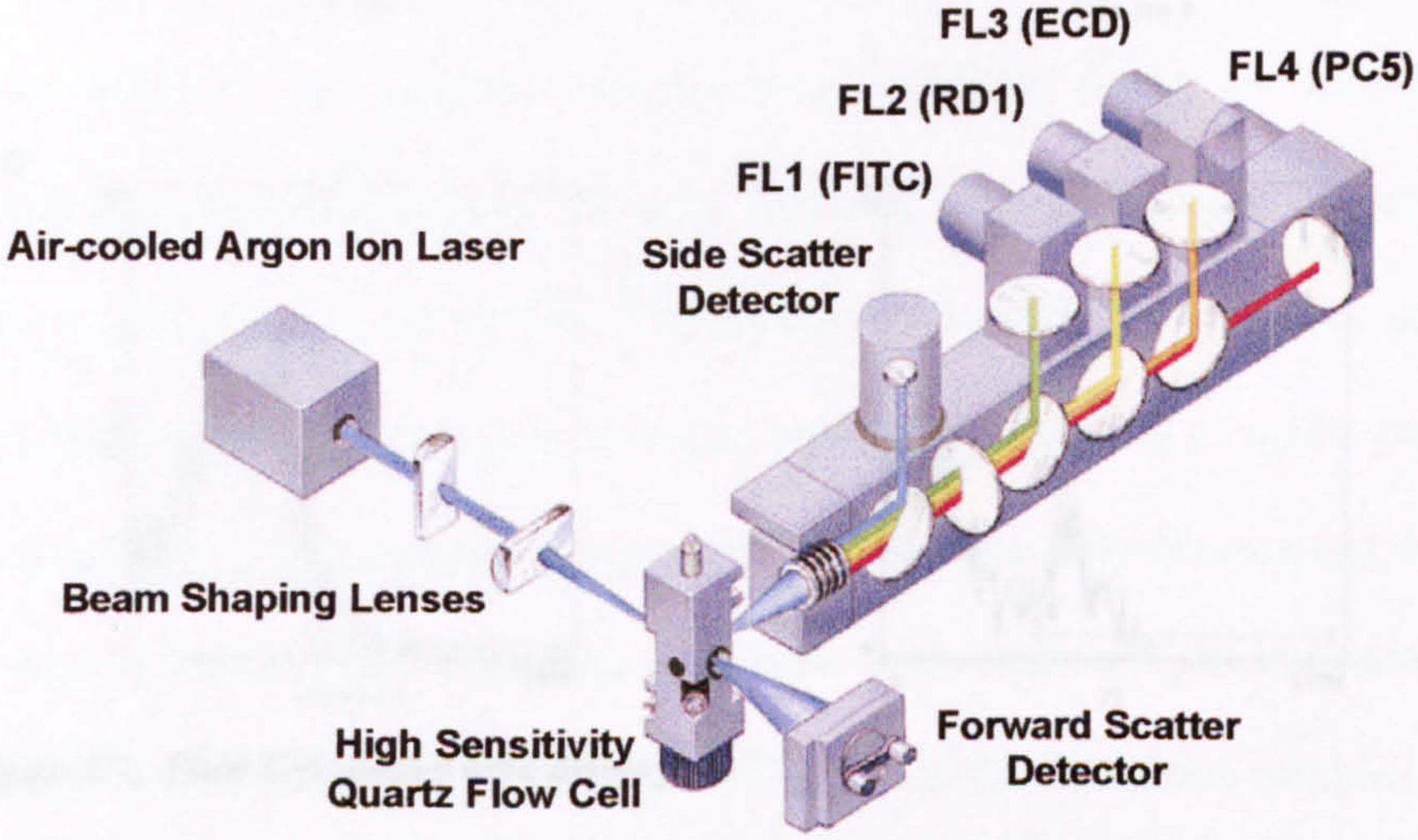

Figure 2.6. Flow cytometer optics from Beckman Coulter tutorial slide

The cell suspension is taken up by the flow cytometer and excited by light at 488nm. Light scattered forward gave an indication of granularity of events, and light scattered sideways gave an indication of size of events. Side scatter light passed through dichroics of various limits and light shorter then the dichroic limit was reflected up to various light filters of 525nm, 575nm and 600nm.

The wavelength of forward scatter light represented size of the particles (events) hit by light and the wavelength of side scatter represented the granularity of particles (events) hit by light. The beam of side scatter light was filtered through a series of dichroic mirrors and filters for different wavelengths as shown in figure 2.5. Emission collected at 525nm (filter 1, green) picked up FITC-conjugated AV labelled cells and emission collected at 600nm picked up PI labelled cells (filter 3, red). The PMT amplified the signal. This was then controlled by the voltage, which acts as a fine control and by the gain, which acts as a coarse adjustment.

2.9.4 Setting up protocols

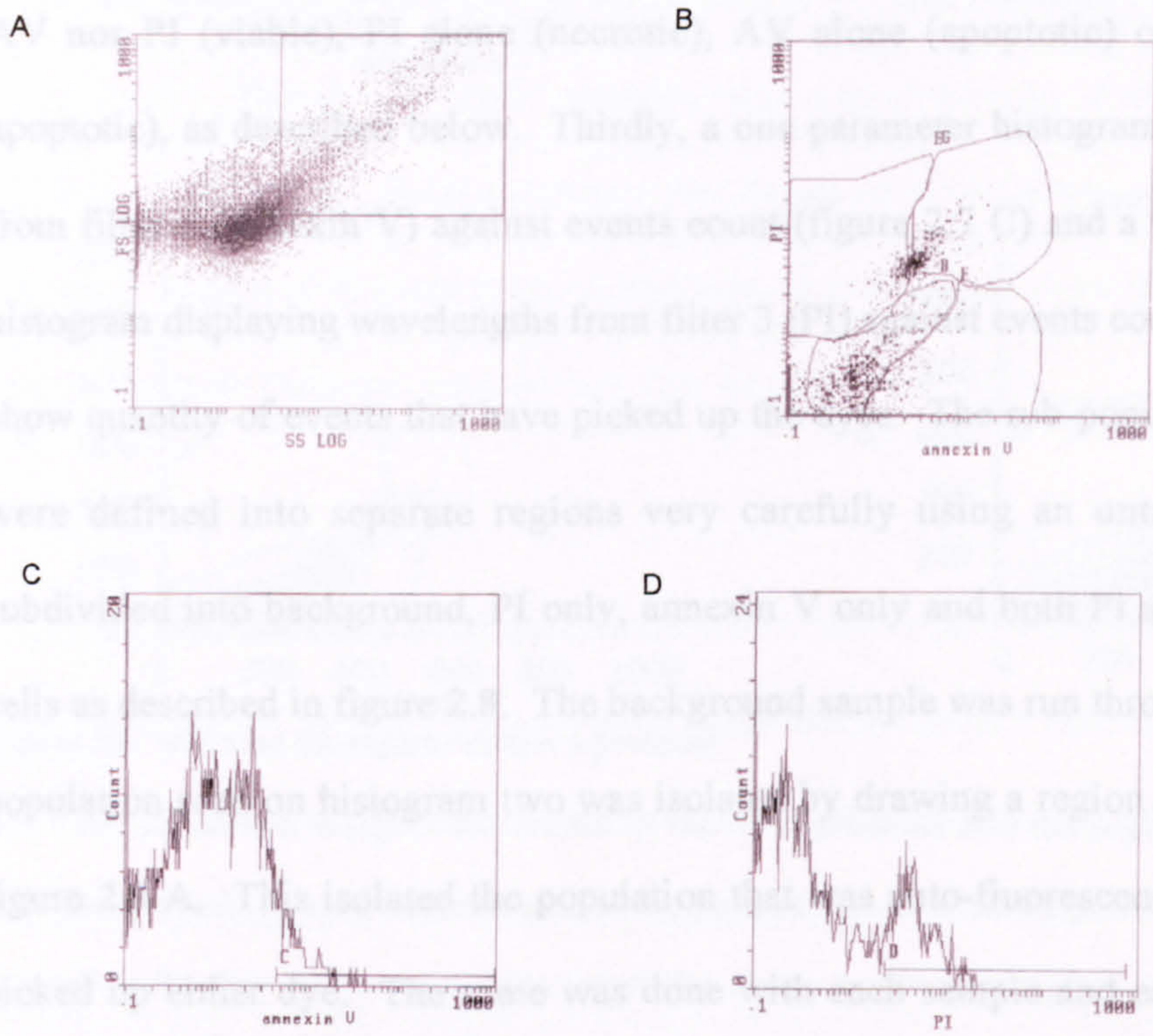

Figure 2.7. Flow Cytometer data display.

A. Forward scatter and side scatter light from each event is displayed, and the gated region defines cells depending on their size and granularity. B. A scatter plot of events detected at 525nm (AV) and at 600nm (PI), showing subpopulations defined by four different regions. C. Count of events with AV binding, showing a linear region to divide the AV bound population from the autofluorescent, or low level AV

bound population. D. Count of events with PI staining, showing a linear region to divide the PI stained population from the autofluorescent, or low level AV bound population.

Data from the cell sample are displayed in four graphs. Firstly, a dot plot of forward scatter against side scatter, which is used to gate an area representative of size and granularity of events (data points) therefore discarding debris (figure 2.7 A). The discriminator was also set on the machine to discard readings below a certain size in order to count only whole cells. Secondly, a scatter plot of events from filter 1 (annexin V) (X axis) was plotted against events from filter 3 (PI) (Y axis) (figure 2.7 B). This histogram separates the entire population of events into sub-populations characterised according to whether they are labelled with neither AV nor PI (viable), PI alone (necrotic), AV alone (apoptotic) or both PI and AV (late apoptotic), as described below. Thirdly, a one parameter histogram displaying wavelengths from filter 1 (annexin V) against events count (figure 2.7 C) and a fourthly a one parameter histogram displaying wavelengths from filter 3 (PI) against events count (figure 2.7 D). These show quantity of events that have picked up the dyes. The sub-populations in histogram two were defined into separate regions very carefully using an untreated sample that was subdivided into background, PI only, annexin V only and both PI and annexin V incubated cells as described in figure 2.8. The background sample was run through the machine and the population seen on histogram two was isolated by drawing a region around it as indicated in figure 2.8 A. This isolated the population that was auto-fluorescent from the cells that had picked up either dye. The same was done with each sample and each new population was isolated by a new region (figure 2.8 B-D). Once the first three samples were run through, the population defined by the last sample was the population that had picked up both PI and annexin V. This inferred that either the cells (events) were in late apoptosis and had lost some membrane integrity (apoptotic cell bodies) or that some necrotic cells (events) had low exposure of PS residues on the surface (figure 2.8 D). The population from the combined

stain sample (figure 2.8 D) that fit into the autofluorescence region (figure 2.8 A) described a viable population, as well as autofluorescent cells, because this cell population picked up neither annexin V nor PI.

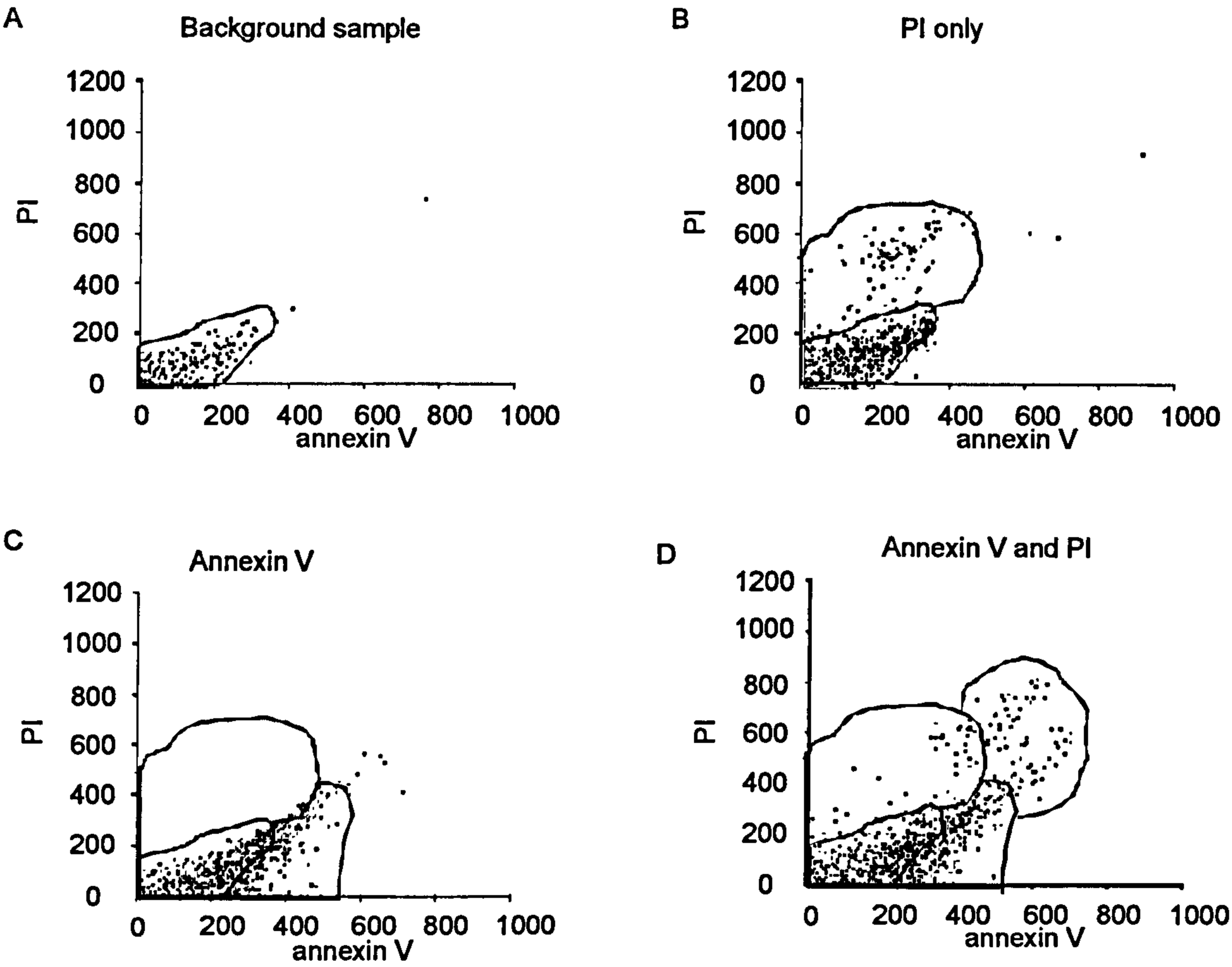

Figure 2.8. Defining the regions within a protocol

A. A cell suspension sample was assayed by the flow cytometer and the population shown by the scatter plot was defined as an autofluorescence/viable population. B. A cell suspension incubated in PI only was assayed by the flow cytometer and the population shown by the scatter plot outside of the autofluorescence region was defined as the necrotic population. C. A cell suspension incubated in FITC conjugated annexin V only was assayed by the flow cytometer and the population shown by the scatter plot outside of the regions already defined was defined as the apoptotic population. D. A cell suspension incubated in both PI and annexin V was assayed by the flow cytometer and the population shown by the scatter plot outside of the regions already defined was defined as the late apoptotic population.

A linear region was also fitted to the last two histograms using the background sample to show auto-fluorescence, defining the region from there onwards. A protocol was set up in this manner for different cell types. Once it had been set up then the populations of all of the samples should fit in the regions defined unless the laser loses its alignment (see calibration below).

2.9.5 Calibration

Every time the flow cytometer was used it was calibrated using fluorescent spheres that fluoresce equally at all three filter wavelengths (Beckman Coulter, Buckinghamshire, UK). They were run through as a sample would be and the data was displayed on a pre-set up "start-up protocol". This data indicated whether there was a blockage in the flow cell or if the laser was out of alignment. Each parameter was tested on a histogram against sphere count. The computer measured the half peak co-efficient of variation of these peaks, which showed that the excited light from the laser did not vary by more than 0.5%.

2.9.6 Analysis

The computer on the flow cytometer quantifies the events in the gates and regions and this data was analysed in Excel with the assumption that all events were cells. Each subpopulation was calculated as a percentage of the total population given by the statistics on the Flow cytometer as follows:

$$\text{Viable population (background)} = POP_{CV}/POP_{T}$$

$$\text{Necrotic population (PI)} = (POP_{CN}-POP_{OA})/POP_{T}$$

$$\text{Apoptotic population (Annexin V)} = (POP_{CA}-POP_{ON})/POP_{T}$$

$$\text{Late apoptotic population (PI and Annexin V)} = (POP_{CLa}-(POP_{OA}+POP_{ON}))/POP_{T}$$

Where POP_T describes the total population calculated as the sum of populations in each region. POP_{XV} depicts the population in the viable region just as POP_{XA}, POP_{XN} and POP_{XLa} depicts the populations in the apoptotic necrotic and late apoptotic regions respectively. POP_{CX} and POP_{OX} describe this populations from combined incubation or incubation with one dye only respectively. An unpaired ANOVA with a Bonferroni post hoc test was used to test for significant differences between cell populations.

2.10 Western Blotting

2.10.1. Protein extraction (adapted from (Wen et al., 1999))

Protein was extracted from confluent cells in a $75cm^3$ tissue culture flask that had been serum starved for 24hrs and then incubated with treatment for various times. Cells were washed once with cold 1x PBS and then scraped into suspension using a cell scraper. Cells were centrifuged at 3000rpm for 5 minutes, the supernatant removed and lysis buffer added depending on the pellet size (~100µl). The lysis buffer contained RIPA buffer consisting of detergents and salts including 1% Nonidet P-40 (ICN Biomedicals, California, USA), 0.5% Sodium deoxycholate, 0.1% sodium dodecyl sulphate (SDS) /water, 1x PBS. It also contained a cocktail of proteinase and phosphatase inhibitors added fresh to the RIPA buffer consisting of 1mM PMSF/isopropanol, 1mM Na_3VO_4/water and 20µg Aprotonin/ml water. The samples were left to rock at 4°C for 20 minutes to mix and then incubated on ice for 60 minutes to lyse the cells. The samples were spun at 13000rpm at 4°C for 15mins and the supernatant transferred to clean Eppendorf tubes. Protein was kept at -20°C until ready to use. Protein extraction from tissue was done in much the same way except that the tissue was chopped finely and homogenised using plastic homogenisers (Fisher Scientific, Leicestershire, UK) then

incubated in lysis buffer and centrifuged in the same way. The lysis buffer added equated to the weight of the tissue.

2.10.2. Protein quantification (Bradford assay using Bio-Rad guide lines)

Protein was quantified from samples that were thawed on ice. A protein standard curve was prepared using normal mouse IgG protein at various dilutions in milli Q ranging from 0 to 30 µg/ml in (total volume 30µl) made up in 7ml sterilised polystyrene containers (Biby Sterilin, Staffordshire, UK). Protein was diluted at 1:10, 1:50 and/or 1:100 in water (total volume 30µl). The Bio-Rad dye was made up 1:5 in water (containing ethanol and phosphoric acid) and 1.5ml added to each of the samples, including the standard curve samples, vortexed and left at room temperature for ~10 minutes. The samples were transferred to plastic 1.6ml cuvettes (Fisher Scientific, Leicestershire, UK). The standard curve absorbence was read on a spectrophotometer at 595nm in order of increasing protein concentration using the 0 µg/ml protein sample to calibrate the machine, then the samples were read. The protein standard curve was then plotted using the optical density (OD) reading against concentration (µg/ml) and the protein quantity of the diluted samples determined from the line of best fit. This concentration of protein was multiplied by the dilution factor used, then divided by 1000 to achieve µg/µl.

2.10.3. SDS Polyacrylamide gel electrophoresis (PAGE)

Proteins were run using SDS PAGE to separate them according to charge and molecular size. First the proteins for each gel were diluted with up to 8µl 1x PBS so that each sample had an equal quantity of protein (70-100µg) and were then diluted in 8µl 1x SDS loading buffer. This contained 100mM Tris/Cl pH 6.8, 4% SDS, 20% (v/v) glycerol (BDH, Pool, UK), 5% β-mercaptoethanol and 0.2% (w/v) bromophenol blue. The β-mercaptoethanol reduces any

disulphide bonds stabilising the protein, the glycerol gives density to the samples when loaded into the gel and the bromophenol blue dye enables visualisation of samples as they run through the gel. The samples were then boiled at 100°C for 5 minutes to denature the protein and expose the entire length of the polypeptide chain to the detergent. The samples were put on ice to stop the reaction. A polyacrylamide gel was made (by the polymerisation of the two monomers acrylamide and N,N-methylene-bis-acrylamide (Sambrook and Russell, 2001c)). The percentage bis-acrylamide varied depending on the molecular weight of the protein in question (i.e. 7.5, 12 and 15%) because the pore size of the gel decreases with increasing proportions of bis-acrylamide. 5ml resolving gel solution was made for each gel using water 30 % bis-acrylamide (BioRad, Hertfordshire, UK) (final concentration varies), 375mM Tris, 0.1% SDS, 0.05% ammonium persulphate, to catalyse the reaction and 0.05% tetramethylethylene diamine (TEMED) to initiate the reaction. The gel was cast using Bio-Rad (Hertfordshire, UK) equipment and allowed to set with a layer of ethanol at the surface to exclude air, which inhibits the reaction. When it had set, a 4% bis-acrylamide stacking gel was made as above but using 125mM Tris, and 0.1% TEMED. The ethanol was drained away from the resolving gel, the stacking gel added and combs put in place. Once the gel had set it was transferred to the electrophoresis tank (Bio-Rad, Hertfordshire, UK) and set up using SDS running buffer (25mM Tris, 250mM glycine (electrophoresis grade BDH, Pool, UK) 0.1% SDS and water). 15µl kaleidoscope ladder (BioRad, Hertfordshire, UK) was loaded on the right hand side of each gel and then each sample was loaded and a current of 90V was run through the gel for ~60-90 minutes until it had separated proteins according to the band size of interest. The gel was trimmed and kept in transfer buffer (50mM Tris, 38mM glycine (electrophoresis grade BDH), 20% methanol, 0.1% SDS and water) for no longer than 24 hrs before use.

2.10.4 Transfer

The protein was transferred from the gel to a polyvinylidine fluoride (PVDF) membrane (Fisher Scientific, Leicestershire, UK) using electrophoresis. Transfer was carried out perpendicular from the direction of travel of proteins. The PVDF membrane was cut to the size of the gel. It was soaked in methanol because it is hydrophobic, then soaked in transfer buffer until use. The PVDF membrane was placed on top of the gel and sandwiched between a set of filters (BioRad, Hertfordshire, UK) and a set of sponges (BioRad, Hertfordshire, UK) pre-soaked in transfer buffer (see above). This was held together in a cassette and placed in the transfer module (BioRad, Hertfordshire, UK). The transfer module was kept at 4°C and the protein was transferred at a constant current of 250mA for 4hrs.

2.10.5 Immunodetection

This procedure was used to identify and measure the size of proteins that are recognised by the specific antibodies. The PVDF membrane was incubated in 10% low fat powdered milk/0.05% PBS-tween blocking solution or filter sterilised 3% bovine serum albumin (BSA)/0.05% PBS-tween depending on the primary antibody used: For example, when probed with an anti-p-Y antibody membranes were blocked with 1% BSA instead of non fat milk, as the latter has been described to provide much greater background, due to endogenous phosphotyrosines. It was incubated for 1hr at room temperature on a roller to block non-specific binding sites on the membrane and suppress non-specific adsorption of antibodies. The membrane was then incubated with the primary antibody that recognises the antigen of the protein of interest, diluted by 50% in the required blocking solution in 0.05% PBS-tween and incubated at 4°C overnight under gentle agitation. Unbound primary antibody was washed away with 5 washes of at least 5 minutes each using 0.05% PBS-tween at room temperature. The membrane was then incubated for one hour at room temperature on a roller

in horseradish peroxidase (HRP) conjugated secondary antibody (Pierce) diluted by 50% in the required blocking solution. The membrane was washed again as above. The luminol enhancer solution and the peroxide solution from an enhanced chemiluminescent kit (ECL) (SuperSignal West Femto Maximum Sensitivity Substrate, Pierce, Cheshire, UK) were mixed 1:1 allowing 0.125ml of total solution per cm^2 of membrane. The membrane was exposed to the ECL for between 5-15 minutes (depending on optimisation for each primary antibody) and light protected. In the presence of hydrogen peroxide HRP it triggers a cyclical chemiluminescent reaction that results in the oxidation of luminol to an excited form of 3-aminophthalate. When this compound returns to ground state it emits blue light that was captured on X-ray film (Sambrook and Russell, 2001c). In a dark room the membrane was laid flat against cling film and taped in place in a film cassette (GRI Molecular Biology, Essex, UK). The membrane was exposed for various amounts of time to X-ray film (Amersham Biosciences, Buckinghamshire, UK) ranging from 1 second to 5 minutes depending on the signal given off and was run through the developing machine (X-ograph Imaging Systems). Membranes were kept in clingfilm at 4°C for long term storage.

2.10.6 Stripping blots

Membranes that had been probed once were stripped of that antibody detection complex so that they could be re-probed with further antibodies. This allowed experiments to be paired. Membranes were wetted with methanol if they had dried out, then incubated at 50°C for 30 minutes with occasional gentle agitation in stripping buffer. This contained 100mM β-mercaptoethanol, 2% SDS, 1M Tris and water. The membrane was then washed twice for ten minutes in 0.05% PBS-tween and then blocked and probed as before.

2.10.7 Analysis

The bands on the film were scanned into the computer (SnapScan 1236, AGFA, Middlesex, UK) and opened in the NIH image software package. This was used to compare the pixel density of each band in question, using an identical area each time. The bands were compared within a membrane using an unpaired *t*-test (comparing two bands) or an unpaired ANOVA (more than two bands) and bands between the same re-probed membrane using paired *t*-test or paired ANOVA.

2.11 Immunoprecipitation

This procedure was used to establish protein association. It used proteins A and G, which are expressed on the surface of gram positive bacteria (different species) and enable the bacteria to invade the host system. They do this by binding to immunoglobulins (Igs) without stimulating an immune response. Protein G only recognises IgGs where as Protein A recognises other types of Igs such as IgM and IgE. Protein A/G can bind to the Fc portion of antibodies so can be used in combination as a binding reagent when conjugated to beads. Protein was extracted from the cells and quantified as above.

2.11.1. Cell lysate pre-clearing

The protein A/G slurry (Santa Cruz Biotechnologies, Heidelberg, Germany) was pre-washed in the lysis buffer used in protein extraction. It was washed twice, centrifuged at 10000rpm for 30 seconds and resuspended in lysis buffer. The lysate was then pre-cleared of non-specific contaminants by incubating it in 2% (v/v) pre-washed protein A/G slurry at 4°C for 1hr under gentle agitation. The sample was then centrifuged at 13000rpm for 15 minutes at 4°C, the supernatant transferred to a fresh Eppendorf and the bead pellet, containing the non-specific contaminants and protein A/G beads discarded. The lysate was incubated again as above, also adding 0.25µg of appropriate control IgG corresponding to the host species of the

primary antibody used in the next step. The sample was spun down as above and again the supernatant kept and the pellet discarded, the slurry was resuspended in lysis buffer 1:1.

2.11.2 Immunoprecipitation

The lysate was incubated overnight at 4°C under gentle agitation with a total of 1µg of primary antibody to react with the antigen of the protein of interest. 1:25 of the 50% protein A/G slurry was added to the lysate and incubated for a further 2hrs at 4°C under gentle agitation to bind to the primary antibody. The lysate was centrifuged at 13000rpm for 15 minutes at 4°C, the supernatant transferred to a fresh Eppendorf and the bead pellet containing the protein of interest was washed three times in lysis buffer, as described for pre-clearing. The pellet and supernatant were kept at -20°C until use. The pellet was resuspended in 10µl 1x SDS loading buffer and the lysate diluted to a standard concentration with 1xPBS and samples were boiled as before. The samples were then subjected to SDS PAGE, transferred to a PVDF membrane and immunodetected as described above.

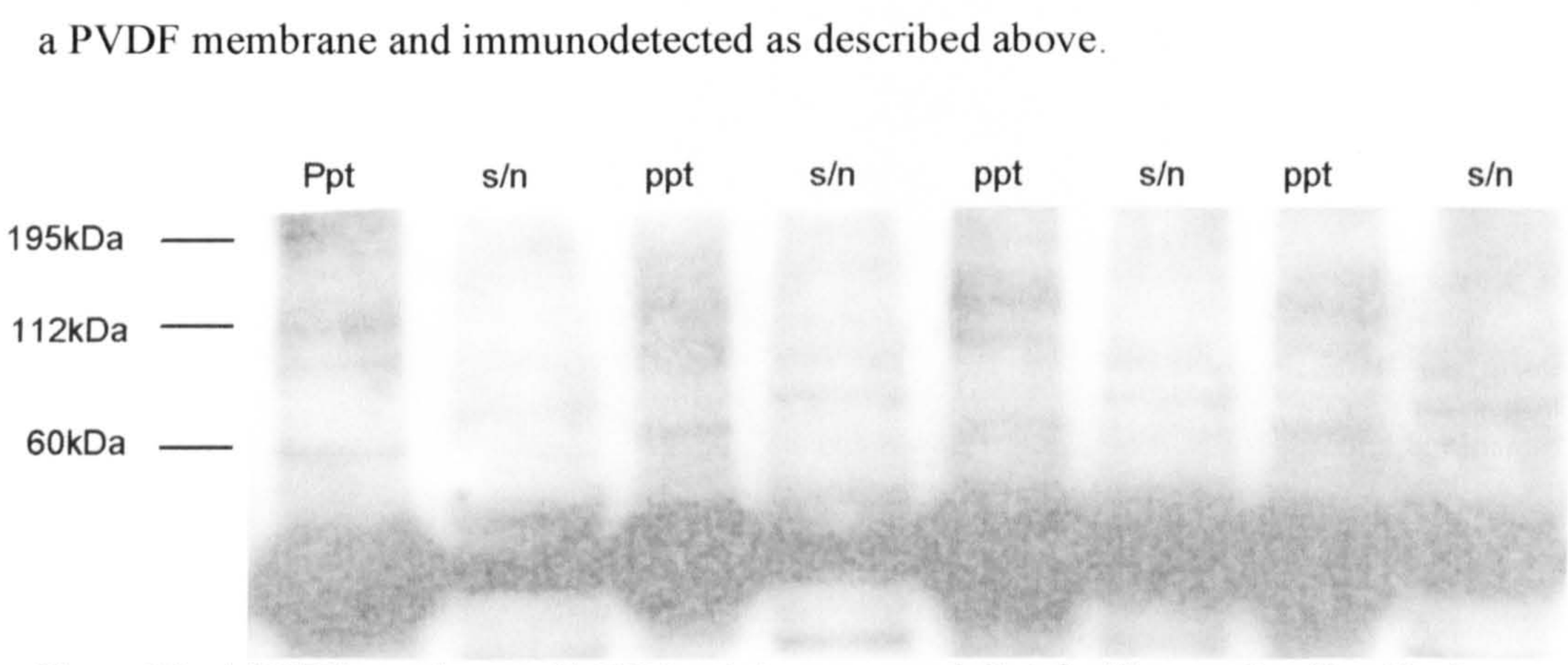

Figure 2.9. A PVDF membrane of hCIP lysate immunoprecipitated with an anti-p-Y antibody.

A number of tyrosine phosphorylated protein bands have been picked up at various molecular weights. The bands are more intense in the precipitate (ppt) compared to the supernatant (s/n).

An example of a PVDF membrane, containing hCIP lysate that had been immunoprecipitated, using an anti-phospho-tyrosine antibody and probed with anti-phospho-tyrosine, is shown in

figure 2.9. This demonstrates that tyrosine phosphorylated proteins were successfully pulled down in the precipitate.

Chapter 3

Characterisation of primary cultured podocytes (PCPs) and the expression of VEGF receptors

3.1 Introduction

To investigate the effects of VEGF on podocytes I chose to study them in isolation from the glomerulus since the glomerulus is a complex microenvironment and may introduce many extraneous variables. Podocytes can be isolated from glomeruli, originated from kidney cortex, from various species including mouse, rat, pig and human. In order to understand the relevance of this study to human physiology the best species from which to isolate podocytes is human. As with any primary cell culture isolation the possibility of contamination by other cell types is a problem and research groups have tried to address these criticisms in primary culture podocytes (PCPs). Yaoita et al outline the main criticism of PCPs isolated from glomeruli: a pure population is dubious and podocytes may change their phenotype in culture (Yaoita et al., 2001). A typical protocol to isolate PCPs from glomeruli was used by Parry et al, 2000: Chopped kidney cortex was pushed through sieves of progressively smaller pore sizes, e.g. sieves with pore sizes of 425μm, 180μm and 125μm. Encapsulated glomeruli were retained in the 125μm pore sieve and cultured in complete RPMI-1640 media containing insulin for a fortnight, to provide the conditions for podocyte outgrowth (Parry, 2000). Using this technique two types of cells have been described as podocytes with similar characteristics; the first are cobblestone polygonal cells, which form outgrowths in the first 6 days of incubation and replicate rapidly. The second are irregular, multinucleated cells with long cytoplasmic extensions that have limited proliferative capacity (Yaoita et al., 2001). The first cell type, however, were suggested to be parietal epithelial cells (PECs) that line the Bowman's space (Yaoita et al., 1991). Instead of pushing the kidney through the sieves, as described above, Yaoita et al rinsed the kidney sections gently with PBS. Individual glomeruli were isolated and decapsulated to avoid PEC outgrowths. They concluded that podocytes isolated under these conditions retained their phenotype, but those grown from encapsulated

glomeruli were derived from PECs or tubular epithelial cells (Yaoita et al., 2001). These authors, therefore, recommend that encapsulated glomeruli should be avoided when isolating PCPs. When isolating PCPs for cell culture, however, encapsulation of each glomerulus is impractical because of the number required. I therefore chose to follow the protocol described by Parry et al, 2000 and to characterise PCPs from each isolation.

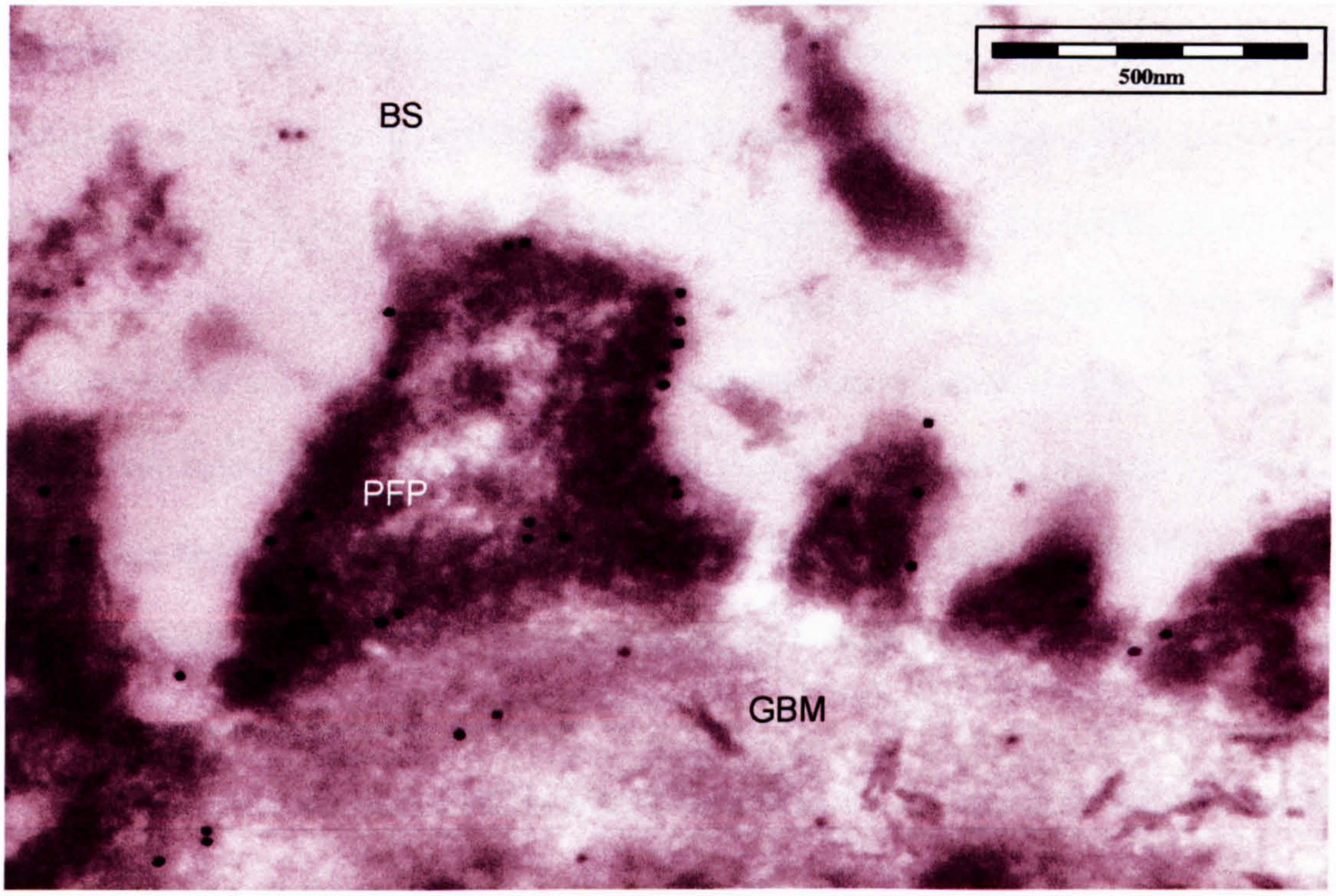

Figure 3.1. Identification of VEGF expression by immuno-gold transmission electron micrograph in a normal human glomerulus.

Sections of human renal cortex were probed with immuno-gold labelled anti-VEGF. Gold particles were clearly seen on the edge of the podocyte foot processes (BS= Bowman's Space, GBM=Glomerular Basement Membrane, PFP = Podocyte Foot process (done by Rachel Hole).

VEGF is thought to play a paracrine role in the glomerulus, acting on the glomerular endothelial cells (Simon et al., 1995) even though there is no overt angiogenesis in the mature kidney. VEGF may be able to act on endothelial cells without causing angiogenesis, due to

the presence of other endogenous factors. It may, however, also be possible that VEGF plays an autocrine role. VEGF is highly expressed in podocytes, which also express Np-1 (Harper et al., 2001), a co-receptor for VEGF-R2. Circumstantial evidence presented itself during an electron microscopy (EM) study investigating VEGF expression in the glomerulus by immuno-gold particles by Rachel Hole at the Academic Renal Unit, Southmead Hospital, Bristol. Immuno-gold labelled anti-VEGF, which was thought to act specifically on glomerular endothelial cells, appeared to be tightly associated with the podocyte plasma membrane (figure 3.1). To confirm these observations, the distance of the immuno-gold labelled anti-VEGF from the plasma membrane was measured and shown in the results. Plasma membrane associated VEGF excreted from the podocytes would be expected to be sequestered to the podocyte glycocalyx, due to the heparin binding abilities of $VEGF_{165}$. If VEGF were bound by the glycocalyx, however, then it would not be expected to be quite so consistently tightly membrane bound as shown in figure 3.1. This suggested that podocyte plasma membrane bound VEGF was binding to the plasma podocyte plasma membrane by some other means, potentially VEGF specific receptors. Therefore, investigations were made into VEGF receptor expression on podocytes, as well as Np-1. This work possibly may have been overlooked in the past because investigations into VEGF activity in the glomerulus concentrated mainly on glomerular endothelial cells and VEGF activation on epithelial cells was thought to be limited.

3.2 Methods

3.2.1 Cell culture-PCP isolation

PCPs were isolated as previously described: Human renal cortex was pushed through successive sieves of progressively smaller pore sizes, and the encapsulated glomeruli were left at 37°C in complete RPMI media (for composition see p.60 of methods) for a fortnight to allow the outgrowth of podocytes. Encapsulated glomeruli were used because it was too time consuming to decapsulate individual glomeruli, as the number required for sufficient podocyte culture was too great. The PCPs were, therefore, characterised for protein and mRNA of podocyte specific markers.

3.2.2 Immunocytochemistry - characterisation of PCPs

Expression of Wilms Tumour-1 (WT-1) and pan endothelial cell adhesion molecule (PECAM-1) protein was examined using immunocytochemical techniques on PCPs and rat glomeruli tissue sections. 5µg/ml rabbit polyclonal IgG anti-WT-1 (C-19) antibody (Santa Cruz Biotechnology, Heidleberg, Germany) was used to detect WT-1 protein and 5µg/ml biotinylated goat anti-rabbit IgG (Vector, California, USA) secondary antibody was used to label the primary antibody. 5µg/ml normal rabbit IgG was used to control for non-specific staining of the secondary antibody (an isotype control) and goat serum was used in the blocking solution. 8µg/ml goat polyclonal IgG anti-PECAM-1 (M 20) antibody (Santa Cruz Biotechnologies, Heidleberg, Germany) was used with 5µg/ml biotinylated horse anti-goat IgG (Vector) secondary antibody. 5µg/ml normal goat serum (Vector, California, USA) was used to control for non-specific staining, and horse serum (Vector, California, USA) was used in the blocking solution. Both were microwaved in TrisHcl/EDTA buffer (pH9).

3.2.3 PCR- characterisation of PCPs and expression of VEGF receptors

RNA was extracted from PCPs, hCIPs, human umbilical vein endothelial cells (HUVECs) and human liver tissue by extraction with phenol:chloroform:guanidine isothiocyanate as described in the methods. RNA was quantified and 1μg RNA was reverse transcribed. PCR was carried out using the primers described in table 3.1.

Table 3.1. Sense and anti-sense primer sequences showing location of primers relative to ATG site

Primer	Sense 5'-3'	Location	Anti-sense 5'-3'	Location
CD45	AGAATACTGGCCGTCAATGG	+1811	GGAGAGTGAATGCCTTCAGC	+2044
vWF	AAGGAGTTCATGGAGGAGGT	+4551	AACCTGGTCTACATGGTCAC	+4823
VEGF-R1	ATGATGCCAGCAAGTGGGAGTTTGC	+2444	CCAACTACCTCAAGAGCAAACGTG	+2776
VEGF-R2	GCATCTCATCTGTTACAG	+2003	CTTCATCAATCTTTACCCC	+2335
VEGF-R3	AACATCACGGAGGAGTCACACG	+97	CGCTCTTGGTCAACAGGAAGGA	+455
Np-1	AAAAGCCCACGGTCATAG	+1888	GGATTGCTGTGGATGACA	+2392
GAPDH	GTCTTCACCACCATGGAG	+301	GCCAAGGCTGTGGGCAAGGT	+659

The amplicon length of each primer is as follows; CD45 233bp (Whittle et al., 1999), vWF 272bp (designed by Dr Bates), VEGF-R1 332bp (designed by Dr Bates), VEGF-R2 332bp (Fakhari et al., 2002), VEGF-R3 358bp (Shushanov et al., 2000), Np-1 504bp (Fakhari et al., 2002) and glyceraldehyde-3-phosphate dehydrogenase (GAPDH) 358bp (designed by Dr Bates). The annealing temperature for each primer pair was 55°C.

3.2.4 VEGF-immunogold labelling EM analysis

I did the analysis on the immuno-gold labelled anti-VEGF probed EM sections, kindly provided by Miss R. Hole. Podocyte (intracellular or membrane associated), glomerular basement membrane and glomerular endothelial cell associated VEGF labelled gold particles were counted in 16 random fields from 4 different kidneys. Colloidal gold particles were considered membrane associated if they were within 2 particle widths (i.e. 30nm) of the membrane on either side. Data were presented as mean + standards errors. Two tailed paired *t*-tests were used to compare paired data on the same cells, unpaired *t*-tests to compare separate cell populations treated differently. ANOVA was used to compare distribution of gold particles.

3.2.5 Western blotting- expression of VEGF receptors

Serum starved PCPs were treated with 1nM recombinant VEGF protein (a kind gift from Professor N. Ferrara, Genetec) for 20 minutes and serum starved hCIPs were treated with 1nM recombinant VEGF-C protein (a kind gift from Professor K. Alitalo). VEGF-C protein was then quantified and subjected to SDS PAGE, transfer to PVDF membrane and immunodetection. The membrane containing VEGF treated PCP protein was probed with 0.6μg/ml goat polyclonal IgG anti-Flt-1 (C-17)-G (VEGF-R1) (Santa Cruz Biotechnology, Heidleberg, Germany) and 0.03μg/ml HRP conjugated donkey polyclonal anti-goat IgG secondary antibody (Santa Cruz Biotechnology, Heidleberg, Germany) in 5% non-fat milk blocking solution. The membrane containing VEGF-C treated hCIP protein was probed with 0.5μg/ml rabbit polyclonal IgG anti-Flt-4 (C-20) (VEGF-R3) (Santa Cruz Biotechnology, Heidleberg, Germany) and 0.03μg/ml HRP conjugated goat polyclonal anti-rabbit IgG secondary antibody in 5% non-fat milk blocking solution.

3.3 Results

3.3.1 Characterisation of PCPs

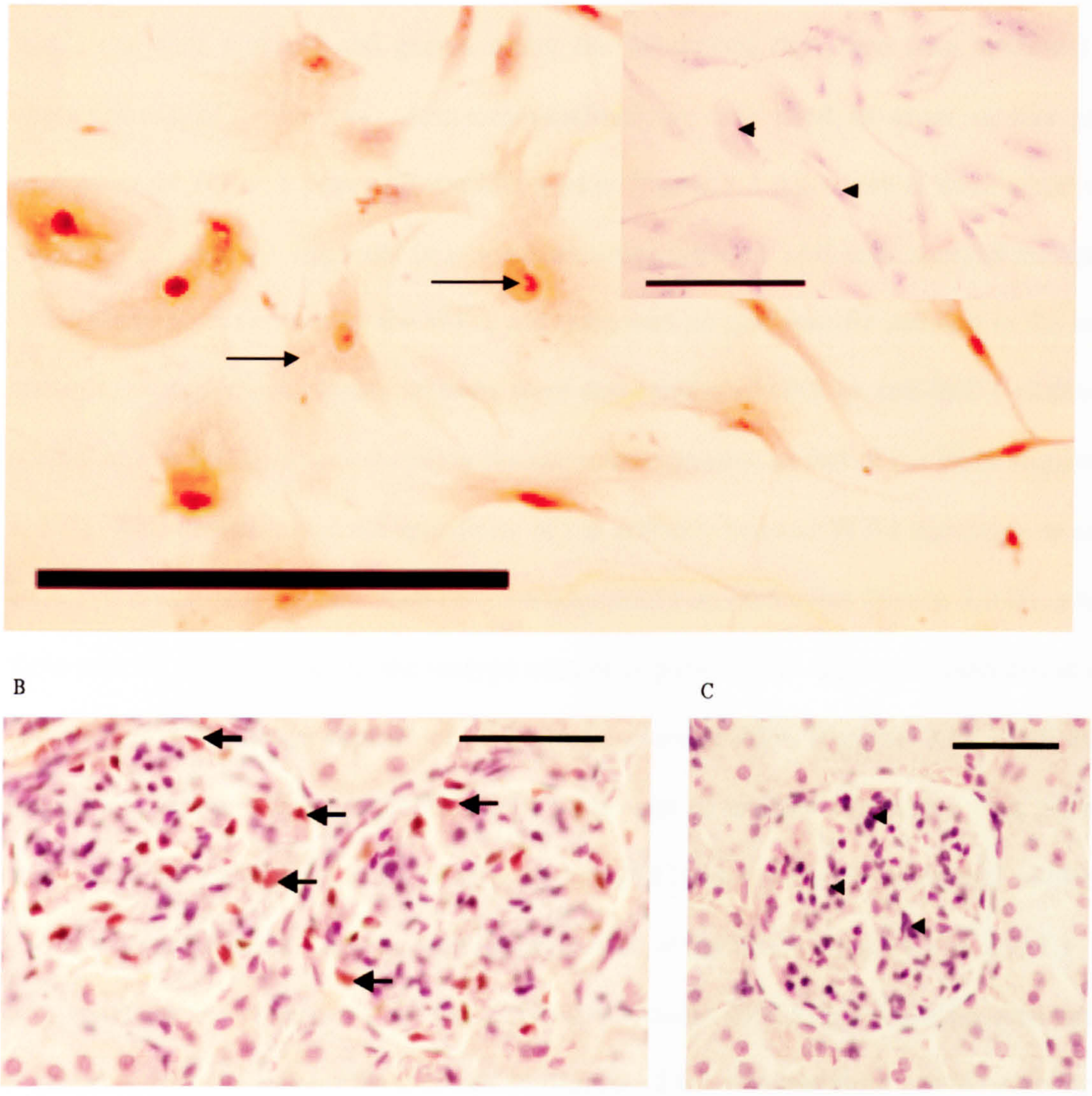

Figure 3.2. PCPs stain positively for WT-1.

A. Podocytes were incubated with an antibody specific to the podocyte marker, WT-1, showed brown nuclear and cytoplasmic staining (shown by arrows), confirming the expression of this molecule. Cells incubated with the normal isotype control (IgG) were counterstained with haematoxylin (inset top RH corner), which is the blue nuclear stain (shown by the arrowheads), and did not show any brown staining.

The anti-WT-1 antibody was optimised using rat glomeruli tissue sections. B. An example of brown nuclear staining (shown by arrow) of podocytes within the rat glomerulus, demonstrating specificity of the antibody. C. An example of rat glomeruli tissue sections incubated with the normal isotype control (IgG) and counterstained with haematoxylin (arrows), which did not show any brown staining (50μm scale bar).

The use of PCPs is widespread but remains controversial. It was necessary to test that in my hands the cells isolated and grown under the conditions described (see methods) were characteristic of podocytes. Immunocytochemistry was used to show *in situ* protein expression of WT-1, a podocyte specific marker (figure 3.2 A), which is not limited to any stage of podocyte development (e.g. not a maturity marker). All cells showed nuclear and cytoplasmic positive staining for WT-1 and there was no non-specific staining in the isotype controls. Rat glomeruli tissue sections were also incubated with an anti-WT-1 antibody or normal mouse IgG (isotype control) at the same concentration as that of the PCPs (figure3.2 B and C). This demonstrated the specificity of the antibody because WT-1 staining was seen in cells that could only be described micro-anatomically as podocytes (figure 3.2 B), whereas there was no staining seen in the isotype control (figure 3.2C). Immunohistochemistry was also used to demonstrate absence of PECAM-1 protein in PCPs (figure 3.3A), a cell surface endothelial cell specific marker. No cells were seen to express PECAM-1. Rat glomeruli tissue sections were also incubated with an anti-PECAM-1 antibody or normal mouse IgG (isotype control) at the same concentration as that of the PCPs (figure3.3 B and C). This demonstrated the specificity of the antibody because PECAM-1 staining was seen in endothelial cells throughout the glomerulus (figure 3.2 B), whereas there was no staining seen in the isotype control (figure 3.2C).

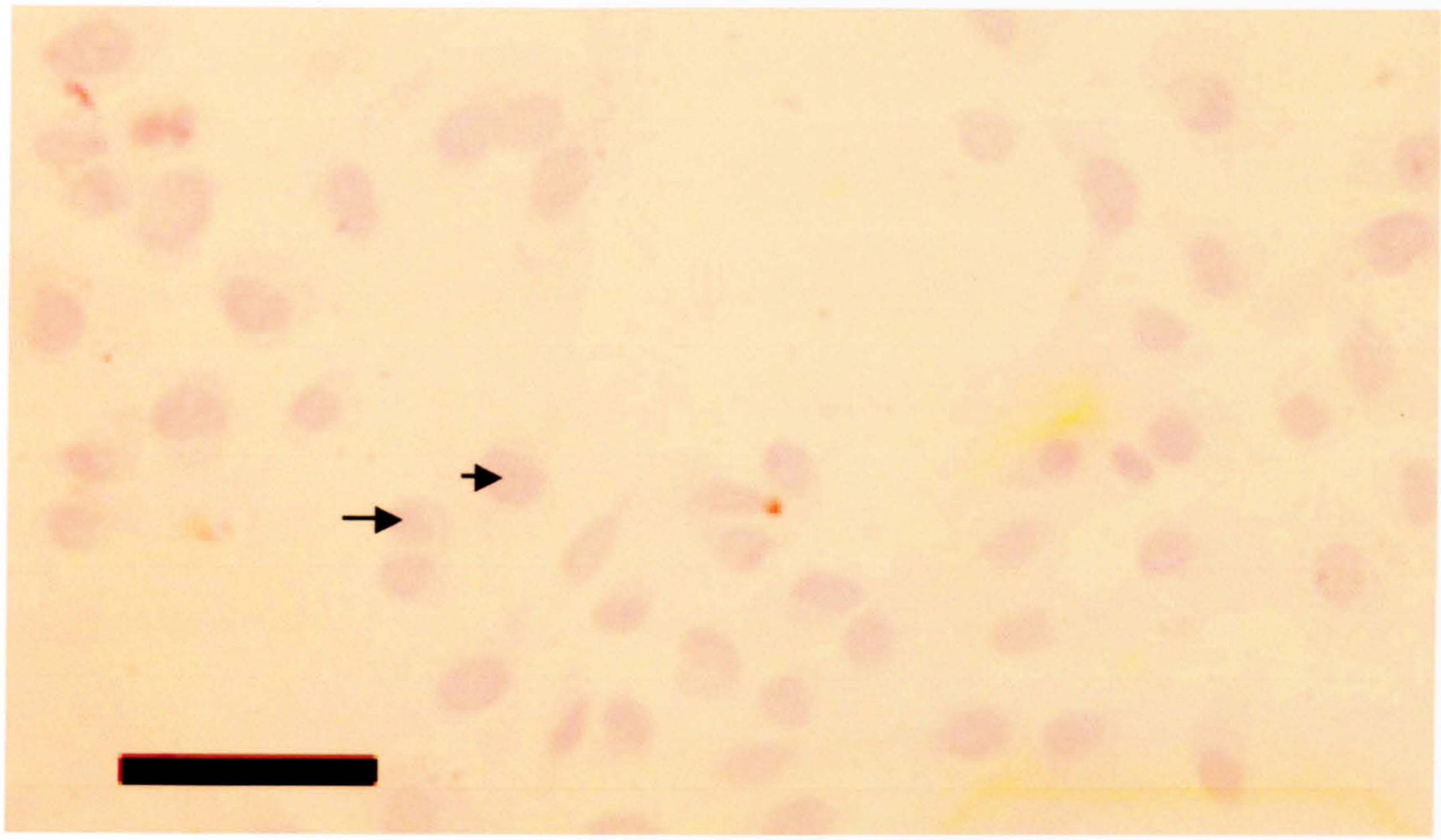

Figure 3.3. PCPs are negative for PECAM-1 staining

A. PCPs, incubated with an antibody to the endothelial specific marker, PECAM-1, did not show brown staining, indicating that this molecule was not expressed and that endothelial contamination of the cell culture was negligible. Cells were counterstained with haematoxylin, which is the blue nuclear stain shown by the arrowheads (scalebar = 100μm). The anti-PECAM-1 antibody was optimised using rat glomeruli tissue sections. B. An example of brown cytoplasmic and nuclear staining (shown by arrow) of enodthelial

cells within the glomerulus, demonstrating specificity of the antibody. C. An example of rat glomeruli tissue sections incubated with the normal isotype control (IgG) and counterstained with haematoxylin (arrows), which did not show any brown staining (50μm scale bar).

The cells were also characterised using PCR, a more sensitive technique, to test if the cell population was contaminated. Primers were chosen or designed to amplify cDNA for von Willebrand Factor (vWF), a vascular endothelial cell marker and CD45, a cell surface marker of leukocytes. HUVECs and human liver tissue cDNA were used to show that the reaction, using the CD45 and vWF primers, was able to result in a product of a length consistent with the sequence the primers were designed against. Dep. H_2O was used to show that the cDNA samples were not contaminated (Figure 3.4). Primers for GAPDH, a housekeeping gene, showed that all of the samples contained mRNA that had been successfully reverse transcribed to cDNA. There were no vWF or CD45 bands in the PCP cDNA samples. Together these results support the view that contamination of the isolated PCPs with endothelial cells or leucocytes was negligible.

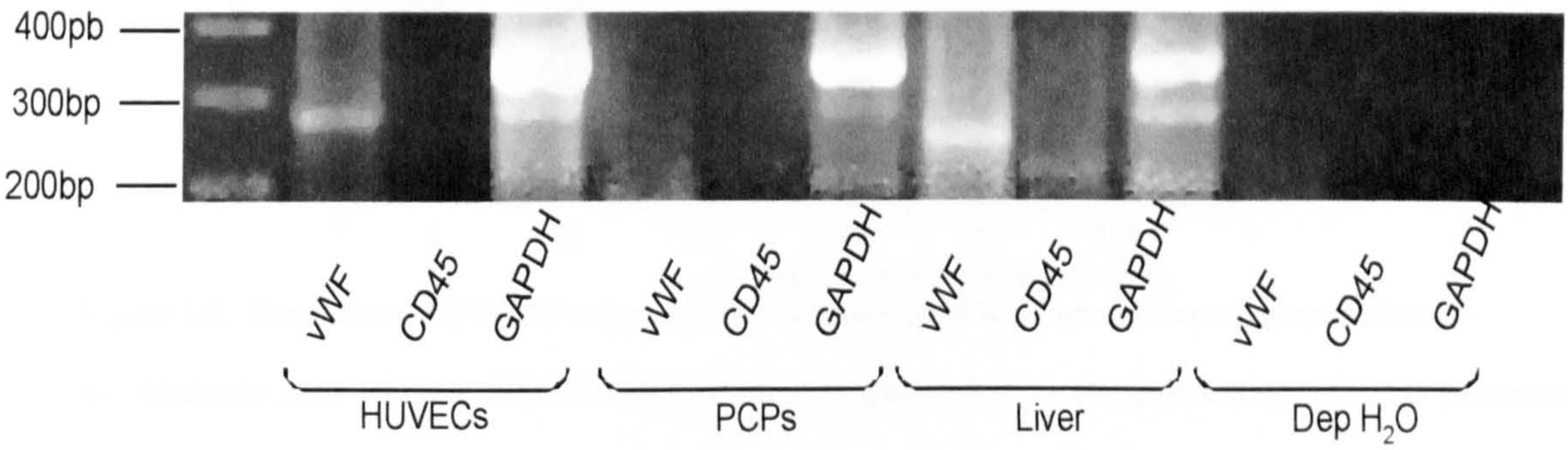

Figure 3.4. PCPs are not contaminated by endothelial cells or leukocytes.

PCP, HUVEC and human liver tissue mRNA was probed with primers specifically designed to amplify vWF (272bp) or CD45 (233bp) mRNA. VWF and CD45 mRNA were amplified in HUVEC and human liver tissue mRNA, but was absent from PCP mRNA. GAPDH (385bp) was amplified in all mRNA samples, and there was no amplification of either vWF or CD45 in samples where mRNA was replaced with Dep. H_2O.

These results demonstrate that the PCP isolation system is suitable to investigate the effects of VEGF on podocyte biology. The first stage of this investigation was to test the means by which VEGF could have an effect on podocytes. The investigation was, therefore, directed towards examining the possible expression of VEGF specific receptors.

3.3.2 VEGF receptor expression in cultured podocytes

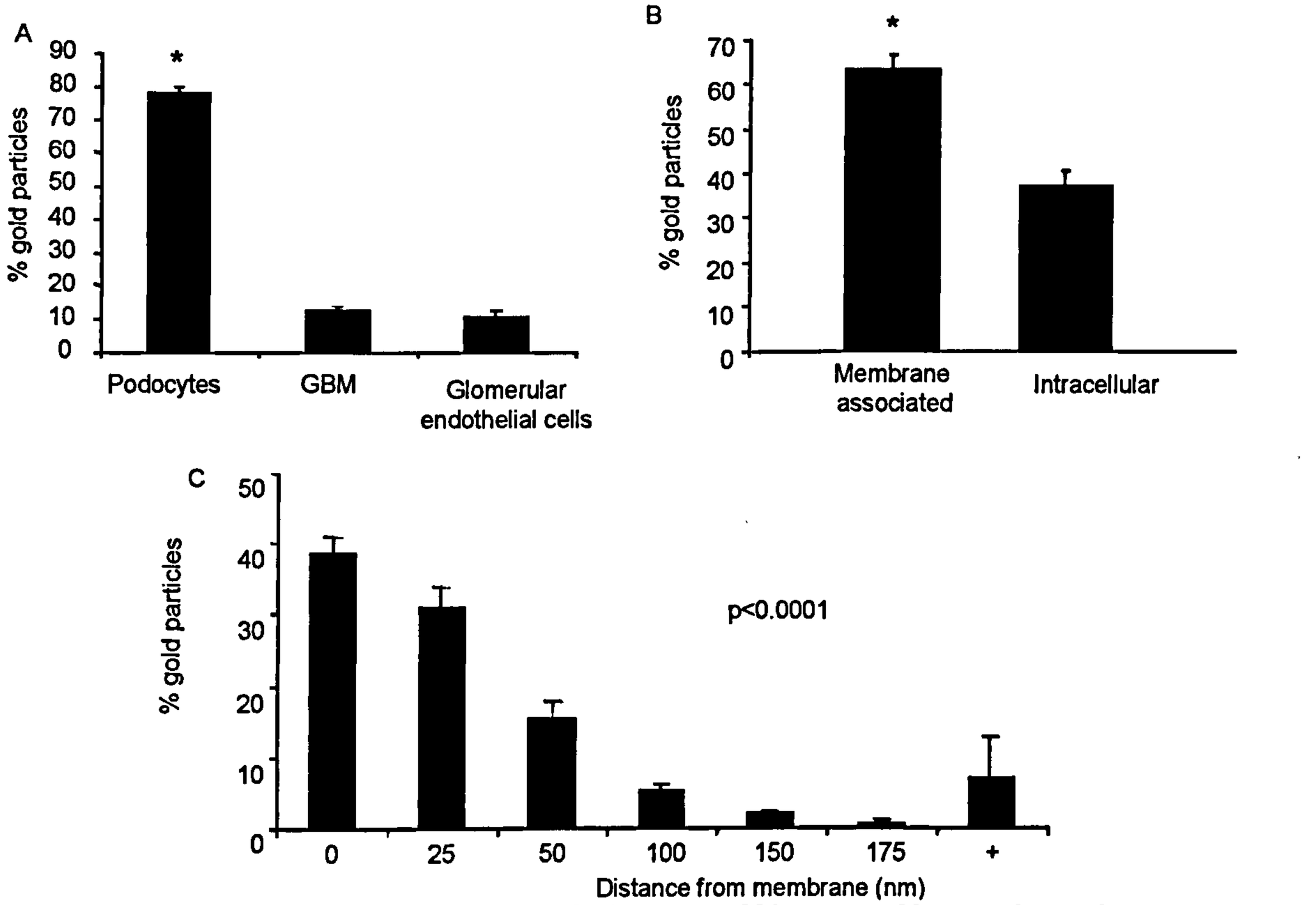

Figure 3.5. Distribution of VEGF expression by immuno-gold in a normal human glomerulus.

A. Immuno-gold labelled VEGF distribution was quantified as the percentage of total immuno-gold particles, the distribution was measured within the three components of the glomerular filtration barrier (Mean+SEM). The majority of immuno-gold labelled VEGF was found in the podocytes of the filtration barrier. B. Immuno-gold labelled VEGF distribution was quantified within podocyte foot processes, and distinguished as either membrane (>25nm) associated or intracellular (<25nm) (mean+SEM). A greater proportion of immuno-gold labelled VEGF was podocyte membrane associated. C. Immuno-gold labelled VEGF distribution was quantified as the percentage of total gold particles, measured at 25nm intervals from the membrane the podocyte plasma membrane. The quantity of immuno-gold labelled VEGF

declined with distance from the podocyte plasma membrane. Results significantly different using ANOVA or unpaired *t*-test. *=p<0.05, n=11

The distribution of glomerular VEGF was examined to provide clues as to the site(s) of VEGF binding activation. EM sections of human renal cortex tissue, which had been probed with immuno-gold labelled anti-VEGF were provided, courtesy of Rachel Hole. The distribution of gold particles was measured and categorised according to whether they were podocyte, endothelial cell or GBM bound. Podocyte bound gold particles were then identified as either membrane associated (within 25nm of the membrane) or intracellular. Podocyte bound gold particles were also categorised into distances from the membrane, in groups of 25nm from 0 to 175nm+ from the plasma membrane. The distribution of immuo-gold labelled anti-VEGF particles were significantly higher in podocytes (77.9±1.81% of total gold particles) than in the GBM (11.9±1.2% of total gold particles) or the glomerular endothelial cells (10.2±1.6% of total gold particles, figure 3.5 A, $p<0.05$, ANOVA). This suggests that although VEGF was diffusing to the endothelial cells much of it was retained within the podocytes or at their surface. This may be because VEGF was expressed, but had not yet been excreted from the podocytes. The majority of immuno-gold labelled anti-VEGF particles, however, were membrane associated and of the podocyte foot process membrane bound immuno-gold labelled anti-VEGF, 63.15±3.29% of total gold particles were plasma membrane associated, whereas only 36.85±3.29% of total gold particles were intracellular (figure 3.5 B, $p<0.05$, unpaired *t* -test). Immuno-gold labelled VEGF membrane association may have been due to glycocalyx bound VEGF, therefore the distribution of VEGF labelled immuno-gold particles from the podocyte plasma membrane were examined. Figure 3.5 C shows that the majority of VEGF immuno-gold labelled particles were tightly membrane associated (<50nm from the membrane) ($P<0.0001$, ANOVA), and that there was progressively reduced immuno-gold labelled VEGF, progressively further from the podocyte plasma membrane. Together, these

results show that the majority of podocyte VEGF is tightly membrane bound, suggesting that VEGF binds to the podocyte plasma membrane. The next stage therefore was to investigate if podocytes express any VEGF receptors, other than Np-1.

mRNA was extracted from human kidney tissue and hCIPs and primers were used to amplify VEGF-R1, VEGF-R2, VEGF-R3 and GAPDH mRNA expression. PCR products of the size predicted for VEGF-R1, R3 and Np-1 were seen after agarose gel electrophoresis of the PCR reaction and ethidium bromide staining (figure 3.6). This technique was used with this particular cell line because of its sensitivity and there was no possibility of amplifying receptors from small contaminating cell populations because hCIPs is a cell line developed from one clone. This experiment was performed once.

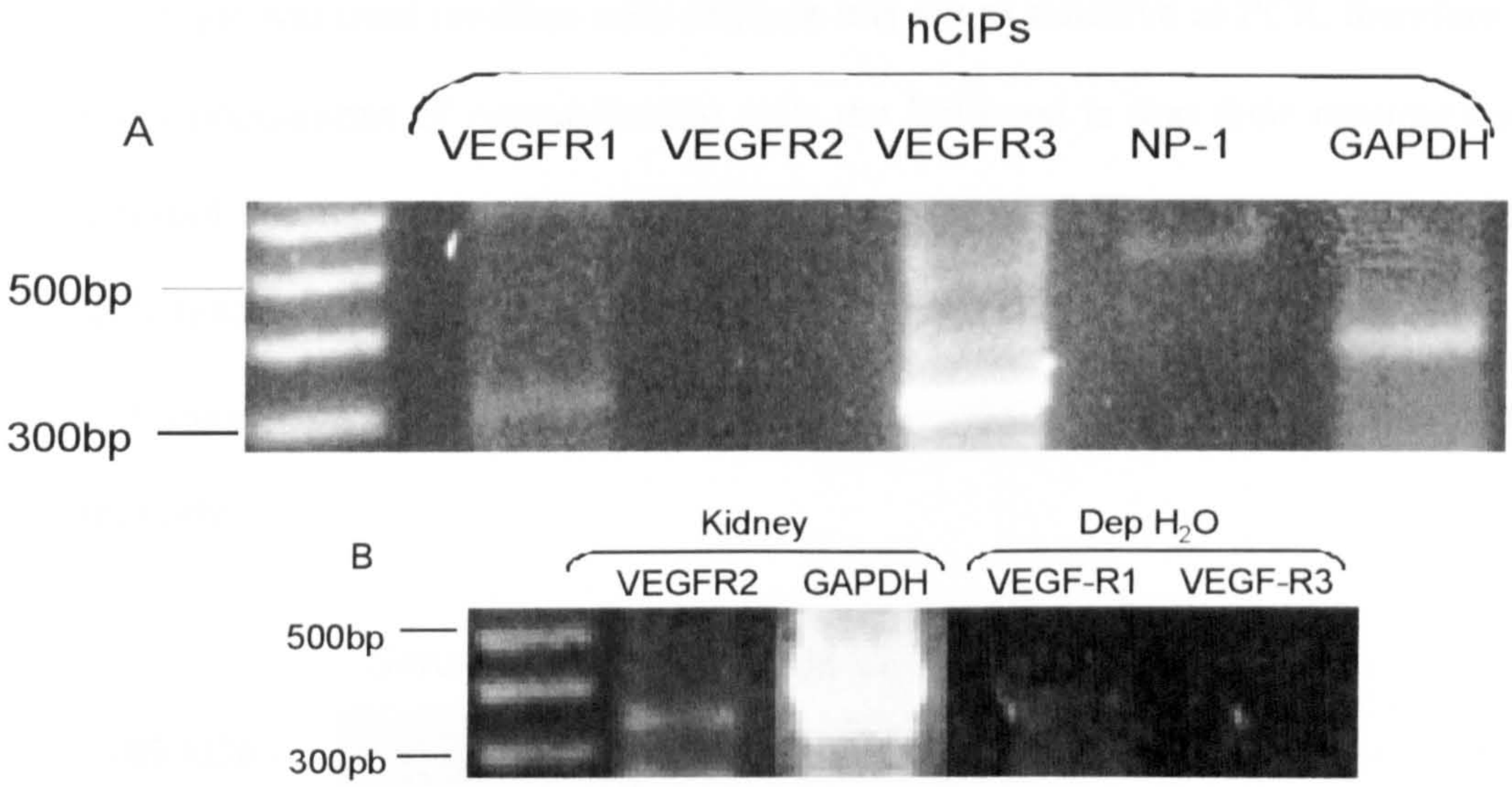

Figure 3.6. mRNA expression of VEGF receptors in cultured podocytes and human kidney tissue

A. PCR products of the predicted size were seen for VEGF-R1 (332bp), VEGF-R3 (358bp), and Np-1 (504bp) hCIP mRNA, whereas a PCR product of the predicted size was not seen for VEGF-R2 (332bp) in hCIPs. A PCR product of the predicted size was seen for GAPDH (358bp), demonstrating that the hCIP mRNA had been successfully reverse transcribed to cDNA. B. PCR products of the predicted size were seen for VEGF-R2 and GAPDH in human kidney tissue, demonstrating that the VEGF-R2 primers could detect VEGF-R2, and that the kidney tissue mRNA had been successfully reverse transcribed. There were

no PCR products of predicted size for VEGF-R1 and VEGF-R3 in Dep. H_2O samples, demonstrating that the PCR products, seen in A, were not due to contamination, n=1.

There were no PCR products of the predicted size for any of the primers when the mRNA was replaced with Dep. H_2O. This demonstrated that PCR products of predicted size were specific to the mRNA sample used. There was no PCR product of predicted size in hCIP mRNA when probed with VEGF-R2 primers (figure 3.6), although there was in human kidney tissue mRNA samples when probed with VEGF-R2 primers. This suggests that although hCIPs do not express VEGF-R2 mRNA, VEGF-R2 primers do amplify PCR products of the predicted length in mRNA samples known to express VEGF-R2 mRNA.

VEGF-R1 protein expression was also examined in PCPs using Western blotting. This technique was used for these cells because it is not as sensitive as PCR, therefore if there were small populations of contaminating cells the liklihood is that their receptors would not be detected because expression levels would be so low. PCPs were serum starved and treated with 1nM VEGF or left untreated for 24hrs. Protein was extracted, subjected to SDS PAGE and transferred to a PVDF membrane. The membrane was probed with an anti-VEGFR-1 antibody.

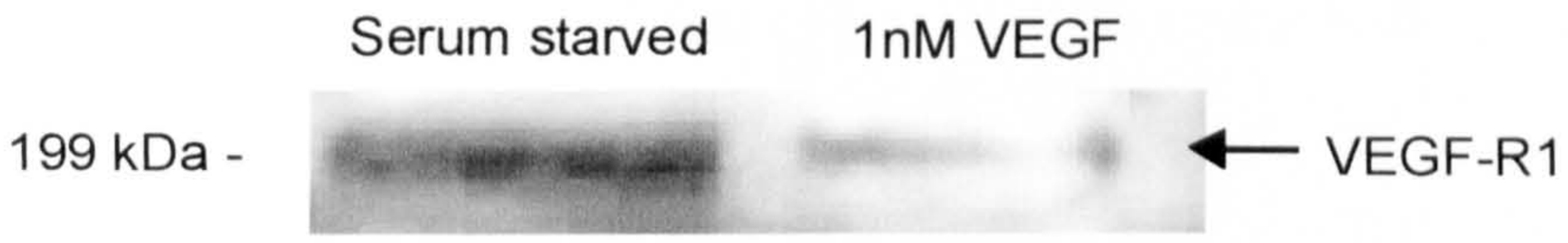

Figure 3.7. Protein expression of VEGF-R1 in PCPs

Serum starved PCPs were treated with 1nM VEGF or left untreated for 24hrs. A PVDF membrane containing the protein from these cells was probed with an anti-VEGF-R1 antibody. A band at the predicted molecular weight of 200kDa was seen, although it appeared less intense in the VEGF treated PCPs that the serum starved PCPs.

Figure 3.7 clearly demonstrates a band corresponding to the predicted size of VEGF-R1 protein (200kDa). These results suggest that VEGF-R1 protein is expressed by PCPs and it appears that treatment with VEGF actually lowered its expression (figure 3.7). These results demonstrate that VEGF-R1 was transcribed from the mRNA in PCPs. To determine whether VEGF-R3 was also transcribed from mRNA in cultured podocytes, a PVDF membrane containing protein, this time from hCIPs treated with 1nM VEGF-C (the ligand for VEGF-R3) and probed with anti-VEGFR-3, showed clear expression of VEGF-R3 protein (figure 3.8). As observed previously, treatment appeared to lower VEGF-R3 expression.

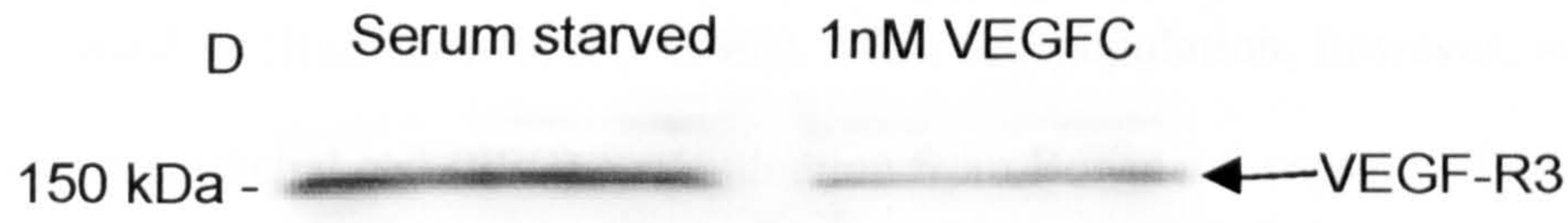

Figure 3.8. Protein expression of VEGF-R3 in hCIPs

A band at the predicted molecular weight of 150 kDa was seen in protein samples extracted from hCIPs, either serum starved or treated with 1nM VEGF -C, when probed with anti-VEGF-R3 antibody.

These results demonstrate for the first time that cultured podocytes express VEGF-R1 and VEGF-R3 mRNA and protein as well as Np-1, which has already been demonstrated. Surprisingly VEGF-R2 mRNA was not expressed.

3.4 Discussion

PCPs were successfully characterised; glomerular endothelial cell and leukocyte contamination was excluded. The cells stained positively for WT-1 mRNA and protein (a marker for podocytes), negative for vWF (a vascular endothelial marker), and CD45 (an adhesive molecule found on leukocytes). The entire immunocytochemical cell population viewed showed positive WT-1 staining and this in itself suggests that there was no significant contamination of either endothelial cells or mesangial cells. In addition, podocytes have a morphology distinct from mesangial cells, which have a rod like or stellate morphology (as discussed in (Buniatian et al., 1999)). The cell population, however, was not checked for parietal epithelial cell (PEC) contamination from Bowmans' capsule. There is some confusion in the literature over PEC specific markers to differentiate PECs from podocytes. Yaoita et al used pan cadherin as a specific marker for PECs (Yaoita et al., 2001). P-cadherin, however, is found in association with the slit diaphragm in differentiated podocytes and is also expressed by de-differentiated podocytes (Reiser et al., 2000a). Pan cadherin, therefore, is not a specific marker for parietal cells. PECs also express WT-1 in the mature kidney (<30% expression of PECs), a marker that was thought to be specific to podocytes (Kanemoto et al., 2003). The immunocytochemistry results in figure 3.2, however, demonstrated a uniform population of WT-1 expressing cells. WT-1 was chosen as a podocyte specific marker in this investigation, instead of a podocyte maturity marker, such as nephrin, which is not expressed by PECs, because the PCPs have a mixed population of differentiation. I cannot exclude some minor PEC contamination but have done my utmost to minimise this. It is worth noting, however, that the PCPs were isolated using the same protocol that was used to isolate and subclone the human conditionally immortalised podocytes, which have been fully characterised. PCPs also responded in the same way as hCIPs in later functional experiments, which suggests they are

of the same origin. Although the PCP isolation technique used in this chapter appears to be successful the cells had to be characterised after each isolation, yet the cells only last a few passages before they become senescent. These cells were used at the beginning of this investigation, mainly because the conditionally immortalised cell line, described in the methods, were not yet fully characterised. PCPs and hCIPs were, therefore, used as appropriate, and when available.

I have shown that cultured podocytes express mRNA for VEGF-R1 in hCIPs and protein for VEGF-R1 in PCPs and that hCIPs express both mRNA and protein for VEGF-R3, but VEGF-R2 was not shown to be expressed in either cell line. In support of VEGF-R1 expression Dr S. Chen (Renal-Electrolyte and Hypertension Division, University of Pennsylvania, Philadelphia) demonstrated VEGF-R1 mRNA expression in mouse CIPs (Mundelocytes) and had it successfully sequenced (unpublished abstract at the 5th International Symposium on Podocyte Biology in Seattle). Further on in the thesis evidence on functional effects of VEGF (especially those blocked with a class III tyrosine kinase inhibitor) support the evidence for VEGF-R1 expression because VEGF has not been shown to be a ligand for VEGF-R3 and it is controversial whether Np-1 can signal independently. In support of VEGF-R3 expression in cultured podocytes Dr S. Satchell (Academic Renal Unit, Southmead Hospital, Bristol) has demonstrated protein expression in hCIPs (a different clone to those used in this thesis) at both de-differentiation and differentiation (unpublished). This evidence for podocyte VEGF receptor expression, other than Np-1 opens up a new area of research. It is surprising that VEGF-R2 was not expressed, as this is the receptor that is involved in most biological functions of VEGF (Zachary and Gliki, 2001).

VEGF-R1 binds VEGF with a greater affinity then VEGF-R2 (Neufeld et al., 1999), but its signalling potential is limited because the tyrosine kinase activity of VEGF-R1 is one order of magnitude lower than that of VEGF-R2 (as reviewed in (Shibuya, 2001)). It has been shown that VEGF can stimulate the induction of hepatocyte growth factor (HGF) through VEGF-R1 activation in sinusoidal endothelial cells (LeCouter et al., 2003). In this manner VEGF-R1 has an indirect survival effect due to the nature of HGF. Interestingly, HGF can protect podocytes from Cyclosporin A induced apoptosis via regulation of Bcl-2_x by the PI3-kinase/AKT pathway (Fornoni et al., 2001) and it is possible that VEGF-R1 can activate a similar pathway in podocytes. Monocytes also express VEGF-R1, but not VEGF-R2 and in these cells VEGF-R1 is capable of mediating a chemotactic response to VEGF (Barleon et al., 1996). This raises possibilities that VEGF-R1, in response to VEGF, may be involved in development or differentiation of podocytes. An important consideration to make is that VEGF-R1 is capable of binding to, and forming complexes with Np-1 (as reviewed in (Neufeld et al., 2002)) and Np-2 (Gluzman-Poltorak et al., 2001), which are also expressed on podocytes at least at the mRNA level (Harper et al., 2001). VEGF-R3 and its ligand VEGF-C are mainly found in the lymphatic system. There is no evidence in the literature to show a direct interaction of VEGF with VEGF-R3. Therefore VEGF-C was used as a ligand for VEGF-R3 in the Western blot shown in figure 3.7. VEGF-C and VEGF-R3 will be discussed in detail later in the thesis.

The protein expression of both VEGF-R2 and VEGF-R3 upon activation with their ligands, compared to serum starvation (figures 3.6 and 3.7), was reduced. This was not significant because there were no replicates, however it was clearly seen in both blots. This may be explained by VEGF/VEGF-R2 complex internalisation by endocytosis in bovine adrenal cortex endothelial cells (Li and Keller, 2000): VEGF labelled with a fluorescent probe was detected in vesicular organelles within three minutes of VEGF treatment, lasting for hours. If

VEGF/VEGF-R1 and VEGF-C/VEGF-R3 complexes were also internalised then this may explain the reduction in protein expression seen: vesicular VEGF would be harder to lyse during protein extraction, if it had not already been taken into the endosome and lysed.

These results suggest that cultured podocytes express VEGF-R1 and VEGF-R3 along with Np-1, and that VEGF protein is frequently tightly associated with the podocyte plasma membrane. VEGF may therefore be capable of acting on podocytes in an autocrine manner. Some of the work from this chapter was published in paper 1 of the list of publications arising from this work.

Chapter 4

VEGF can exert a signalling response in cultured podocytes

4.1 Introduction

In the previous chapter I showed that podocytes express VEGF receptors. VEGF has been shown to exert its effects through many signalling pathways in endothelial cells. The first pathway identified stimulated an increase in $[Ca^{2+}]_i$ (Criscuolo et al., 1989). In endothelial cells, VEGF induces a rapid transient increase in $[Ca^{2+}]_i$, via a phospholipase C γ (PLC) (Brock et al., 1991)-diacylglycerol (DAG) dependent, calcium store-independent transient receptor potential (TRP) channel pathway. This allows influx of extracellular calcium (Pocock et al., 2004). The increase in $[Ca^{2+}]_i$ can result in a number of biological actions in endothelial cells, such as nitric oxide dependent increased vessel dilatation (Ku et al., 1993), vessel permeability (Pocock et al., 2000) and alterations in the actin cytoskeleton (Criscuolo and Balledux, 1996). To investigate, therefore, if VEGF can exert an autocrine effect on podocytes $[Ca^{2+}]_i$ was measured to signify a cellular response to VEGF.

4.2 Methods

$[Ca^{2+}]_i$ measurements-VEGF signalling in podocytes

PCPs and hCIPs were incubated in Hanks' Balanced Salt Solution (HBSS) containing either minimal calcium (~200μM) or physiological levels of calcium (1.3mM) (for composition of HBSS see p.75 and p.76 of methods). Cells were loaded with Fura 2-AM for a minimum of 1hr and a maximum of 2hrs. They were treated with 1nM VEGF (0.4μl of 100ng/μl stock) or 0.4μl HBSS containing appropriate levels of calcium. Changes in Fura-2 fluorescence intensity were recorded and $[Ca^{2+}]_i$ concentrations were calculated from this, as described in the methods.

4.3 Results

4.3.1 The effects of VEGF on $[Ca^{2+}]_i$ in cultured podocytes

When PCPs, which had been loaded with Fura-2, were incubated in HBSS containing physiological levels of calcium (1.3mM), treatment with VEGF did not cause a change in $[Ca^{2+}]_i$ (Figure 4.1 A). The ratio (R) (treatment $[Ca^{2+}]_i$/baseline $[Ca^{2+}]_i$) did not significantly change (0.98±0.065) (Figure 4.1 E). When incubated in HBSS containing minimal calcium ($[Ca^{2+}]_o$), however, there was a reduction in $[Ca^{2+}]_i$ in VEGF treated cells, which was significant (0.69±0.07, $p<0.05$) (figure 4.1 E). The 2 fold reduction in $[Ca^{2+}]_i$ was rapid, occurring within the first four minutes, then reaching a plateau (figure 4.1 B). VEGF was then washed away using HBSS and left for 20 minutes, but it was observed that $[Ca^{2+}]_i$ levels did not return to original baseline levels. This was mirrored in differentiated hCIPs: there was no change in $[Ca^{2+}]_i$ in hCIPs, treated with VEGF, in the presence of 1.3mM $[Ca^{2+}]_o$ (figure 4.1 C). There was, however, a reduction in $[Ca^{2+}]_i$ in minimal $[Ca^{2+}]_o$ (figure 4.1 D), which was significant (minimal $[Ca^{2+}]_o$: R0.71±0.03 compared to 1.3mM $[Ca^{2+}]_o$ R1.03±0.2, $p<0.05$, figure 4.1 F). The 2 fold reduction in $[Ca^{2+}]_i$ in hCIPs, treated with VEGF and incubated in minimal $[Ca^{2+}]_o$ was again rapid and reached a plateau within the first five minutes (figure 4.1 D). Observations revealed that $[Ca^{2+}]_i$ levels did not return to original baseline levels after VEGF had been washed out of these cells either. These results demonstrate that not only did VEGF induce a reduction in $[Ca^{2+}]_i$ in cultured podocytes incubated in minimal $[Ca^{2+}]_o$, but that there was no difference in response to VEGF between the two types of cultured podocytes. This reduction in $[Ca^{2+}]_i$, in response to VEGF was the opposite to that seen in endothelial cells, and a reduction in $[Ca^{2+}]_i$ in response to VEGF has not actually been documented before in any cell type.

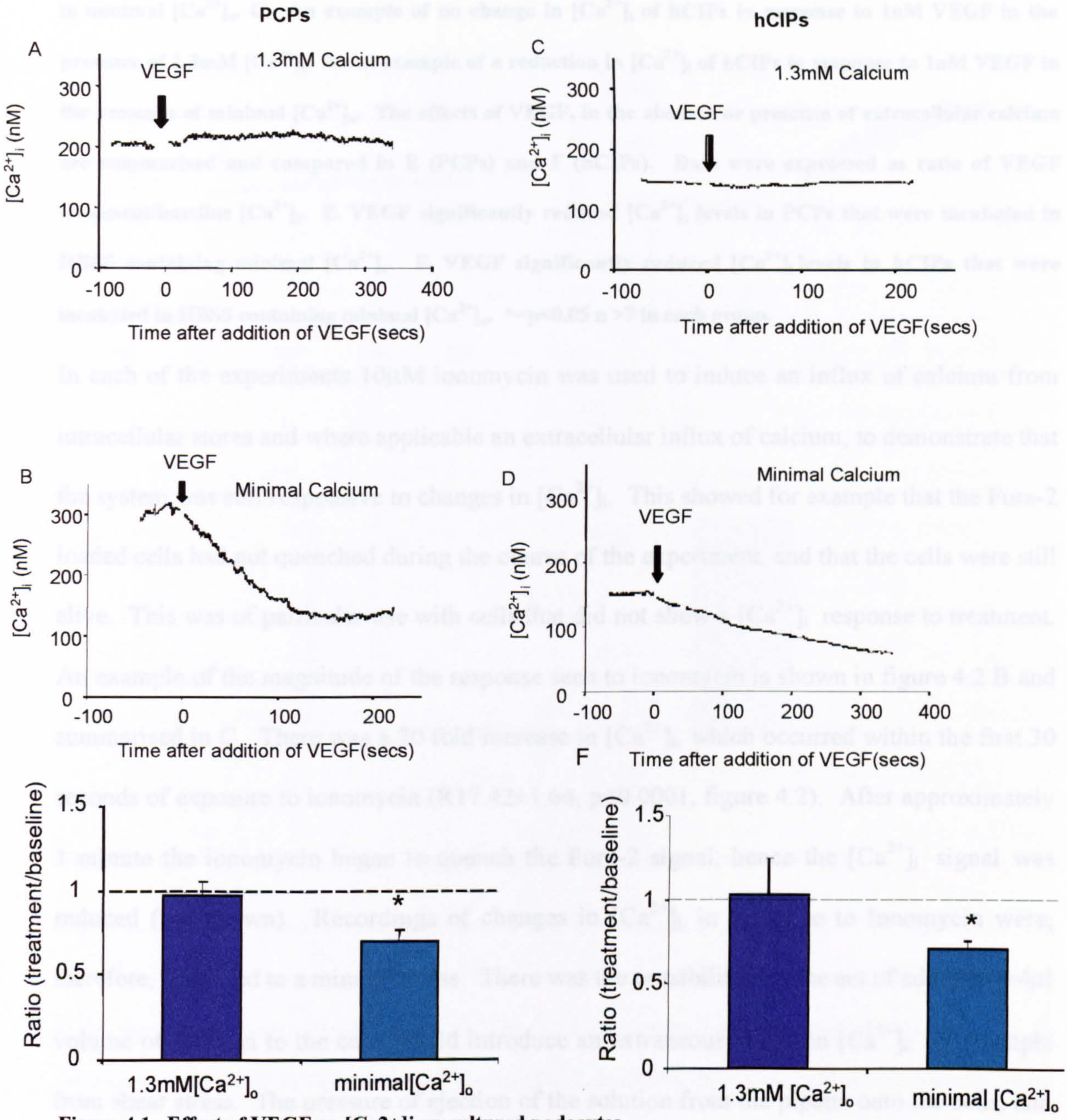

Figure 4.1. Effect of VEGF on [Ca2+]i on cultured podocytes.

PCPs and hCIPs were incubated in HBSS containing either minimal [Ca2+]o or 1.3mM [Ca2+]o , and were either treated with 1nM VEGF or left untreated. When cells were treated with 1nM VEGF in the presence of 1.3mM $[Ca^{2+}]_o$, no change was seen for either PCPs or hCIPs (A and C). When cells were treated with 1nM VEGF in minimal $[Ca^{2+}]_o$, however, a significant reduction in $[Ca^{2+}]_i$ was seen for both PCPs and hCIPs (B and D) .A. An example of no change in $[Ca^{2+}]_i$ of PCPs in response to 1nM VEGF in the presence of 1.3mM $[Ca^{2+}]_o$. B. An example of a reduction in $[Ca^{2+}]_i$ of PCPs in response to 1nM VEGF

in minimal $[Ca^{2+}]_o$. C. An example of no change in $[Ca^{2+}]_i$ of hCIPs in response to 1nM VEGF in the presence of 1.3mM $[Ca^{2+}]_o$. D. An example of a reduction in $[Ca^{2+}]_i$ of hCIPs in response to 1nM VEGF in the presence of minimal $[Ca^{2+}]_o$. The effects of VEGF, in the absence or presence of extracellular calcium are summarised and compared in E (PCPs) and F (hCIPs). Data were expressed as ratio of VEGF treatment/baseline $[Ca^{2+}]_i$. E. VEGF significantly reduced $[Ca^{2+}]_i$ levels in PCPs that were incubated in HBSS containing minimal $[Ca^{2+}]_o$. F. VEGF significantly reduced $[Ca^{2+}]_i$ levels in hCIPs that were incubated in HBSS containing minimal $[Ca^{2+}]_o$. *=$p<0.05$ n >7 in each group.

In each of the experiments 10μM ionomycin was used to induce an influx of calcium from intracellular stores and where applicable an extracellular influx of calcium, to demonstrate that the system was still responsive to changes in $[Ca^{2+}]_i$. This showed for example that the Fura-2 loaded cells had not quenched during the course of the experiment, and that the cells were still alive. This was of particular use with cells that did not show a $[Ca^{2+}]_i$ response to treatment. An example of the magnitude of the response seen to ionomycin is shown in figure 4.2 B and summarised in C. There was a 20 fold increase in $[Ca^{2+}]_i$, which occurred within the first 30 seconds of exposure to ionomycin (R17.42±1.64, $p<0.0001$, figure 4.2). After approximately 1 minute the ionomycin began to quench the Fura-2 signal, hence the $[Ca^{2+}]_i$ signal was reduced (not shown). Recordings of changes in $[Ca^{2+}]_i$, in response to Ionomycin were, therefore, restricted to a minute or less. There was the possibility that the act of adding a 0.4μl volume of solution to the cells would introduce an extraneous effect on $[Ca^{2+}]_i$, for example from shear stress. The pressure of ejection of the solution from the pipette onto the cells, and the disturbance of the cell surface of the media in which the cells were incubated, by the pipette tip could contribute to a change in $[Ca^{2+}]_i$. To test these variables 0.4μl of HBSS was added to the cells incubated in HBSS in the same manner as VEGF. The calcium concentration of HBSS used was appropriate to the calcium concentration used in that particular experiment. Addition of 0.4μl HBSS did not stimulate a change in $[Ca^{2+}]_i$ in hCIPs, as shown in figure 4.2 A and summarised in C (R0.96±0.02, n.s).

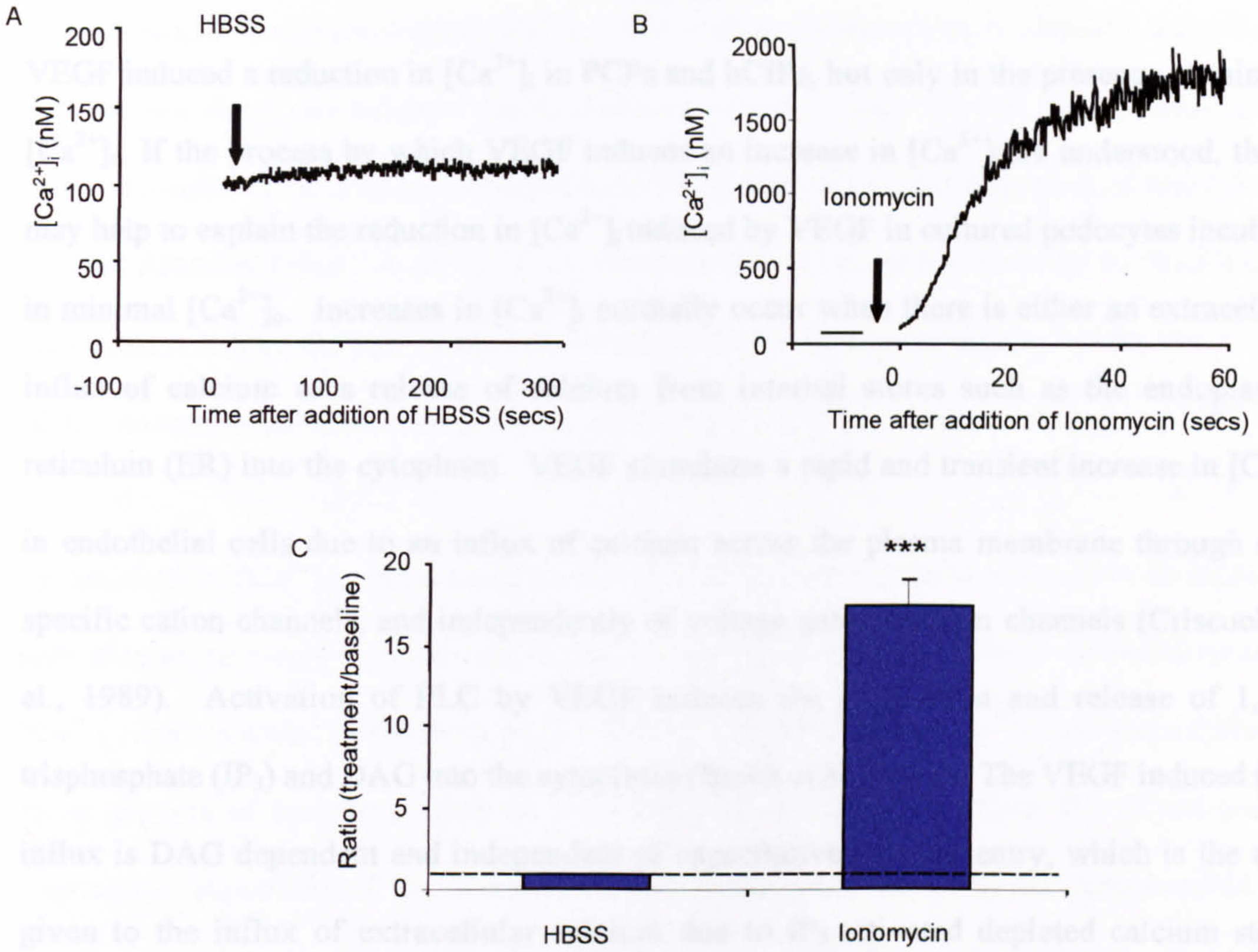

Figure 4.2. $[Ca^{2+}]_i$ responses to 0.4μl HBSS and to 10μM ionomycin in PCPs and hCIPs.

hCIPs and PCPs were loaded with Fura-2. The $[Ca^{2+}]_i$ response was measured when 0.4μl HBSS was added to hCIPs, showing no significant $[Ca^{2+}]_i$ response (A), and when 10μM ionomycin (1μl) was added to PCPs, showing a massive increase in $[Ca^{2+}]_i$ (B). A: An example of no significant change in $[Ca^{2+}]_i$ in response to 0.4μl HBSS in the presence of 1.3mM $[Ca^{2+}]_o$ in hCIPs. B. An example of a transient increase in $[Ca^{2+}]_i$ in PCPs in response to 10μM ionomycin. C. Data were expressed as mean+SEM of the changes in ratio of $[Ca^{2+}]_i$ (treatment/baseline). There was no change in $[Ca^{2+}]_i$ response to 0.4μl HBSS but there was a large increase in $[Ca^{2+}]_i$ in response to 10mM ionomycin in hCIPs. (n=6,*=p<0.0001, paired *t*-test).**

These results show that exogenous VEGF can act elicit a reduction in podocytes $[Ca^{2+}]_i$, but the actual role of VEGF in podocyte signalling or function has yet to be elucidated.

4.4 Discussion

VEGF induced a reduction in $[Ca^{2+}]_i$ in PCPs and hCIPs, but only in the presence of minimal $[Ca^{2+}]_o$. If the process by which VEGF induces an increase in $[Ca^{2+}]_i$ are understood, then it may help to explain the reduction in $[Ca^{2+}]_i$ induced by VEGF in cultured podocytes incubated in minimal $[Ca^{2+}]_o$. Increases in $[Ca^{2+}]_i$ normally occur when there is either an extracellular influx of calcium or a release of calcium from internal stores such as the endoplasmic reticulum (ER) into the cytoplasm. VEGF stimulates a rapid and transient increase in $[Ca^{2+}]_i$ in endothelial cells due to an influx of calcium across the plasma membrane through non-specific cation channels, and independently of voltage gated calcium channels (Criscuolo et al., 1989). Activation of PLC by VEGF induces the production and release of 1,4,5-trisphosphate (IP_3) and DAG into the cytoplasm (Brock et al., 1991). The VEGF induced Ca^{2+} influx is DAG dependent and independent of capacitative calcium entry, which is the term given to the influx of extracellular calcium due to IP_3 activated depleted calcium stores (Putney and McKay, 1999). The $[Ca^{2+}]_i$ response of podocytes to VEGF was the opposite of that seen in endothelial cells. This may be because VEGF induced $[Ca^{2+}]_i$ signalling in endothelial cells is thought to be VEGF-R2 activation dependent (Brock et al., 1991), and the VEGF induced $[Ca^{2+}]_i$ signalling in podocytes would have to be via a different VEGF receptor. The VEGF induced reduction in $[Ca^{2+}]_i$ in cultured podocytes indicates that calcium is either being pumped from the cytosol into intracellular stores by the sarco-endoplasmic reticulum calcium ATPase pump (SERCA), that ensures the re-uptake of calcium into the sarcoplasm (Lytton et al., 1991), or being pumped from the cytosol out of the cell by plasma membrane calcium ATPases (PMCA). It seems unlikely that the Na^+/Ca^{2+} exchange would be involved in this process as there is no evidence in the literature to suggest that it is expressed on podocytes and it tends to contribute more to Ca^{2+} transport in excitable cells (Sedova and

Blatter, 1999). The effects of VEGF on $[Ca^{2+}]_i$ in podocytes was masked, when incubated in HBSS containing a physiological $[Ca^{2+}]_o$. This may mean that there is normally a small leak into the cell down the calcium concentration gradient, or that the cell equilibrates itself if $[Ca^{2+}]_i$ is reduced. It is not understood how VEGF can induce the activation of these pumps or what function it has. A series of experiments would be needed in order to elucidate the mechanisms behind the $[Ca^{2+}]_i$ decline, which could be done in the future, but for the purpose of this investigation it has been accepted simply that VEGF can induce a change in $[Ca^{2+}]_i$.

An increase in $[Ca^{2+}]_i$ is often associated with detrimental effects in cells, such as increased necrosis (due to a very high increase in $[Ca^{2+}]_i$ levels) and apoptosis (due to lower increases in $[Ca^{2+}]_i$) (as reviewed in (Rizzuto et al., 2003)). An increase in $[Ca^{2+}]_i$ has been linked to many aspects of apoptosis, such as via release of cytochrome c from the mitochondrial membrane: Movement of Ca^{2+} from the ER, and subsequent uptake by the mitochondria (via the cytoplasm) can cause mitochondrial Ca^{2+} overloading. This induces the opening of the permeability transition pore in the mitochondrial membrane, leading to swelling of the mitochondria and the release of cytochrome c (as reviewed in (Rizzuto et al., 2003) (Gogvadze et al., 2001)). An increase in $[Ca^{2+}]_i$ can instigate cytotoxicity in many ways in many cell types, but increased $[Ca^{2+}]_i$ can also induce podocyte specific effects. For example Angiotensin-II stimulates a rapid, transient increase in $[Ca^{2+}]_i$. in podocytes, which is dependent on release from calcium stores and influx of extracellular calcium (Nitschke et al., 2000), probably via capacitative calcium store release (Putney and McKay, 1999). This demonstrates that the effects of angiotensin-II are dependent on an increase in $[Ca^{2+}]_i$. In addition Benigni et al show that the reduction in nephrin expression, seen in rats with severe nephrosis, could be fully inhibited by blocking the effects of angiotensin-II (Benigni et al., 2001). Nephrin is intricately linked to the actin cytoskeleton, as discussed in the introduction,

and any changes in nephrin expression are likely to have a knock-on effect on the actin cytoskeleton. The possible effects of the VEGF induced reduction in $[Ca^{2+}]_i$ therefore may be to regulate $[Ca^{2+}]_i$ homeostasis within the podocyte. This would only regulate changes in $[Ca^{2+}]_i$ levels within the same range as VEGF induced $[Ca^{2+}]_i$ changes, but may regulate podocyte cytoskeletal retraction via nephrin redistribution, or may regulate the other consequences of raised $[Ca^{2+}]_i$ levels, such as apoptosis.

In summary, these results show that VEGF can induce signalling in podocytes. I have therefore attempted to determine the effects of VEGF signalling on podocyte cell function. This work was published in paper 1 of the list of publications arising from this work.

Chapter 5

The effects of VEGF on proliferation and cytotoxicity in cultured podocytes

5.1 Introduction

The results from the previous chapter show that VEGF can induce a reduction in cytosolic calcium in podocytes. VEGF is a pluripotent growth factor and many of its functions relate to proliferation and survival. The next aim therefore was to decipher the role of VEGF in these signalling pathways in podocytes. To understand potential proliferation and survival signalling pathways in podocytes these pathways can be examined in endothelial cells in which VEGF promotes both proliferation and survival (as reviewed in (Ruhrberg, 2003)). In endothelial cells proliferation is regulated by the activation of VEGF-R2 by VEGF, which induces the activation of MAPK in a protein kinase C (PKC) dependent manner (Rousseau et al., 2000) (Wu et al., 2000). The activation of VEGF-R2 by VEGF in endothelial cells also induces the activation of PI3-kinase, which induces the phosphorylation of AKT (Gerber et al., 1998b). Subsequently, pro-apoptotic Bcl-2 family members are phosphorylated and de-activated by phosphorylated AKT (Gerber et al., 1998a). The activation of MAPK p38 by auto-phosphorylation of VEGF-R2 regulates migration via actin based motility in endothelial cells (Rousseau et al., 2000). Interestingly, the MAPK p38 migration pathway seems to negatively regulate the PI3-kinase/AKT survival pathway and vice versa in endothelial cells (Gratton et al., 2001) (figure 1.5, chapter 1) suggesting that survival signalling is greater when cells are not migrating. When podocytes are mature and terminally differentiated they have very limited proliferation, a very low turnover of cells and presumably relatively low migration compared to developing podocytes, which are proliferative. VEGF may therefore be exerting a proliferative and possibly migratory effect on podocytes during glomerulogenesis and may promote survival in podocytes in mature glomeruli. The effect of VEGF on PCP proliferation and on hCIP survival was therefore investigated using a ^{3}H-thymidine incorporation assay and a lactate dehydrogenase (LDH) assay respectively. The

effect of endogenous VEGF was also examined with the use of a neutralising monoclonal antibody to VEGF.

5.2 Methods

5.2.1 ^{3}H-thymidine assay-the effects of VEGF on podocyte proliferation

Serum starved PCPs were treated with 1nM VEGF (12 wells) in fresh serum free RPMI media or in fresh serum free RPMI media alone for 24hrs. ^{3}H-thymidine was added to all of the wells for just 4hrs and the cells were then counted, using a Students' haemocytometer and assayed for ^{3}H-thymidine incorporation using a scintillation counter.

5.2.2 LDH assay-the effects of VEGF on podocyte cytotoxicity

Serum starved PCPs and hCIPs were treated with 1nM VEGF (48 wells) in fresh serum free RPMI media or in fresh serum free RPMI media alone for 48 or 24hrs. In order to assess the role of endogenous VEGF PCPs were also treated with 0.32μg/ml mouse monoclonal IgG_{2A} neutralising anti-VEGF antibody (VEGF-Mab) in fresh serum free RPMI media by itself or with 1nM VEGF for 24hrs. Serum starved human embryonic kidney (HEK) 293 cells were also treated with VEGF and a neutralising monoclonal antibody to VEGF in serum free fresh Dulbeccos' Modified Eagles Media (DMEM, containing inorganic salts; 0.265g/L $CaCL_2 \cdot 2H_2O$, 0.0001g/L $Fe(NO_3)_3 \cdot 9H_2O$, 0.098g/L $MgSO_4$, 0.4g/L KCL, 3.7g/L $NaHCO_3$, 6.4g/L NaCl and 0.109g/L NaH_2PO_4) to demonstrate the effects were podocyte specific. The amount of LDH release into the media was quantified using a colourimetric assay for the low, experimental and high controls, as described in the methods. The percent of cytotoxicity was then calculated from this.

5.3 Results

5.3.1 The effects of VEGF on PCP proliferation

VEGF plays a role in endothelial organisation in glomerulogenesis, yet the role of VEGF on podocytes during glomerulogenesis had never been documented. The reason for this is mainly that VEGF receptor expression on podocytes has not been published. A prime role of VEGF during development is mitogenesis, therefore the effects of VEGF on cultured podocyte proliferation was examined first. PCPs are proliferative, whereas differentiated hCIPs are not, therefore PCPs were used to investigate the effects of VEGF on podocyte proliferation.

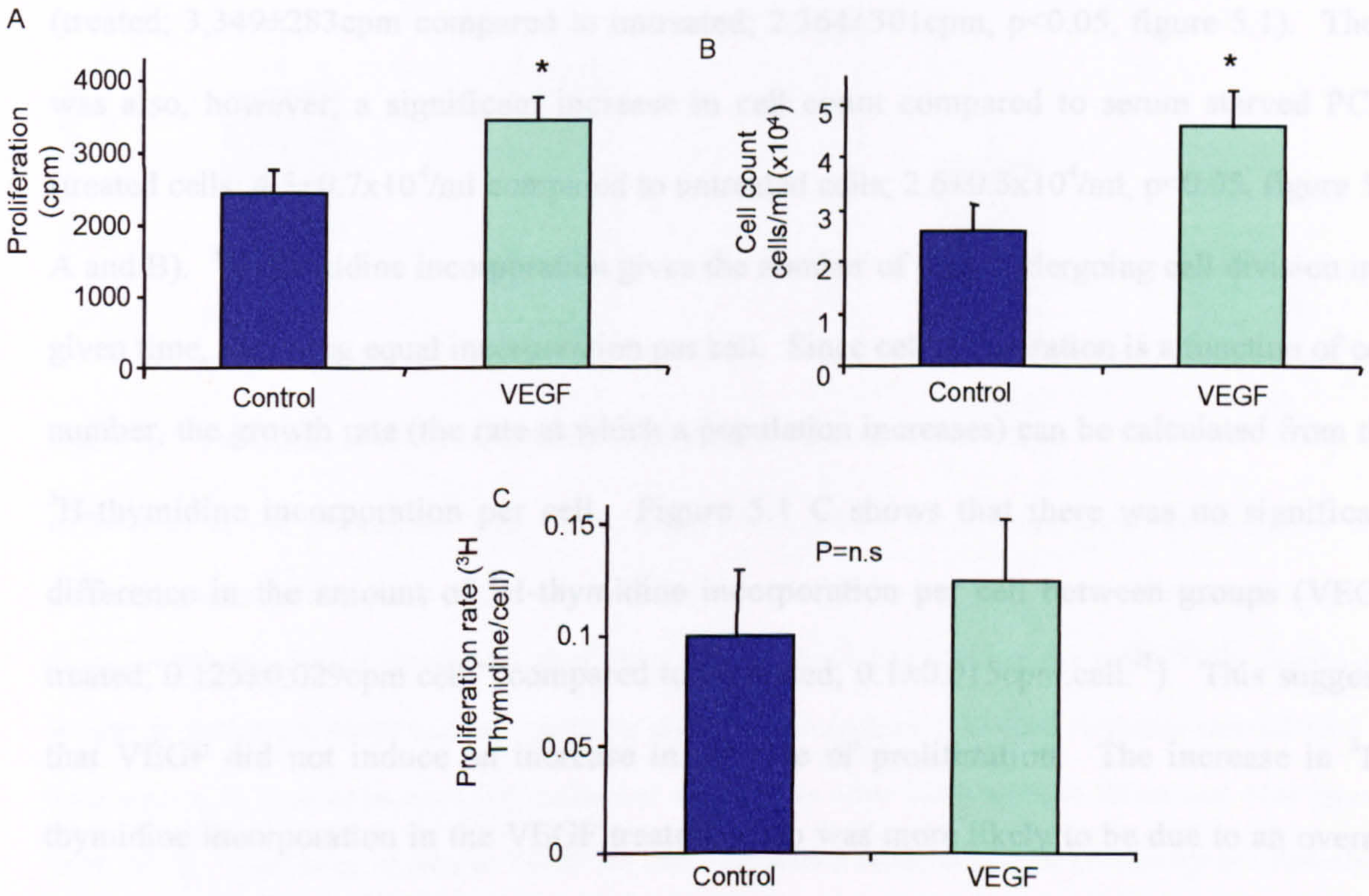

Figure 5.1. The effects of VEGF on PCP proliferation.

Serum starved PCPs were incubated in 1nM VEGF or left untreated. ^{3}H-thymidine was added and the cells were counted, then assayed for ^{3}H-thymidine incorporation. A. Data were expressed as mean+SEM cpm/^{3}H-thymidine of serum starved PCPs without (blue) and with (green) 1nM VEGF. ^{3}H-thymidine incorporation was significantly greater in PCPs incubated with VEGF then that of PCPs. B. Data were

expressed as mean+SEM cell count (cells/mlx10^4) without (blue) and with (green) 1nM VEGF. PCPs incubated with VEGF had a significantly higher cell count than untreated PCPs. C. Data were expressed as mean+SEM proliferation rate (^{3}H-thymidine/cpm.cell^{-1}) without (blue) and with (green) 1nM VEGF, *=p<0.05 compared to control, unpaired *t*-test, n = 12. There was no significant difference, however, in proliferation rate between PCPs incubated with VEGF or left untreated.

PCPs were serum starved in a 24 well plate for 16hrs, then were treated with 1nM VEGF or left untreated for 24 hrs. 1μCi ^{3}H-thymidine was added to each of the wells for 4hrs and then the cells were trypsinised, counted using a haemocytometer and then the samples were assayed for ^{3}H-thymidine incorporation using a scintillation counter. PCPs incubated with VEGF had a significantly greater amount of ^{3}H-thymidine incorporation compared to serum starved PCPs (treated; 3,349±283cpm compared to untreated; 2,364±301cpm, $p<0.05$, figure 5.1). There was also, however, a significant increase in cell count compared to serum starved PCPs (treated cells; 4.5±0.7x10^4/ml compared to untreated cells; 2.6±0.5x10^4/ml, $p<0.05$, figure 5.1 A and B). ^{3}H-thymidine incorporation gives the number of cells undergoing cell division in a given time, assuming equal incorporation per cell. Since cell proliferation is a function of cell number, the growth rate (the rate at which a population increases) can be calculated from the ^{3}H-thymidine incorporation per cell. Figure 5.1 C shows that there was no significant difference in the amount of ^{3}H-thymidine incorporation per cell between groups (VEGF treated; 0.125±0.029cpm.cell.$^{-1}$ compared to untreated; 0.1±0.015cpm.cell.$^{-1}$). This suggests that VEGF did not induce an increase in the rate of proliferation. The increase in ^{3}H-thymidine incorporation in the VEGF treated group was more likely to be due to an overall larger population of cells, which may be explained by a reduction in cell loss compared to the serum starved control, i.e. a reduction in cell death.

5.3.2 The effects of VEGF on cytotoxicity in podocytes

As there appeared to be an increase in cell survival stimulated by VEGF, the effect of VEGF on cytotoxicity of cultured podocytes was primarily tested on PCPs. PCPs were serum starved for 16 hrs then treated with 1nM VEGF or left untreated for either 24hrs or 48hrs. LDH release from the cells was quantified using a colourimetric assay and the percent of cytotoxicity was calculated from this. The experiments were carried out at two time points to optimise the effects of VEGF.

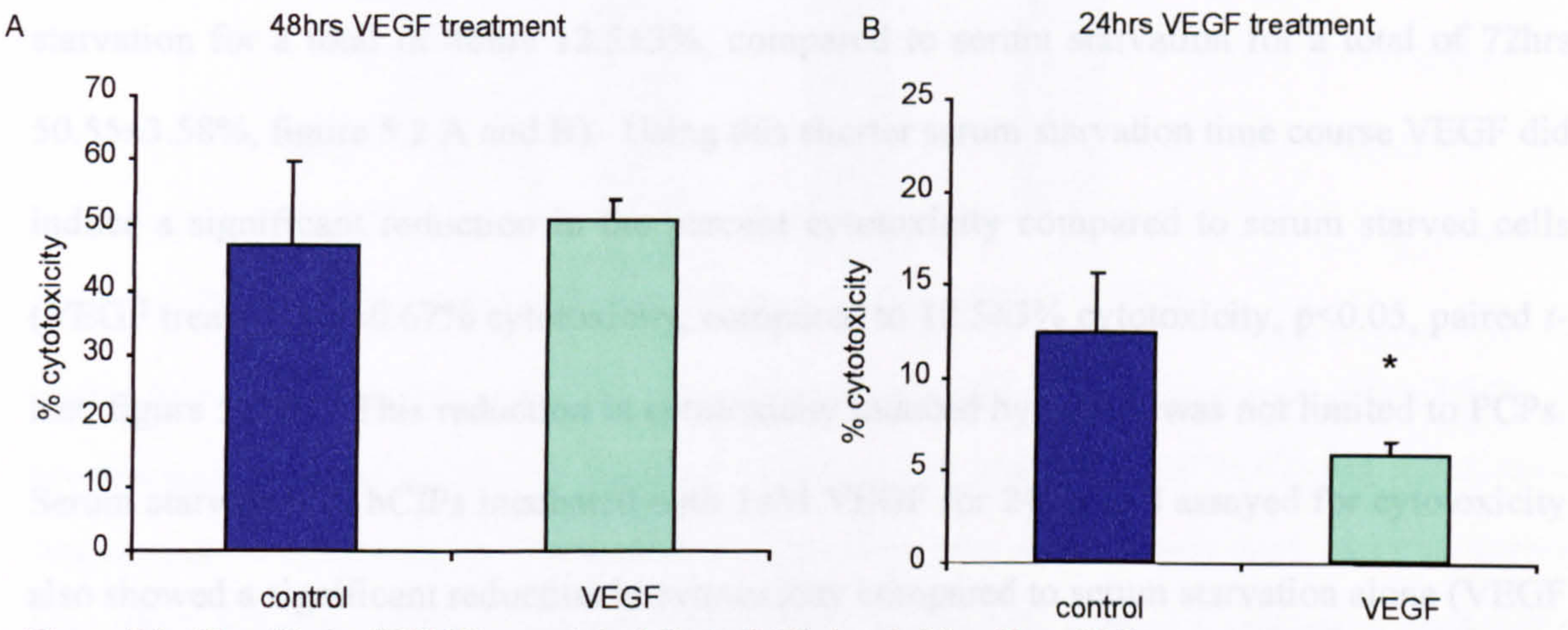

Figure 5.2. The effects of VEGF on cytotoxicity in PCPs treated for 48 and 24hrs.

PCPs were serum starved for 24hrs then treated with VEGF or left untreated, under serum free conditions, for a further 48hrs (A) or 24hrs (B), before cytotoxicity was assayed. A. Data were expressed as mean+SEM percent of cytotoxicity after 48hrs without (blue) and with (green) 1nM VEGF. Incubation of cells in VEGF for 48hrs had no significant effect on cytotoxicity compared to serum starved cells. B. Data were expressed as mean+SEM percent of cytotoxicity after 24hrs without (blue) and with (green) 1nM VEGF. Incubation of cells in VEGF for 24hrs induced a reduction in the percentage of cytotoxicity compared to that of serum starvation. *=$p<0.05$ compared to control, unpaired *t*-test, n = 48.

There was no significant difference in the percent of cytotoxicity between podocytes treated with VEGF for 48hrs and those serum starved for 48hrs (VEGF treated; 47.02±12.7% cytotoxicity compared to untreated; 50.55±3.58% cytotoxicity, figure 5.2 A). The percent of

cytotoxicity was very high in both cell populations (note the Y axis scale in A compared to B). It is possible that the absence of serum over a total of 64hrs induced too much cytotoxicity. This would mean that either VEGF could not exert an effect of a significant magnitude, or that VEGF did exert an effect at some time point during the course of the experiment, but it was not sustained over that time period. The serum starved cells were, therefore, incubated with VEGF for just 24hrs to examine whether VEGF could induce a significant change in cytotoxicity during a shorter time course of serum starvation. The percentage cytotoxicity, induced by 24hrs of serum starvation in cells was much lower using this time course (serum starvation for a total of 48hrs 12.5±3%, compared to serum starvation for a total of 72hrs 50.55±3.58%, figure 5.2 A and B). Using this shorter serum starvation time course VEGF did induce a significant reduction in the percent cytotoxicity compared to serum starved cells (VEGF treated; 5.9±0.67% cytotoxicity, compared to 12.5±3% cytotoxicity, $p<0.05$, paired *t*-test, figure 5.2 B). This reduction in cytotoxicity induced by VEGF was not limited to PCPs. Serum starvation of hCIPs incubated with 1nM VEGF for 24hrs and assayed for cytotoxicity also showed a significant reduction in cytotoxicity compared to serum starvation alone (VEGF treated; 10.3±0.96% cytotoxicity compared to untreated: 19.8±1.3% cytotoxicity, $p<0.05$, figure 5.3 A). This provides further support for similarities between PCPs and hCIPs. The cytotoxicity induced by a total of 48hrs serum starvation (24hrs VEGF treatment) in hCIP cytotoxicity experiments was approximately 7% higher than in the PCP cytotoxicity experiments (24hr VEGF treatment).

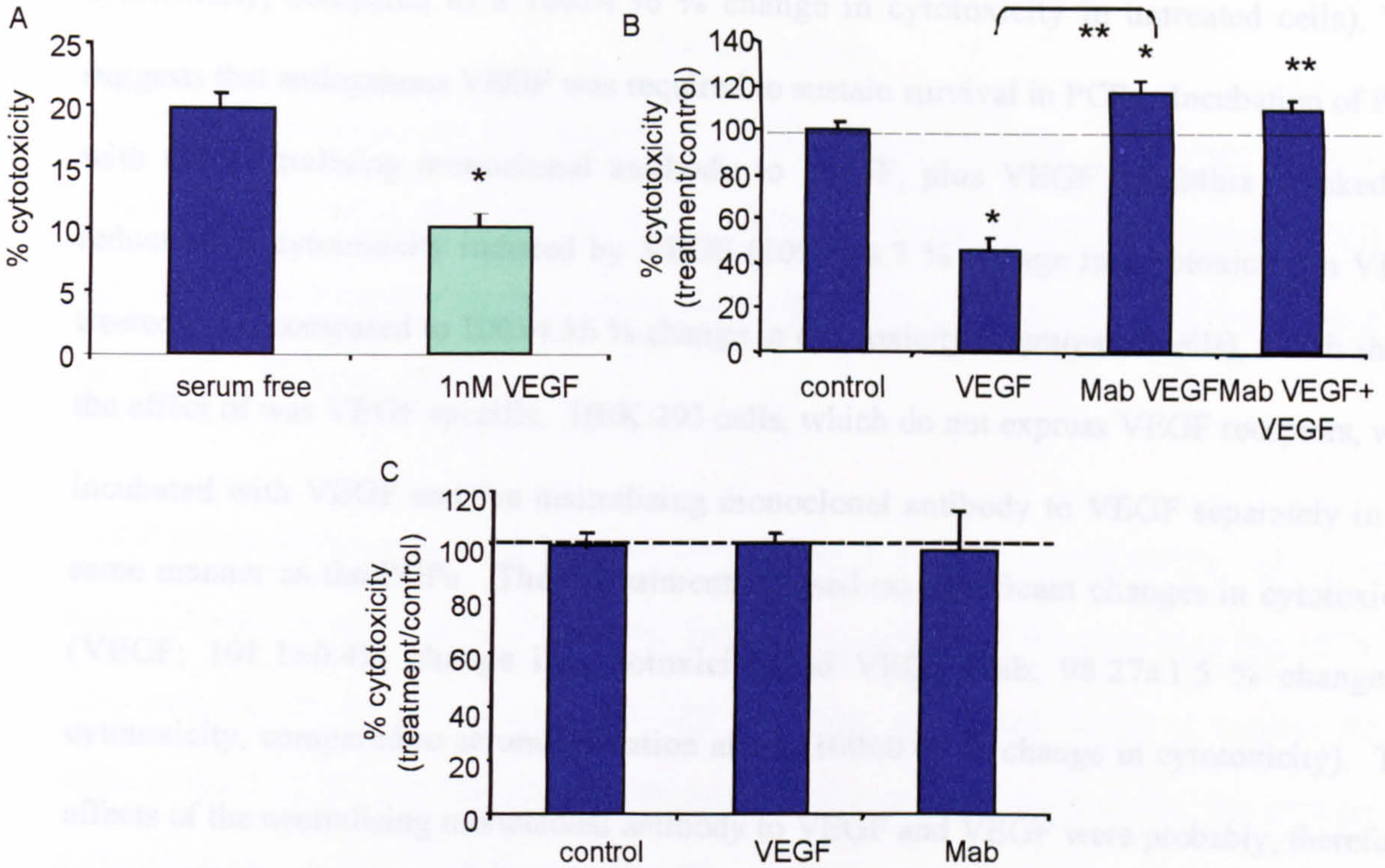

Figure 5.3. Effects of exogenous VEGF on hCIPs and endogenous VEGF on PCPs.

hCIPs, PCPs and HEK 293 cells were serum starved for 24hrs then treated with either VEGF, a neutralising monoclonal antibody to VEGF (VEGF-Mab) or a combination of VEGF with VEGF-Mab, then assayed for cytotoxicity. A. Mean+SEM % cytotoxicity after 24hrs without (blue) and with (green) 1nM VEGF in hCIPs. hCIPs incubated in VEGF had a significantly reduced percentage of cytotoxicity than serum starved cells. B. Mean+SEM % change in cytotoxicity (treatment/control) comparing VEGF treated cells with VEGF-Mab, and VEGF combined with VEGF-Mab. PCPs incubated in VEGF-Mab had a significantly increased %cytotoxicity compared to both VEGF treated cells, and serum starved cells, as did PCPs treated with a combination of VEGF with VEGF-Mab. C. Mean+SEM % change in cytotoxicity (treatment/control) after 24hrs with VEGF and VEGF-Mab compared to control in HEK 293 cells. Neither VEGF treatment nor VEGF-Mab treatment in HEK 293 cells induced a significant change in the percentage of cytotoxicity compared to serum starved cells. *=$p<0.05$ ** = $p< 0.01$ compared to control or as indicated, n = 48

Serum starvation of PCPs incubated with a neutralising monoclonal antibody specific to VEGF (VEGF-Mab) for 24hrs and assayed for cytotoxicity demonstrated an increase in cytotoxicity compared to that of serum starvation (VEGF treatment: 117.27±5.46 % change in

cytotoxicity, compared to a 100±4.56 % change in cytotoxicity in untreated cells). This suggests that endogenous VEGF was required to sustain survival in PCPs. Incubation of PCPs with the neutralising monoclonal antibody to VEGF, plus VEGF for 24hrs blocked the reduction in cytotoxicity induced by VEGF (109.4±4.7 % change in cytotoxicity in VEGF treated cells, compared to 100±4.56 % change in cytotoxicity in untreated cells), which shows the effect of was VEGF specific. HEK 293 cells, which do not express VEGF receptors, were incubated with VEGF and the neutralising monoclonal antibody to VEGF separately in the same manner as the PCPs. These treatments caused no significant changes in cytotoxicity (VEGF; 101.1±0.4% change in cytotoxicity and VEGF-Mab; 98.27±1.5 % change in cytotoxicity, compared to serum starvation alone; 100±0.46 % change in cytotoxicity). The effects of the neutralising monoclonal antibody to VEGF and VEGF were probably, therefore, mediated through the receptors expressed on the podocytes. These results support the ^{3}H-thymidine incorporation/cell results: Exogenous and endogenous VEGF promotes survival in cultured podocytes.

5.4 Discussion

VEGF did not stimulate proliferation in PCPs (figure 5.1 C). This may be because proliferation in endothelial cells is mainly mediated through VEGF-R2 whereas VEGF-R1 signalling in endothelial cells contributes about one tenth of the total tyrosine kinase signal (as reviewed in (Shibuya, 2001)).

VEGF treatment induced a reduction in cytotoxicity in both PCPs and hCIPs. There was a slight increase in cytotoxicity induced by serum starvation in hCIPs relative to that of PCPs. This may be due to variations in seeding densities, which are harder to control for in differentiated hCIPs because they go through significant cell death during the process of differentiation. A lower confluency of cells would be more exposed. When the effects of endogenous VEGF were blocked by a neutralising monoclonal antibody to VEGF, levels of cytotoxicity induced by serum starvation were significantly increased (figures 5.1 and 5.3) suggesting that endogenous as well as exogenous VEGF promotes survival in cultured podocytes. A similar effect was also seen when the effects of endogenous VEGF in astrocytes, upregulated in the central nervous system (CNS) after various types of injury, were blocked with the use of a neutralising monoclonal antibody to VEGF (Krum and Khaibullina, 2003). This resulted in astroglial degeneration, due to increased apoptosis as well as a reduction in mitogenicity. The authors have pointed out that blocking the effects of endogenous VEGF may increase the effects or expression of basic fibroblast growth factor because the two have a synergistic relationship in this system (Krum and Khaibullina, 2003). This suggests that blocking the effects of endogenous VEGF in podocytes may imbalance the system and affect the expression or signalling of other synergistic molecules (discussed later in the thesis). Interestingly, astrocytes express VEGF-R1 but not VEGF-R2, which indicates

that endogenous VEGF induced its effects via VEGF-R1 signalling (Krum and Khaibullina, 2003). I made the assumption that the reduction in cytotoxicity induced by VEGF in podocytes was mediated through VEGF-R1 for reasons mentioned for the proliferation assay. VEGF-R2 has again been shown to be the receptor implicated in VEGF mediated survival in endothelial cells. VEGF induced AKT signalling in microglial cells, which express VEGF-R1 but not VEGF-R2, was very limited and if anything, AKT phosphorylation induced by VEGF was reduced compared to that of serum starvation (Forstreuter et al., 2002). These results are interesting because VEGF is known to signal in these cells (Forstreuter et al., 2002), but suggests that survival signalling through VEGF-R1 may be limited, or at least survival pathways mediated by AKT phosphorylation. It has, however, been shown that VEGF can induce the activation of PI3-Kinase and AKT phosphorylation via VEGF-R1 signalling in rat hepatic stellate cells, which do not express VEGF-R2 (Takahashi et al., 2003). Surprisingly, this PI3-Kinase/AKT signalling was dependent on MAPK phosphorylation. Together this suggests that cell differences determine the signalling effects of VEGF on VEGF-R1, hence it is possible that VEGF activates the PI3-Kinase/AKT survival pathway via VEGF-R1 in podocytes.

Conclusions drawn from these results suggest that both exogenous and endogenous VEGF promote survival in cultured podocytes, via a reduction in cytotoxicity. This will be dependent on either inhibition of apoptosis or necrosis, although, due to the nature of VEGF it is more likely to be due to a reduction in apoptosis. The work from this chapter was published in paper 1 of the list of papers arising from this work.

Chapter 6

VEGF promotes survival in cultured podocytes through inhibition of the apoptosis pathway

6.1 Introduction

In chapter 5 it was shown that treatment with VEGF resulted in a reduction in cytotoxicity in cultured podocytes incubated in VEGF. The mechanism through which VEGF results in this reduction in cytotoxicity is not clear. The mechanisms by which cells die, however, have been extensively studied. Cytotoxicity can manifest itself in two ways: necrosis or apoptosis. Necrosis is accidental or pathological cell death, which results in an inflammatory response. The most characteristic features of necrosis are nuclear changes starting with pyknosis; the condensation of the chromatin, then karyorrhexis; the uncontrolled fragmentation of nuclear material and finally karyolysis; where the nucleus is completely broken down (Burkitt et al., 1997). The cytoplasm also forms an amorphous mass and the cell membrane integrity is lost (cytolysis), due to excess cell swelling (Burkitt et al., 1997). The term apoptosis was first used by Kerr et al, "apoptosis" meaning the "dropping off" of leaves from trees (Kerr et al., 1972). It describes programmed cell death either spontaneously, or in response to physiological stimuli. There are two distinct stages of apoptosis; firstly, the formation of apoptotic bodies, which are small membrane bound spheres consisting of condensed cytoplasmic and nuclei fragments, and secondly, phagocytosis by other cells thus avoiding an inflammatory response (Kerr et al., 1972) (Uthaisang et al., 2003). The pathways involved in apoptosis are both varied and complex. The pathways can be divided into the death receptor cascade pathway and the physiological stimuli induced pathway as shown in figure 6.1, although there is interaction between the two. Activation of the death receptors, such as FasL, (Fas ligand), TRAIL-R1 (TNF-related apoptosis-inducing ligand) and TNF-R1 (Tumor necrosis Factor-Receptor 1), by their ligands induces receptor clustering.

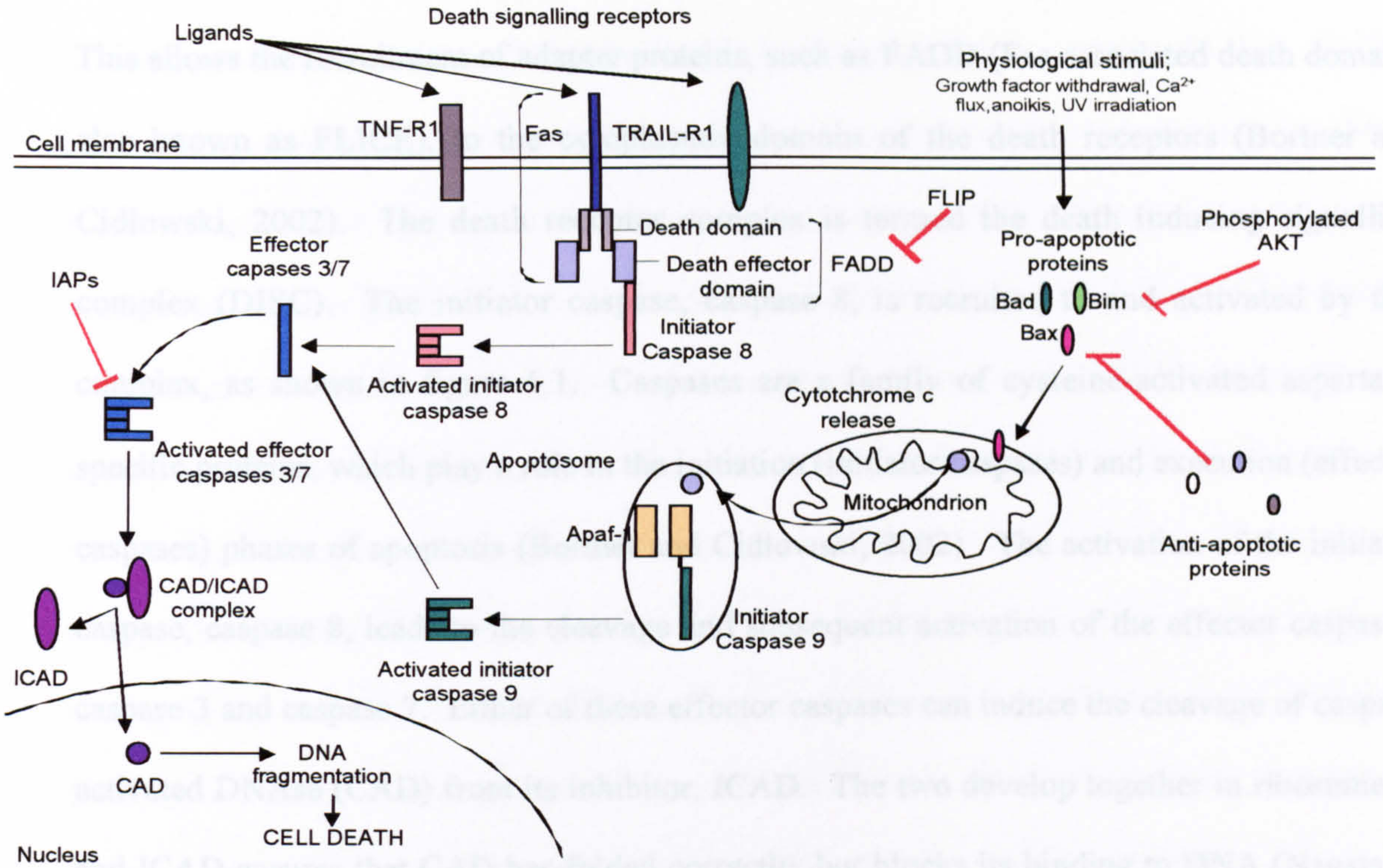

Figure 6.1. Simplified schematic of apoptosis signalling cascades.

Apoptosis signalling pathways have been split into death receptor signalling cascades and cascades due to physiological stimuli. Death receptors, such as TNF-R1, Fas and TRAIL-R1 are activated by their ligands; TNF FasL and TRAIL respectively. Death inducing signalling complexes (DISCs) are formed at each death receptor and in the case of Fas it involves FADD (containing a death domain and a death effector domain). This complex induces the cleavage, and activation of caspase 8, but its binding can be inhibited by FLIP. Activated caspase 8 leads to the cleavage and activation of the effector caspases, which are either inhibited by IAPs, or induce the cleavage of CAD from ICAD. Activated CAD then translocates to the nucleus and induces DNA fragmentation, which leads to cell death. Physiological stimuli on the other hand can induce the activation of pro-apoptotic members of the Bcl-2 family. Homodimers of these pro-apoptotic proteins insert into the mitochondrial membrane, leading to cytochrome c release. The insertion of the pro-apoptotic proteins into the mitochondria depends on whether the homodimers are cleaved and competitively replaced by anti-apoptotic Bcl-2 family members and retained in the cytoplasm, or if the pro-apoptotic proteins are phosphorylated by phosphorylated AKT. The cytochrome c forms a complex in the cytoplasm with Apaf-1, a caspase recruiting domain, and caspase 9. This induces the cleavage, and activation of caspase 9, which leads to the cleavage and activation of effector caspases resulting in the activation of CAD and DNA fragmentation and death.

This allows the recruitment of adapter proteins, such as FADD (Fas-associated death domain, also known as FLICE), to the cytoplasmic domain of the death receptors (Bortner and Cidlowski, 2002). The death receptor complex is termed the death inducing signalling complex (DISC). The initiator caspase, caspase 8, is recruited to and activated by this complex, as shown in figure 6.1. Caspases are a family of cysteine-activated aspartate-specific proteins, which play a role in the initiation (initiator caspases) and execution (effector caspases) phases of apoptosis (Bortner and Cidlowski, 2002). The activation of the initiator caspase, caspase 8, leads to the cleavage and subsequent activation of the effector caspases, caspase 3 and caspase 7. Either of these effector caspases can induce the cleavage of caspase activated DNAse (CAD) from its inhibitor, ICAD. The two develop together in ribosome's, and ICAD ensures that CAD has folded correctly, but blocks its binding to DNA (Nagata et al., 2003b). This complex resides in the cytoplasm, but CAD translocates to the nucleus after ICAD has been cleaved away by the effector caspases, as shown in figure 6.1. CAD is a member of the histidine nuclease family, and, within the nucleus, generates DNA fragments with blunt ends, carrying a 5' phosphate and a 3' hydroxyl group (Nagata et al., 2003b). DNA fragmentation invariably leads to cell death. Various physiological stimuli, summarised in figure 6.1, can induce the upregulation of pro-apoptotic proteins, which insert into the mitochondrial membrane (Bortner and Cidlowski, 2002). The method by which pro-apoptotic proteins can induce activation of apoptosis at the mitochondrial level is controversial, but invariably leads to the release of various pro-apoptotic factors, such as cytochrome c (figure 6.1). Cytochrome c forms a complex (apoptosome) with Apaf-1, a caspase recruitment domain, and the initiator caspase, caspase 9, which results in its activation. The activated initiator caspase, caspase 9, cleaves and activates the effector caspases, which then cleave CAD from ICAD and induce DNA fragmentation and cell death (figure 6.1). The apoptosis pathways can be inhibited at a number of levels, in various ways. For example, apoptosis can

be inhibited at the level of the DISC by FLICE (FADD)-inhibitory proteins (FLIPs). FLIPs are recruited to the DISC due to their death effector domains blocking recruitment of caspase 8 and its subsequent activation (Bortner and Cidlowski, 2002). Apoptosis can also be inhibited at the level of the Bcl-2 family of proteins by heterodimeric binding of anti-apoptotic members of the Bcl-2 family to pro-apoptotic members (Gross et al., 1999). Apoptosis can also be inhibited at the level of the Bcl-2 pro-apoptotic family of proteins by phosphorylated AKT, which phosphorylates and inactivates pro-apoptotic family members (Gross et al., 1999). The inhibitor of apoptosis proteins (IAPs) can inhibit apoptosis at the caspase level, by binding to the activated effector caspases, caspase-3 and caspase-7 (Bortner and Cidlowski, 2002). The authors of this paper have suggested that the ratio of activated effector caspases to IAPs is likely to be a key point in determining whether apoptosis will be inhibited.

The pathway involved in the VEGF induced reduction in apoptosis in endothelial cells, however, is thought to be due to VEGF/VEGF-R2 dependent activation of PI3-Kinase leading to the phosphorylation of AKT. This results in the phosphorylation and inactivation of members of the pro-apoptotic family, thus preventing cytochrome c release from the mitochondria. To investigate whether VEGF had an effect on either necrosis or apoptosis, cells were assayed using a technique that distinguished between both necrotic and apoptotic sub populations using a flow cytometer. An analogy could be made between de-differentiated hCIPs *in vitro* and proliferative immature podocytes *in vivo* and between differentiated hCIPs *in vitro* and non-proliferative, mature podocytes *in vivo*. The effects of VEGF on hCIPs were investigated using both de-differentiated and differentiated cells. This set of experiments were carried out to provide clues as to whether VEGF has a different role in podocyte function in development and maturity.

6.2 Methods

6.2.1 Apoptosis assay-the effects of VEGF on podocyte apoptosis

De-differentiated and differentiated hCIPs were serum starved either for a total of 24hrs (acutely) or for a total of 48hrs (chronically). The cells were serum starved for 16hrs then incubated in 1nM VEGF for either 4hrs (acutely) or 8hrs (chronically), or left untreated. 24hrs later, the cells in the chronic assay were serum starved for 16hrs then incubated once more with VEGF for a further 4hrs, or left untreated. Each sample was incubated with either annexin V (AV), propidium iodide (PI), a combination of both AV and PI or left untreated. A comparison was made between VEGF treated and untreated de-differentiated hCIPs using the 24hr serum starvation assay. The induction of apoptosis by a total of 24hrs serum starvation and a total of 48hrs serum starvation was compared. A comparison was also made between VEGF treated and untreated differentiated hCIPs using the 48hr serum starvation assay.

6.3 Results

6.3.1 The effects of VEGF on apoptosis in hCIPs

An apoptosis assay was used to differentiate between necrotic and apoptotic sub-populations of the total cell population. To investigate whether VEGF had an effect on de-differentiated hCIPs they were serum starved for 16hrs, treated with VEGF or left untreated in serum free media for 4hrs, then scraped into suspension and rolled for 4hrs, in serum free media (total 24hrs serum starvation). The cell suspension samples were incubated in AV, PI, AV and PI or left untreated, as described in the methods.

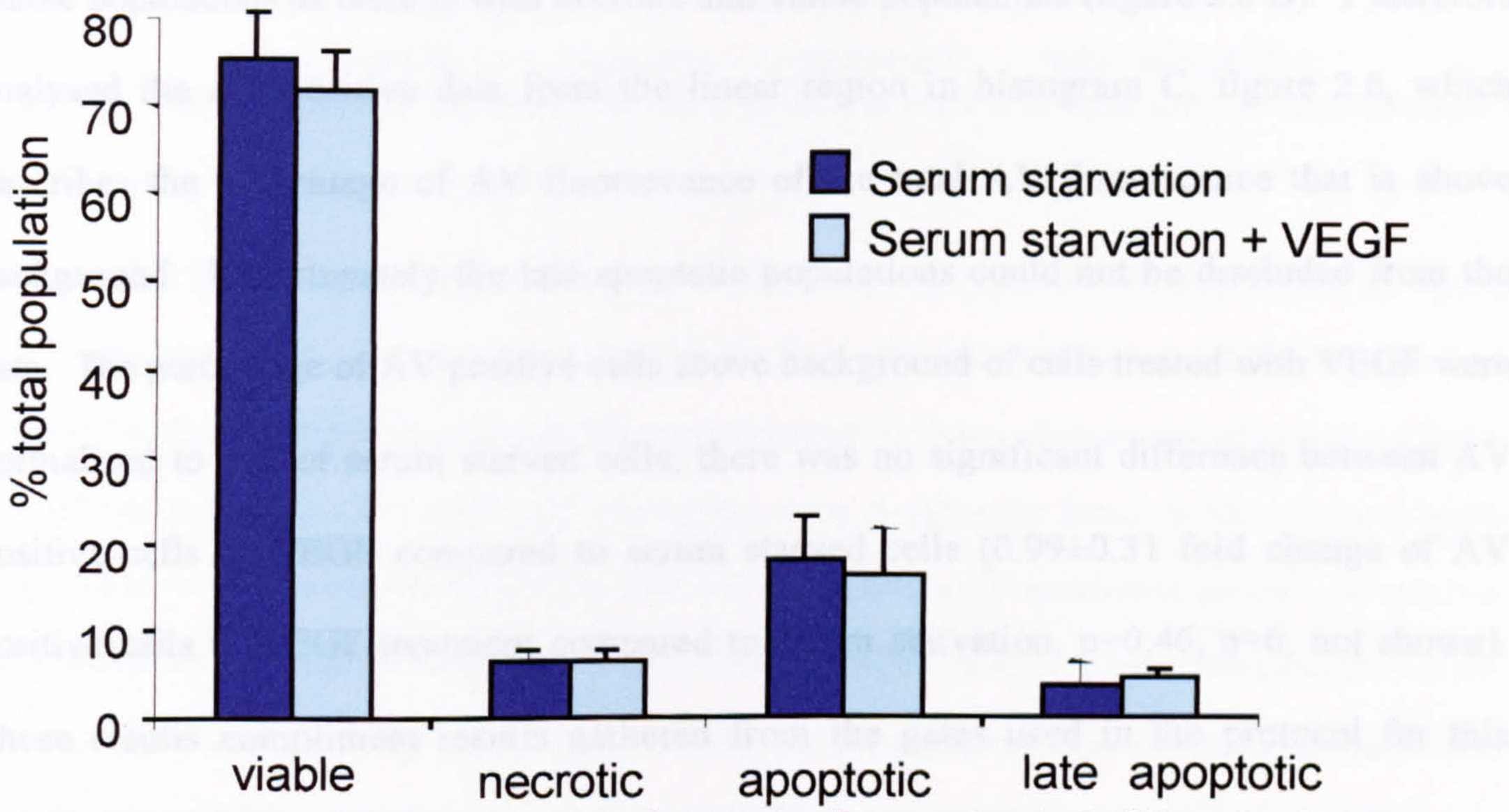

Figure 6.2. The effects of VEGF on necrotic and apoptotic cell populations in de-differentiated hCIPs.

Serum starved, de-differentiated hCIPs were either treated with VEGF for 4hrs, or serum starved for another 4hrs. Cells in both groups were in serum free media for a total of 24hrs, before being incubated in AV, PI, AV and PI or left untreated. Cells were then assayed, using the flow cytometer and sub-populations of cells were compared between serum starved and VEGF treated de-differentiated hCIPs. Data were expressed as mean+SEM % total population for apoptotic, necrotic, late apoptotic and viable sub populations. There was no significant difference between VEGF treated and untreated samples, in any of the cell populations. N.s. unpaired AVOVA, n = 7.

Of the total cell population 70.4±5.45% stained with neither AV nor PI (i.e. met the criteria for viable cells), in the serum starved group 20.0±5.17% stained with AV (i.e. met the criteria for apoptotic cells), 6.24±1.4% stained with PI (i.e. met the criteria for necrotic cells) and 6.14±2.25% stained with a combination of both AV and PI (i.e. met the criteria for late apoptotic cells) (figure 6.2). There was no significant difference between sub-populations of cells in the serum starved group compared to the VEGF treated group. These results show that apoptosis was induced under these conditions, although necrotic levels were relatively low. These cells do autofluoresce at 525nm (the wavelength at which FITC conjugated AV fluoresces) to a certain extent and so there is not a clear distinction between apoptotic and viable populations as there is with necrotic and viable populations (figure 2.6 B). I therefore analysed the AV positive data from the linear region in histogram C, figure 2.6, which describes the percentage of AV fluorescence of the total AV fluorescence that is above background. Unfortunately the late apoptotic populations could not be discluded from the data. The percentage of AV positive cells above background of cells treated with VEGF were normalised to that of serum starved cells; there was no significant difference between AV positive cells in VEGF compared to serum starved cells (0.99±0.31 fold change of AV positive cells in VEGF treatment compared to serum starvation, $p=0.46$, $n=6$, not shown). These results compliment results gathered from the gates used in the protocol for this experiment.

To investigate whether 24hrs serum starvation had the same effect on differentiated hCIPs, as it did on de-differentiated hCIPs, differentiated hCIPs were serum starved for 16hrs, the media replaced with fresh serum free media and left for 4hrs. The cells were then scraped into a cell suspension and rolled for a further 4hrs in serum free media, then incubated in AV, PI, AV with PI or left untreated and assayed using the flow cytometer. The response of differentiated

hCIPs to a total of 24hrs serum starvation was quite different to that of de-differentiated hCIPs (figure 6.3).

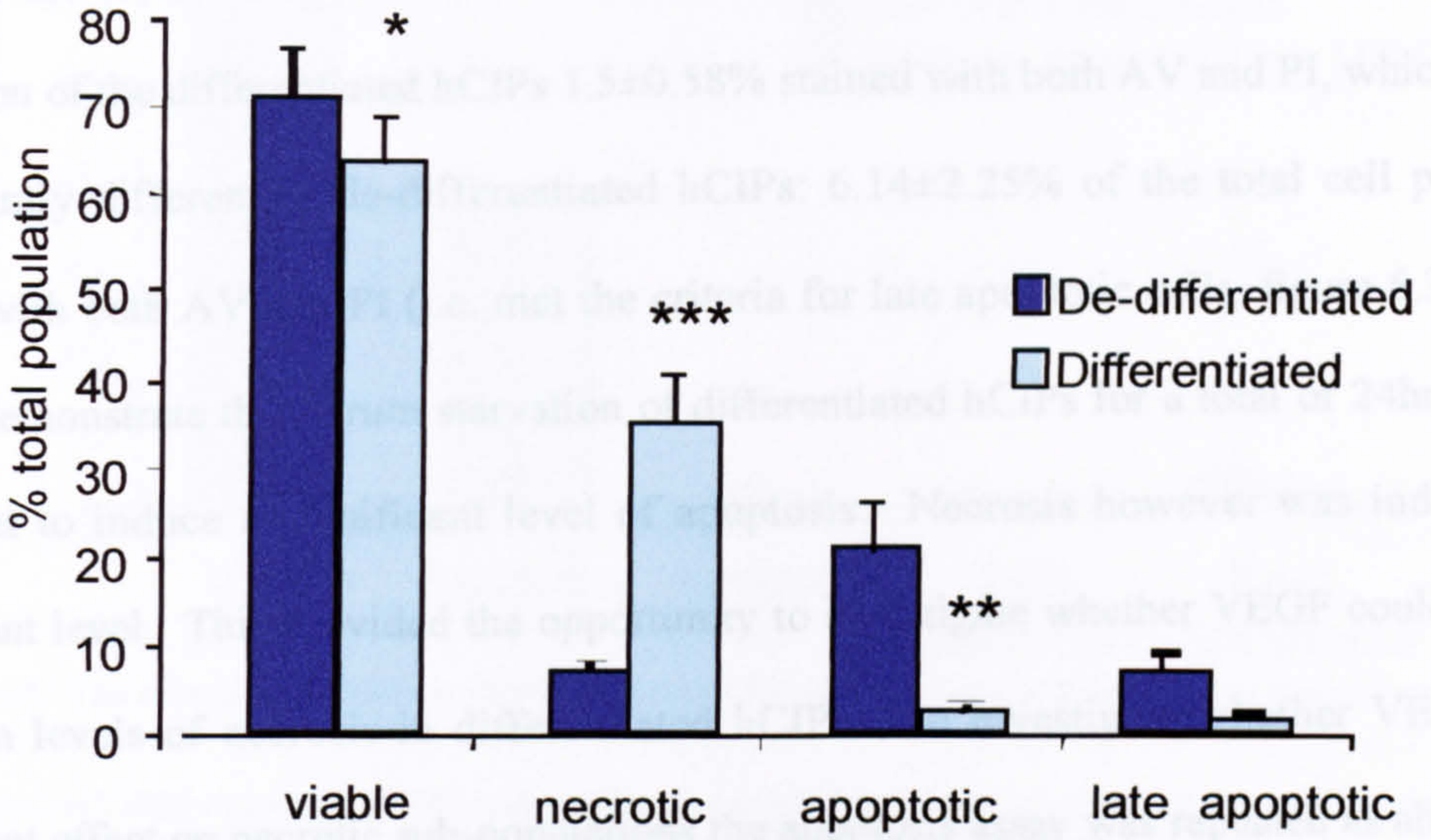

Figure 6.3. Effect of 24hrs (acute) serum starvation on differentiated hCIPs compared to de-differentiated hCIPs.

Differentiated hCIPs were serum starved for a total of 24hrs, before being incubated in AV, PI, AV and PI or left untreated. Cells were then assayed, using the flow cytometer and sub-populations of cells were compared to those of de-differentiated hCIPs, serum starved for 24hrs. Data expressed as mean+SEM % of total cell population. The viable cell populations were significantly lower in differentiated hCIPs compared to de-differentiated hCIPs, but necrotic cell populations were significantly greater and apoptotic cell populations were significantly lower in differentiated hCIPs, compared to de-differentiated hCIPs. There was no significant difference between late apoptotic cell populations in differentiated, compared to de-differentiated hCIPs. *=p<0.05, **=p<0.01, **=P<0.001, unpaired ANOVA, n≥4.

Of the total population of cells, 61.7±4.5% stained with neither AV nor PI (i.e. met the criteria for viable cells), which was significantly lower than de-differentiated hCIPs; 70.44±5.45%, of the total population of cells stained with neither AV nor PI (figure 6.3, $p<0.05$, ANOVA). Of the total cell population of differentiated hCIPs 2.16±0.4% stained with AV, which was significantly lower than with de-differentiated hCIPs; of the total cell population 20±5.17% stained with AV (i.e. met the criteria for apoptotic cells, $p<0.01$, ANOVA, figure 6.3). Of the

total population in differentiated hCIPs 33.49±4.5% stained with PI, which was significantly greater than in de-differentiated hCIPs; 6.24±1.4% of the total cell population stained with PI (i.e. met the criteria for necrotic cells, $p<0.001$, ANOVA, figure 6.3). Of the total cell population of the differentiated hCIPs 1.5±0.58% stained with both AV and PI, which was not significantly different to de-differentiated hCIPs: 6.14±2.25% of the total cell population stained with both AV and PI (i.e. met the criteria for late apoptotic cells, figure 6.3). These results demonstrate that serum starvation of differentiated hCIPs for a total of 24hrs was not sufficient to induce a significant level of apoptosis. Necrosis however was induced to a significant level. This provided the opportunity to investigate whether VEGF could exert an effect on levels of necrosis in differentiated hCIPs. To investigate whether VEGF had a significant effect on necrotic sub-populations the apoptosis assay was repeated as above using differentiated hCIPs, which had been serum starved for 16hrs, then incubated in VEGF in serum free media for 4hrs, and scraped into suspension and rolled for a further 4hrs.

There was no significant difference in any of the cell sub-population of differentiated cells, incubated in VEGF, compared to untreated differentiated hCIPs (figure 6.4). To verify that this was not due to a miscalculation of apoptosis due to an overlap of viable and apoptotic populations the percentage of AV positive cells of total AV fluorescence minus background (autofluorescence) was calculated for each treatment. There was no significant decrease in AV positive cells, expressed as a ratio of VEGF treated hCIPs to serum starved hCIPs (0.6±0.19, $p=0.124$, $n=3$, not shown). This indicates that VEGF does not induce a reduction in cytotoxicity in differentiated hCIPs via a reduction in necrosis.

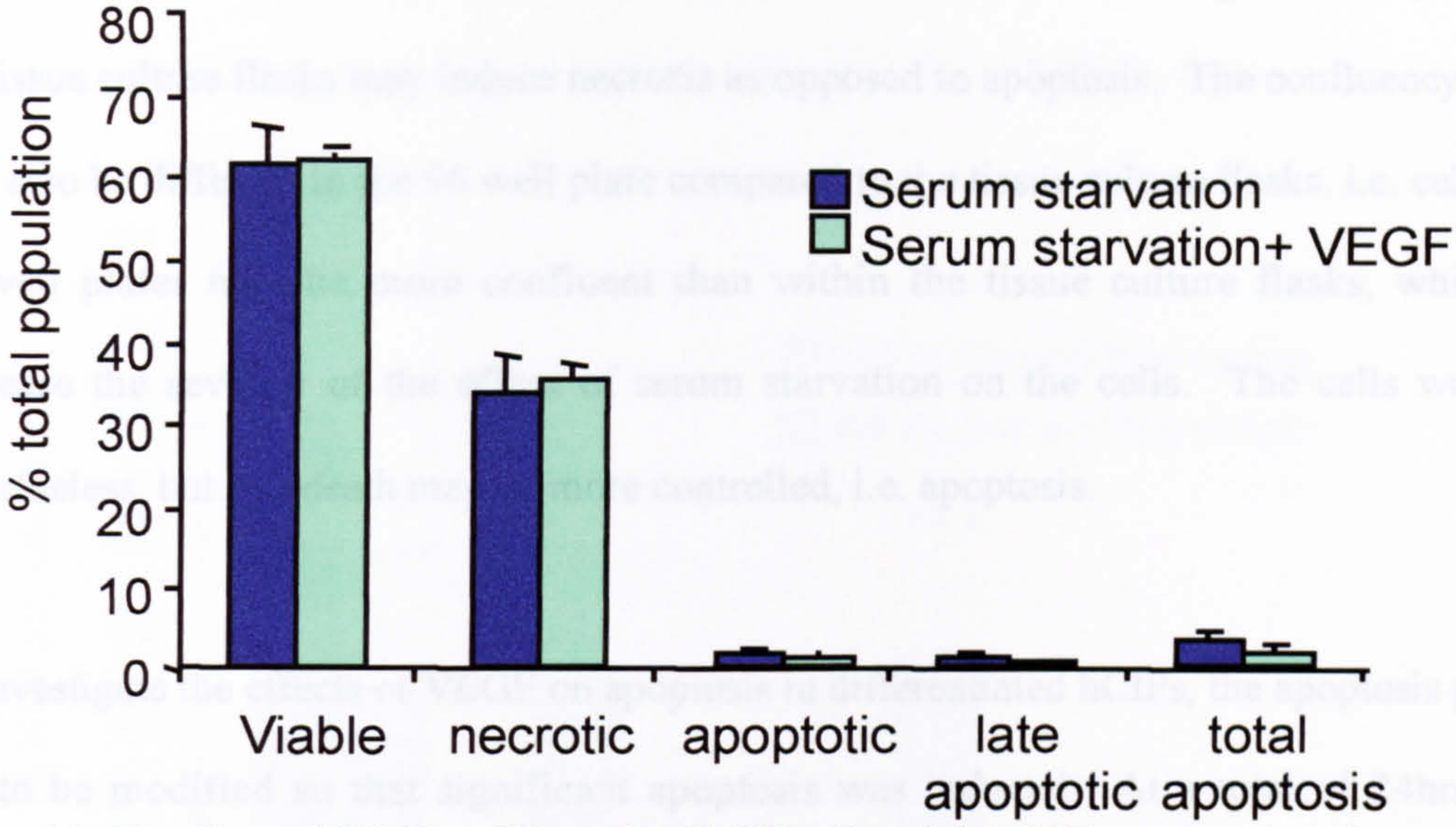

Figure 6.4. The effects of VEGF on differentiated hCIPs after a total of 24hrs serum starvation

Serum starved, differentiated hCIPs were either treated with VEGF for 4hrs, or serum starved for another 4hrs. Cells in both groups were in serum free media for a total of 24hrs, before being incubated in AV, PI, AV and PI or left untreated. Cells were then assayed using the flow cytometer and sub-populations of cells were compared between serum starved and VEGF treated differentiated hCIPs. Data were expressed as mean+SEM % total population for apoptotic, necrotic, late apoptotic and viable sub populations. There was no significant difference, in any of the cell sub-populations, between VEGF treated and untreated samples. N.s. unpaired AVOVA, n = 7.

These results contradict the results from chapter 5 (figure 5.3), showing that VEGF induced a reduction in cytotoxicity in differentiated hCIPs, serum starved for a total of 24hrs. This may be because apoptosis was induced in the cytotoxicity assay to a greater extent than necrosis. Although the cells were serum starved for the same period of time in the cytotoxicity assay, and the apoptosis assay they were treated under different conditions. The cells in the cytotoxicity assay were grown in 96 well plates, not in $75cm^2$ tissue culture flasks, as in the apoptosis assay. This means that the cells were exposed to different amounts of media, and possibly different concentrations of oxygen or CO_2. The cells in the 96 well plate would have a greater ratio of media to cells than in the tissue culture flask, therefore CO_2 levels would not

be as affected as in the tissue culture flask and therefore not as toxic. Higher toxicity levels in the tissue culture flasks may induce necrosis as opposed to apoptosis. The confluency of cells may also be different in the 96 well plate compared to the tissue culture flasks, i.e. cells in the 96 well plates may be more confluent than within the tissue culture flasks, which may decrease the severity of the effect of serum starvation on the cells. The cells would die nevertheless, but cell death may be more controlled, i.e. apoptosis.

To investigate the effects of VEGF on apoptosis in differentiated hCIPs, the apoptosis protocol had to be modified so that significant apoptosis was induced. At a total of 24hrs serum starvation there was no significant level of apoptosis in differentiated hCIPs, therefore these cells either undergo apoptosis over a shorter time course than de-differentiated hCIPs or over a longer time course than de-differentiated hCIPs. The latter has been more implied in the literature and this theory applies well to immature and mature podocytes *in vivo*. A serum starvation protocol was, therefore, developed over a more chronic time period. Cells were serum starved for 16hrs, treated with VEGF or left untreated in serum free media for 8hrs, left to recover in complete media for 48hrs, serum starved for another 16hrs and treated again with VEGF or left untreated in serum free media for 4hrs. Cells were then scraped into suspension and rolled in serum free media for a further 4hrs. This protocol was developed by accident, but was the only one out of many to induce significant apoptosis. Of the total cell population in the group that had been serum starved for a total of 48hrs 33.8±6.67% stained with neither AV nor PI, which was significantly lower than the group that had been serum starved for a total of 24hrs; 61.66±4.5% stained with neither AV nor PI (i.e. met the criteria for viable cells, $p<0.001$, AVOVA, figure 6.5). Of the total cell population in the group that had been serum starved for a total of 48hrs 37.6±6.08% stained with AV, which was significantly greater than

the group that had been serum starved for a total of 24hrs; 2.16±0.4% of the total cell population (i.e. met the criteria for apoptotic cells, $p<0.001$, ANOVA, figure 6.5).

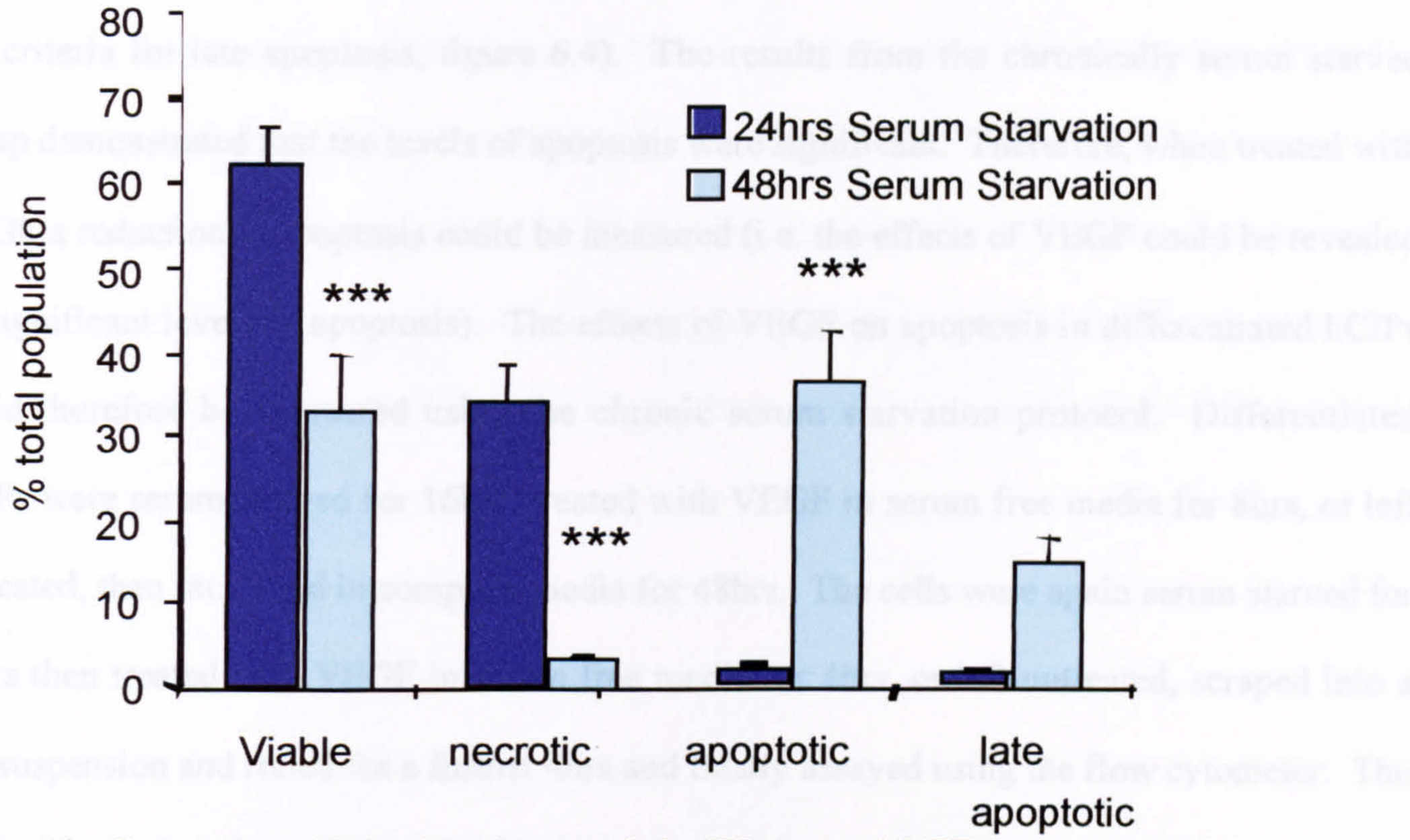

Figure 6.5. Comparison of induction of apoptosis in differentiated hCIPs, serum starved for a total of 48hrs, compared to a total of 24hrs.

Differentiated hCIPs were serum starved for 16hrs, the media was replaced with fresh serum free media for either 4hrs (acute assay) or 8hrs (chronic assay). Cells in the acute assay were then scraped into suspension, rolled for a further 4hrs, then assayed. The cells in the chronic assay were incubated in complete media for 48hrs, then serum starved again for 16hrs. The media was replaced with fresh serum free media and the cells were incubated for a further 4hrs, before being scraped into suspension and rolled for 4hrs, then assayed. Data expressed as mean+SEM % total population for apoptotic, necrotic, late apoptotic and viable sub populations. There was a significant reduction in the viable and necrotic cell populations, but a significant increase in apoptotic cell populations, as well as a non-significant increase in the late apoptotic cell populations in cells starved for a total of 48hrs, compared to 24hrs. ***=$p<0.001$, ANOVA, $n\geq3$.

3.34±7.5% of the total population of cells that had been serum starved for a total of 48hrs stained with PI, which was significantly lower than in cells serum starved for 24hrs:

33.49±4.5% of the total cell population (i.e. met the criteria for necrotic cells, $p<0.001$, ANOVA, figure 6.5). There was a small, but not significant, increase in cells staining for both PI and AV in cells serum starved for 48hrs compared to cells serum starved for 24hrs (i.e. met the criteria for late apoptosis, figure 6.4). The results from the chronically serum starved group demonstrated that the levels of apoptosis were significant. Therefore, when treated with VEGF a reduction in apoptosis could be measured (i.e. the effects of VEGF could be revealed by significant levels of apoptosis). The effects of VEGF on apoptosis in differentiated hCIPs could therefore be measured using the chronic serum starvation protocol. Differentiated hCIPs were serum starved for 16hrs, treated with VEGF in serum free media for 8hrs, or left untreated, then incubated in complete media for 48hrs. The cells were again serum starved for 16hrs then treated with VEGF in serum free media for 4hrs, or left untreated, scraped into a cell suspension and rolled for a further 4hrs and finally assayed using the flow cytometer. The results show that there was a significant reduction in cells that stain for AV (i.e. met the criteria for apoptotic cells) in chronically serum starved cells incubated in VEGF (19.49±5.57% of the total cell population) compared to untreated chronically serum starved cells (37.6±6.08%, of the total cell population, p,0.05, ANOVA, figure 6.6). Of note there was also an increase in cells incubated in VEGF that stained for neither AV nor PI (i.e. met the criteria for viable cells), although it was not significant. Cells, incubated in VEGF also demonstrated a small, but non-significant increase in cells staining with PI (i.e. met the criteria for necrosis) compared to untreated cells. There was no difference between cells staining for both AV and PI (i.e. met the criteria for late apoptosis), between cells incubated VEGF and untreated cells. To confirm there was no miscalculation in AV positive cells due to the regions used in the protocol, the percentage of AV positive cells of the total AV fluorescence of VEGF treated cells were normalised to that of serum starved cells. There was a 0.5±0.07

fold reduction in AV positive cells in VEGF treatment compared to serum starvation ($p<0.05$, one sample *t*-test, n=3, not shown), which confirms the results in figure 6.6.

These results show that: 1) VEGF does not have a significant effect on apoptotic or necrotic sub-populations in de-differentiated hCIPs; 2) de-differentiated hCIPs are more sensitive to apoptosis than differentiated hCIPs; 3) VEGF does not significantly affect necrotic sub-populations in differentiated hCIPs; 4) chronic serum starvation induces significant apoptosis in differentiated hCIPs; 5) VEGF induces a significant reduction in apoptosis in differentiated hCIPs.

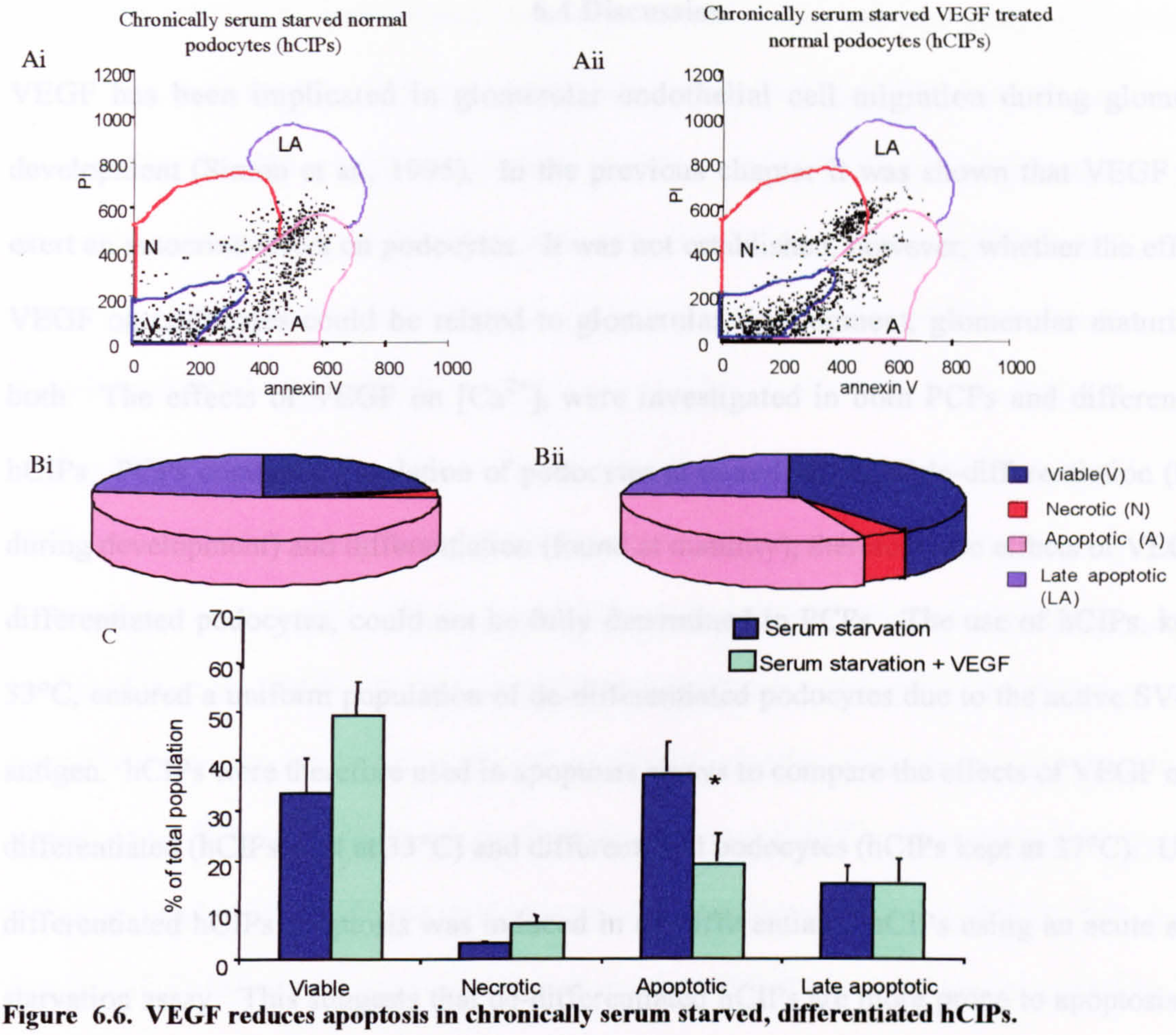

Figure 6.6. VEGF reduces apoptosis in chronically serum starved, differentiated hCIPs.

Differentiated hCIPs were serum starved for 16hrs, cells were then incubated in fresh serum free media, either containing VEGF or not for or 8hrs. Cells were then incubated in complete media for 48hrs then serum starved again for 16hrs. The media was replaced with fresh serum free media either containing VEGF or not and the cells were incubated for a further 4hrs, before being scraped into suspension and rolled for 4hrs then assayed. A. Comparison of AV and PI labelling of 1nM VEGF treated, serum starved hCIPs compared to serum starved hCIPs. There is more apoptosis in this example of untreated cells (i) compared to cells treated with VEGF (ii), but, what appears to be a smaller necrotic population in serum starved (i) compared to cells incubated in VEGF (ii). B. Characteristics of cell populations in chronically serum starved 1nM VEGF treated hCIPs compared to untreated hCIPs. Values are expressed as a percentage of the total cell population. There is more apoptosis in the serum starved group (i) whereas there is more necrosis and viable cells in the VEGF treated group (ii). C. Mean+SEM sub-population as a percentage of the total cell population. Compared to serum starvation alone, VEGF treatment significantly reduced apoptotic cells. $p<0.05$, ANOVA, n=3.

6.4 Discussion

VEGF has been implicated in glomerular endothelial cell migration during glomerular development (Simon et al., 1995). In the previous chapter it was shown that VEGF could exert an autocrine effect on podocytes. It was not established, however, whether the effect of VEGF on podocytes could be related to glomerular development, glomerular maturity, or both. The effects of VEGF on $[Ca^{2+}]_i$ were investigated in both PCPs and differentiated hCIPs. PCPs contain a population of podocytes at mixed stages of de-differentiation (found during development) and differentiation (found at maturity), therefore, the effects of VEGF on differentiated podocytes, could not be fully determined in PCPs. The use of hCIPs, kept at 33°C, ensured a uniform population of de-differentiated podocytes due to the active SV40 T-antigen. hCIPs were therefore used in apoptosis assays to compare the effects of VEGF on de-differentiated (hCIPs kept at 33°C) and differentiated podocytes (hCIPs kept at 37°C). Unlike differentiated hCIPs apoptosis was induced in de-differentiated hCIPs using an acute serum starvation assay. This suggests that de-differentiated hCIPs are more prone to apoptosis than differentiated hCIPs. The de-differentiated hCIPs are still held in the cell cycle because the genes that lead to growth arrest are not transactivated by p53, which has been inactivated. This makes de-differentiated hCIPs more vulnerable to cytototoxic processes than terminally differentiated podocytes: Exit from the cell cycle in differentiated cells coincides with an upregulation in CDK inhibitors, which promote cell survival (Fujio et al., 1999) (as discussed in for figure 1.3). There was no significant difference in any of the cell sub-populations of de-differentiated hCIPs incubated in VEGF compared to those that were not incubated in VEGF (figure 6.2). This was in contrast to the reduction in apoptosis in differentiated hCIPs incubated in VEGF compared to serum starved cells (figure 6.4). De-differentiated hCIPs share similar characteristics with immature podocytes *in vivo*; they are proliferative, do not form foot processes and do not express maturity markers whereas differentiated podocytes

share characteristics with mature podocytes *in vivo*; they are non-proliferative, develop secondary and tertiary foot processes and express maturity markers associated with differentiation. There is the possibility, therefore, that VEGF acts as a maturity specific podocyte survival factor: VEGF induces a reduction in apoptosis in terminally differentiated podocytes, *in vivo*, but not in proliferative, de-differentiated podocytes *in vivo*, as discussed by Saleem et al, 2002 (Saleem et al., 2002).

Differentiated hCIPs incubated in VEGF demonstrated reduced cytotoxicity due to a reduction in apoptosis (figure 6.6). This agrees with known VEGF survival signalling pathways mediated through VEGF-R2. Signalling through VEGF-R1 though is quite different. VEGF can induce the upregulation of the PI3-Kinase/AKT signalling pathway in primary rat hepatic stellate cells. When these cells are kept in culture for more then 10 days VEGF-R2 expression is diminished, but VEGF-R1 expression is upregulated (Takahashi et al., 2003). This suggests that if VEGF mediates its survival effects through VEGF-R1 in podocytes it could induce the activation of the PI3-Kinase/AKT pathway. VEGF-R1 can bind to Np-1 and Np-2 as discussed earlier, Np-1 and Np-2 can form heterodimers (Giger et al., 1998) and it has been speculated that VEGF-R3 can bind to Np-2 (Yuan et al., 2002). It is possible, therefore, that VEGF-R1 and VEGF-R3 form heterodimers in podocytes. VEGF-R3 is involved in similar signalling pathways to VEGF-R2 in lymphatic endothelial cells in response to VEGF-C. It activates the PI3-Kinase/AKT pathway, protects cells from apoptosis and activates the PKC/MAPK pathway (Makinen et al., 2001). Interestingly, VEGF-C stimulation induced the formation of VEGF-R3/VEGF-R2 heterodimers in lymphatic endothelial cells and it was shown that the phosphorylation sites in this signalling complex were distinct from VEGF-R3 homodimers (Dixelius et al., 2003). VEGF-R1/VEGF-R3 heterodimers on podocytes would enable recognition of VEGF by VEGF-R1, although the activation of PI3-Kinase by

phosphorylation sites on both receptors would be hard to predict to due a conformational change of the intracellular domain of the receptors on heterodimerisation. There is no evidence available from the literature, however, that VEGF-R1 and VEGF-R3 can form heterodimers. Equally, however, this heterodimerisation has not been shown to be impossible or the hypothesis even tested. The reduction in apoptosis in podocytes induced by VEGF may stimulate more than one signalling pathway. VEGF protected podocytes from apoptosis induced by serum starvation, but it may only be effective in resisting certain apoptotic stimuli.

From these results we can deduce that VEGF signals in podocytes in an autocrine manner, potentially through VEGF-R1/VEGF-R3/Np-1/Np-2 complexes, to promote survival via a reduction in apoptosis. The signalling pathways that mediate these effects, though, still have to be elucidated in order to fully understand the effects of VEGF on podocyte biology. Much of the work from this chapter has been accepted for publication in paper 3 of the list of papers arising from this work

Chapter 7

VEGF intracellular signalling pathways in cultured podocytes

7.1 Introduction

The results from the previous chapters showed that VEGF could stimulate an autocrine effect on podocytes stimulating an unknown pathway, which ultimately resulted in promoting survival via a reduction in apoptosis. To elucidate the effects of VEGF in podocytes the survival pathway that VEGF activates was investigated.

Likely signalling pathways through which VEGF may signal in epithelial cells lacking VEGFR-2, but containing VEGFR-1 include VEGFR-1 tyrosine phosphorylation and activation of downstream signalling molecules known to be involved in regulation of apoptosis. These include PI3 kinase, which has also been shown to be activated after VEGF-R1 stimulation in activated hepatic stellate cells (Takahashi et al., 2003). It would therefore be useful to use inhibitors of these molecules, particularly VEGF-R1 and PI3 Kinase as a starting point for the investigation of the mechanism through which VEGF acts on podocytes.

1-[4-Chloroanilino]-4-[4-pyridylmethyl]-dihydrochloride (PTK787/ZK222584) is a class III tyrosine kinase receptor inhibitor developed by Novartis Pharmaceuticals (a kind gift from Dr J Wood, Novartis AG, Switzerland), which acts by binding to the ATP-binding sites of these types of receptor tyrosine kinases. Class III RTKs include VEGFR-1, VEGF-R2, VEGF-R3, placental growth factor receptor (PDGF-R) and c-Kit (a receptor for cell stem factor) with an IC_{50} of less than 1μM (Wood et al., 2000). PTK787/ZK222584 can inhibit VEGF-R1 phosphorylation at an IC_{50} of 77nM and VEGF-R2 at 130nM, whereas PDGF-R and VEGF-R3 require higher concentrations with an IC_{50} of 580nM and 660nM respectively (Wood et al., 2000). This inhibitor was used at 1μM in $[Ca^{2+}]_i$ experiments to block the effects of all of the above class III tyrosine kinases, and at 100nM in cytotoxicity experiments to examine whether the VEGF effects on cultured podocytes were VEGF-R1 dependent.

VEGF promotes survival by reducing apoptosis in cultured podocytes, shown in chapter 6. In endothelial cells the survival pathway commonly activated by VEGF is the PI3-Kinase/AKT survival pathway, as discussed in the introduction. Wortmannin is a fungal metabolite, which selectively and irreversibly blocks the catalytic activity of PI3-Kinase by binding to the ATP binding site of the pre-phosphorylated p85/p110 PI3-Kinase complex at residue Lys-802 (Wymann et al., 1996). This inhibitor was used to investigate whether the VEGF induced reduction in cytotoxicity was PI3-Kinase dependent in podocytes. VEGF has been shown to be able to exert its effects both externally, via VEGF receptors expressed at the plasma membrane, and internally, via in-side-out VEGF receptor expression on the membrane of caveolae within the cytosol (Labrecque et al., 2003) (Feng et al., 1999). Wortmannin is cell permeant (Wymann et al., 1996) and therefore can inhibit VEGF signalling both externally and internally.

A neutralising monoclonal antibody to VEGF was also used in these experiments. It binds to an epitope of VEGF on the receptor-binding site and therefore VEGF cannot recognise and bind to its receptors (MAB393, R&D Systems, Abingdon, UK). The neutralising monoclonal antibody to VEGF is not cell permeant and can only neutralise exogenous or endogenous VEGF externally to the cell plasma membrane, therefore it has no neutralising effect on internal VEGF signalling. The neutralising monoclonal antibody to VEGF was used to ensure that the effects of exogenous VEGF were VEGF specific, and was also used to block the external effects of endogenous VEGF.

7.2 Methods

7.2.1 $[Ca^{2+}]_i$ measurements-VEGF-R signalling

hCIPs and PCPs were incubated in HBSS containing minimal calcium (minimal $[Ca^{2+}]_o$) so that the reduction in $[Ca^{2+}]_i$ in hCIPs induced by VEGF could be detected. Cells were pre-incubated for 10 minutes with 1μM of the class III tyrosine kinase inhibitor, PTK787/ZK222584, then treated with 1nM VEGF as described in the methods. The cells were washed three times with HBSS containing minimal calcium, then left for 20 minutes to wash out the inhibitor before being treated once more with 1nM VEGF. Cells were not treated with VEGF before incubation with PTK787/ZK222584 because the VEGF-induced reduction in $[Ca^{2+}]_i$ did not reverse during the experiment, which may affect the magnitude of the $[Ca^{2+}]_i$ response. Cells were also treated with 0.32μg/ml of a neutralising monoclonal antibody to VEGF (R&D Systems, Abingdon, UK) and 0.32μg/ml of normal mouse IgG in the same manner as with treatment of VEGF. The analysis of these experiments was carried out in two ways; the measurement of the mean $[Ca^{2+}]_i$ values at the peak of the response or the mean $[Ca^{2+}]_i$ values taken at the end of the experiment, once a plateaux had been reached. This enabled both increases and reductions in $[Ca^{2+}]_i$ to be measured in response to a stimulus.

7.2.2 Cytotoxicity assay-VEGF-R signalling

Serum starved PCPs were incubated for 24hrs in fresh RPMI media containing 100nM PTK787/ZK222584, not 1μM, so that the effects of VEGF-R1 could be distinguished from VEGF-R3 or PDGF-R signalling. Serum starved PCPs were also incubated in 1nM VEGF, VEGF with PTK787/ZK222584, or left untreated for 24hrs. The percentage of cytotoxicity was quantified in low, experimental and high controls, and compared between treatments, as described in the methods.

7.2.3 Cytotoxicity assay-PI3-Kinase signalling

Serum starved hCIPs and PCPs were incubated in fresh RPMI media containing a range of Wortmannin concentrations, a PI3-Kinase inhibitor) including 0, 50, 100, 200 and 400nM, either alone, to assess endogenous levels of PI3-Kinase activity, or with 1nM VEGF for 24hrs. % cytotoxicity was quantified in low, experimental and high controls, and compared between treatments, as described in the methods.

7.3 Results

7.3.1 Signalling through VEGF-Rs

Incubation of hCIPs with VEGF loaded with Fura-2 and pre-incubated with the class III tyrosine kinase inhibitor, PTK787/ZK222584, induced a 2 fold transient increase in $[Ca^{2+}]_i$. It peaked approximately 2 minutes after the addition of VEGF and reached a plateaux approximately 4 minutes from the addition of VEGF (figure 7.1 A). This increase in $[Ca^{2+}]_i$ in response to VEGF in the presence of PTK787/ZK222584 was significantly greater than baseline recordings over the course of 5 experiments (a ratio (treatment/baseline $[Ca^{2+}]_i$) of 1.48±0.25) compared to baseline (a ratio (baseline/average baseline $[Ca^{2+}]_i$) of 1±0.16, figure 7.1 B, $p<0.01$). The recovering $[Ca^{2+}]_i$ baseline (at the end of the experiment) in cells pre-incubated in PTK787/ZK222584, then treated with VEGF was if anything slightly higher than the original baseline and was significantly higher than the recovering $[Ca^{2+}]_i$ baseline in cells treated with VEGF alone (a ratio (baseline/average baseline $[Ca^{2+}]_i$) of 1.23±0.13 compared to that of 0.72±0.09, figure 7.1 C, $p<0.05$). The data were analysed in this manner so that these experiments could be compared to similarly analysed historical experiments and also demonstrated that there was no decrease in $[Ca^{2+}]_i$ from original baseline recordings in the presence of VEGF. This suggests that pre-incubation of hCIPs with PTK787/ZK222584 blocked the VEGF induced reduction in $[Ca^{2+}]_i$ shown previously in figure 4.1F and it also induced an increase in $[Ca^{2+}]_i$. The phosphorylation of all class III tyrosine kinases in question was blocked, in principle, because the concentration of inhibitor used was at an IC_{50} much greater then was required. These results indicate that VEGF induces its effects on $[Ca^{2+}]_i$ in hCIPs via class III tyrosine kinase receptors.

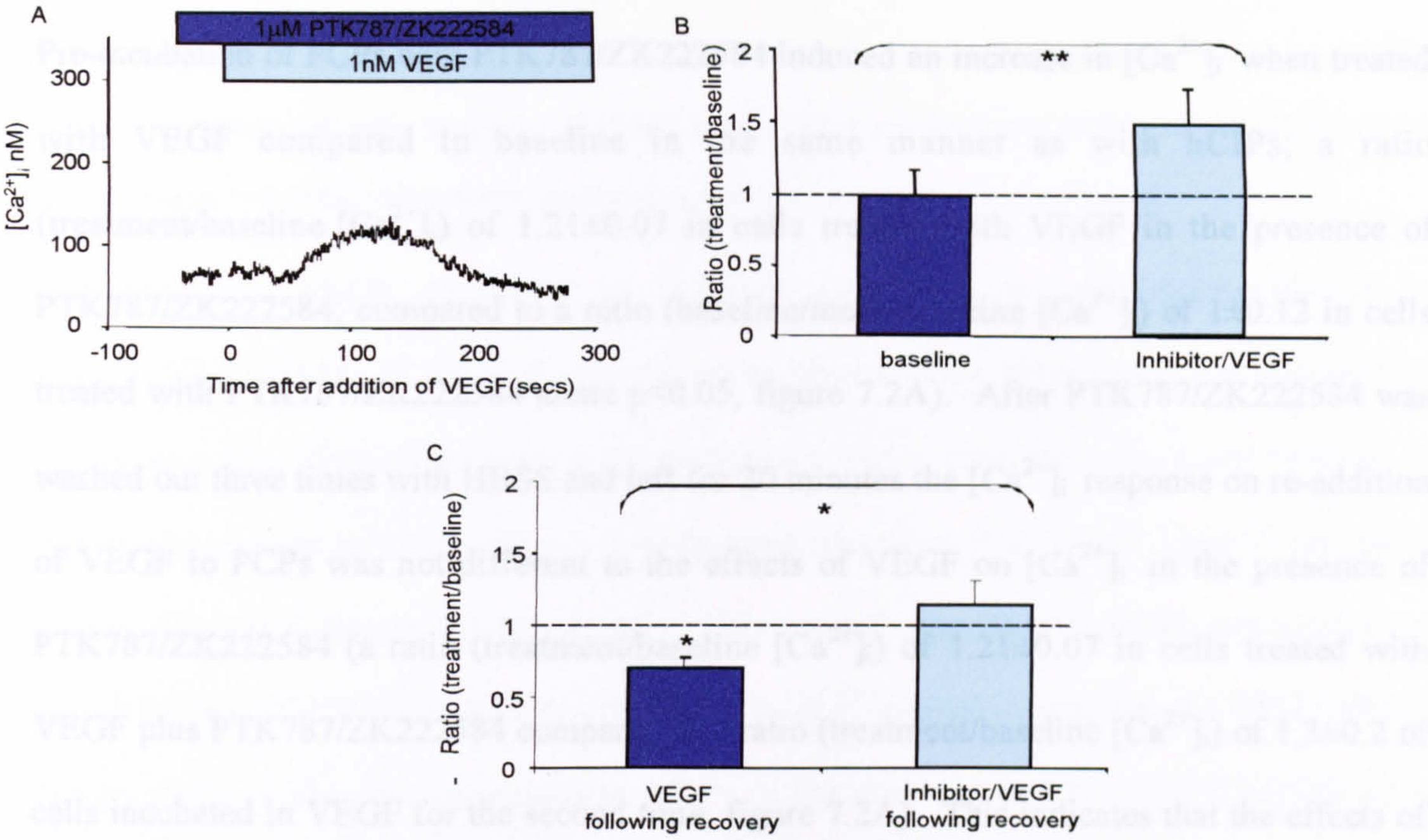

Figure 7.1. PTK787/ZK222584 blocks the reduction in $[Ca^{2+}]_i$ induced by VEGF in hCIPs.

Serum starved hCIPs, loaded with Fura-2, were pre-incubated with PTK787/ZK222584 for 10 minutes before the addition of 1nM VEGF in the presence of minimal $[Ca^{2+}]_o$. Fluorescent inensity changes were recorded and used to calculate $[Ca^{2+}]_i$ concentrations and then the ratio (treatment/baseline $[Ca^{2+}]_i$) was used for comparisons between experiments in hCIPs. A. An example of the peak $[Ca^{2+}]_i$ response to 1nM VEGF in cells pre-incubated with PTK787/ZK222584 (incubated in minimal $[Ca^{2+}]_o$). VEGF induced an increase in $[Ca^{2+}]_i$ in hCIPs pre-incubated in PTK787/ZK222584. B. The peak $[Ca^{2+}]_i$ response in hCIPs pre-incubated in PTK787/ZK222584 after the addition of 1nM VEGF (pale blue) was significantly higher compared to baseline in the presence of PTK787/ZK222584 (dark blue) ($p<0.05$; two-tailed t-test). C. Comparison of $[Ca^{2+}]_i$ following recovery of the response to the addition of 1nM VEGF in hCIPs pre-incubated in PTK787/ZK222584 (pale blue) to that of hCIPs treated with VEGF alone (dark blue, historical data as shown in figure 4.1F). The change in $[Ca^{2+}]_i$, expressed as the ratio of treatment/control, following recovery was significantly higher compared to those of historical VEGF experiments, but was not significantly different from one (ie not different from baseline; one tailed *t*-test). The $[Ca^{2+}]_i$ following recovery in the PTK787/ZK222584 and VEGF experiments was significantly lower than the peak $[Ca^{2+}]_i$ resonse ($p>0.05$, paired *t*-test, not shown). *=$p<0.05$, **=$p<0.01$ compared to baseline or as indicated, paired *t*-test, n=5.

Pre-incubation of PCPs with PTK787/ZK222584 induced an increase in $[Ca^{2+}]_i$ when treated with VEGF compared to baseline in the same manner as with hCIPs; a ratio (treatment/baseline $[Ca^{2+}]_i$) of 1.21±0.07 in cells treated with VEGF in the presence of PTK787/ZK222584; compared to a ratio (baseline/mean baseline $[Ca^{2+}]_i$) of 1±0.12 in cells treated with PTK787/ZK222584 alone $p<0.05$, figure 7.2A). After PTK787/ZK222584 was washed out three times with HBSS and left for 20 minutes the $[Ca^{2+}]_i$ response on re-addition of VEGF to PCPs was not different to the effects of VEGF on $[Ca^{2+}]_i$ in the presence of PTK787/ZK222584 (a ratio (treatment/baseline $[Ca^{2+}]_i$) of 1.21±0.07 in cells treated with VEGF plus PTK787/ZK222584 compared to a ratio (treatment/baseline $[Ca^{2+}]_i$) of 1.3±0.2 of cells incubated in VEGF for the second time, figure 7.2A). This indicates that the effects of PTK787/ZK222584 did not reverse.

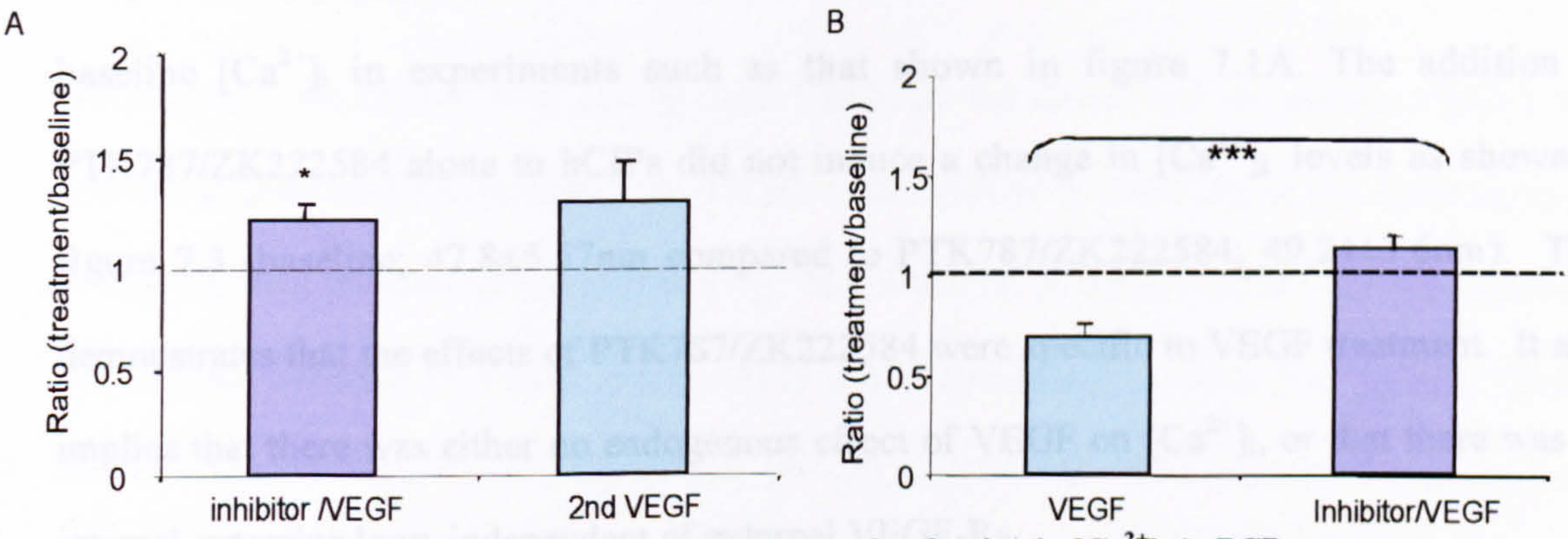

Figure 7.2. PTK787/ZK222584 blocks the VEGF induced reduction in $[Ca^{2+}]_i$ in PCPs.

Serum starved PCPs, were loaded with Fura-2 and pre-incubated with PTK787/ZK222584 for 10 minutes before the addition of 1nM VEGF. Fluorescent intensity changes were recorded and used to calculate $[Ca^{2+}]_i$ and were compared to baseline $[Ca^{2+}]_i$ recordings in the presence of PTK787/ZK222584 in PCPs. Data were expressed as mean+SEM ratio (treatment/baseline $[Ca^{2+}]_i$). A. The $[Ca^{2+}]_i$ response of PCPs to 1nM VEGF in the presence (blue) of PTK787/ZK222584 and a second treatment with VEGF in the absence (green) of PTK787/ZK222584. VEGF induced a significant increase in $[Ca^{2+}]_i$ in PCPs, pre-incubated in PTK787/ZK222584 compared to baseline recordings. The re-addition of VEGF after the PTK787/ZK222584 had been washed from the cells for 20 minutes did not significantly change the $[Ca^{2+}]_i$

levels compared to in the presence of PTK787/ZK222584. B. A comparison of the recovering $[Ca^{2+}]_i$ baseline recordings following treatment of VEGF in cells either pre-incubated in PTK787/ZK222584 (blue) or not (green). *=p<0.05, ***=p<0.001, paired *t*-test compred to baseline or as indicated.

Not only did VEGF stimulate an increase in $[Ca^{2+}]_i$ in cells pre-incubated in PTK787/ZK222584 in PCPs but the recovering baseline in these experiments was also slightly higher than the original baseline and significantly higher than the recovering baseline in historical responses to VEGF alone; a ratio (treatment/baseline $[Ca^{2+}]_i$) of 1.13±0.07 compared to that of 0.7±0.07 (figure 7.2 B, $p<0.001$). This suggests that, as with hCIPs, pre-incubation with PTK787/ZK222584 blocks the reduction in $[Ca^{2+}]_i$ seen in response to VEGF alone. Observations of baseline recordings in hCIPs in the presence of PTK787/ZK222584 were made to test that PTK787/ZK222584 itself was not having an effect, other than blocking class III tyrosine kinase receptors. These observations revealed that there was no elevation of baseline $[Ca^{2+}]_i$ in experiments such as that shown in figure 7.1A. The addition of PTK787/ZK222584 alone to hCIPs did not induce a change in $[Ca^{2+}]_i$ levels as shown in figure 7.3 (baseline; 47.8±5.57nm compared to PTK787/ZK222584; 49.24±3.6nm). This demonstrates that the effects of PTK787/ZK222584 were specific to VEGF treatment. It also implies that there was either no endogenous effect of VEGF on $[Ca^{2+}]_i$, or that there was an internal autocrine loop, independent of external VEGF-Rs.

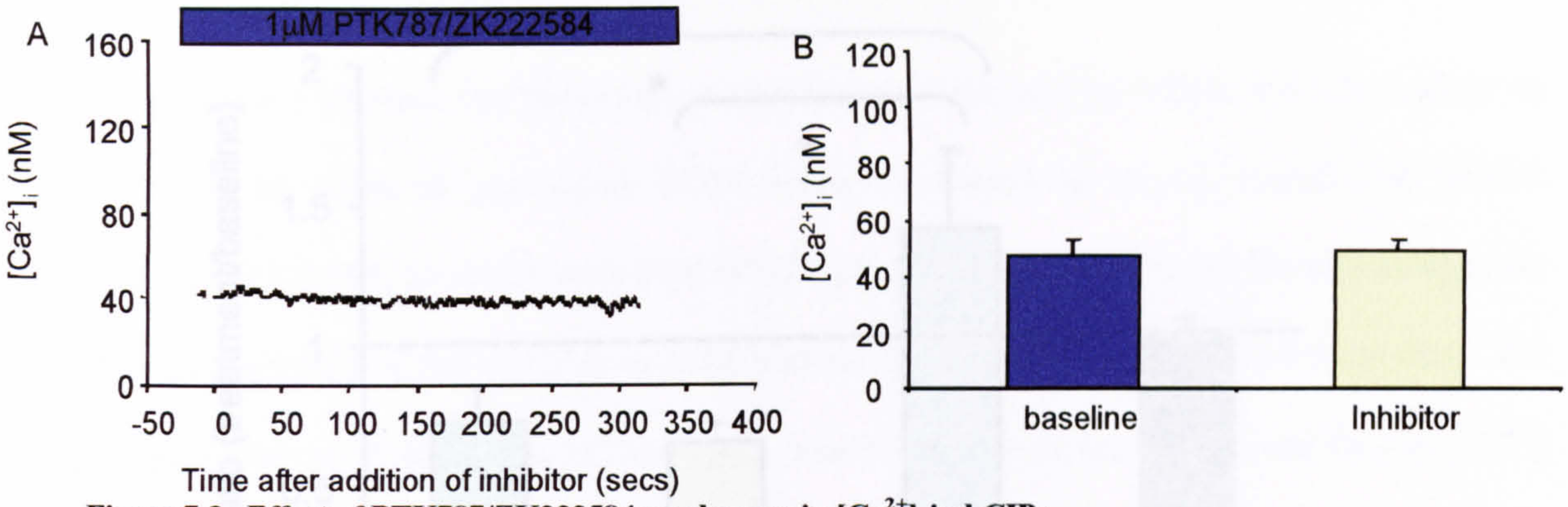

Figure 7.3. Effect of PTK787/ZK222584 on changes in $[Ca^{2+}]_i$ in hCIPs.

Serum starved hCIPs, loaded with Fura-2 were incubated with PTK787/ZK222584. Changes in fluorescent intensity were recorded, and used to calculate $[Ca^{2+}]_i$ and then compared to baseline recordings of changes in $[Ca^{2+}]_i$ in hCIPs. A. An example of an $[Ca^{2+}]_i$ measurement in response to treatment with PTK787/ZK222584 alone showed no change in $[Ca^{2+}]_i$. B. Mean+SEM of $[Ca^{2+}]_i$ in cells before (blue) and after yellow) pre-incubation with PTK787/ZK222584 shows no significant difference in $[Ca^{2+}]_i$ concentration. N.s. n=6.

Surprisingly, the inhibition of endogenous VEGF (in the absence of exogenous VEGF), by a neutralising monoclonal antibody to VEGF, reduced $[Ca^{2+}]_i$ in hCIPs to the same extent as VEGF (a ratio (treatment/baseline $[Ca^{2+}]_i$) of 0.64±0.06 in cells treated with a neutralising monoclonal antibody to VEGF, compared to a ratio (treatment/baseline $[Ca^{2+}]_i$) of 0.72±0.13 in cells treated with VEGF, figure 7.4, $p<0.05$, ANOVA). The effects of a neutralising monoclonal antibody to VEGF, combined with VEGF, not only blocked the effects of VEGF on $[Ca^{2+}]_i$, in hCIPs but also significantly increased $[Ca^{2+}]_i$ from baseline recordings (a ratio (treatment/baseline $[Ca^{2+}]_i$) of 1.38±0.29 in cells treated with VEGF plus a neutralising monoclonal antibody to VEGF, $p<0.01$, figure 7.4). These results were similar to the effects of VEGF on changes in $[Ca^{2+}]_i$ in cells pre-incubated with PTK787/ZK222584.

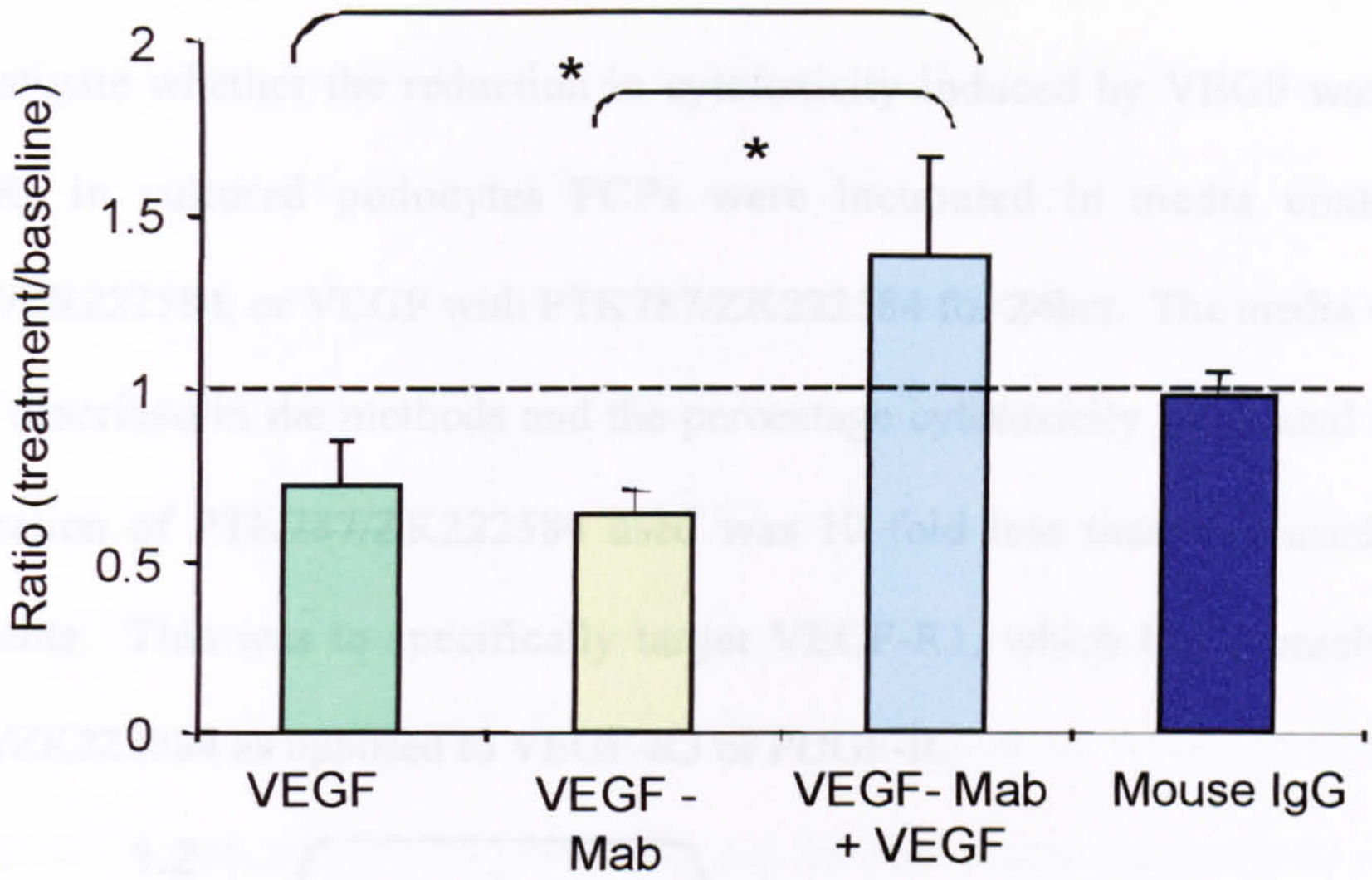

Figure 7.4. The effect of VEGF-Mab on the reduction in $[Ca^{2+}]_i$ induced by VEGF in hCIPs.

Serum starved hCIPs, loaded with Fura-2, were incubated in VEGF, VEGF-Mab, VEGF plus VEGF-Mab or normal mouse IgG. Changes in fluorescent intensity were recorded, and used to calculate $[Ca^{2+}]_i$, Data were expressed as mean+SEM ratio (treatment/baseline $[Ca^{2+}]_i$). There was a significant reduction in $[Ca^{2+}]_i$ in cells treated with both VEGF (green) and VEGF-Mab (yellow) to cells treated with a combination of VEGF plus VEGF-Mab (light blue). There was no significant effect on $[Ca^{2+}]_i$ in cells treated with normal mouse IgG. Student-Newmann-Keuls Test, *=$p<0.05$, $n\geq6$.

Treatment of hCIPs with normal mouse IgG did not induce a significant change in $[Ca^{2+}]_i$ compared to baseline $[Ca^{2+}]_i$ (a 0.97±0.07 fold change in ratio of (treatment/baseline $[Ca^{2+}]_i$) in cells treated with mouse IgG, figure 7.4). This shows that the effect of the neutralising monoclonal antibody to VEGF was not due to a non-specific mouse IgG effect (the species in which the neutralising monoclonal antibody to VEGF was raised). Together, these results demonstrate that exogenous VEGF induced a class III tyrosine kinase dependent reduction in $[Ca^{2+}]_i$ in cultured podocytes. To investigate whether VEGF survival signalling was also dependent on class III tyrosine kinases, the effect of PTK787/ZK222584 on the VEGF induced reduction in cytotoxicity was assayed.

To investigate whether the reduction in cytotoxicity induced by VEGF was dependent on VEGF-Rs in cultured podocytes PCPs were incubated in media containing VEGF, PTK787/ZK222584, or VEGF with PTK787/ZK222584 for 24hrs. The media was assayed for LDH as described in the methods and the percentage cytotoxicity calculated from this. The concentration of PTK787/ZK222584 used was 10 fold less than that used in the $[Ca^{2+}]_i$ experiments. This was to specifically target VEGF-R1, which has a much lower IC_{50} to PTK787/ZK222584 as opposed to VEGF-R3 or PDGF-R.

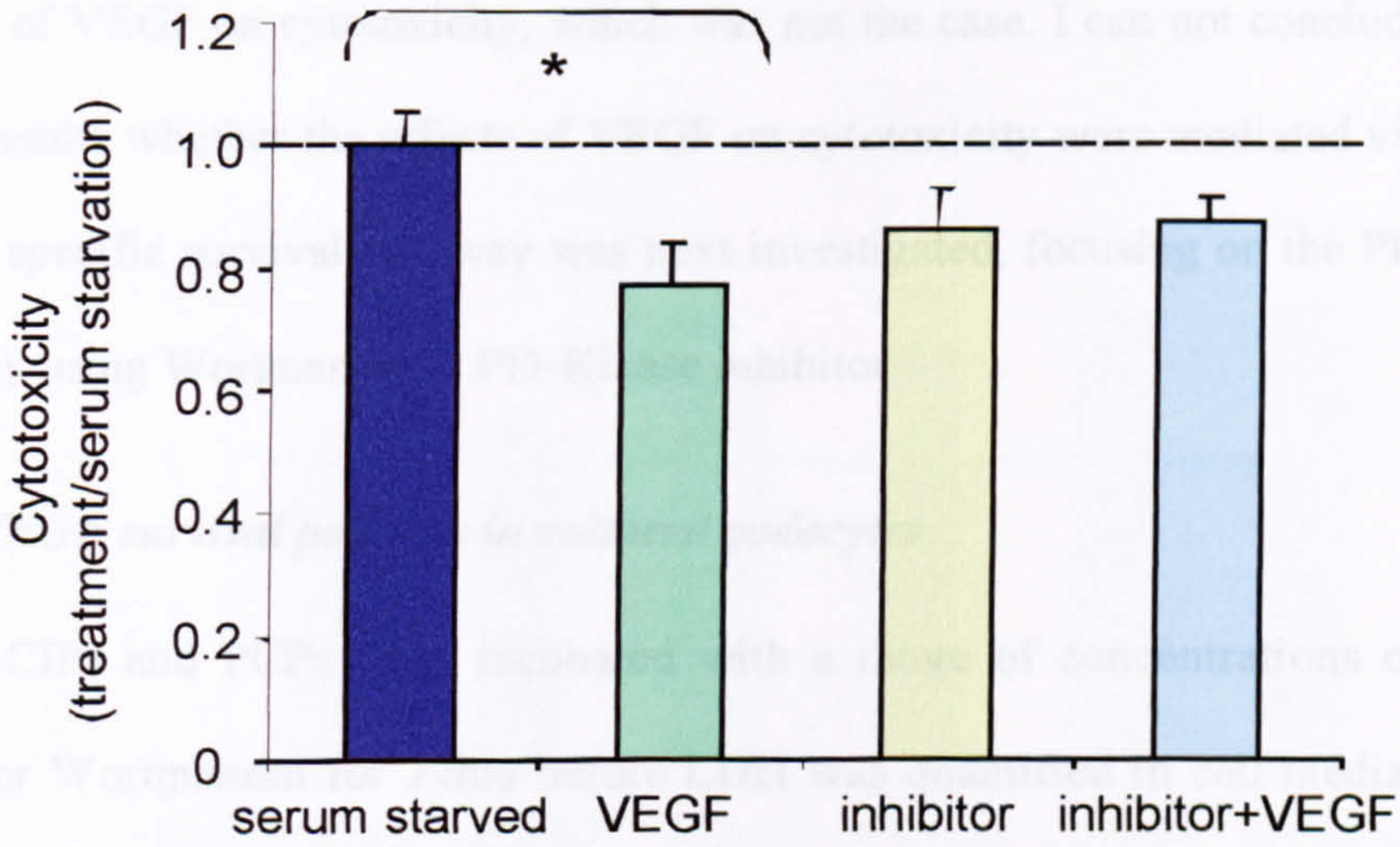

Figure 7.5. The effects of PTK787/ZK222584 on the reduction in cytotoxicity induced by VEGF in PCPs.

Serum starved PCPs were incubated in VEGF, PTK787/ZK222584, VEGF plus PTK787/ZK222584 or left untreated for 24hrs. The percentage of cytotoxicity was then assayed and compared between treatments. The bar graph shows mean+SEM ratio of (percentage cytotoxicity treatment/baseline). There was no significant difference in ratio between cells treated with PTK787/ZK222584 or cells treated with PTK787/ZK222584 plus VEGF, with either cells that were serum starved or cells that were treated with VEGF. * =p<0.05, Bonferroni test, n=18.

There was a small, but not significant reduction in cytotoxicity in PCPs treated with a combination of the inhibitor and VEGF compared to that of serum starved cells (a 0.87±0.43 fold reduction of ratio (treatment/serum starvation) in cells treated with VEGF plus

PTK787/ZK222584, figure 7.5). These results imply that either PTK787/ZK222584 did not fully block the effects of VEGF and that the effects of VEGF on cytotoxicity are only partially dependent on VEGF-R1, or that PTK787/ZK222584 did not have an effect on the VEGF induced reduction in cytotoxicty. Figure 5.3B shows that treatment of cultured podocytes with a neutralising monoclonal antibody to VEGF increased cytotoxicity compared to control. This indicates that the endogenous effects of VEGF on cytotoxicity act via an external autocrine loop because the neutralising monoclonal antibody to VEGF acts externally. It was predicted, therefore, that treatment of PCPs with PTK787/ZK222584 alone would block the endogenous effects of VEGF on cytotoxicity, which was not the case. I can not conclude either way from these results whether the effects of VEGF on cytotoxicity were mediated via VEGF-R1. The VEGF specific survival pathway was next investigated, focusing on the PI3-Kinase survival pathway using Wortmannin, a PI3-Kinase inhibitor.

7.3.2 VEGF survival pathway in cultured podocytes

Both hCIPs and PCPs were incubated with a range of concentrations of the PI3-Kinase inhibitor Wortmannin for 24hrs before LDH was quantified in cell media and cytotoxicity calculated to assess how Wortmannin effected cytotoxicity levels. Wortmannin induced a dose dependent increase in cytotoxicity in PCPs, becoming significant at a concentration of 200nM Wortmannin ($p<0.01$, ANOVA, figure 7.6 A). Wortmannin also induced a dose dependent increase in cytotoxicity in hCIPs, becoming significant at a lower concentration than with PCPs, at 50nM Wortmannin ($p<0.01$, ANOVA, figure 7.6 B). The increase in cytotoxicity, induced by Wortmannin in cultured podocytes could be either due to an inhibition of baseline levels of PI3-Kinase in serum starved cells, resulting in increased apoptosis or due to a non-specific toxic effect resulting in increased cell death.

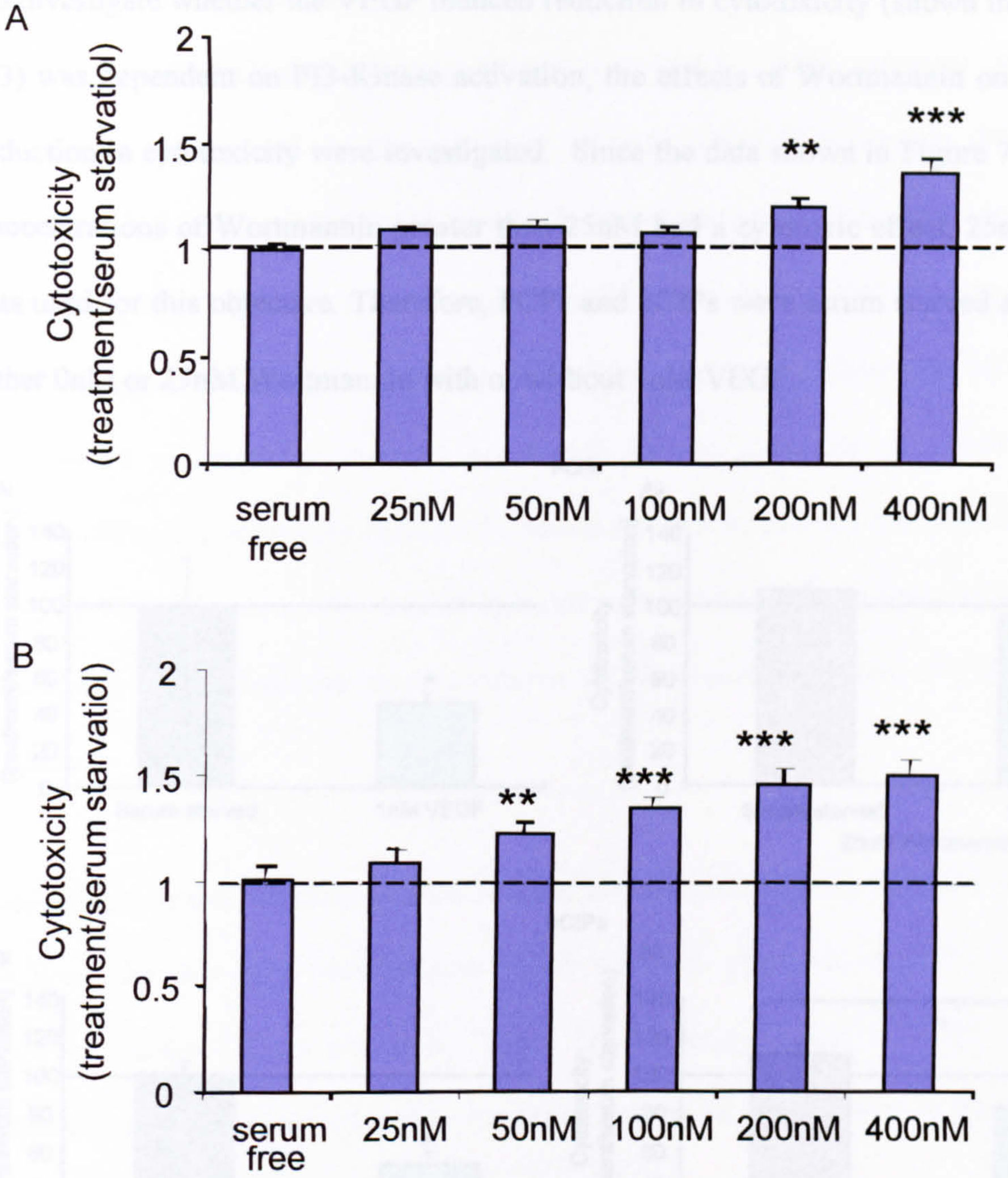

Figure 7.6. Cytotoxicity dose response of PCPs and hCIPs to Wortmannin.

Serum starved PCPs and hCIPs were incubated in increasing doses of Wortmannin for 24 hrs. Cytotoxicity was then assayed and compared between treatments. Data were expressed as mean+SEM ratio of (percentage of cytotoxicity of treatment/serum-starvation). Wortmannin dose dependently increased cytotoxicity in PCPs (A) and hCIPs (B). Wortmannin caused a significant increase in cytotoxicity in PCPs from 200nM upwards whilst in hCIPs it was active at lower concentrations; from 50nM upwards. *=p<0.05 **=p<0.01,*p<0.001 compared to serum starvation, one way ANOVA, Student-Newmann Keuls posthoc test.**

To investigate whether the VEGF induced reduction in cytotoxicity (shown in figures 5.2 and 5.3) was dependent on PI3-Kinase activation, the effects of Wortmannin on VEGF induced reduction in cytotoxicity were investigated. Since the data shown in Figure 7.6 indicates that concentrations of Wortmannin greater than 25nM had a cytotoxic effect, 25nM Wortmannin was used for this objective. Therefore, PCPs and hCIPs were serum starved and incubated in either 0nM or 25nM Wortmannin with or without 1nM VEGF.

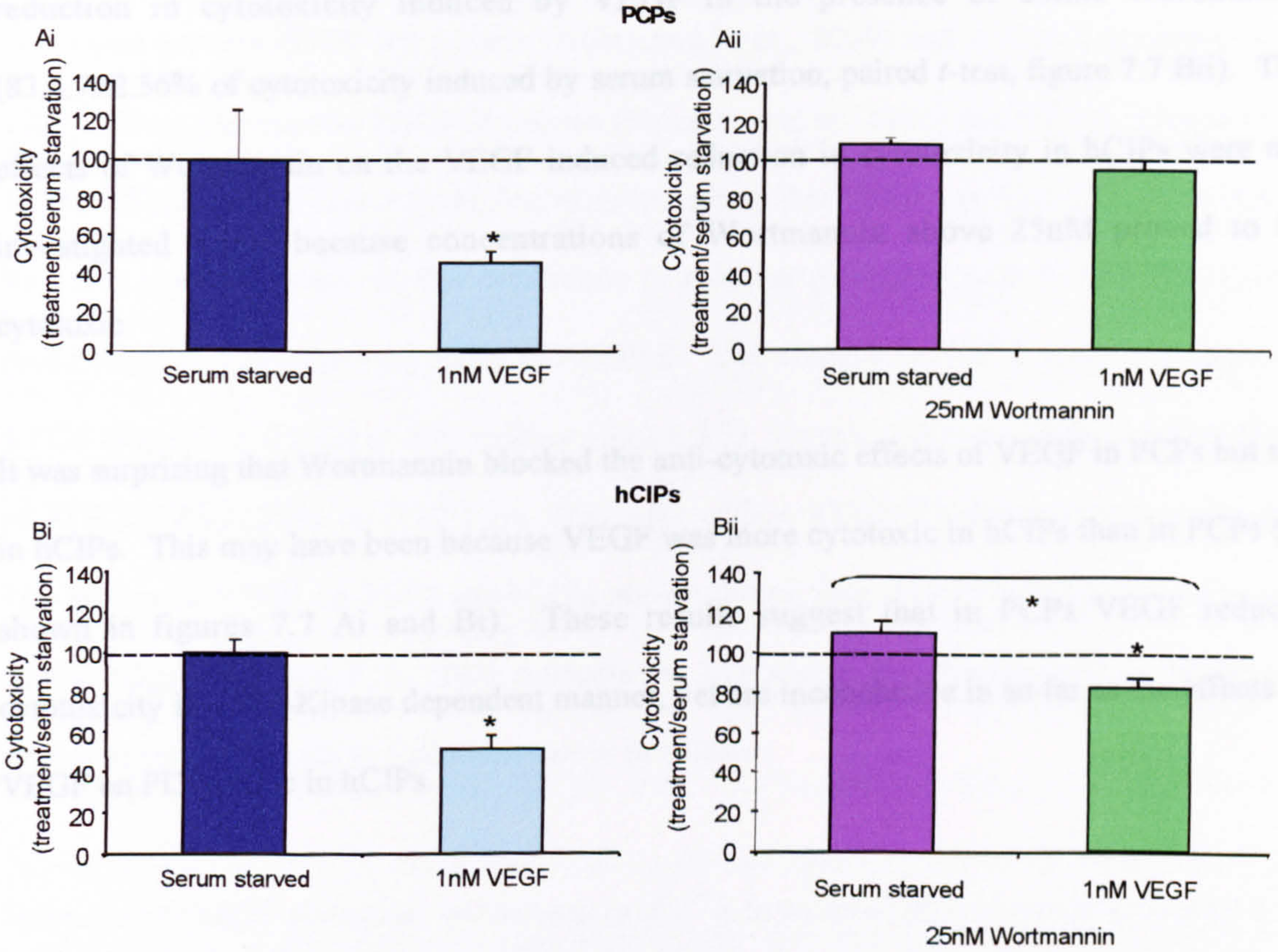

Figure 7.7. The effects of Wortmannin on the VEGF mediated reduction in cytotoxicity.

Ai. Data from figure 5.2B re-expressed as change in cytotoxicity (treatment/serum starvation). Aii. The effect of VEGF on cytotoxicity in PCPs in the presence of 25nM Wortmannin. Bi. Data from figure 5.3A re-expressed as change in cytotoxicity (treatment/baseline). Bii. The effect of VEGF on cytotoxicity in hCIPs in the presence of 25nM Wortmannin. *=$p<0.05$, paired *t*-test.

As expected, this concentration of Wortmannin did not have a cytotoxic effect on serum-starved PCPs (108.4±2% cytotoxicity compared to 94.63±5.63%, unpaired *t*-test, figure 7.7 Aii). On the other hand, in the presence of just 25nM Wortmannin the reduction in cytotoxicity induced by VEGF (45.5±5.76% of cytotoxicity induced by serum starvation, paired *t*-test, figure 7.7 Ai) was blocked (94.63±5.63% of cytotoxicity induced by serum starvation, paired *t*-test, figure 7.7 Aii). In hCIPs, conversely, there was still a significant reduction in cytotoxicity induced by VEGF in the presence of 25nM Wortmannin (83.4.7±2.56% of cytotoxicity induced by serum starvation, paired *t*-test, figure 7.7 Bii). The effects of Wortmannin on the VEGF induced reduction in cytotoxicity in hCIPs were not investigated futher because concentrations of Wortmannin above 25nM proved to be cytotoxic.

It was surprising that Wortmannin blocked the anti-cytotoxic effects of VEGF in PCPs but not in hCIPs. This may have been because VEGF was more cytotoxic in hCIPs than in PCPs (as shown in figures 7.7 Ai and Bi). These results suggest that in PCPs VEGF reduces cytotoxicity in a PI3-Kinase dependent manner, yet are inconclusive in so far as the effects of VEGF on PI3-Kinase in hCIPs.

7.4 Discussion

Pre-incubation of PCPs and hCIPs with the class III tyrosine kinase receptor inhibitor, PTK787/ZK222584, blocked the VEGF induced reduction in $[Ca^{2+}]_i$ when incubated in minimal $[Ca^{2+}]_o$. This suggests the effects of VEGF on $[Ca^{2+}]_i$ in hCIPs were class III tyrosine kinase receptor dependent. The receptors that could be inhibited at the concentration of inhibitor used were VEGF-R1, VEGF-R2, VEGF-R3 and PDGF-R. Differentiated, cultured podocytes express PDGF-Rβ protein (Nakagawa et al., 2000) and mRNA (Asanuma et al., 2002). They also express PDGF-B protein (Nakagawa et al., 2000) and mRNA (Floege et al., 1993). There is no evidence in the literature to suggest that VEGF can bind directly to PDGF-Rs. It is possible, however, that incubation of cultured podocytes with PTK787/ZK222584 could block an autocrine loop effect of PDGF-B. Yet, changes in $[Ca^{2+}]_i$ were in response to VEGF (figure 7.1 A), not to the inhibitor (figure 7.3). Hence, it is most likely that the effects of PTK787/ZK222584 on $[Ca^{2+}]_i$ are VEGF-R1 and/or VEGF-R3 dependent in podocytes. The effects of VEGF on PCPs and hCIPs pre-incubated with PTK787/ZK222584 were very similar (figure 7.1 and 7.2). This supports the hypothesis that the two cell types express similar receptors and act in a similar manner in culture.

Surprisingly, VEGF stimulated an increase in $[Ca^{2+}]_i$ in cultured podocytes pre-incubated with PTK787/ZK222584. This rapid transient response was similar to the *in vivo* response of endothelial cells to VEGF (Pocock et al., 2000). If activation of VEGF-R1 and/or VEGF-R3 by VEGF activates either the SERCA or PMCA (as discussed in chapter 3) then the inhibitor may act by blocking the active pumping of calcium from the cytosol. Thus, it would be predicted that cells would no longer respond to VEGF, not respond in an opposite manner. It may be possible that VEGF can act through another receptor in podocytes, which is not a class

III tyrosine kinase receptor. For example, if VEGF was capable of signalling independently through Np-1 or Np-2, as suggested by Wang et al 2003 this may induce an increase in $[Ca^{2+}]_i$ via a different signalling pathway than when VEGF-R1 and VEGF-R3 are activated by VEGF.

Blocking the effects of exogenous VEGF, using a neutralising monoclonal antibody to VEGF also resulted in a significant increase in $[Ca^{2+}]_i$ compared to untreated cells (figure 7.4). This suggests that because the neutralising monoclonal antibody to VEGF binds directly to VEGF and thus prevents it from binding to its receptors this increase in $[Ca^{2+}]_i$ was not dependent on VEGF receptor activation by VEGF. Yet the reduced $[Ca^{2+}]_i$ response was mediated by the addition of VEGF. Interestingly, inhibition of endogenous VEGF by a neutralising monoclonal antibody to VEGF induced a significant reduction in $[Ca^{2+}]_i$ similar to that of VEGF. This will be discussed further in more detail later in the thesis, as will the implications of natural VEGF inhibitors within the glomerulus.

The VEGF induced reduction in cytotoxicity in cultured podocytes was not significantly blocked by PTK787/ZK222584, which was used at a concentration too low to affect VEGF-R3, but able to inhibit VEGF-R1 (figure 7.5). This indicated that either the effects of exogenous VEGF on cytotoxicity were only partially dependent on VEGF-R1 and that they were also dependent on another receptor, most likely VEGF-R3 or that the effects of VEGF on cytotoxicity were not VEGF-R1 dependent. A similar response was also seen when the cells were incubated in PTK787/ZK222584 alone at the same concentration; it did not significantly block the effects of endogenous VEGF. It has been suggested that PTK787/ZK222584 inhibits VEGF mediated VEGF-R signalling at different concentrations depending on the signalling pathway, for example in HUVECs VEGF mediated proliferation is blocked at an IC_{50} of 16nM, whereas cell survival and migration are blocked at an IC_{50} of 58nM (Traxler et

al., 2001). When PTK787/ZK222584 was used to block the auto-phosphorylation of VEGF-R1 by VEGF in Multiple Myeloma cells, which do not express VEGF-R2 or VEGF-R3, the proliferative effects of VEGF were significantly blocked at 500nM PTK787/ZK222584 (a lower concentration was not used) (Lin et al., 2002). The effects of PTK787/ZK222584 on VEGF-R1 auto-phosphorylation mediated by VEGF have not yet been examined with respect to survival signalling. The IC_{50} of PTK787/ZK222584 needed to block this signalling pathway may therefore be higher than the concentration of PTK787/ZK222584 used podocytes in this chapter. If a higher concentration of PTK787/ZK222584 was needed to block the reduced cytotoxicity induced by VEGF activation of VEGF-R1 in podocytes then this may explain why the use of PTK787/ZK222584 did not significantly block the survival effect of exogenous and endogenous VEGF (figure 7.5). PTK787/ZK222584 does not appear to have been used experimentally in the literature to block the effects of VEGF-R3 auto-phosphorylation by VEGF. These results demonstrate that external VEGF mediated $[Ca^{2+}]_i$ effects are at least partially VEGF-R1 dependent and are possibly also VEGF-R3 dependent. I can not draw any conclusions on VEGF-R1 mediated VEGF survival signalling in cultured podocytes.

Wortmannin, a PI3-Kinase inhibitor, dose dependently increased cytotoxicity in PCPs within the range whereby Wortmannin had no non-specific toxic effects (figure 7.6), although in hCIPs the concentration at which Wortmannin blocked the reduction in cytotoxicity induced by VEGF was beyond the range whereby Wortmannin only had an effect on PI3-Kinase. This suggests Wortmannin had non-specific cytotoxic effects past a given concentration, as discussed by Wyman et al, 1996 (Wymann et al., 1996), particularly in hCIPs. This may be due to a number of factors, for example hCIPs may have had lower serum starved induced levels of PI3-Kinase, or they may have been seeded at a lower density, as discussed for figure

3.11B in chapter 3. In PCPs Wortmannin is most likely to be acting on PI3-kinase activated by VEGF-R1 auto-phosphorylation. VEGF-R2 is not expressed and VEGF cannot interact directly with VEGF-R3. VEGF-R1 auto-phosphorylation can induce the activation of PI3-Kinase in VEGF-R1-expressing insect cells (Yu et al., 2001b), but the effects of Wortmannin on the activity of VEGF-R1 induced PI3-Kinase activity have not yet been assessed. It is therefore not known if Wortmannin can block the activation of PI3-Kinase, by VEGF-R1 autophosphorylation at the same concentration as it is effective against VEGF-R2 and VEGF-R3. It is possible that PI3-Kinase can also be activated by the indirect auto-phosphorylation of VEGF-R3.

These results demonstrate that the VEGF induced reduction in $[Ca^{2+}]_i$ in cultured podocytes was class III tyrosine kinase dependent. Although the receptor and the mechanism by which VEGF induced a reduction in cytotoxicity in cultured podocytes are as yet undefined, the data are consistent with the involvement of VEGF-R1 and PI3-Kinase. To investigate this survival pathway further the direct effects of VEGF on AKT phosphorylation will be determined. Reduced cytotoxicity in cultured podocytes has also been associated with nephrin phosphorylation (reduced apoptosis) in a PI3-Kinase/AKT phosphorylation dependent manner, as discussed in the introduction. This is another potential mechanism to investigate the role of VEGF in podocyte survival. Much of the work from this chapter was published in paper 1 of the list of publications arising from this work.

Chapter 8

VEGF mediated induction of nephrin phosphorylation and survival signalling in cultured podocytes

8.1 Introduction

The results of the previous chapter were consistent with the hypothesis that VEGF reduced cytotoxicity in cultured podocytes by activating PI3-Kinase. I therefore continued to persue this line of investigation. There is some evidence in the literature to show that the phosphorylation of nephrin at the podocyte slit diaphragm induces the activation of PI3-Kinase, which induces the phosphorylation of AKT (Huber et al., 2003c). Phosphorylated AKT is known to induce the phosphorylation and inactivation of the pro-apoptotic family member, Bad, resulting in inhibition of apoptosis (Gerber et al., 1998a). Nephrin and VEGF have therefore both been linked to survival signalling in podocytes. Nephrin can be phosphorylated by various members of the Src family kinases including Fyn, Lyn and Yes (Lahdenpera et al., 2003) (Verma et al., 2003). In vascular endothelial cells VEGF can activate members of the Src family kinases (Chou et al., 2002). Interestingly, in these cells Fyn and Lyn show preferential binding to VEGF-R1 whereas Src preferentially binds to VEGF-R2 (Chou et al., 2002). It is possible, therefore, that VEGF can activate members of Src family kinases in podocytes and induce the phosphorylation of nephrin via VEGF-R1, which may allow activation of PI3-Kinase and result in reduced apoptosis. I therefore investigated whether VEGF could induce the phosphorylation of nephrin. Various parameters of the PI3-Kinase/AKT pathway were then studied in relation to VEGF-nephrin signalling such as AKT phosphorylation and apoptosis to verify that VEGF did activate the PI3-Kinase/AKT phosphorylation survival pathway in cultured podocytes. The human conditionally immortalised nephrin mutated (NMhCIP) and nephrin deficient (NDhCIP) cell lines provided useful tools in this chapter to elucidate nephrin signalling in relation to VEGF and apoptosis.

8.2 Methods

8.2.1 Immunoprecipitation (IP)-VEGF induced phosphorylation of nephrin

Serum starved, differentiated hCIPs were treated with 1nM recombinant VEGF protein for 20 minutes, a neutralising monoclonal antibody to VEGF for 24hrs, or left untreated for an appropriate length of time. Protein was extracted and quantified. Cell lysates were incubated with a total of 1μg of mouse monoclonal IgG_{2b} anti-phospho-tyrosine primary antibody (p-Y) overnight then incubated for 2hrs with protein A/G slurry, as described in the methods. The pellet and supernatant were subjected to SDS PAGE and transferred to a PVDF membrane. The membrane was probed with 1:300 rabbit polyclonal IgG anti-nephrin primary antibody (a kind gift from Karl Tryggvasson) in 5% non-fat milk blocking solution and 0.03μg/ml HRP conjugated goat polyclonal anti-mouse IgG secondary antibody in 5% non-fat milk blocking solution. The membranes were stripped and re-probed with 0.05μg/ml anti-p-Y primary antibody in 1.5% BSA blocking solution and 0.003μg/ml of HRP conjugated anti-mouse secondary antibody. The p-Y probe was used to show that tyrosine phosphorylated proteins had been immunoprecipitated and also showed other bands of unidentified proteins that had also been tyrosine phosphorylated by treatment with VEGF or serum starvation.

8.2.2 Apoptosis assay-VEGF induced nephrin signalling

Nephrin mutated and nephrin deficient podocyte cell lines (NMhCIPs and NDhCIPs) were serum starved for either 16hrs or 4hrs then treated with 1nM VEGF in serum free media for 4hrs or left untreated. Cells were scraped into suspension in serum free media and rolled for a further 4hrs. Each treatment group was then incubated with either AV, PI AV with PI or left untreated. Samples were assayed using the flow cytometer and necrotic and apoptotic sub-populations were quantified, as a percentage of the total cell population.

8.2.3 Western blotting-VEGF-induced AKT signalling

Serum starved hCIPs and NDhCIPs were either treated with 1nM VEGF for 20 minutes, a neutralising monoclonal antibody to VEGF for 24hrs or left untreated for the appropriate amount of time. Serum starved HUVECs were either left untreated or treated with 100mM ethanol for 30 minutes to act as a positive control for AKT phosphorylation (Liu et al., 2002). Membranes were probed with 1μg/ml mouse monoclonal anti-phospho-AKT (p-ser 472/473) primary antibody (BD Bioscience,Oxford, UK) in 5% non-fat milk blocking solution and 0.01μg/ml HRP conjugated anti-mouse secondary antibody in 5% non-fat milk blocking solution. Membranes were then stripped and re-probed with 1μg/ml mouse monoclonal anti-AKT antibody (200μg/ml) and 0.01μg/ml HRP conjugated anti-mouse secondary antibody. Densitometry analysis of the appropriate bands (at 60kDa) was carried out using NIH image software, and then phospho-AKT was normalised to total AKT.

8.3 Results

8.3.1 VEGF induced phosphorylation of nephrin.

hCIPs were incubated with VEGF, a neutralising monoclonal antibody to VEGF, or left untreated. Tyrosine phosphorylated proteins were immunoprecipitated and then PVDF membranes, containing protein from immunoprecipitate and supernatant, were probed with an anti-nephrin antibody to assess whether nephrin had been tyrosine phosphorylated in any of the treatments. There was a greater intensity of a band corresponding to nephrin (180kDa) when hCIPs were incubated in VEGF in the phospho-tyrosine precipitate compared to the supernatant (figure 8.1 A, lanes 2 and 3). The intensity of the band corresponding to nephrin was of a similar intensity in the phospho-tyrosine precipitate compared to the supernatant of serum starved hCIPs with no VEGF treatment (figure 8.1 A, lanes 4 and 5). Nephrin phosphorylation, normalised to total nephrin (the sum of the supernatant and precipitate bands) in cells treated with VEGF was 3.36±1.21 fold greater than that in serum starved cells ($p<0.05$, figure 8.1 B). Nephrin appeared to be constitutively phosphorylated in serum starved hCIPs (figure 8.1 A, lanes 4 and 5) and approximately 50% of total nephrin expression was in the precipitate. To investigate if this constitutive phosphorylation was induced by endogenous VEGF cells were incubated with a neutralising monoclonal antibody to VEGF. The intensity of the band corresponding to nephrin in cells incubated with the neutralising monoclonal antibody to VEGF was barely detectable in the phospho-tyrosine precipitate compared to the supernatant. Nephrin phosphorylation normalised to total nephrin in hCIPs incubated in a neutralising monoclonal antibody to VEGF was 0.21±0.09 fold lower than that in serum starved cells (Figure 8.1 B). The reduction in nephrin phosphorylation induced by the neutralising monoclonal antibody to VEGF suggested that the majority of constitutive nephrin phosphorylation was due to endogenous VEGF.

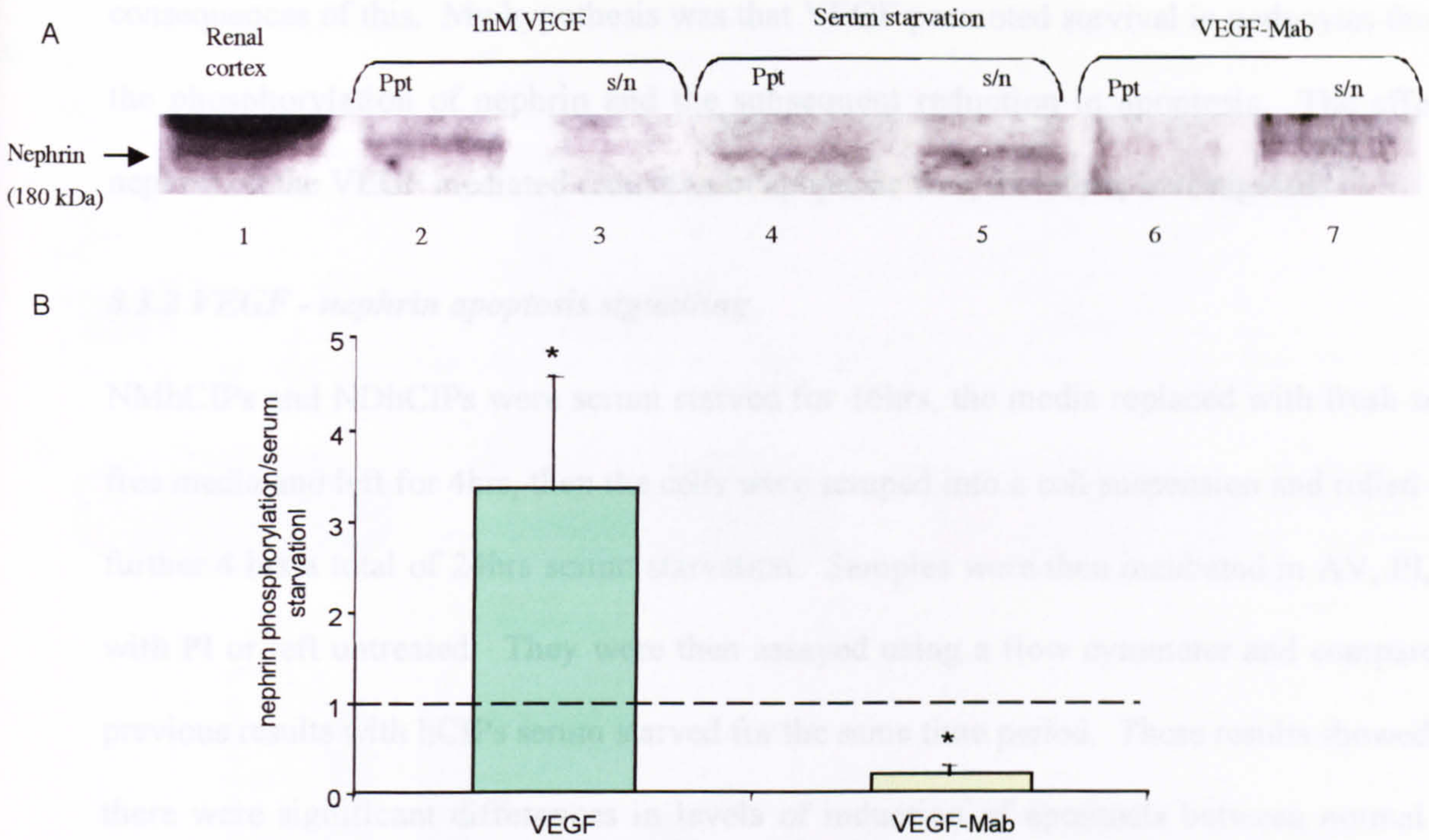

Figure 8.1. Exogenous and endogenous VEGF induces nephrin phosphorylation in hCIPs.

Serum starved hCIPs were treated with VEGF, VEGF-Mab, or left untreated. Protein was immunoprecipitated using an anti-p-Y antibody. Both the lysate and precipitate were subjected to SDS PAGE, transferred to a PVDF membrane and probed with an anti-nephrin antibody. A. An example of immunodetection with an anti-nephrin antibody for lysate and precipitate is shown for each treatment group. VEGF treatment resulted in increased nephrin phosphorylation compared to that of serum starved cells (2 vs 4), whereas there was attenuated constitutive nephrin phosphorylation in cells that were pre-incubated with VEGF-Mab compared to that of serum starved cells (6 vs 4). Protein extracted from renal cortex demonstrated the correct molecular weight for nephrin (180kDa) (1). B. Data were expressed as mean+SEM of densitometry ratios: (treated ppt/serum starved ppt)/(treated s-n/serum starved s-n). VEGF treatment resulted in an increase in nephrin phosphorylation compared to that of serum starved cells whereas VEGF-Mab treatment resulted in a decrease in nephrin phosphorylation compared to that of serum starved cells. *=$p<0.05$ unpaired *t*-test, n=6 and 4 respectively. Ppt = precipitate, s-n = supernatant.

These results show that both exogenous and endogenous VEGF induce the phosphorylation of nephrin. It is known that VEGF reduces cytotoxicity in cultured podocytes and that VEGF induces phosphorylation of nephrin. The next stage of the investigation was to assess the

consequences of this. My hypothesis was that VEGF promoted survival in podocytes through the phosphorylation of nephrin and the subsequent reduction in apoptosis. The effect of nephrin on the VEGF mediated reduction in apoptosis was, therefore, investigated.

8.3.2 VEGF - nephrin apoptosis signalling

NMhCIPs and NDhCIPs were serum starved for 16hrs, the media replaced with fresh serum free media and left for 4hrs, then the cells were scraped into a cell suspension and rolled for a further 4 hrs a total of 24hrs serum starvation. Samples were then incubated in AV, PI, AV with PI or left untreated. They were then assayed using a flow cytometer and compared to previous results with hCIPs serum starved for the same time period. These results showed that there were significant differences in levels of induction of apoptosis between normal and nephrin-mutated podocytes. Of the total cell population 4.43±0.52% of NMhCIPs stained with PI alone (i.e. met the criteria for necrotic cells), which was significantly lower than hCIPs (33.5±4.65) and NDhCIPs (29.1±4.23%, $p<0.01$, AVOVA, figure 8.2). There was only a significant induction of cells staining with just AV (i.e. met the criteria for apoptotic cells) in NMhCIPs; 25.3±2.1% of the total cell population compared to 2.17±0.4% in hCIPs and 9.12±2.7% in NDhCIPs ($p<0.01$, ANOVA figure 8.2). The induction of a significant AV stained population in NMhCIPs indicated that these cells were more sensitive to apoptosis, presumably due to the mutation in the Ig5 domain of the extracellular domain in nephrin, which may interfere with nephrin–nephrin interaction. This may make the cells less stable in culture, or may detrimentally affect normal nephrin survival signalling.

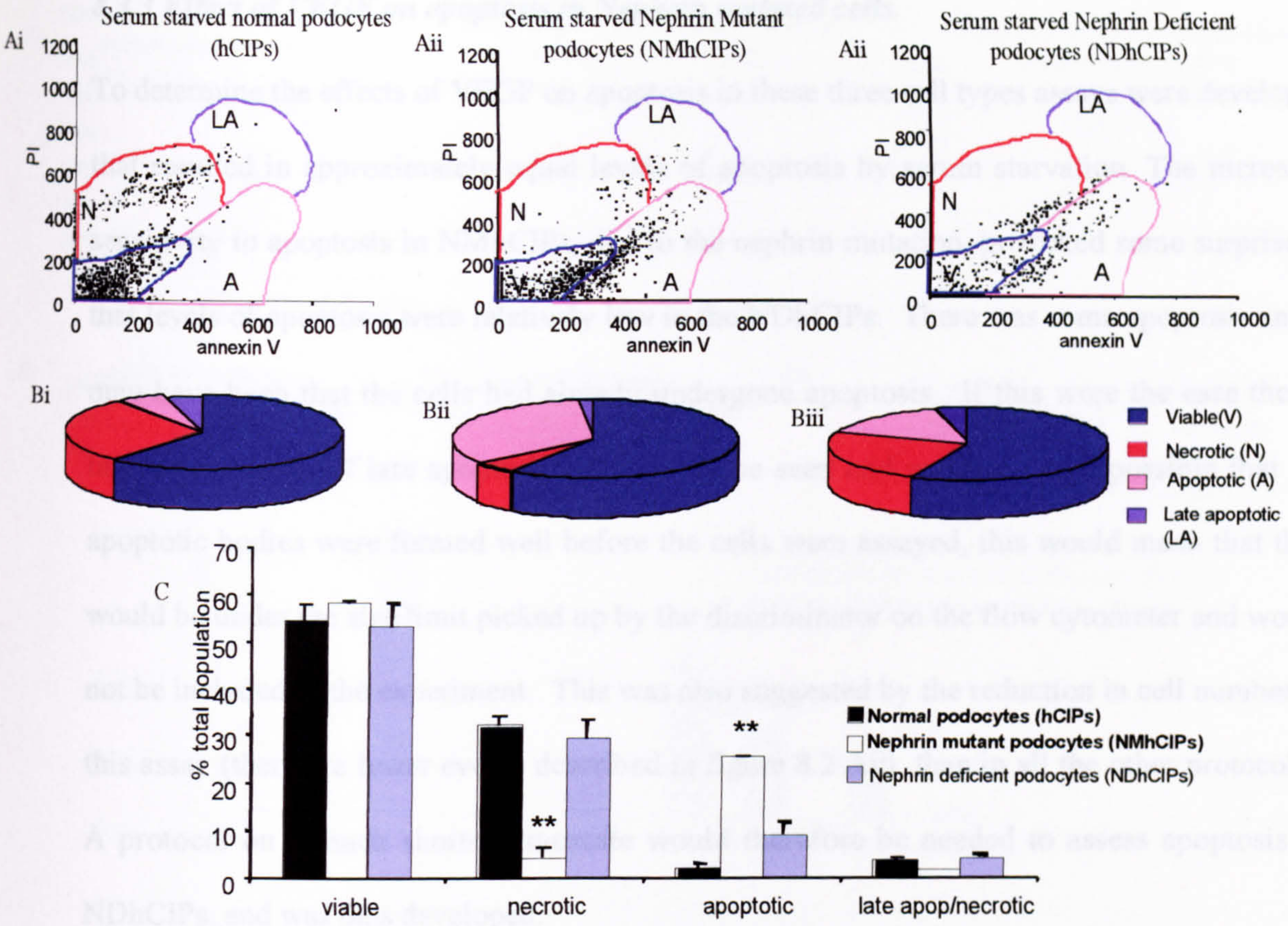

Figure 8.2. The induction of apoptosis in nephrin mutated/deficient hCIPs compared to normal hCIPs for a total of 24hrs.

Cells were serum starved for 16hrs, the media replaced and left for 4hrs, then the cells were scraped into suspension and rolled for a further 4hrs. Cells were then assayed using a flow cytometer. A. Comparison of AV and PI labelling of hCIPs, NMhCIPs and NDhCIPs, serum starved for a total of 24hrs. NMhCIPs and NDhCIPs show a greater apoptotic cell population than hCIPs. B. Characteristics of cell populations in serum starved hCIPs compared to NMhCIPs and NDhCIPs. Necrotic hCIPs account for a significant proportion of the total population, whereas in NMhCIPs apoptotic cells account for a significant proportion of the cell population. With NDhCIPs necrotic cells accounted for a greater proportion of the cell population than apoptotic cells. Data were expressed as mean+SEM percentage of total population. Serum starvation in NMhCIPs significantly increased apoptosis and significantly decreased necrosis compared to hCIPs and NDhCIPs. $p<0.05$ unpaired ANOVA., **= $p<0.01$ Bonferroni test.

8.3.3 Effect of VEGF on apoptosis in Nephrin mutated cells.

To determine the effects of VEGF on apoptosis in these three cell types assays were developed that resulted in approximately equal levels of apoptosis by serum starvation. The increased sensitivity to apoptosis in NMhCIPs, due to the nephrin mutation, provoked some surprise in that levels of apoptosis were relatively low in the NDhCIPs. There was some apoptosis and it may have been that the cells had already undergone apoptosis. If this were the case then a larger population of late apoptotic cells would be seen and was not. It is possible that the apoptotic bodies were formed well before the cells were assayed, this would mean that they would be under the size limit picked up by the discriminator on the flow cytometer and would not be included in the experiment. This was also suggested by the reduction in cell number in this assay (there are fewer events described in figure 8.2 Aiii, than in all the other protocols). A protocol on a much shorter timescale would therefore be needed to assess apoptosis in NDhCIPs, and was thus developed.

Even though the 24hr time course protocol was based on that used for the cytotoxicity assay, it did not induce apoptosis in normal podocytes (hCIPs). There was, however, a lot of necrosis induced in hCIPs, but this was not significantly reduced with VEGF treatment, as discussed for figure 6.4. Due to the robust nature of normal differentiated podocytes it was assumed that the hCIPs had not yet undergone apoptosis at this time in this specific assay. An assay over a longer time period was therefore developed, which induced significant apoptosis and was significantly reduced by VEGF (as discussed for figure 6.6). The NDhCIPs were serum starved for just 4hrs, scraped into a cell suspension and rolled for a further 4hrs, then assayed by flow cytometry. The results of this are compared, in figure 8.3, to the NMhCIPs, serum starved for a total of 24hrs, as described for figure 8.2, and hCIPs serum starved for a total of 72hrs, as described for figure 6.6.

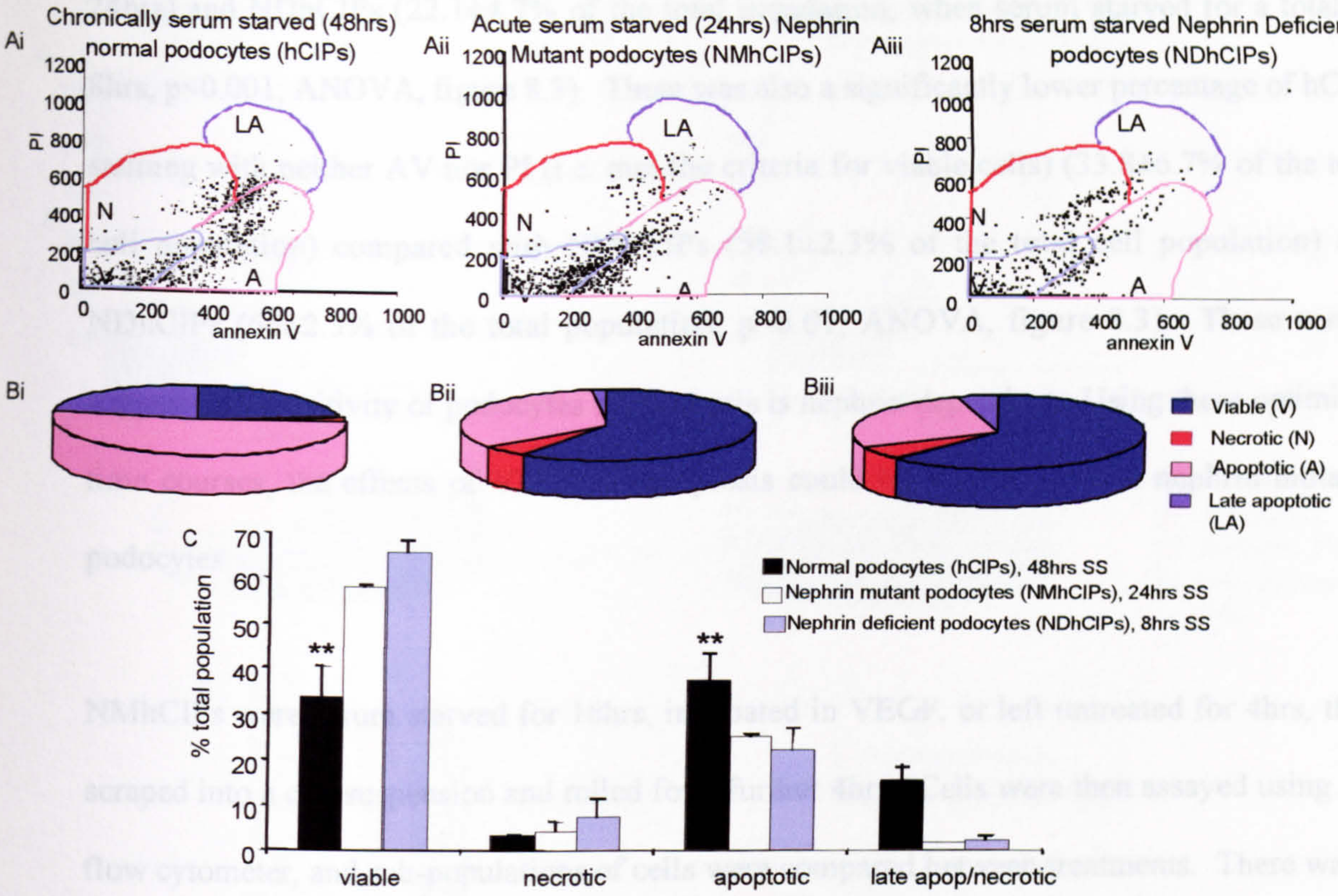

Figure 8.3. Time courses used to induce apoptosis in hCIPs, NMhCIPs and NDhCIPs.

hCIPs were serum starved for a total of 48hrs, NMhCIPs were serum starved for a total of 24hrs and NDhCIPs for a total of 8hrs. Cells were then assayed using a flow cytometer. A. A comparison of AV and PI labelling of hCIPs, NMhCIPs and NDhCIPs that had been serum starved. A Substantial apoptotic population was seen for all cell types. B. Characteristics of cell populations in serum starved hCIPs compared to NMhCIPs and NDhCIPs. A significant proportion of the total population was apoptotic in all cell types, although the greatest induction of apoptosis was seen in hCIPs, under the serum starvation time course used. C. Data were expressed as mean+SEM percentage of total population. Chronic serum starvation in hCIPs resulted in a significant reduction in viable cells and a significant increase in apoptosis compared to NMhCIPs and NDhCIPs. **=p<0.01 unpaired ANOVA. SS = serum starvation.

A significant level of AV staining (i.e. met the criteria for apoptotic cells) was induced in each of the cell types under the time period of serum starvation chosen: 37.6±6.1% of the total cell population of hCIPs serum starved for a total of 48 hrs, which was significantly greater than both NMhCIPs (25.32±2% of the total cell population, when serum starved for a total of

24hrs) and NDhCIPs (22.1±4.7% of the total population, when serum starved for a total of 8hrs, $p<0.001$, ANOVA, figure 8.3). There was also a significantly lower percentage of hCIPs staining with neither AV nor PI (i.e. met the criteria for viable cells) (33.8±6.7% of the total cell population) compared with NMhCIPs (58.1±2.3% of the total cell population) and NDhCIPs (66±2.5% of the total population, $p<0.01$, ANOVA, figure 8.3). These results suggest that sensitivity of podocytes to apoptosis is nephrin dependent. Using these optimised time courses, the effects of VEGF on apoptosis could be investigated on nephrin mutated podocytes.

NMhCIPs were serum starved for 16hrs, incubated in VEGF, or left untreated for 4hrs, then scraped into a cell suspension and rolled for a further 4hrs. Cells were then assayed using the flow cytometer, and sub-populations of cells were compared between treatments. There was a significant reduction in NMhCIPs stained with AV (i.e. met the criteria for apoptotic cells) in those cells incubated in VEGF (15.1±1.53% of the total cell population) compared to untreated cells (25.3±2.01% of the total cell population, $p<0.05$, ANOVA, figure 8.4). The population stained with neither PI nor AV (i.e. met the criteria for viable cells) was slightly although not significantly larger in NMhCIPs incubated in VEGF (62.6±2.40% of the total cell population) compared to untreated (58.1±2.25% of the total population). This was probably because there was also a similar small, but not significant, increase in NMhCIPs stained only with PI (i.e. met the criteria for necrosis), incubated in VEGF (8.7±0.93% of the total cell population) compared to untreated (4.43±0.52% of the total cell population).

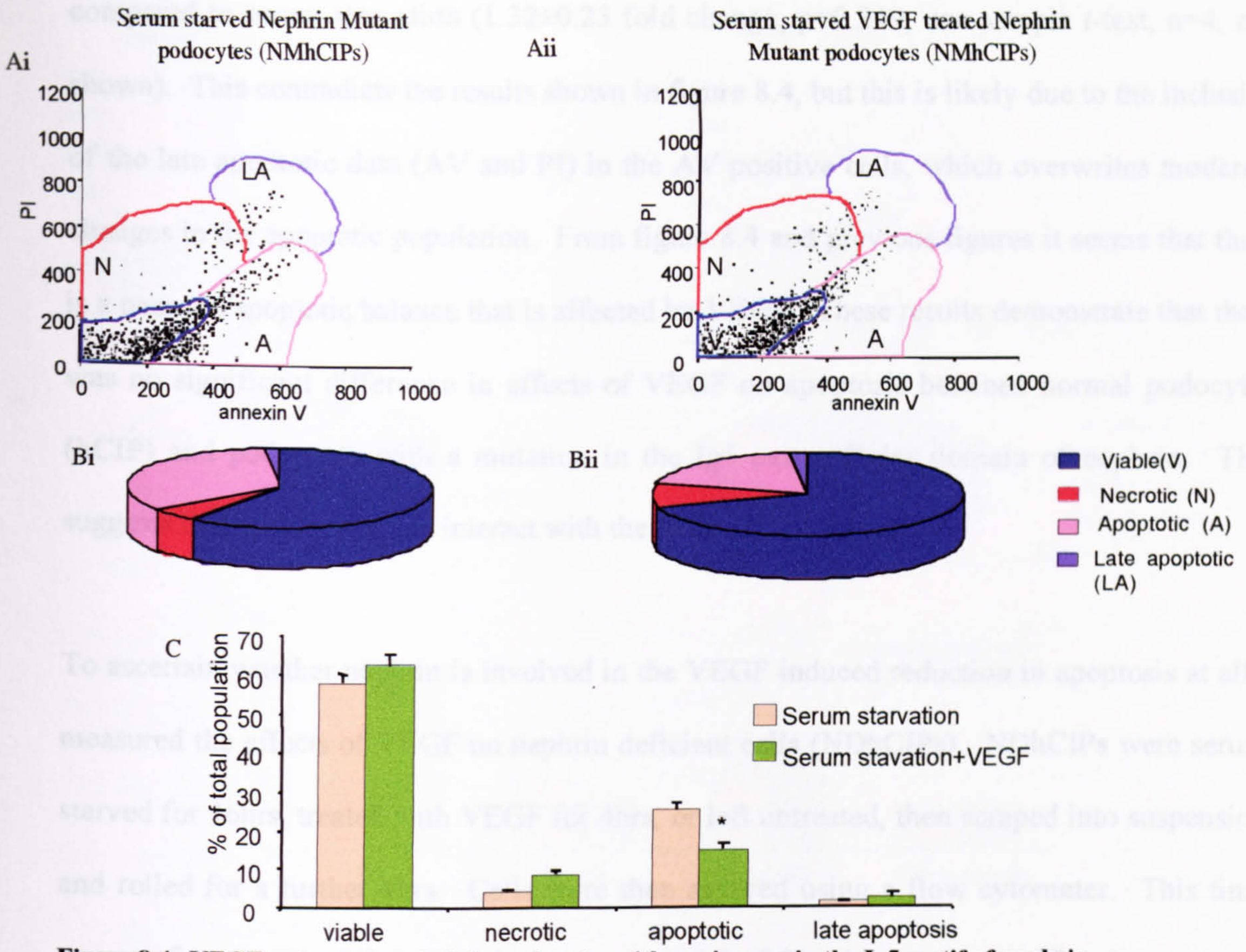

Figure 8.4. VEGF reduces apoptosis in podocytes with a missense in the Ig5 motif of nephrin.

NMhCIPs were serum starved for 16hrs, incubated in VEGF for 4hrs or left untreated, then scraped into suspension and rolled for 4hrs. Cells were then assayed by a flow cytometer. A. Comparison of AV and PI labelling of 1nM VEGF treated NMhCIPs compared to serum starved NMhCIPs. There was a reduction of cells in the apoptotic population of NMhCIPs, treated with VEGF, compared to untreated. B. Characteristics of cell populations in 1nM VEGF treated NMhCIPs compared to serum starved NMhCIPs. There was a reduction in apoptosis as a proportion of the total cell population in cells treated with VEGF compared to untreated. C. Data were expressed as mean+SEM of the total cell population. Compared to serum starvation alone, VEGF treatment significantly reduced apoptotic cells. *=$p<0.05$, Bonferroni n=4 in all.

The percentage of AV positive cells of the total fluorescence picked up at 525nm (minus the background) in the VEGF treatment were normalised to that of cells that had been serum starved. There was no significant reduction in AV positive cells when treated with VEGF

compared to serum starvation (1.32±0.23 fold change, p=0.249, one sample *t*-test, n=4, not shown). This contradicts the results shown in figure 8.4, but this is likely due to the inclusion of the late apoptotic data (AV and PI) in the AV positive cells, which overwrites moderate changes in the apoptotic population. From figure 8.4 and previous figures it seems that there is a necrotic/apoptotic balance that is affected by VEGF. These results demonstrate that there was no significant difference in effects of VEGF on apoptosis between normal podocytes (hCIP) and podocytes with a mutation in the Ig5 extracellular domain of nephrin. This suggests that VEGF does not interact with the Ig5 motif of nephrin.

To ascertain whether nephrin is involved in the VEGF induced reduction in apoptosis at all I measured the effects of VEGF on nephrin deficient cells (NDhCIPs). NDhCIPs were serum starved for 16hrs, treated with VEGF for 4hrs, or left untreated, then scraped into suspension and rolled for a further 4hrs. Cells were then assayed using a flow cytometer. This time course of serum starvation was chosen over a total of 8hrs because a significant amount of both apoptotic and necrotic populations were seen in figure 8.3 Biii, which allows the effects of VEGF on necrosis and apoptosis to be measured simultaneously. There was no significant difference seen in any of the cell sub-populations between VEGF treated and untreated NDhCIPs (figure 8.5). There was also no significant change in AV positive cells (expressed as a percentage of total fluorescence picked up at 525nm) in VEGF treated cells when normalised to serum starved cells (1.03±0.11 fold change, p=0.78, n=3, not shown).

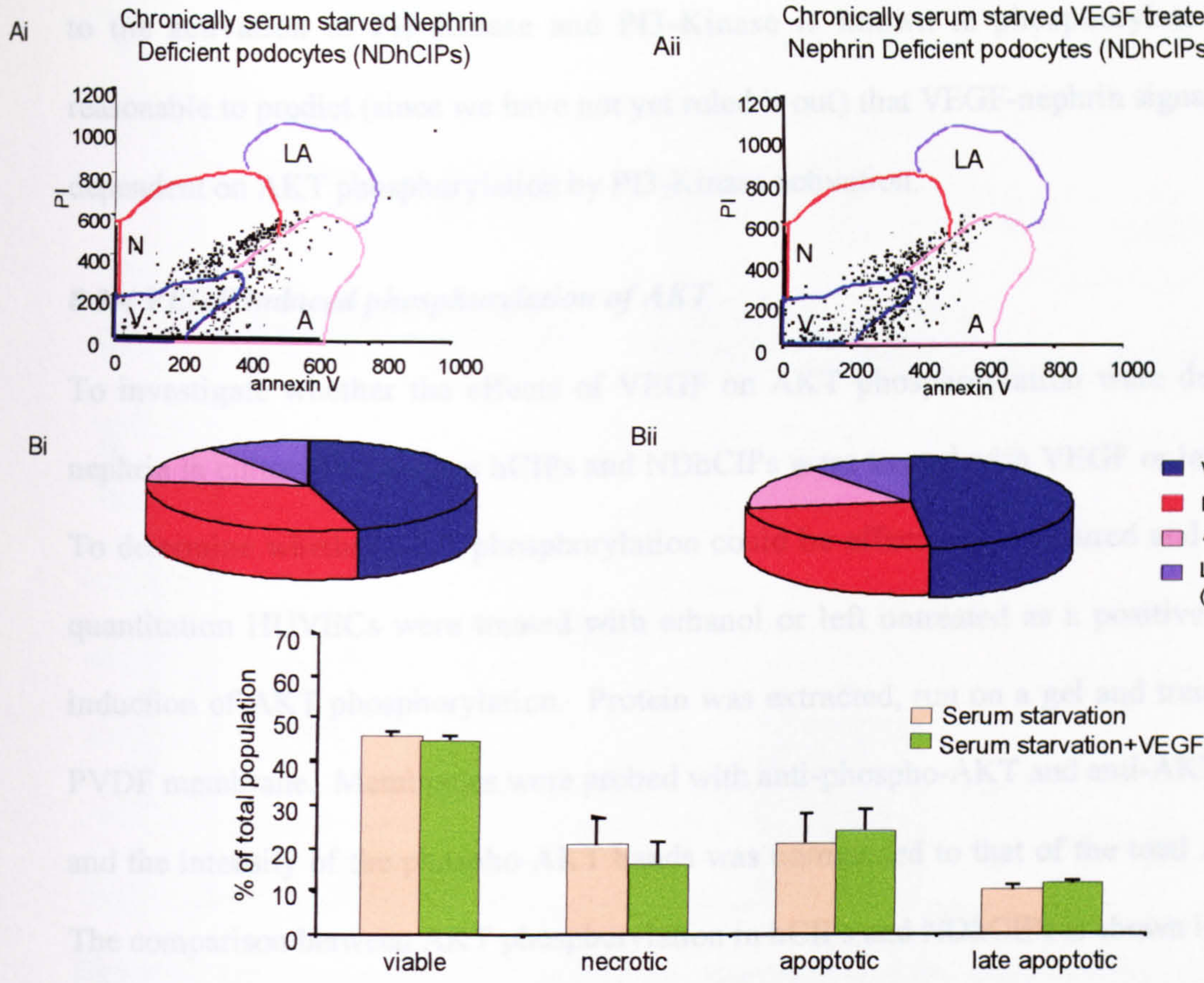

Figure 8.5. The effects of VEGF on serum starved nephrin deficient podocytes (NDhCIPs)

NDhCIPs were serum starved for 16hrs, then treated with VEGF for 4hrs, or left untreated. Cells were then scraped into suspension and rolled for a further 4hrs then assayed using a flow cytometer. A. A Comparison of AV and PI labelling of 1nM VEGF treated NDhCIPs compared to serum starved NDhCIPs. There was no difference seen between cell sub-populations of cells treated with VEGF compared to those left untreated. B. Characteristics of cell populations in chronically serum starved 1nM VEGF treated NDhCIPs compared to untreated NDhCIPs. The cell sub-populations, expressed as a percentage of the total cell population were the same in both VEGF treated and untreated cells. C. Data were expressed as mean+SEM percentage of the total cell population. Compared to serum starvation alone VEGF treatment had no significant effect on any of the cell populations (n.s. ANOVA, n=5).

These results demonstrate that VEGF had no significant effect on apoptosis induced by serum starvation in podocytes deficient in nephrin. The reduction in apoptosis in cultured podocytes induced by VEGF may, therefore, be nephrin dependent. Since nephrin phosphorylation leads

to the activation of PI3-Kinase and PI3-Kinase is known to phosphorylate AKT it is reasonable to predict (since we have not yet ruled it out) that VEGF-nephrin signalling is also dependent on AKT phosphorylation by PI3-Kinase activation.

8.3.4 VEGF induced phosphorylation of AKT

To investigate whether the effects of VEGF on AKT phosphorylation were dependent on nephrin in cultured podocytes hCIPs and NDhCIPs were treated with VEGF or left untreated.

To determine whether AKT phosphorylation could be effectively measured and to facilitate quantitation HUVECs were treated with ethanol or left untreated as a positive control for induction of AKT phosphorylation. Protein was extracted, run on a gel and transferred to a PVDF membrane. Membranes were probed with anti-phospho-AKT and anti-AKT antibodies and the intensity of the phospho-AKT bands was normalised to that of the total AKT bands. The comparison between AKT phosphorylation in hCIPs and NDhCIPs is shown in figure 8.6. I predicted that there would be an increase in AKT phosphorylation in hCIPs treated with VEGF, but a decrease in AKT phosphorylation in NDhCIPs treated with VEGF was seen when compared to untreated cells. An example of membranes from the experiments described are shown in figure 8.6 A. Membranes containing protein of both hCIPs and NDhCIPs treated with VEGF or left untreated showed a band that corresponded to total AKT (60kDa) of similar intensities. The membrane containing hCIP protein was stripped and re-probed with an anti-phospho-AKT antibody and surprisingly demonstrated a lower intensity of band corresponding to phospho-AKT in VEGF treated cells compared to untreated cells. The membrane containing NDhCIP protein was also stripped and re-probed with an anti phospho-AKT antibody and surprisingly demonstrated a greater intensity of band corresponding to phospho-AKT in VEGF treated cells compared to untreated cells.

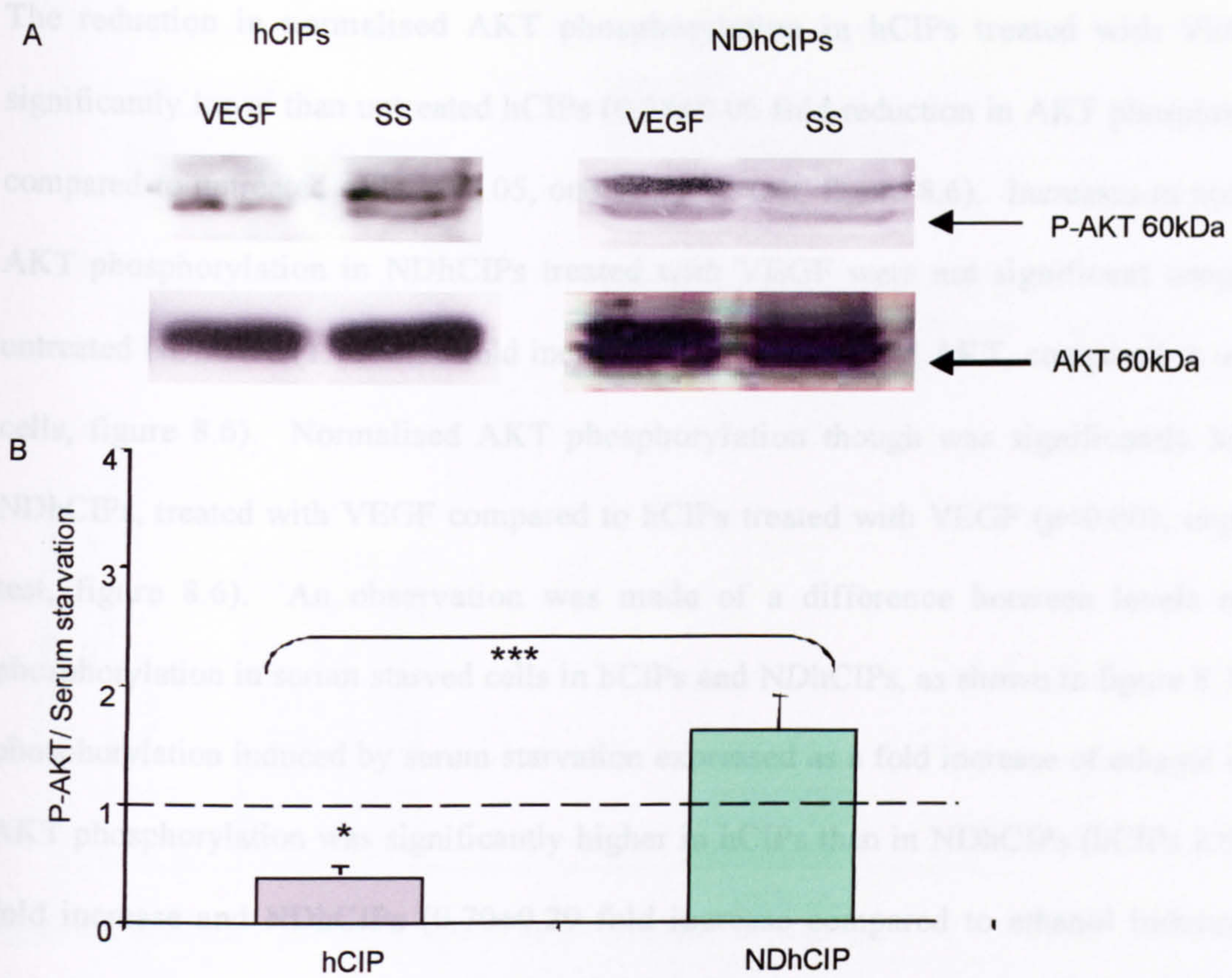

Figure 8.6. The effects of 1nM VEGF on AKT phosphorylation in hCIPs compared to that of NDhCIPs.

PVDF membranes containing protein extracted from hCIPs and NDhCIPs, which were treated with 1nM VEGF, or left untreated, were probed with an anti phospho-AKT antibody, stripped and re-probed with an anti-AKT antibody. A. An example of membranes probed with anti-AKT and anti-phospho-AKT antibodies from each experiment. Bands corresponding to phospho-AKT (60kDa) were less intense in VEGF treated hCIPs, compared to untreated hCIPs and were more intense in NDhCIPs treated with VEGF compared to untreated. B. Data were expressed as mean+SEM ratios: phospho-AKT (treatment/control)/total AKT (treatment/control). AKT phosphorylation induced by 1nM VEGF was significantly lower in hCIPs then in NDhCIPs. AKT phosphorylation induced by VEGF in NDhCIPs was not significantly different to serum starvation. *= $p<0.05$, ***= $p<0.001$ unpaired *t*-test compared to serum starved cells or as indicated, n=5. Treated =1nM VEGF, SS = serum starved.

The reduction in normalised AKT phosphorylation in hCIPs treated with VEGF was significantly lower than untreated hCIPs (0.35±0.06 fold reduction in AKT phosphorylation, compared to untreated cells, $p<0.05$, one sample *t*-test, figure 8.6). Increases in normalised AKT phosphorylation in NDhCIPs treated with VEGF were not significant compared to untreated NDhCIPs (1.73±0.29 fold increase in phosphorylated AKT, compared to untreated cells, figure 8.6). Normalised AKT phosphorylation though was significantly higher in NDhCIPs, treated with VEGF compared to hCIPs treated with VEGF ($p<0.001$, unpaired *t*-test, figure 8.6). An observation was made of a difference between levels of AKT phosphorylation in serum starved cells in hCIPs and NDhCIPs, as shown in figure 8.7. AKT phosphorylation induced by serum starvation expressed as a fold increase of ethanol induced AKT phosphorylation was significantly higher in hCIPs than in NDhCIPs (hCIPs 2.91±0.93 fold increase and NDhCIPs (0.70±0.29 fold increase compared to ethanol induced AKT phosphorylation). This may affect how VEGF exerts its effects on AKT in the two cell types.

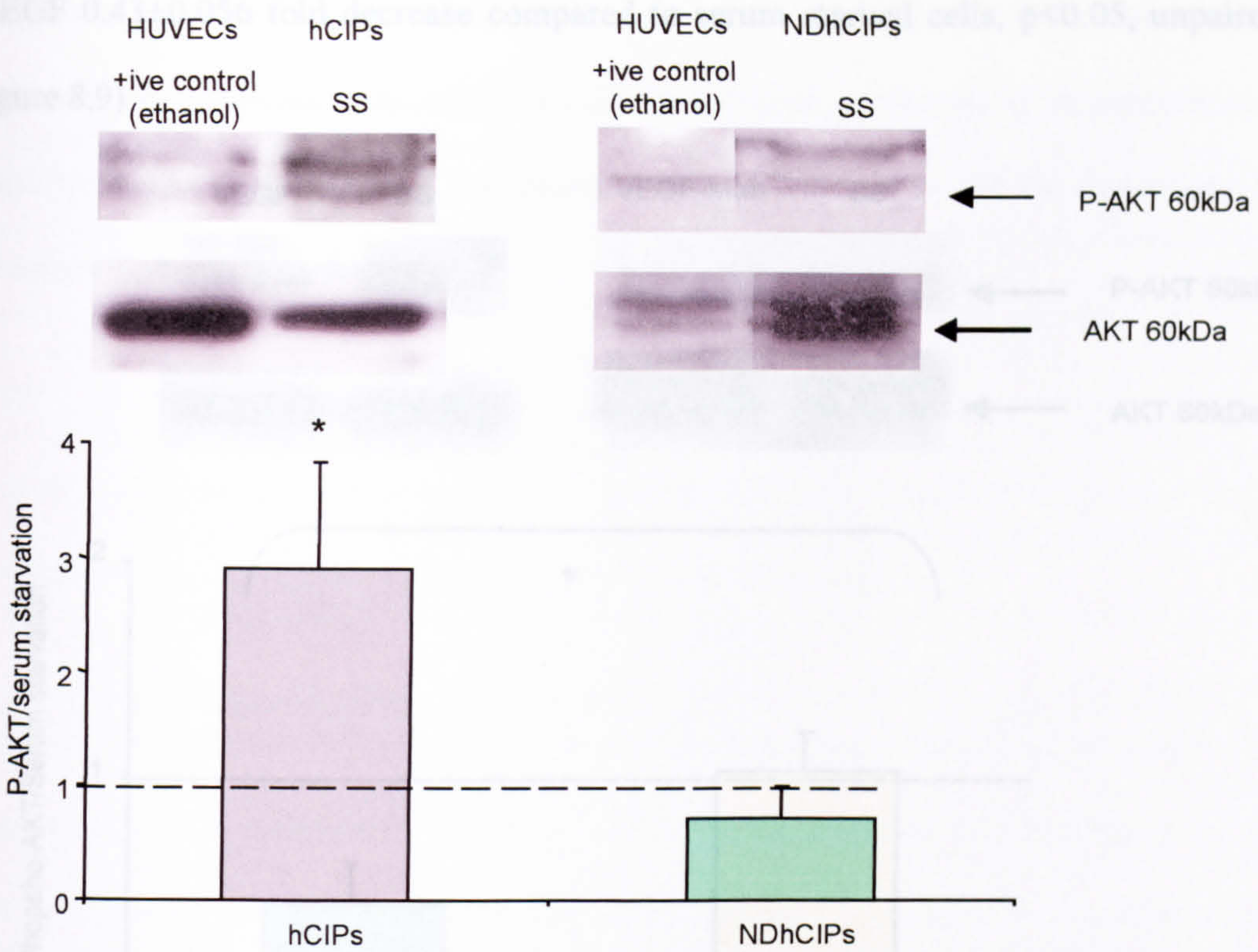

Figure 8.7. Basal AKT phosphorylation in hCIPs compared to NDhCIPs.

A comparison was made between levels of AKT phosphorylation in serum-starved hCIPs and NDhCIPs.

The data were re-analysed from the experiments shown in figure 8.6. Data were expressed as mean+SEM ratios: phospho-AKT (serum starvation/positive control)/total AKT (serum starvation/positive control). Basal AKT phosphorylation was significantly higher in hCIPs then it was in NDhCIPs. *= $p<0.05$ unpaired *t*-test, n=3 and 5 respectively). Ethanol = ethanol treated HUVECs, SS = serum starved

If endogenous VEGF could also induce an effect on AKT phosphorylation in hCIPs then it might be predicted that treatment of hCIPs with a neutralising monoclonal antibody to VEGF would significantly increase phosphorylated AKT compared to serum starvation. This was not the case as shown in figure 8.8. Treatment of hCIPs with a neutralising monoclonal antibody to VEGF had no significant effect on normalised AKT phosphorylation compared to serum starved cells. AKT-phosphorylation was significantly increased however compared to cells treated with VEGF (VEGF-Mab 1.02±0.19 fold increase compared to serum starved cells,

VEGF 0.43±0.056 fold decrease compared to serum starved cells, $p<0.05$, unpaired *t*-test, figure 8.9).

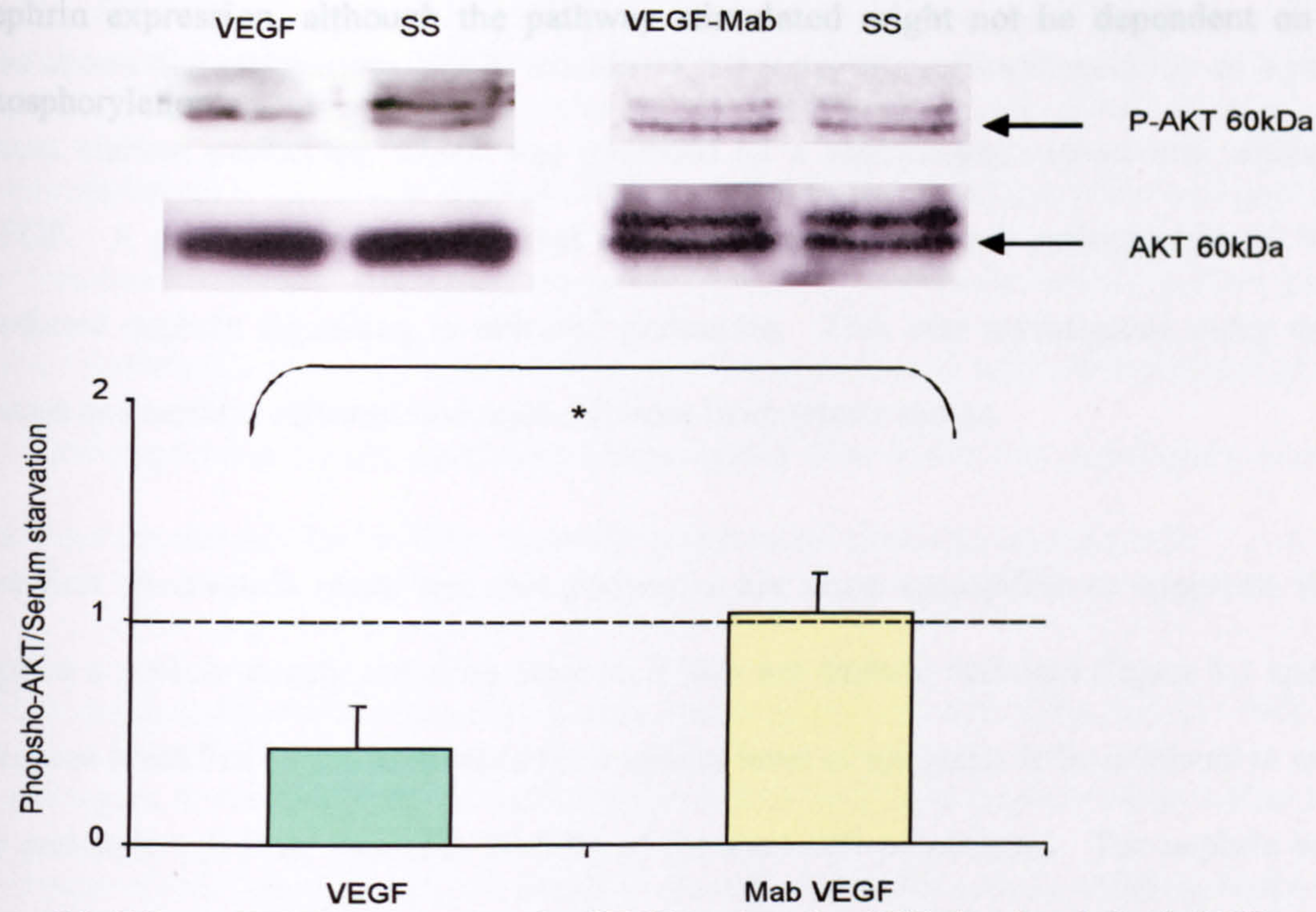

Figure 8.8. Effects of VEGF-Mab compared to VEGF treatment on AKT phosphorylation in hCIPs.

Serum starved hCIPs were either treated with VEGF, VEGF-Mab or left untreated. Protein was extracted, subjected to SDS PAGE, transferred to a PVDF membrane and probed with an anti-phospho-AKT antibody, stripped and re-probed with an anti-AKT antibody. Data were expressed as mean+SEM ratio: phospho-AKT (treatment/control)/total AKT (treatment/control). VEGF-Mab did not significantly effect phospho-AKT levels compared to control but was significantly different to the VEGF induced reduction in AKT phosphorylation. *= $p<0.05$ unpaired *t*-test, n=5. SS = serum starved.

These results suggest that endogenous VEGF does not have an effect on AKT phosphorylation in hCIPs, or at least not external effects of endogenous VEGF; if endogenous VEGF acted externally, then the neutralising monoclonal antibody to VEGF would be able to block the effects of endogenous VEGF.

Together, these results show that VEGF can induce nephrin phosphorylation and that the reduction in apoptosis induced by VEGF in cultured podocytes is dependent on normal nephrin expression, although the pathway stimulated might not be dependent on AKT phosphorylation.

8.4 Discussion

VEGF has been shown to induce nephrin phosphorylation, as shown in figure 8.1. This figure also shows that endogenous VEGF stimulated the constitutive phosphorylation of nephrin in serum starved podocytes, which was inhibited by a neutralising monoclonal antibody to VEGF. A proportion of cell survival was hypothesised to be a consequence of VEGF-mediated nephrin signalling in cultured podocytes. This was investigated using nephrin mutant and nephrin deficient podocyte cell lines in apoptosis assays.

The first observation made was that podocytes are more susceptible to apoptosis if they express a nephrin mutant and even more so if they are nephrin deficient (figure 8.2 and 8.3). This was identified by the time taken for a similar level of apoptosis to be achieved in each of the podocyte cell lines (between 20-40% of the total cell population). The nephrin mutant cells (NMhCIPs) have a mutation in the Ig5 motif of the extracellular domain of nephrin. This should not directly influence nephrin survival signalling because survival signalling is postulated to occur at the tyrosine residues of the intracellular domains. It is possible that head to head nephrin-nephrin interactions may be disrupted as is postulated to occur using the first 6 Ig motifs (figure 1.9, chapter 1). This may have a number of effects. For example it may make the cultured podocytes less stable due to the disruption of cell-cell interactions (Khoshnoodi et al., 2003). Isolation of podocytes from each other in culture may increase their vulnerability, just as lower confluency would. Nephrin–nephrin interactions may result in constitutive nephrin phosphorylation in the same way that overexpression of nephrin on HEK 293 cells causes clustering and phosphorylation of nephrin (Lahdenpera et al., 2003). A mutation in the part of the nephrin extracellular domain that mediates homophilic binding, therefore, may indirectly affect nephrin phosphorylation and PI3-Kinase activation. This

would ultimately result in increased susceptibility to apoptosis induced by serum starvation. Using this reasoning I predicted that nephrin deficient podocytes would have lower constitutive PI3-Kinase activity and would be susceptible to apoptosis to an even greater degree. It became clear when comparing these different serum starvation time course apoptosis assays between the different cell types that necrotic and apoptotic sub-populations were mutually exclusive. When apoptosis levels were high necrotic levels were low and vice versa. Looking at figures 8.2 to 8.4 it seems that necrotic and apoptotic subpopulations in each cell population always equates to approximately 40% of the total population. It may be that there is cross talk between the apoptotic and necrotic pathways in podocytes.

VEGF reduced apoptosis induced by serum starvation in NMhCIPs (figure 8.4). This is not surprising as it was thought that VEGF could induce nephrin phosphorylation indirectly via activation of Src family kinases. A mutation limited to the extracellular domain should not in theory therefore affect the intracellular tyrosine kinase activation of nephrin by cytosolic Src family kinases. The extracellular domain of nephrin is thought to be predominantly involved in integrin interaction. Therefore, it is unlikely that VEGF would be able to bind to the extracellular domain to induce intracellular signalling. VEGF had no significant effect on NDhCIPs (figure 8.5). This demonstrates that the VEGF mediated reduction in apoptosis is nephrin dependent.

It has been shown that VEGF mediated survival signalling is dependent on nephrin signalling in podocytes and that VEGF can induce the phosphorylation of nephrin. It is also known that the phosphorylation of nephrin can induce the activation of PI3-Kinase, therefore it is reasonable to assume that AKT phosphorylation was also implicated (Gerber et al., 1998a). The effects of VEGF on AKT phosphorylation were therefore investigated in hCIPs and

NDhCIPs. Surprisingly, VEGF induced a reduction in serum starvation induced AKT phosphorylation (figure 8.6). The effects of VEGF on AKT phosphorylation in NDhCIPs were assessed to see if nephrin was mediated in the VEGF intracellular apoptosis-signalling pathway. This also provided unexpected results: VEGF increased AKT-phosphorylation, induced by serum-starvation in NDhCIPs (figure 8.6). The evidence in chapter 7 suggesting that VEGF reduced cytotoxicity by activating PI3-Kinase was inconclusive, but it may be that VEGF-nephrin mediated survival signalling is independent of AKT phosphorylation. It is worth noting that normal podocytes (hCIPs) have elevated levels of AKT phosphorylation when serum starved compared to that of nephrin deficient podocytes (NDhCIPs) and hCIPs enter apoptosis after a longer time period compared to NDhCIPs. This suggests that levels of AKT phosphorylation in podocytes are dependent on normal nephrin expression and play a role in cytoprotection, independent to that of VEGF. This was supported by figure 8.8 where the external effects of endogenous VEGF were blocked using a neutralising monoclonal antibody to VEGF. When endogenous VEGF was blocked there was no significant change in AKT phosphorylation compared to serum starvation.

These results suggest that the VEGF induced reduction in apoptosis in cultured podocytes is dependent on nephrin phosphorylation. VEGF does not appear to signal through AKT phosphorylation. Much of the work from this chapter has been accepted for publication in paper 3 of the list of publications arising from this work.

Chapter 9

The effects of VEGF-C on cultured podocytes

9.1 Introduction

It is intriguing that podocytes express VEGF-R3, a receptor activated by members of the VEGF family VEGF-C and VEGF D. VEGF-R3 is expressed on various tissues such as the spleen, brain, and epithelial cells of fetal lung (Pajusola et al., 1992), although it is predominantly expressed on lymphatic endothelial cells (as reviewed in (Jussila and Alitalo, 2002)). There is no evidence to date to suggest that VEGF can activate VEGF-R3, however it has been suggested that VEGF-R3 can negatively modulate VEGF-R2 (Matsumura et al., 2003). This would suggest that VEGF-R2 and VEGF-R3 can interact and VEGF may then be able to modulate VEGF-R3 via VEGF-R2. Podocytes do not express VEGF-R2 however and there is no evidence as yet to indicate that VEGF-R1 and VEGF-R3 can interact. The question therefore remains; is VEGF-R3 functional in podocytes?

Recent unpublished results from this laboratory show *in situ* VEGF-C protein expression in human kidney tissue sections (figure 9.1 A and B). These sections demonstrate that although VEGF-C protein is expressed by podocytes it is not expressed by every podocyte and it is possible that other glomerular cells also express VEGF-C. If podocytes do produce VEGF-C protein then it is possible that it may also be involved in an autocrine loop binding and activating VEGF-R3 (as reviewed in (Jussila and Alitalo, 2002)). VEGF-C promotes similar survival pathways via VEGF-R3 (Makinen et al., 2001) as VEGF does via VEGF-R2. This VEGF-R3 activation by VEGF-C leads to phosphorylation of AKT and reduced apoptosis as well as PKC dependent activation of p42/p44 MAPK, which has also been linked to survival in human dermal microvascular endothelial cells (HMVECs) (Makinen et al., 2001).

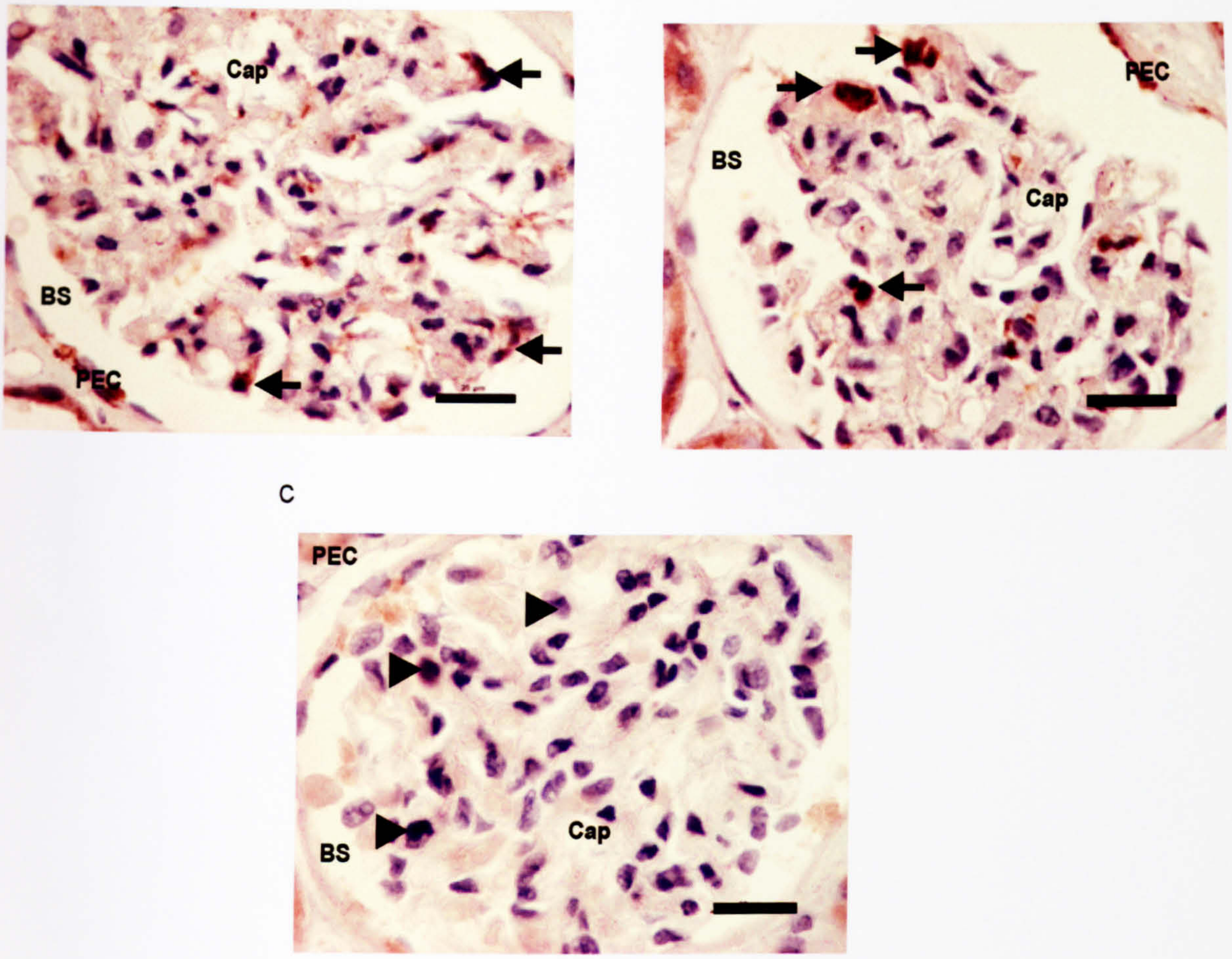

Figure 9.1. ***In situ*** **VEGF-C protein expression by podocytes (courtesy of Miss K. Joory).**

Immunohistochemistry was carried out on sections of human renal cortex using an antibody specific to VEGF-C. A-C show sections through a glomerular tuft surrounded by Bowmans' space (BS) and encapsulated by parietal epithelial cells (PECs). An example of a capillary is shown in each section (Cap) and the scale bar for each section is 20μM. A and B show examples of brown positive VEGF-C staining in podocytes (arrows) situated on the periphery of the glomerular tuft indicating that this protein is expressed. It is possible that other glomerular cells, such as mesangial cells, also express VEGF-C, because not all of the brown staining can be defined micrco-anatomically as podocytes. C. Cells incubated with just the normal IgG were counterstained with haematoxylin (top RH corner), which is the blue nuclear stain (shown by the arrowheads) and did not show any brown staining.

The VEGF/VEGF-C survival pathways are very similar, but follow different time courses. For example in HMVECs AKT phosphorylation by VEGF peaked between 20 and 30 minutes after initial exposure whereas AKT phosphorylation by VEGF-C peaked at 10 minutes and VEGF-C induced a more prolonged upregulation of phosphorylated MAPK (Makinen et al., 2001). Interestingly, AKT phosphorylation induced by VEGF-C is independent of PI3-Kinase activation in these cells. To investigate whether VEGF-C plays a signalling role in podocytes a similar approach was used to that of investigating VEGF signalling in podocytes. The effects of VEGF-C on $[Ca^{2+}]_i$, cytotoxicity and apoptosis was investigated in cultured podocytes to assess if VEGF-C could exert an effect in podocytes and whether it promoted survival in a similar manner to VEGF. AKT/MAPK signalling pathways were studied to investigate similarities between VEGF and VEGF-C signalling.

9.2 Methods

9.2.1 $[Ca^{2+}]_i$ measurements- VEGF-C signalling

hCIPs were incubated in HBSS containing minimal $[Ca^{2+}]_o$. If the effects of VEGF-C were similar to that of VEGF then a reduction in $[Ca^{2+}]_i$ would not be detected in the presence of 1.3mM $[Ca^{2+}]_o$. Cells were treated with 1nM human recombinant VEGF-C protein (a kind gift from Kari Alitalo) as described for 1nM VEGF. Ionomycin was used towards the end of each experiment to ensure that the system was still measuring changes in $[Ca^{2+}]_i$ i.e. the Fura-2 had not quenched and the cells were still alive. Manganese was used at the end of each experiment to quench the Fura-2 signal, to achieve an R_{min} measurement.

9.2.2 Cytotoxicity assay-VEGF-C signalling

Serum starved hCIPs were treated with 1nM VEGF-C in fresh serum free RPMI media or with fresh serum free RPMI media for 24hrs. Low, experimental and high LDH controls were assayed using a colourimetric assay, and cytotoxicity was calculated as described in the methods.

9.2.3 Apoptosis assay-VEGF-C signalling

hCIPs were chronically serum starved for 16hrs, treated with fresh serum free RPMI media containing 1nM VEGF-C, or not for 8hrs. Cells were left for 48hrs in complete RPMI media, serum starved for 16hrs, then treated with fresh RPMI media containing 1nM VEGF-C or not for 4hrs, scraped into suspension and rolled for a further 4hrs. Cells were then incubated with AV, PI, AV and PI or left untreated and then assayed by a flow cytometer.

9.2.4 Western Blotting-VEGF-C survival signalling

Serum starved hCIPs were treated with 1nM VEGF for 20 minutes, 1nM VEGF-C for 10 minutes, a neutralising monoclonal antibody to VEGF for 24hrs or left untreated for the appropriate amounts of time. Protein was extracted, quantified and subjected to SDS PAGE. Protein was transferred to a PVDF membrane, which was then probed with an anti-phospho-AKT and anti-AKT antibody as described previously. Membranes were also probed with 0.4μg/ml rabbit polyclonal IgG anti-p44/42 MAPK primary antibody (Cell signalling, Beverly, USA) and 0.005μg/ml HRP conjugated goat anti-rabbit IgG secondary antibody (Pierce, Cheshire, UK). Membranes were stripped and re-probed with 0.5μg/ml mouse monoclonal anti-phospho p44/42 MAPK (T202/Y204) (Cell Signalling, Beverly, USA) and 0.005μg/ml HRP conjugated goat anti-mouse IgG secondary antibody (Pierce, Cheshire, UK). Data were expressed as ratio of treatment/control to total amount of protein.

9.2.5 Immunoprecipitation- VEGF-C-VEGF-R3/nephrin signalling

Serum starved hCIPs were either treated with 1nM VEGF for 20 minutes, 1nM VEGF-C for 10 minutes or left untreated for the appropriate amount of time. Protein was extracted and quantified. Tyrosine phosphorylated proteins were immunoprecipitated from the lysate, and both pellet and supernatant were subjected to SDS PAGE and transferred to PVDF membrane. The membrane was probed with anti-p-Y, and mouse anti-nephrin as previously described. Membranes were also probed with 0.5μg/ml rabbit polyclonal IgG anti-Flt-4 (C-20) (VEGF-R3) primary antibody and 0.003μg/ml HRP conjugated goat anti-rabbit IgG secondary antibody.

9.3 Results

9.3.1 VEGF-C intracellular signalling in cultured podocytes

To investigate whether VEGF-C exerted a response in hCIPs the $[Ca^{2+}]_i$ response of hCIPs to VEGF-C was measured. $[Ca^{2+}]_i$ measurements were chosen as a method for studying the response of hCIPs to VEGF-C for the same reason that it was chosen to investigate whether VEGF exerted an effect in cultured podocytes; because $[Ca^{2+}]_i$ is a general secondary messenger that is involved in many cell signalling pathways. This technique was also chosen to compare the $[Ca^{2+}]_i$ signalling effects of VEGF-C with those of VEGF. hCIPs were incubated in HBSS containing minimal $[Ca^{2+}]_o$ and were treated with 1nM VEGF-C as described previously. Changes in $[Ca^{2+}]_i$ were measured and compared to the effects of VEGF on $[Ca^{2+}]_i$ in hCIPs. Interestingly, VEGF-C also reduced $[Ca^{2+}]_i$ in hCIPs compared to baseline $[Ca^{2+}]_i$ recordings (figure 9.2 B). The reduction in $[Ca^{2+}]_i$ in response to VEGF-C was immediate and rapid and approximately 2 fold lower than baseline $[Ca^{2+}]_i$. After approximately 2 minutes the $[Ca^{2+}]_i$ response levelled off and remained a constant concentration until the end of the experiment. VEGF-C significantly reduced $[Ca^{2+}]_i$ by 0.74 ± 0.09 fold of baseline $[Ca^{2+}]_i$ (figure 9.2 C, $p<0.05$, one sample *t*-test), similarly VEGF induced a significant reduction in $[Ca^{2+}]_i$ by 0.7 ± 0.1 fold of baseline $[Ca^{2+}]_i$ (figure 9.2C, $p<0.05$, one sample *t*-test).

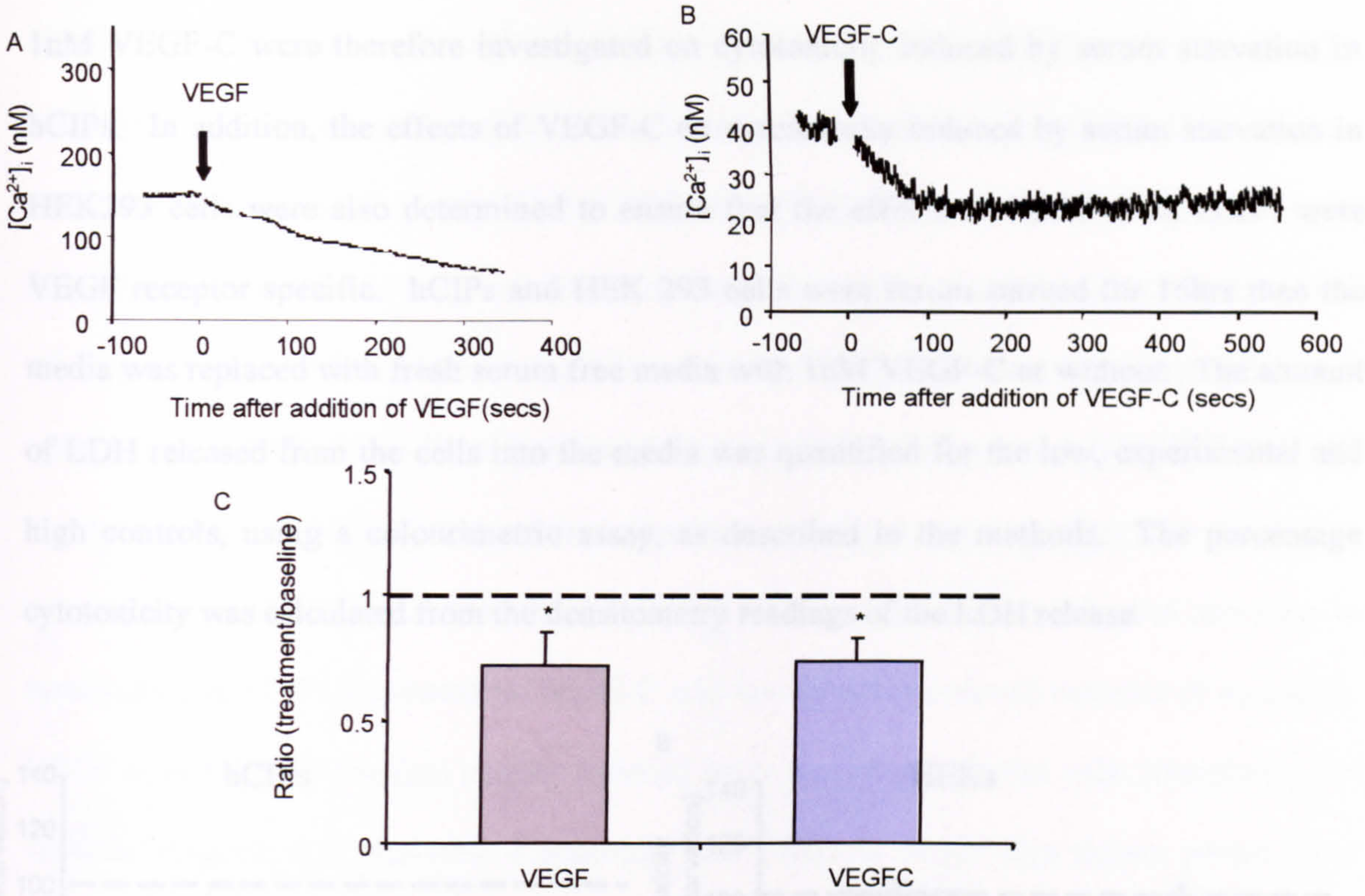

Figure 9.2. The effects of VEGF and VEGF-C on the change in $[Ca^{2+}]_i$ in hCIPs incubated in HBSS containing $[Ca^{2+}]_o$.

hCIPs were serum starved and loaded with Fura-2. VEGF-C was then added to the cells in the presence of HBSS containing minimal $[Ca^{2+}]_o$. Fluorescence intensity changes were recorded and used to calculate $[Ca^{2+}]_i$. Changes in $[Ca^{2+}]_i$ in hCIPs treated with VEGF-C were compared to previous effects of VEGF on changes in $[Ca^{2+}]_i$ in hCIPs. A. An example of the effect of VEGF on the change in $[Ca^{2+}]_i$ on hCIPs showing a reduction in $[Ca^{2+}]_i$ B. An example of the effect of VEGF-C on the change in $[Ca^{2+}]_i$ on hCIPs, showing a reduction in $[Ca^{2+}]_i$. C. Data expressed as mean+SEM ratio of treatment/baseline $[Ca^{2+}]_i$. $[Ca^{2+}]_i$ levels were reduced in hCIPs when treated with both 1nM VEGF and 1nM VEGF-C. One sample *t*-test compared to baseline. *= $p<0.05$, n=5 and 8 respectively.

These results suggest that VEGF-C may activate a similar $[Ca^{2+}]_i$ signalling pathway to VEGF in hCIPs. The function of reduced $[Ca^{2+}]_i$ in hCIPs is debatable, yet these results clearly show that VEGF-C can stimulate an effect in cultured podocytes. The similar effects of VEGF-C and VEGF on $[Ca^{2+}]_i$ suggests that the function of VEGF-C is also similar. The effects of

1nM VEGF-C were therefore investigated on cytotoxicity induced by serum starvation in hCIPs. In addition, the effects of VEGF-C on cytotoxicity induced by serum starvation in HEK293 cells were also determined to ensure that the effects of VEGF-C on hCIPs were VEGF receptor specific. hCIPs and HEK 293 cells were serum starved for 16hrs then the media was replaced with fresh serum free media with 1nM VEGF-C or without. The amount of LDH released from the cells into the media was quantified for the low, experimental and high controls, using a colourimetric assay, as described in the methods. The percentage cytotoxicity was calculated from the densitometry readings of the LDH release.

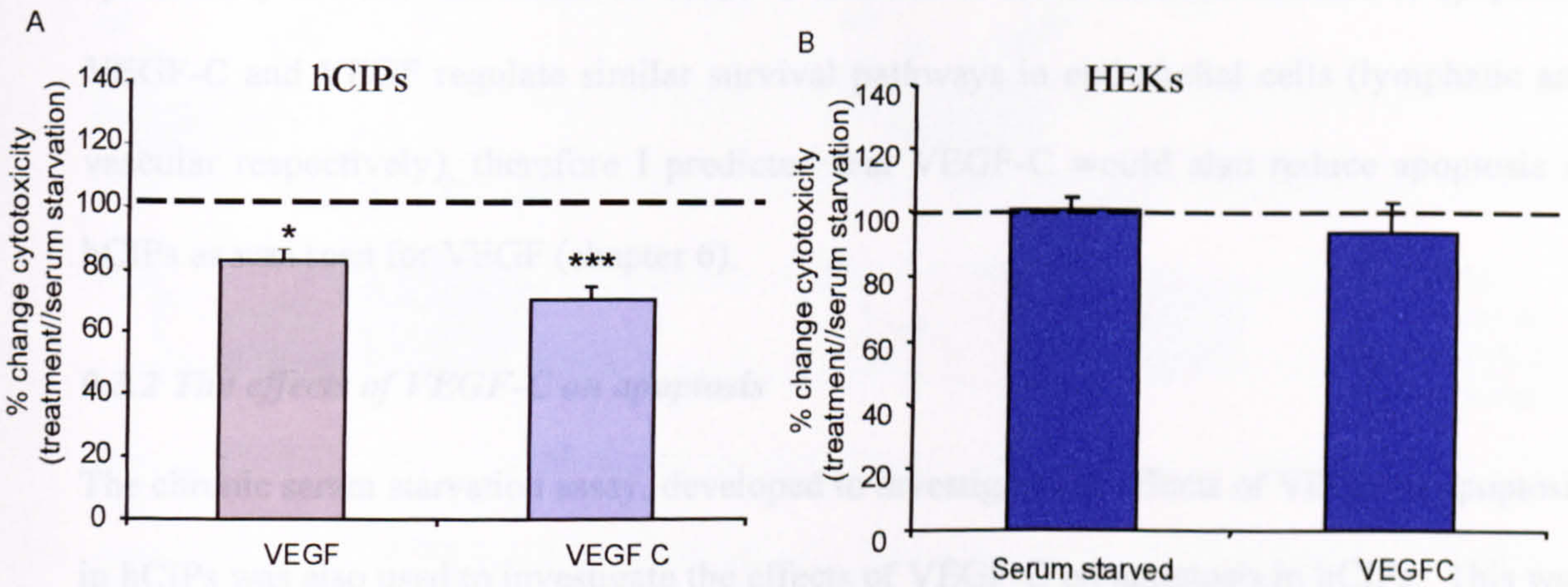

Figure 9.3. A comparison between the effects of 1nM VEGF and 1nM VEGF-C on cytotoxicity in hCIPs and between the effects of VEGF-C and serum starvation in HEK293 cells.

hCIPs and HEK293 cells were serum starved then treated with 1nM VEGF-C, or left untreated for 24hrs. LDH release from the cells was quantified and the percentage of cytotoxicity was then calculated. Data were expressed as mean+SEM the ratio of the percentage of cytotoxicity (treatment/serum starvation). A. The effects of VEGF-C on the percentage of cytotoxicity were compared to previous results showing the effects of VEGF on the percentage of cytotoxicity in hCIPs. Both VEGF-C and VEGF significantly reduced the percent of cytotoxicity (treatment/serum starvation), induced by serum starvation. B. There was no significant difference in the effects of VEGF-C compared to serum starvation in HEK293 cells. Unpaired *t*-test, *=p<0.05, ***=p<0.001, n=16.

VEGF-C reduced serum starved induced cytotoxicity in hCIPs as predicted (figure 9.3). VEGF-C appeared to reduce cytotoxicity to a greater extent than VEGF. There was a reduction in the ratio of cytotoxicity by VEGF-C of 70.8±3.8% of cells that had been serum starved ($p<0.001$, figure 9.3 A) compared to a reduction in the ratio of cytotoxicity by VEGF of 77.3±4.% ($p<0.04$, figure 9.3 A). In contrast, VEGF-C had no significant effect on cytotoxicity in HEK 293 cells, which had been serum starved (figure 9.3 B). HEK 293 cells do not express any VEGF receptors therefore these results demonstrate that the reduction in cytotoxicity in hCIPs, induced by VEGF-C was cell specific. Presumably, the reduction in cytotoxicity in hCIPs incubated in VEGF-C was due to either reduced necrosis or apoptosis. VEGF-C and VEGF regulate similar survival pathways in endothelial cells (lymphatic and vascular respectively), therefore I predicted that VEGF-C would also reduce apoptosis in hCIPs as was seen for VEGF (chapter 6).

9.3.2 The effects of VEGF-C on apoptosis

The chronic serum starvation assay, developed to investigate the effects of VEGF on apoptosis in hCIPs was also used to investigate the effects of VEGF-C on apoptosis in hCIPs. This was so that a significant level of apoptosis was achieved by serum starvation in differentiated hCIPs, as discussed in chapter 6. hCIPs were serum starved for 16hrs then the media was replaced with fresh serum free media either with VEGF-C or without, for 8hrs and then the media was replaced again with complete media, which was left for 48hrs. The cells were serum starved again for 16hrs, the media was replaced with fresh serum free media either with VEGF-C or without for 4hrs and the cells were then scraped into suspension and rolled for a further 4hrs. Surprisingly, VEGF-C did not have a significant effect on AV stained cell sub-populations even though a significant proportion of serum starved cells stained for AV (17.4±3.2% of the total cell population, figure 9.4 C). VEGF-C did not have a significant

effect on any of the other cell sub-populations either (figure 9.4 C). To verify that a change in apoptosis was not lost due to the definitions of the regions in the flow cytometry protocol, the percentage of AV positive cells (expressed as a percentage of total fluorescence picked up at 525nm) in VEGF treated cells was normalised to that of serum starved cells. There was, however, no significant difference in AV positive cells between treatments (1.29±0.32 fold change, p=0.46 one sample *t*-test, n=3, not shown).

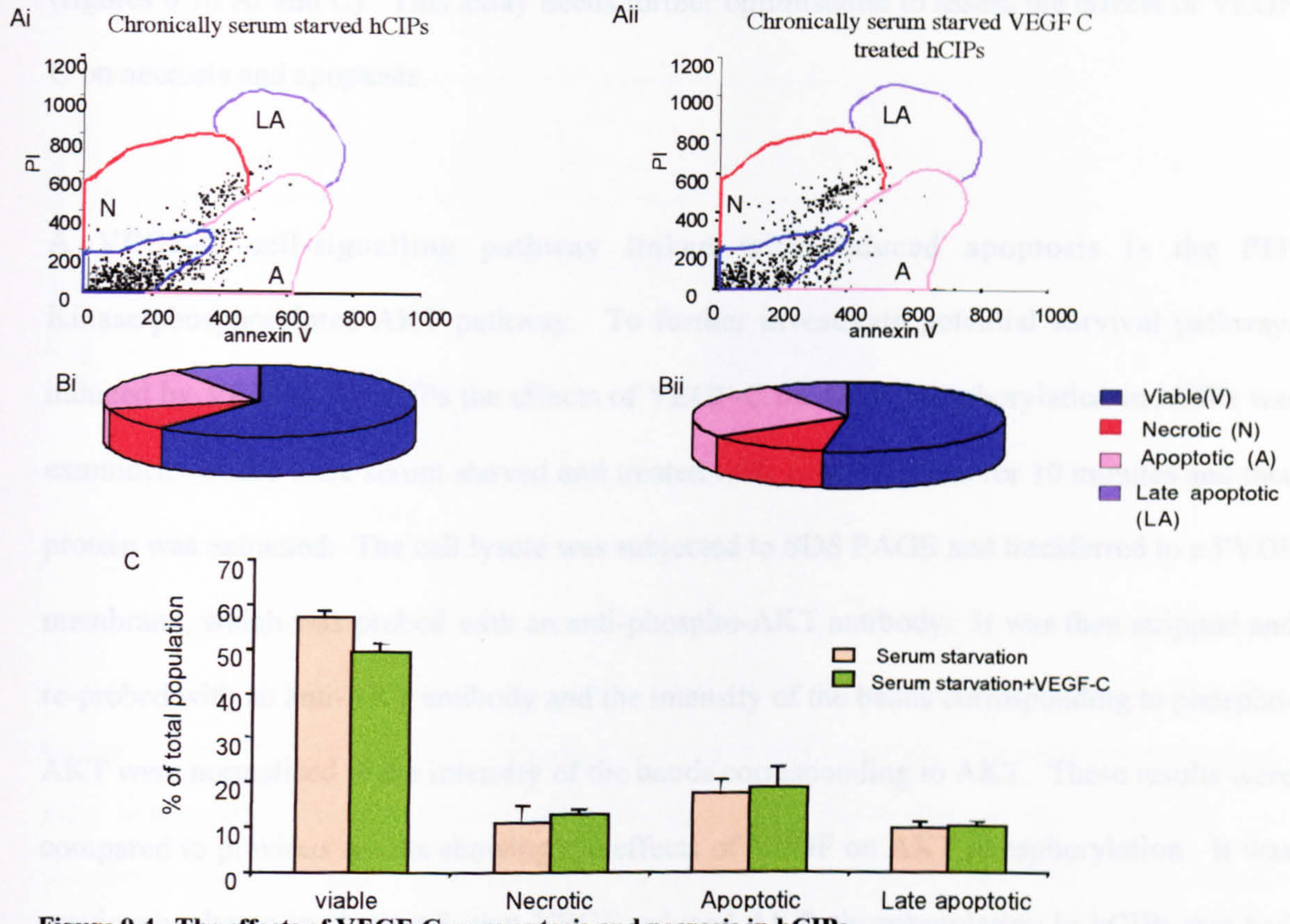

Figure 9.4. The effects of VEGF-C on apoptosis and necrosis in hCIPs.

hCIPs were chronically serum starved and treated with VEGF-C or left untreated. Cells were assayed by flow cytometry. A. A comparison of AV and PI labelling of 1nM VEGF-C treated hCIPs compared to untreated hCIPs, showing no visual difference in cell sub-populations. B. Characteristics of cell sub-populations in chronically serum starved 1nM VEGF-C treated hCIPs compared to untreated hCIPs. There was no significant difference in cell sub-populations treated with VEGF-C and left untreated. C. Data were expressed as mean+SEM percentage of total cell population. Compared to serum starvation alone, VEGF-C had no significant effect on any of the cell sub-populations (n.s. Bonferroni, n=3).

VEGF-C does however reduce cytotoxicity (figure 9.3 A) so it is reasonable to assume that it does affect either necrotic or apoptotic sub-populations. It is possible that VEGF-C works over a different time course to VEGF. Thus, it is difficult to investigate the effect of VEGF-C on apoptosis, using this assay, because apoptosis in hCIPs can only be induced under chronically serum starved conditions. It may be that VEGF-C acts to reduce necrosis, not apoptosis. Necrotic sub populations can be induced in hCIPs using a much shorter time course (figures 6.10 Ai and C). This assay needs further optimisation to assess the effects of VEGF-C on necrosis and apoptosis.

A VEGF-C cell-signalling pathway linked with reduced apoptosis is the PI3-Kinase/phosphorylated AKT pathway. To further investigate potential survival pathways induced by VEGF-C in hCIPs the effects of VEGF-C on AKT phosphorylation in hCIPs was examined. hCIPs were serum starved and treated with 1nM VEGF-C for 10 minutes and then protein was extracted. The cell lysate was subjected to SDS PAGE and transferred to a PVDF membrane, which was probed with an anti-phospho-AKT antibody. It was then stripped and re-probed with an anti-AKT antibody and the intensity of the bands corresponding to phospho-AKT were normalised to the intensity of the bands corresponding to AKT. These results were compared to previous results showing the effects of VEGF on AKT phosphorylation. It was previously shown in chapter 8, that VEGF reduced AKT phosphorylation in hCIPs that had been serum starved. I predicted that VEGF-C would have the same effect on phosphorylated AKT as VEGF in hCIPs. This however was not the case. There was no significant effect on AKT phosphorylation induced by serum starvation in cells that were treated with VEGF-C (0.87±0.12 fold lower than that in cells that had been serum starved, figure 9.5). The phosphorylated AKT levels in hCIPs treated with VEGF, however, were significantly lower than that in hCIPs treated with VEGF-C; in VEGF treated cells AKT phosphorylation was

0.37±0.08 fold lower and in VEGF-C treated cells it was 0.87±0.12 fold lower than serum starved cells ($p<0.05$, figure 9.5).

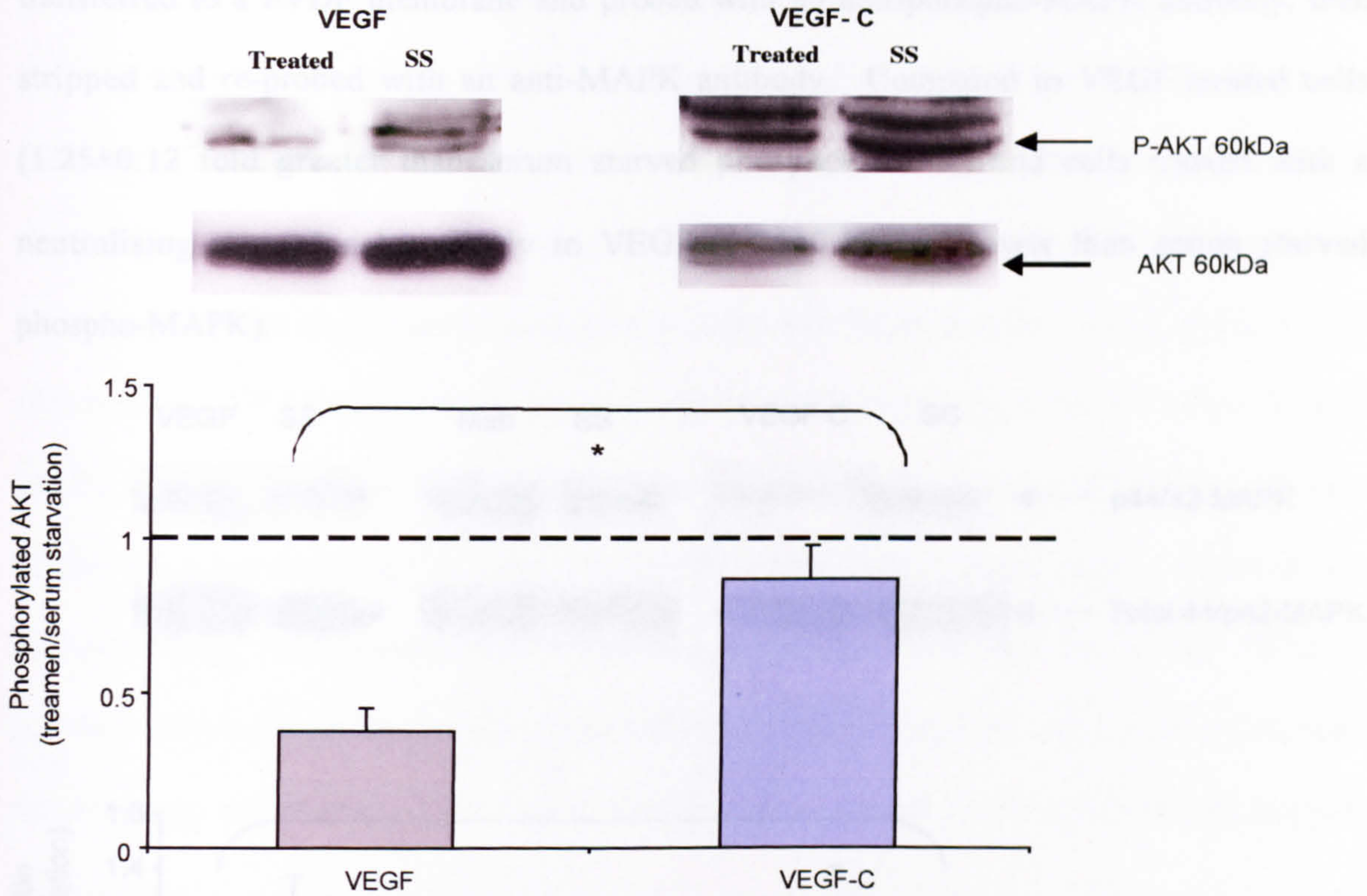

Figure 9.5. Effects of 1nM VEGFC on AKT phosphorylation compared to VEGF in hCIPs.

hCIPs were serum starved and treated with VEGF for 20 minutes, VEGF-C for 10 minutes, or the cells were left untreated for the appropriate amount of time. PVDF membranes containing this protein were probed with an anti-phospho-AKT antibody then stripped and re-probed with an anti-AKT antibody. Data were expressed as mean+SEM ratios: phospho-AKT (treatment/serum starvation)/total AKT (treatment/serum starvation). AKT phosphorylation induced by 1nM VEGFC was not significantly different to serum starved levels, but it was significantly greater than in 1nM VEGF treated. Unpaired *t*-test. *=$p<0.05$, n=3 and 5 respectively. SS = serum starved cells.

These results indicate that VEGF-C does not activate the AKT survival pathway in hCIPs. VEGF-C survival signalling has also been associated with elevated levels of phosphorylated MAPK in HMVECs. Hence, the effect of VEGF-C on MAPK phosphorylation in hCIPs was investigated. hCIPs were serum starved, then treated with VEGF for 20 minutes, VEGF-C for

10 minutes, a neutralising monoclonal antibody to VEGF for 24hrs or left untreated for the appropriate amount of time. Protein was extracted and subjected to SDS PAGE, then transferred to a PVDF membrane and probed with an anti-phospho-MAPK antibody, then stripped and re-probed with an anti-MAPK antibody. Compared to VEGF treated cells (1.25±0.12 fold greater than serum starved phospho-MAPK) and cells treated with a neutralising monoclonal antibody to VEGF (0.94±0.17 fold lower than serum starved phospho-MAPK).

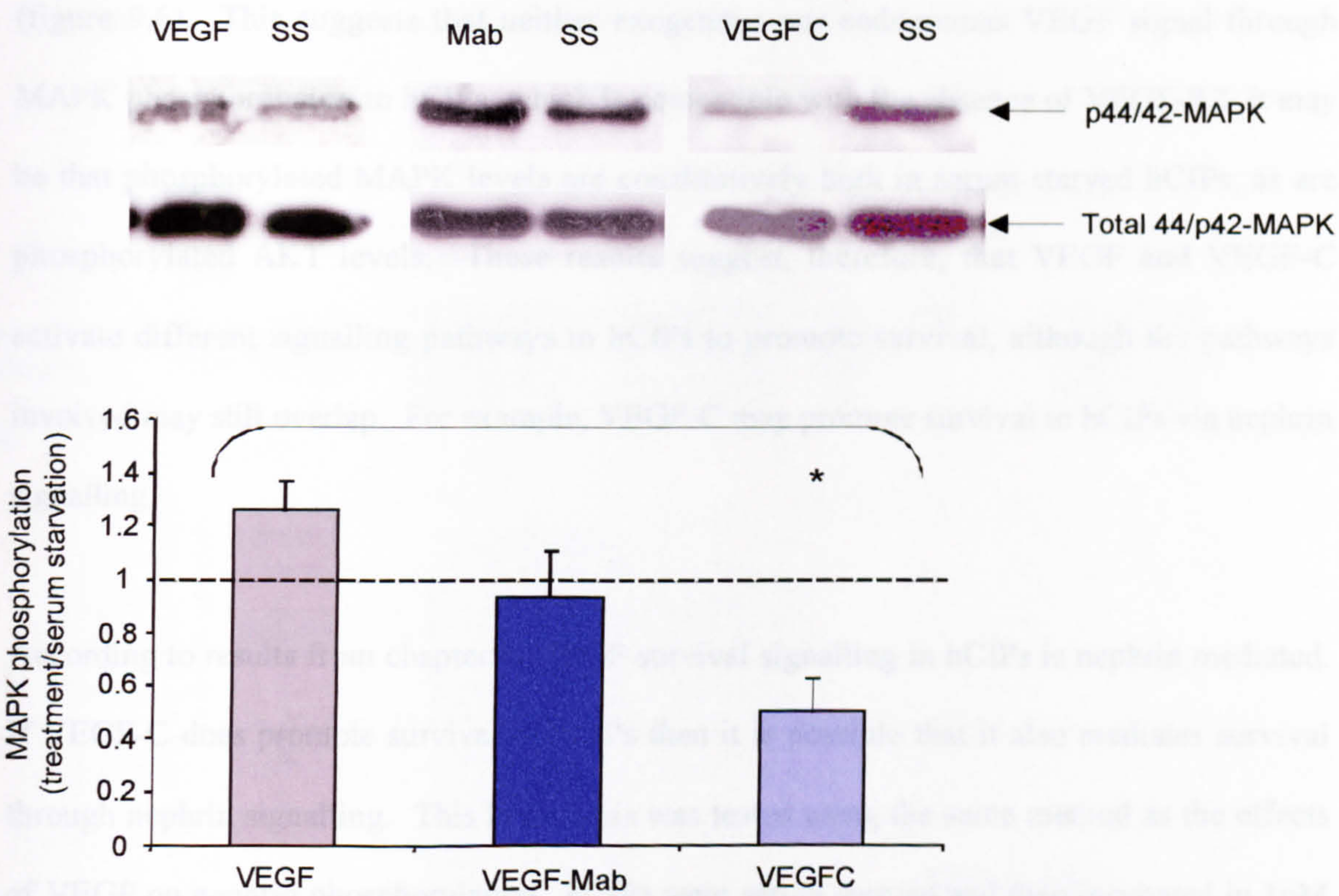

Figure 9.6. Effects of exogenous and endogenous VEGF and VEGF-C on MAPK phosphorylation in hCIPs.

hCIPs were serum starved and incubated in VEGF, VEGF-Mab, VEGF-C or left untreated for the appropriate amount of time. PVDF membranes containing this protein were probed with an anti-phospho-MAPK antibody and then stripped and re-probed with an anti-MAPK antibody. Data were expressed as mean+SEM ratios: phospho- MAPK (treatment/control)/total MAPK (treatment/control). 1nM VEGF-C significantly reduced p-MAPK compared to VEGF treatment in hCIPs. *=$p<0.05$, ANOVA, Bonferroni post hoc test n=4.

The intensity of the band corresponding to phospho-MAPK was normalised to the intensity of the band corresponding to MAPK. Surprisingly, VEGF-C induced a significant reduction in phosphorylated MAPK levels (0.5±0.13 fold lower in than serum starved phospho-MAPK, $p<0.05$, ANOVA, figure 9.6). The increase in phosphorylated MAPK levels in cells treated with VEGF compared to that of serum starved cells was not significant (one sample *t*-test, n=4, not shown). It was interesting to note that neither VEGF nor the neutralising monoclonal antibody to VEGF significantly increased phospho-MAPK in cells that were serum starved (figure 9.6). This suggests that neither exogenous nor endogenous VEGF signal through MAPK phosphorylation in hCIPs, which is compatible with the absence of VEGF-R2. It may be that phosphorylated MAPK levels are constitutively high in serum starved hCIPs, as are phosphorylated AKT levels. These results suggest, therefore, that VEGF and VEGF-C activate different signalling pathways in hCIPs to promote survival, although the pathways involved may still overlap. For example, VEGF-C may promote survival in hCIPs via nephrin signalling.

According to results from chapter 8, VEGF survival signalling in hCIPs is nephrin mediated. If VEGF-C does promote survival in hCIPs then it is possible that it also mediates survival through nephrin signalling. This hypothesis was tested using the same method as the effects of VEGF on nephrin phosphorylation. hCIPs were serum starved and then incubated in 1nM VEGF-C for 10 minutes, or left untreated for the appropriate amount of time. Protein was extracted and the cell lysate was subjected to immunoprecipitation, using an anti-p-Y antibody. The supernatant and precipitate were then subjected to SDS PAGE, transferred to a PVDF membrane and then probed with an anti-nephrin antibody. The mean intensity of the band corresponding to nephrin in the precipitate of each sample, measured by NIH image, was divided by the mean intensity of the band corresponding to nephrin in the supernatant of each

sample. This experiment was only repeated twice, so the results could not be tested for significance. Clearly though, there was a band of greater intensity corresponding to nephrin in the precipitate of VEGF-C treated cells compared to the intensity of the band corresponding to nephrin in the precipitate of the serum starved cells (figure 9.7 A). The intensity of the band corresponding to nephrin in the precipitate of each of the samples normalised to that in the supernatant is summarised in figure 9.7 B, which demonstrates graphically the greater intensity of the band corresponding to nephrin in the precipitate of VEGF-C treated cells. This suggests that VEGF-C can induce the phosphorylation of nephrin in hCIPs.

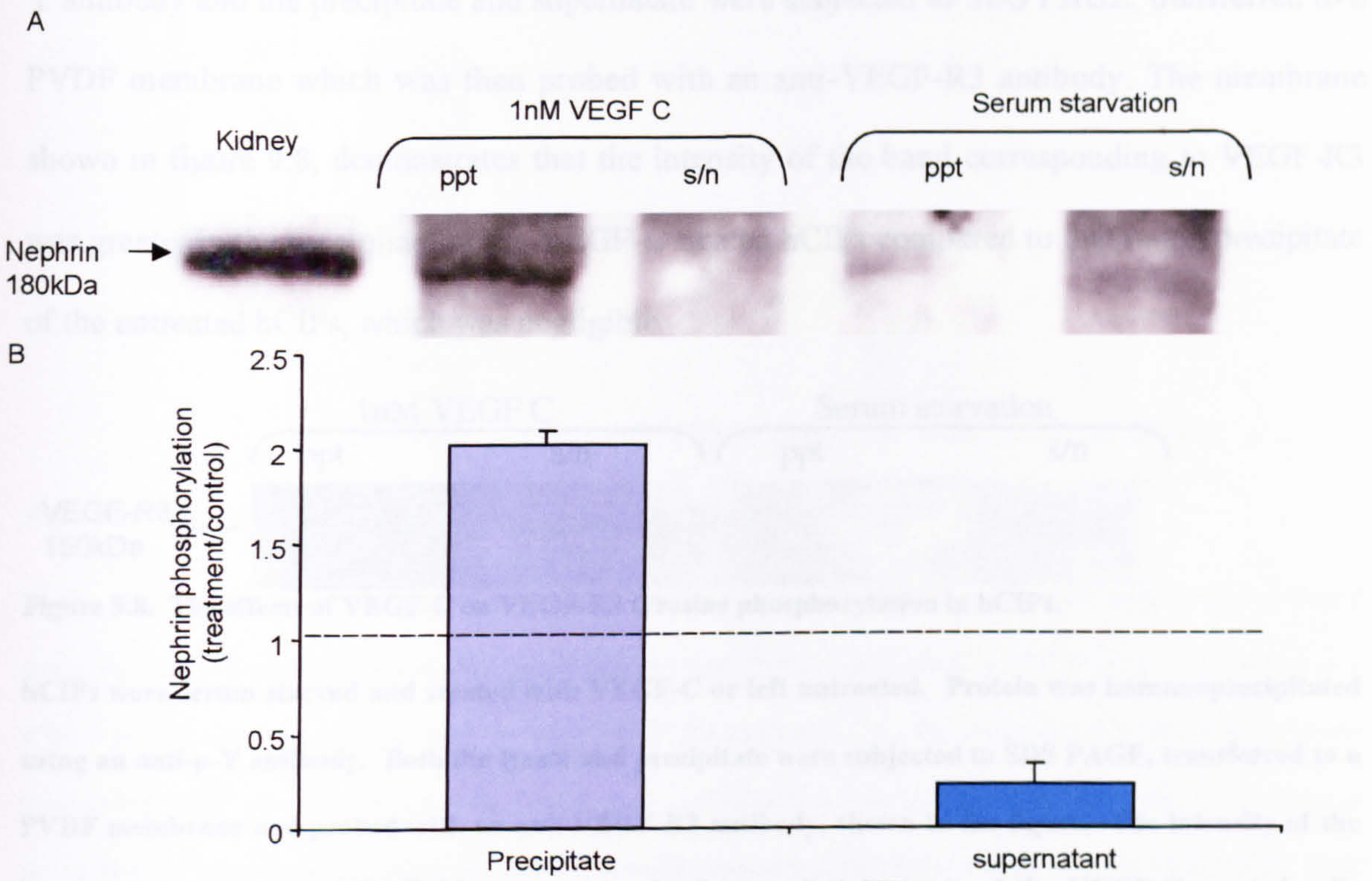

Figure 9.7. The effects of VEGF-C on nephrin phosphorylation in hCIPs.

hCIPs were serum starved and treated with VEGF-C, or left untreated. Protein was immunoprecipitated using an anti-p-Y antibody. Both the lysate and precipitate were subjected to SDS PAGE, transferred to a PVDF membrane and probed with an anti-nephrin antibody. A. An example of a PVDF membrane probed with an anti-nephrin antibody. 1nM VEGF-C treatment induced a more intense nephrin band in the precipitate compared to that of the band in the serum starved hCIPs. B Data expressed as mean+SEM ratio of treatment/control: 1nM VEGF-C treatment resulted in a two fold increase in nephrin

phosphorylation compared to serum starvation whereas non-phosphorylated nephrin was less in VEGF-C treated cells, n=2.

In HMVECs VEGF-C can mediate its effects through VEGF-R2 and VEGF-R3. Podocytes do not express VEGF-R2, therefore the phosphorylation of nephrin by VEGF-C was predicted to be VEGF-R3 dependent. To confirm that VEGF-C signalling in hCIPs was VEGF–R3 dependent an immunoprecipitation was carried out to assess the effects of VEGF-C on VEGF-R3 tyrosine phosphorylation. hCIPs were serum starved and treated with VEGF-C or left untreated for 10 minutes. The protein was extracted and immunoprecipitated using an anti- p-Y antibody and the precipitate and supernatant were subjected to SDS PAGE, transferred to a PVDF membrane which was then probed with an anti-VEGF-R3 antibody. The membrane shown in figure 9.8, demonstrates that the intensity of the band corresponding to VEGF-R3 was greater in the precipitate of the VEGF-C treated hCIPs compared to that in the precipitate of the untreated hCIPs, which was negligible.

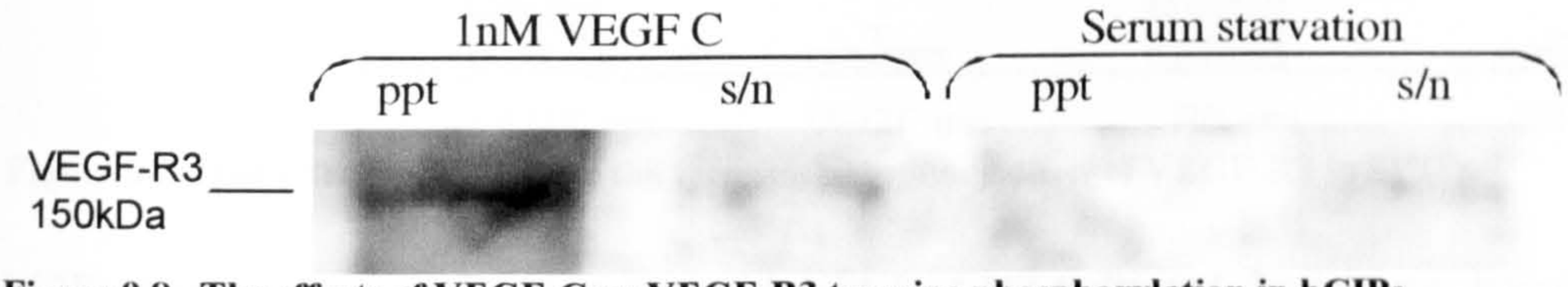

Figure 9.8. The effects of VEGF-C on VEGF-R3 tyrosine phosphorylation in hCIPs.

hCIPs were serum starved and treated with VEGF-C or left untreated. Protein was immunoprecipitated using an anti-p-Y antibody. Both the lysate and precipitate were subjected to SDS PAGE, transferred to a PVDF membrane and probed with an anti-VEGF-R3 antibody, shown in the figure. The intensity of the band corresponding to VEGF-R3 was greater in the precipitate (ppt) of the VEGF-C treated cells compared to that of the serum starved cells. s/n =supernatant, n=1.

The intensity of the band corresponding to VEGF-R3 in the supernatant of both the VEGF-C treated cells and the untreated cells was very faint. This preliminary data (n=1) suggests that VEGF-C can induce the auto-phosphorylation of VEGF-R3 in hCIPs. Some interesting preliminary results were observed during the optimisation of the anti-VEGF-R3 antibody on

old PVDF membranes containing precipitate and supernatant of hCIPs treated with VEGF. The intensity of the band corresponding to VEGF-R3 was more intense in the precipitate of VEGF treated hCIPs compared to that of serum starved cells as shown in figure 9.9A.

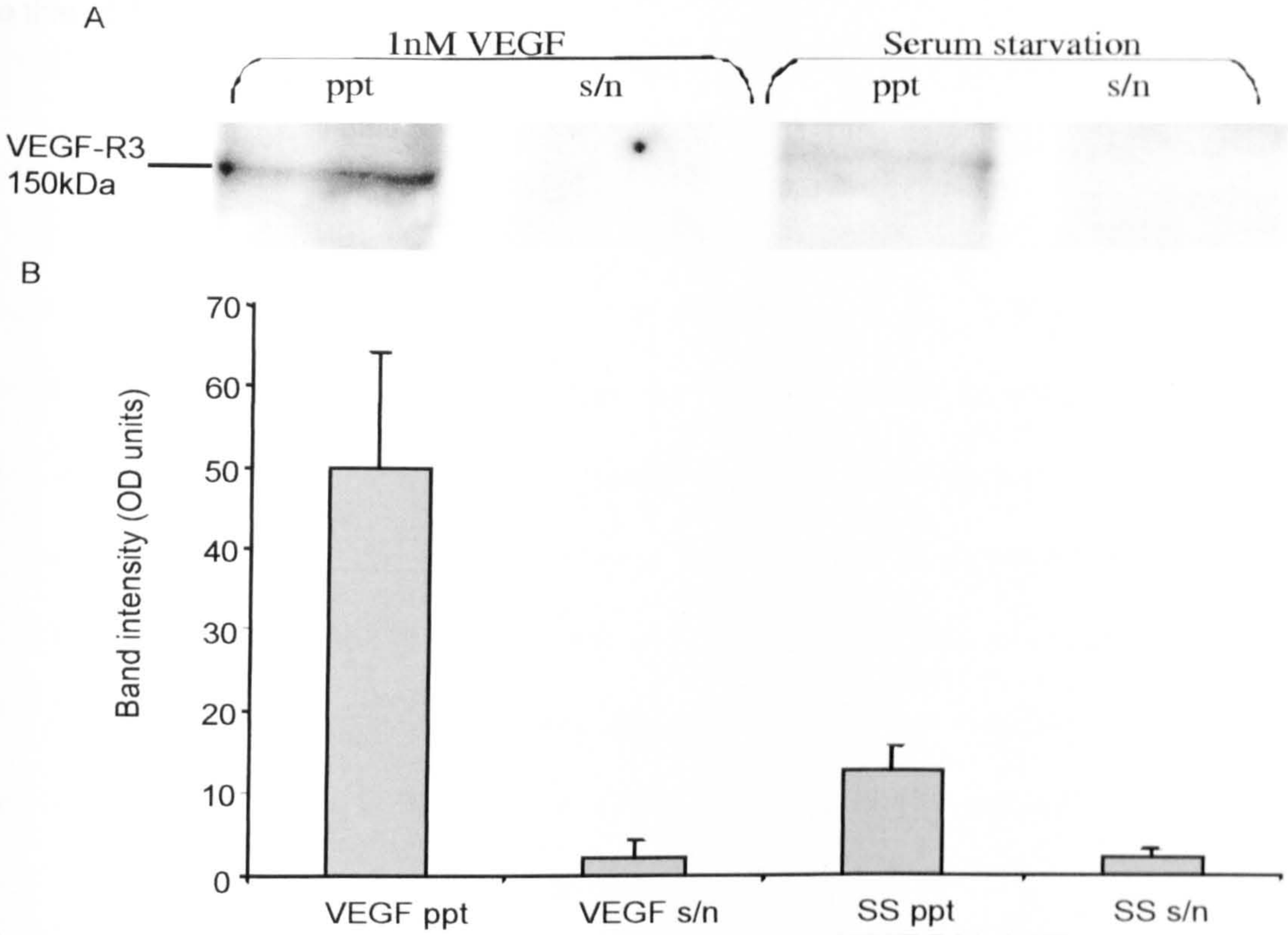

Figure 9.9. The effects of VEGF on the tyrosine phosphorylation of VEGF-R3 in hCIPs.

hCIPs were serum starved and treated with VEGF or left untreated. Protein was immunoprecipitated using an anti-p-Y antibody. Both the lysate and precipitate were subjected to SDS PAGE, transferred to a PVDF membrane and probed with an anti-VEGF-R3 antibody. A. An example of a PVDF membrane containing hCIP protein treated with VEGF and probed with an anti-VEGF-R3 antibody. There was a more intense band corresponding to VEGF-R3 in the immunoprecipitate of cells treated with VEGF than that of serum starved cells. B. Data are expressed as mean+SEM ratio of band intensity–background intensity. Ppt = precipitate, s/n = supernatant, n=2.

The results from two experiments were summarised graphically in figure 9.9 B, but due to the small n value they were not analysed statistically. These results suggest that VEGF can also induce the auto-phosphorylation of VEGF-R3 in hCIPs directly or indirectly. This was

unexpected, but indicates that VEGF may signal through VEGF-R1 and VEGF-R3 in cultured podocytes. These results demonstrate that VEGF-C can promote survival in cultured podocytes, probably through VEGF-R3 signalling, but through a different signalling pathway to that of VEGF.

9.4 Discussion

There has been very little research to date concerning VEGF-C expression or function in podocytes. This is because until now it was not known that podocytes express VEGF-R3, a receptor for VEGF-C. This allows the possiblility that VEGF-C is functional in podocytes.

VEGF-C is predominantly expressed in the lymphatics and promotes survival, growth and migration of lymphatic endothelial cells (Makinen et al., 2001). Yet during an immunohistochemical human tissue screen for VEGF-C protein recently in this laboratory, results were presented showing *in situ* VEGF-C protein expression in human renal cortex tissue sections (figure 9.1). VEGF-C protein was expressed in glomeruli in some cells that could only be described micro-anatomically as podocytes. This does not necessarily mean that VEGF-C is produced by podocytes-only mRNA expression can determine that definitively. Therefore, this study was to determine if VEGF-C could promote survival in podocytes, but it was not assumed that VEGF-C served an autocrine role.

VEGF-C induced a reduction in $[Ca^{2+}]_i$ in hCIPs, which was proportionally similar to the reduction seen with VEGF. The baseline $[Ca^{2+}]_i$ levels in the VEGF-C set of experiments were much lower than those in the VEGF set of experiments. This may be due to a number of experimental variables such as the cells may have been less confluent in the VEGF-C experiments than the VEGF $[Ca^{2+}]_i$ experiments, so that no matter how well the cells had loaded, if $[Ca^{2+}]_i$ changes were measured in fewer cells then overall fluorescence levels would be lower. The lower the fluorescent signal the higher the background, which is demonstrated by a higher noise ratio on figure 9.2 B compared to figure 9.2 A. The possibility that VEGF-C does not have as much physiological significance as VEGF cannot be ruled out: if VEGF-C

reduces $[Ca^{2+}]_i$ by the same amount in cells with a higher baseline $[Ca^{2+}]_i$ then the proportional effect of VEGF-C on podocyte $[Ca^{2+}]_i$ homeostasis, as discussed for VEGF, would be negligible. This is unlikely, however, as VEGF-C has quite obvious effects on podocytes as discussed below.

VEGF-C induced a reduction in cytotoxicity in hCIPs that had been serum starved to an even greater extent than VEGF in cultured podocytes (figure 9.3). These results, together with the $[Ca^{2+}]_i$ results indicate that VEGF-C activates a signalling cascade, which results in similar affects to VEGF, governed by VEGF-R3 and VEGF-R1 respectively. In HMVECs VEGF-C has a more pronounced effect on signalling than VEGF, even though HMVECs express both VEGF-R2 and VEGF-R3 (Makinen et al., 2001). It was suggested that this was due to activation of both VEGF-R2 and VEGF-R3 by VEGF-C, unlike VEGF. The signalling pathways of both receptors were therefore suggested to be cumulative. This explanation cannot be applied to podocytes, which do not express VEGF-R2 unless VEGF-R3 can interact with, or modulate VEGF-R1.

It is not known whether VEGF-C reduces cytotoxicity through the same means as VEGF, because the VEGF-C apoptosis assays were inconclusive and need to be optimised futher. Another approach was taken to investigate if VEGF-C induced survival, through AKT phosphorylation. The results showed that VEGF-C did not significantly affect AKT phosphorylation (figure 9.5), in contrast to VEGF. This was surprising, yet it narrows down the possibilities for VEGF-C survival signalling.

MAPK phosphorylation, usually associated with mitogenesis in VEGF signalling, has been implicated in VEGF-C survival signalling in HMVECs (Makinen et al., 2001); MAPK

activates a signalling cascade, which increases transcription of pro-survival genes such as Bcl-2 and has also been shown to result in the phosphorylation of BAD at serine 112, a different serine residue to the one phosphorylated by activated AKT (Bonni et al., 1999). I therefore predicted that VEGF-C would increase MAPK phosphorylation in podocytes, but the results showed the opposite (figure 9.6). It is interesting that a similar effect was seen with VEGF on AKT phosphorylation. The results remain inconclusive as to how VEGF-C promotes survival, but they do show that VEGF-C signals through a separate pathway to VEGF in podocytes.

If it was known that VEGF-C could signal through nephrin this would support the hypothesis that VEGF-C reduces apoptosis, because nephrin phosphorylation induced by VEGF is associated with reduced apoptosis. Immunoprecipitation studies demonstrated that VEGF-C could induce the phosphorylation of nephrin to a greater extent than in serum starved cells (figure 9.7). These results do provide huge potential for VEGF-C signalling and imply that VEGF-C promotes survival in podocytes by inhibiting apoptosis pathways. The means by which VEGF-C/VEGF-R3 signalling induces nephrin phosphorylation are as yet unclear as is the VEGF-C survival signalling pathway in podocytes and therefore should be investigated further and clarified.

I assumed that VEGF-C signalling in podocytes was VEGF-R3 dependent. Preliminary data confirmed this, shown in figure 9.8, which demonstrated that VEGF-C could induce the phosphorylation of VEGF-R3. Surprisingly, VEGF could also induce the phosphorylation of VEGF-R3 (figure 9.9). Due to the inability of VEGF to bind directly to VEGF-R3 it is more likely that activation of VEGF-R3 by VEGF is via heterodimerisation of the VEGF receptors. Heterodimerisation has previously been shown between VEGF-R2 and VEGF-R3 by VEGF-C in lymphatic endothelial cells (Dixelius et al., 2003). This provides potential for VEGF-R3

and VEGF-R1 heterodimerisation. This hypothesis may explain results seen in figure 6.4: a neutralising monoclonal antibody to VEGF induced a reduction in $[Ca^{2+}]_i$. I had predicted that when endogenous VEGF was blocked the VEGF induced reduction in $[Ca^{2+}]_i$ would also be blocked. Blocking endogenous VEGF ensured that it could not bind to the receptor complex, yet a reduction in $[Ca^{2+}]_i$ was still seen. VEGF-C, however, would still be able to bind to the putative VEGF-1/VEGF-R3 complexes, if indeed podocytes do produce VEGF-C. Inhibition of endogenous VEGF would therefore allow an increased effect of VEGF-C, which may account for the reduction in $[Ca^{2+}]_i$ in cultured podocytes treated with a neutralising monoclonal antibody to VEGF.

These results demonstrate that VEGF-C promotes survival in cultured podocytes through a separate signalling pathway to that of VEGF, via activation of VEGF-R3 and possibly a VEGF-R3/VEGF-R1 complex. The signalling pathway includes nephrin phosphorylation, and effects MAPK phosphorylation. It is postulated that the end result is inhibition of apoptosis.

Chapter 10

The effects of $VEGF_{165}b$ on cultured podocytes

10.1 Introduction

The recent discovery of a new VEGF isoform in this laboratory (Bates et al., 2002) has complicated the potential interpretation of experiments investigating the effects of $VEGF_{165}$ on podocytes. The new isoform is identical to $VEGF_{165}$ except for the last six amino acids (figure 10.1). The first 18 nucleotides of exon 8 of the VEGF gene are encoded in $VEGF_{165}$, but this encoded region is replaced by a more distal splice site selection within exon 8, termed exon 8b (figure 10.1 A). The distal exon 8b is translated to the same number of amino acids as exon 8 in the $VEGF_{165}$ protein (figure 10.1 C). This new isoform has been termed $VEGF_{165}b$ (Bates et al., 2002), (Cui et al., 2003). The consequence of the homology between these isoforms is that detection of what was previously thought to be $VEGF_{165}$, using antibodies or primers, could be $VEGF_{165}$, $VEGF_{165}b$ or both. This is interesting since the function of $VEGF_{165}b$ is different to that of $VEGF_{165}$ in endothelial cells. $VEGF_{165}b$ does not stimulate proliferation or migration of endothelial cells as $VEGF_{165}$ does (Bates et al., 2002). $VEGF_{165}b$ actually competitively binds to VEGF-R2 on endothelial cells, thus blocking $VEGF_{165}$ binding to VEGF-R2. When bound to VEGF-R2, $VEGF_{165}b$ does not seem to activate any signalling pathways, hence it blocks the proliferation and migration induced by $VEGF_{165}$ in endothelial cells (Bates et al., 2002). $VEGF_{165}b$ is expressed endogenously in human tissue, including the kidney, but is downregulated in renal and prostate carcinomas (Bates et al., 2002). The major implications of $VEGF_{165}b$ to this project are outlined by Cui et al. Primers designed to distinguish $VEGF_{165}b$ from $VEGF_{165}$, and short interference RNA (siRNA) designed to degrade $VEGF_{165}b$ specifically, showed that $VEGF_{165}b$ is primarily expressed by non-proliferative, differentiated hCIPs, rather than by de-differentiated, proliferative PCPs (Cui et al., 2003).

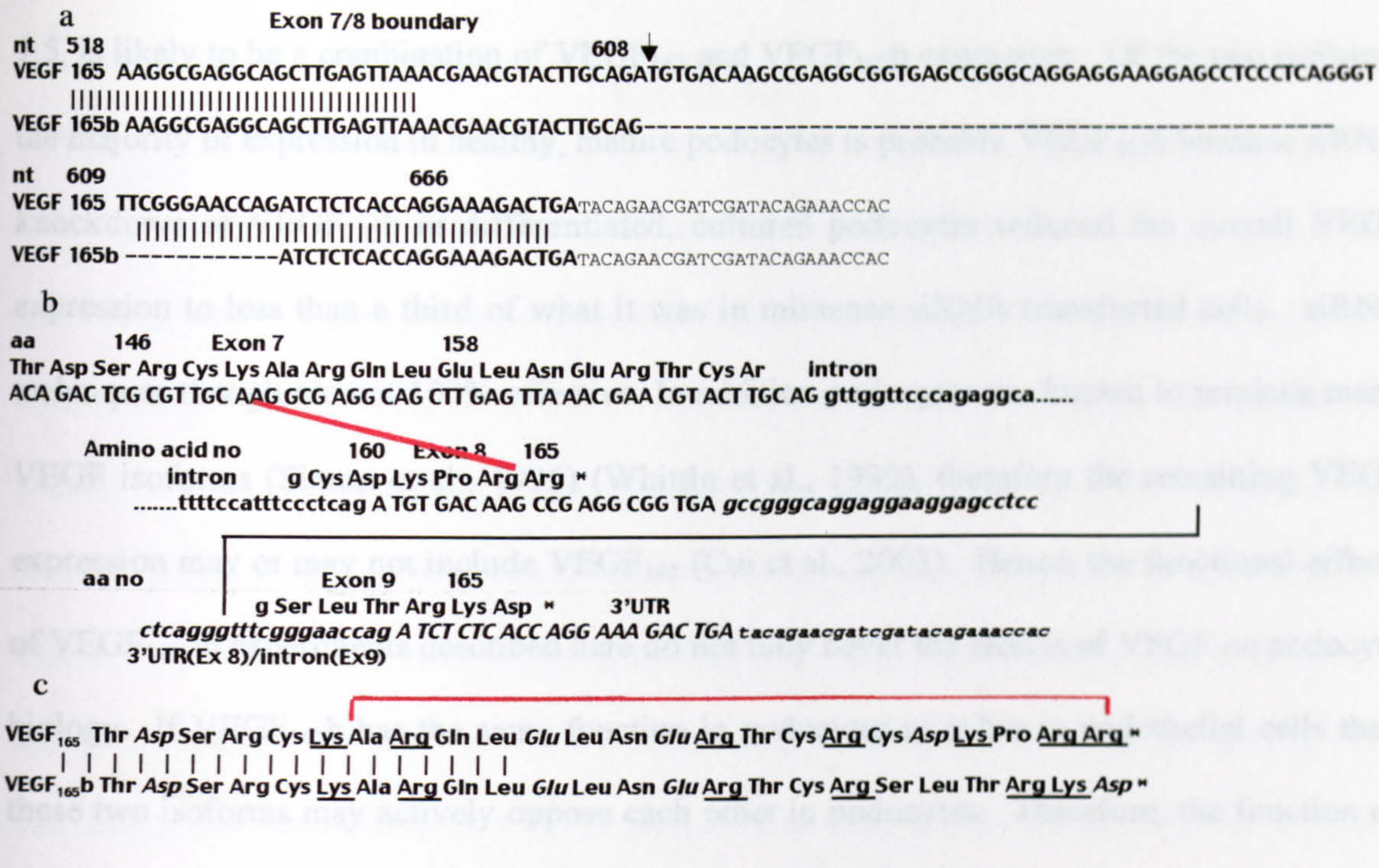

Figure 10.1. Sequence and putative structure and amino acid differences between $VEGF_{165}b$ and $VEGF_{165}$

A. A comparison of the nucleotide sequences of $VEGF_{165}$ and $VEGF_{165}b$; the 66bp downstream of exon 7 are missing from $VEGF_{165}b$. B. The exon structure of the COOH-terminal end of $VEGF_{165}$ and $VEGF_{165}b$. The 3'UTR sequence of exon 8 contains a consensus intronic sequence for exon 9, a CT-rich region and a CAG immediately prior to the splice site. The nucleotide sequence results in an alternate 6-amino acid COOH terminus. Capital letters are open reading frames; lowercase letters are either introns or 3'UTR (italics, $VEGF_{165}$; bold $VEGF_{165}b$). C. The predicted amino acid sequence of $VEGF_{165}$ comapred to $VEGF_{165}b$. The six alternative amino acids result in a different COOH-terminal structure of the VEGF likely to affect receptor activation but not receptor binding or dimerization. The Cys is replaced with a Ser, and the COOH-terminal amino acids are a basic (underlined) and an acidic (italics) moiety instead of two basic ones. Therefore, the net charge on this end of the molecule will be altered (Genbank ref. No. AF430806). Taken from figure 5, (Bates et al., 2002).

It has been hypothesised that $VEGF_{165}b$ expression in non-proliferative, differentiated podocytes reflects the VEGF isoform expression in podocytes in the normal, mature kidney. Furthermore, $VEGF_{165}b$ expression is downregulated in proliferative, de-differentiated podocytes, as it is in proliferative renal carcinomas compared to normal renal tissue (Bates et al., 2002). Therefore, VEGF expression by podocytes, shown by *in situ* hybridisation in figure

1.5, is likely to be a combination of $VEGF_{165}$ and $VEGF_{165}b$ expression. Of the two isoforms the majority of expression in healthy, mature podocytes is probably $VEGF_{165}b$ because siRNA knockdown of $VEGF_{165}b$ in differentiated, cultured podocytes reduced the overall VEGF expression to less than a third of what it was in missense siRNA transfected cells. siRNA techniques though are not 100% effective. In addition podocytes are known to produce many VEGF isoforms (Simon et al., 1995) (Whittle et al., 1999), therefore the remaining VEGF expression may or may not include $VEGF_{165}$ (Cui et al., 2003). Hence, the functional effects of $VEGF_{165}$ in experiments described here do not fully cover the effects of VEGF on podocyte biology. If $VEGF_{165}b$ has the same function in podocytes as it has in endothelial cells then these two isoforms may actively oppose each other in podocytes. Therefore, the function of both isoforms will be considered separately.

At the time of the cytotoxicity experiments in this chapter there was no source of recombinant purified $VEGF_{165}b$ protein. $VEGF_{165}b$ protein was therefore produced in house by Dr J. Woolard: A $pcDNA_3$ vector containing $VEGF_{165}b$ cDNA was transfected into non-VEGF expressing cells (CHO cells). These cells then expressed $VEGF_{165}b$ protein into the tissue culture media, which was quantified and used neat or diluted on cells.

10.2 Methods

10.2.1 Conditioned media from Chinese Hamster Ovary (CHO) cells

CHO cells were transfected using the LipofectAmine Plus method (Invitrogen) with a $pcDNA_3$ vector containing either 2μg $VEGF_{165}b$ cDNA or left empty. Cells were grown to confluency with the aid of 0.1% Geneticin (Gibco), to select for transfected cells. The F-12 CHO cell media was removed, the cells washed once with 1XPBS and serum free RPMI media was added to the cells. CHO cells do not grow well in RPMI media so the incubation time was limited to a period of 48hrs. After this time the serum free RPMI media, conditioned by CHO cells that had been transfected with $VEGF_{165}b$ or an empty $pcDNA_3$ vector, was removed (10ml) and kept separately at -20°C until ready for use. The CHO cells were allowed to recover in complete F-12 media for at least 48hrs and then the process was repeated.

10.2.2 Enzyme linked immunoabsorbancy assay (ELISA)- quantification $VEGF_{165}b$ protein in conditioned media (CM).

A 500μl sample was taken from each lot of CM before it was frozen down. The amount of $VEGF_{165}b$ protein was quantified using a commercially available pan-VEGF ELISA (R&D, Systems, Abingdon, UK) according to manufacturers instructions. CHO cells do not produce VEGF normally (and cells transfected with empty vector produced no VEGF), so the VEGF protein quantified was known to be $VEGF_{165}b$ produced by the transfected cells.

10.2.3 $VEGF_{165}b$ antibody

An antibody specific to the last nine amino acids of $VEGF_{165}b$ (see figure 10.1 A) was raised in mice in this laboratory. The antibody was cloned, purified and the specificity against $VEGF_{165}$ was confirmed by Western Blotting.

10.2.4 Western blotting-expression of $VEGF_{165}b$ in hCIPs

Protein was extracted from serum starved hCIPs and quantified. A total of 20ng recombinant $VEGF_{165}$ and $VEGF_{165}b$ protein (R&D, Systems, Abingdon, UK, developed after the cytotoxicity and apoptosis assays were carried out) plus the hCIP protein were subjected to SDS PAGE. Protein was transferred to a PVDF membrane and was then probed with 0.4μg/ml anti mouse monoclonal IgG anti-$VEGF_{165}b$ primary antibody and 0.006μg/ml HRP conjugated goat anti-mouse IgG secondary antibody (Pierce, Cheshire, UK). The membrane was stripped and re-probed with 1μg/ml mouse monoclonal IgG_{2a} anti-VEGF (C-1) primary antibody (Santa Cruz, Heidelberg, Germany) and 0.006μg/ml HRP conjugated goat anti-mouse IgG secondary antibody (Pierce, Cheshire, UK).

10.2.5 Cytotoxicity assay- effects of $VEGF_{165}b$ alone or in combination with $VEGF_{165}$

hCIPs were serum starved overnight using $pcDNA_3$ CM. Cells were then treated with a range of concentrations of $VEGF_{165}b$ CM, a range of concentrations of $VEGF_{165}b$ CM combined with 1nM VEGF, or left untreated in $pcDNA_3$ CM for 24hrs. Low, experimental and high controls were assayed and quantified as described previously.

10.2.6 Apoptosis assay-effects of $VEGF_{165}b$ alone or in combination with $VEGF_{165}$.

hCIPs were serum starved for 16hrs using $pcDNA_3$ CM. Cells were then treated with 298pM $VEGF_{165}b$ CM, 1nM $VEGF_{165}b$ in $pcDNA_3$ CM, 298pM $VEGF_{165}b$ and 1nM $VEGF_{165}$ or left untreated in $pcDNA_3$ CM for 4hrs. Cells were then scraped into suspension and rolled for a further 4hrs. Cells were then assayed using the flow cytometer as previously described.

10.3 Results

10.3.1 The expression of $VEGF_{165}b$ protein in differentiated podocytes

To confirm that differentiated podocytes express $VEGF_{165}b$ protein a PVDF membrane containing protein from serum starved hCIPs and recombinant $VEGF_{165}$ and $VEGF_{165}b$ protein was probed with anti-VEGF, stripped and re-probed with anti-$VEGF_{165}b$. The results were intriguing: A ladder of bands were seen in both blots and were reproducible (figure 10.2 A). These bands correspond to a number of VEGF isoforms that are summarised in table 10.1. The bands are split into three groups; VEGF monomers, VEGF dimers and large VEGFs.Larger molecular weight VEGFs are generated by an alternate translation initiation process at the CUG start codon in the 5'UTR region, upstream from the normal ATG start codon (Huez et al., 2001). Lower molecular weight VEGF fragments are produced by the cleavage of the carboxy-terminal domain by plasmin (c-terminal fragments) (Keyt et al., 1996).

The $VEGF_{165}b$ antibody was raised to the terminal 9 amino acids encoded for by the last three codons of exon 7 and the whole of exon 8b (see figure 10.1 A), yet the same bands were detected with the anti-$VEGF_{165}b$ antibody as with the anti-$VEGF_{165}$ antibody. This indicates that other common VEGF isoforms also have sister splice variants. These results confirm that differentiated podocytes express various VEGF isoforms, but that at least some of those isoforms are $VEGF_{xxx}b$. These isoforms are also expressed in different proportions to each other in differentiated hCIPs.

The intensity of each band, from both cell lysates, was expressed as a percentage of the intensity of band e (figure 10.2 B-D). Anything over 100% was above saturation levels and

could not be measured relative to the intensity of band e. The intensity of bands, a, b and c of the putative isoform monomers were lower than that of band e in the anti pan-VEGF blot (data expressed as a percentage of the intensity of band e: band a. 2.3±1.8%, band b. 3.7±2.8% and band c. 4.1±3.3%, figure 10.2 B), yet only the intensities of bands a appeared lower in the anti-$VEGF_{xxx}b$ blot (band a. 73.5±10.2% of the intensity of band e, figure 10.2 B). Of the bands corresponding to VEGF dimers, bands f and g appeared to have a lower intensity than that of band e in the anti-pan VEGF blot (data expressed as a percentage of the intensity of band e: band f. 64±7.2 %, band g. 70.3±5.4%, figure 10.2 C). The same was seen in the anti-$VEGF_{xxx}b$ blot; of the VEGF dimers bands f and g appeared to have a lower intensity than that of band e (data expressed as a percentage of the intensity of band e: band f. 85.9±3%, band g. 77±9%, figure 10.2 C). Of the large VEGFs, neither the intensity of the bands in the pan-anti-VEGF blot, nor the intensity of the bands on the anti-$VEGF_{xxx}b$ blot were lower than that of band e (figure 10.2 D).

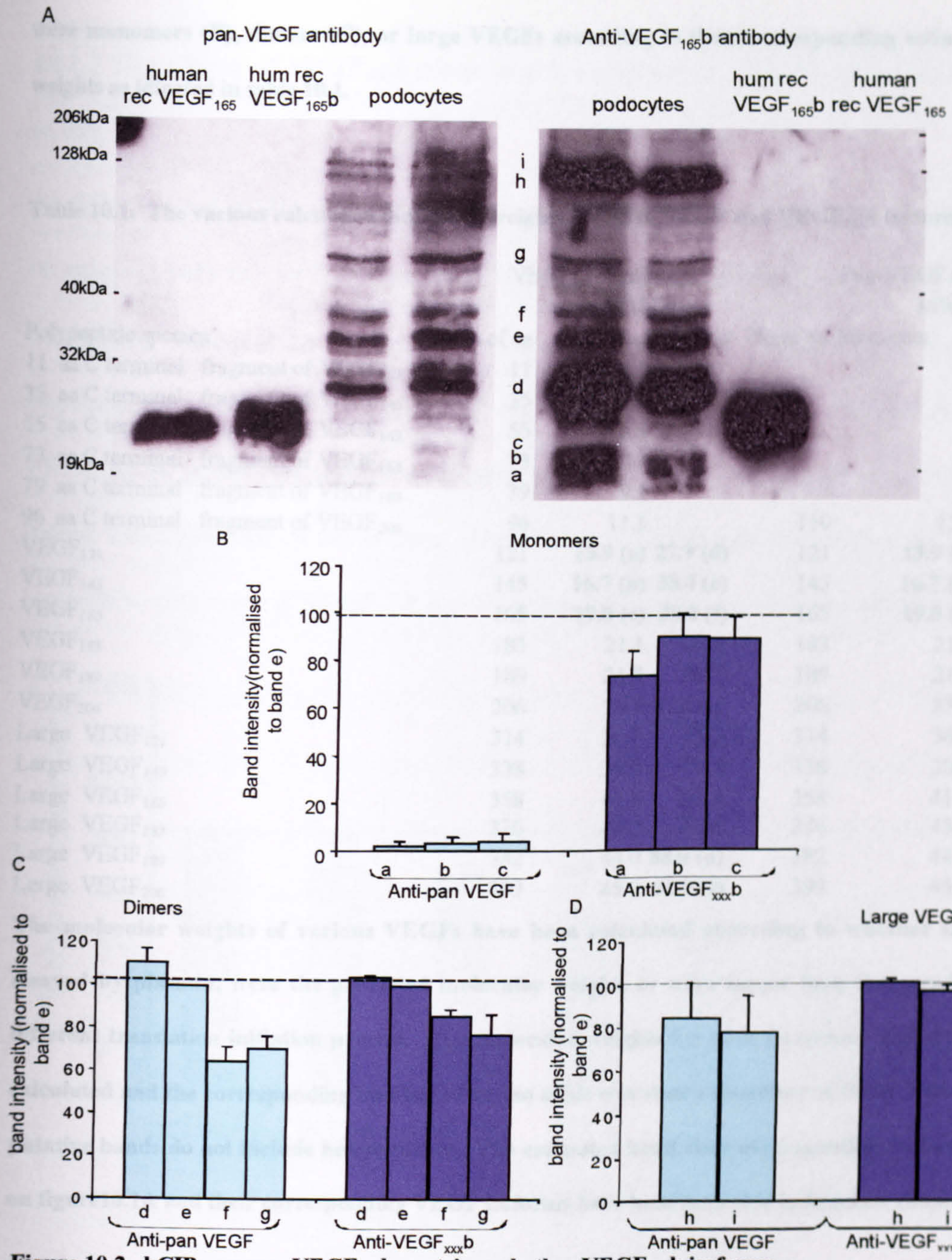

Figure 10.2. hCIPs express $VEGF_{165}b$ protein and other $VEGF_{xxx}b$ isoforms

A. Multiple bands were seen when a PVDF membrane, containing hCIP protein, recombinant $VEGF_{165}$ and $VEGF_{165}b$ protein was probed with an anti pan-VEGF and an anti-$VEGF_{165}b$ antibody. Similar bands were seen with both probes; the multiple bands corresponded to postulated sister splice variants of the common isoforms $VEGF_{189}b$, $VEGF_{165}b$, $VEGF_{145}b$, $VEGF_{121}b$ etc. Human recombinant $VEGF_{165}$ and $VEGF_{165}b$ protein was used to demonstrate the specificity of the antibodies. The intensity of each band was expressed as mean+SEM percentage of intensity of band e (B-D). Bands were defined by whether they

were monomers (B), dimers (C), or large VEGFs according to their corresponding estimated molecular weights as idicated in table 10.1.

Table 10.1. The various calculated molecular weights (MW) of VEGF and $VEGF_{xxx}b$ isoforms.

	$VEGF_{xxx}b$ antibody MW (kDa)			Pan-VEGF antibody MW (kDa)		
Polypeptide species	No of aa	Monomer	Dimer	No of aa	Monomer	Dimer
11 aa C terminal fragment of $VEGF_{121}$	11	1.3				
35 aa C terminal fragment of $VEGF_{145}$	35	4.0				
55 aa C terminal fragment of $VEGF_{165}$	55	6.3				
73 aa C terminal fragment of $VEGF_{183}$	73	8.4				
79 aa C terminal fragment of $VEGF_{189}$	79	9.1				
96 aa C terminal fragment of $VEGF_{206}$	96	11.1		110	12.7	25.3
$VEGF_{121}$	121	**13.9 (a)**	**27.9 (d)**	121	**13.9 (a)**	**27.9 (d)**
$VEGF_{145}$	145	**16.7 (b)**	**33.4 (e)**	145	**16.7 (b)**	**33.4 (e)**
$VEGF_{165}$	165	**19.0 (c)**	**38.0 (f)**	165	**19.0 (c)**	**38.0 (f)**
$VEGF_{183}$	183	21.1	42.1	183	21.1	42.1
$VEGF_{189}$	189	21.8	43.5	189	21.8	43.5
$VEGF_{206}$	206	23.7	**47.4 (g)**	206	23.7	**47.4 (g)**
Large $VEGF_{121}$	314	36.2	72.3	314	36.2	72.3
Large $VEGF_{145}$	338	38.9	77.8	338	38.9	77.8
Large $VEGF_{165}$	358	41.2	82.4	358	41.2	82.4
Large $VEGF_{183}$	376	43.3	86.6	376	43.3	86.6
Large $VEGF_{189}$	382	44.0	**88.0 (h)**	382	44.0	**88.0 (h)**
Large $VEGF_{206}$	399	45.9	**91.9 (I)**	399	45.9	**91.9 (I)**

The molecular weights of various VEGFs have been calculated according to whether they have been cleaved by plasmin, were the predicted molecular weight, or were larger than that predicted due to a different translation initiation process. The molecular weights for both monomers and dimers were also calculated and the corresponding number of amino acids was shown (courtesy of Dr D. Bates). Note; these putative bands do not include heterodimers. The estimated band sizes corresponding to bands a-I labelled on figure10.1A and their corresponding VEGF isoforms have been indicated in brackets (bold).

10.3.2 The effects of $VEGF_{165}b$ alone and in conjunction with $VEGF_{165}$ on cytotoxicity in hCIPs.

As differentiated hCIPs do express $VEGF_{165}b$ I proceeded to compare the effects of $VEGF_{165}b$ on survival with that of $VEGF_{165}$ in hCIPs. The function of $VEGF_{165}b$ in podocytes may be completely different to its function in endothelial cells. In order to comprehend the implications of possible expression of both VEGF isoforms in podocytes the function of $VEGF_{165}b$ in podocytes was investigated. In endothelial cells $VEGF_{165}b$ does not seem to induce functional effects on its own. The effects of $VEGF_{165}b$ on cytotoxicity in hCIPs were assessed to determine if $VEGF_{165}b$ had functional effects on survival in cultured podocytes.

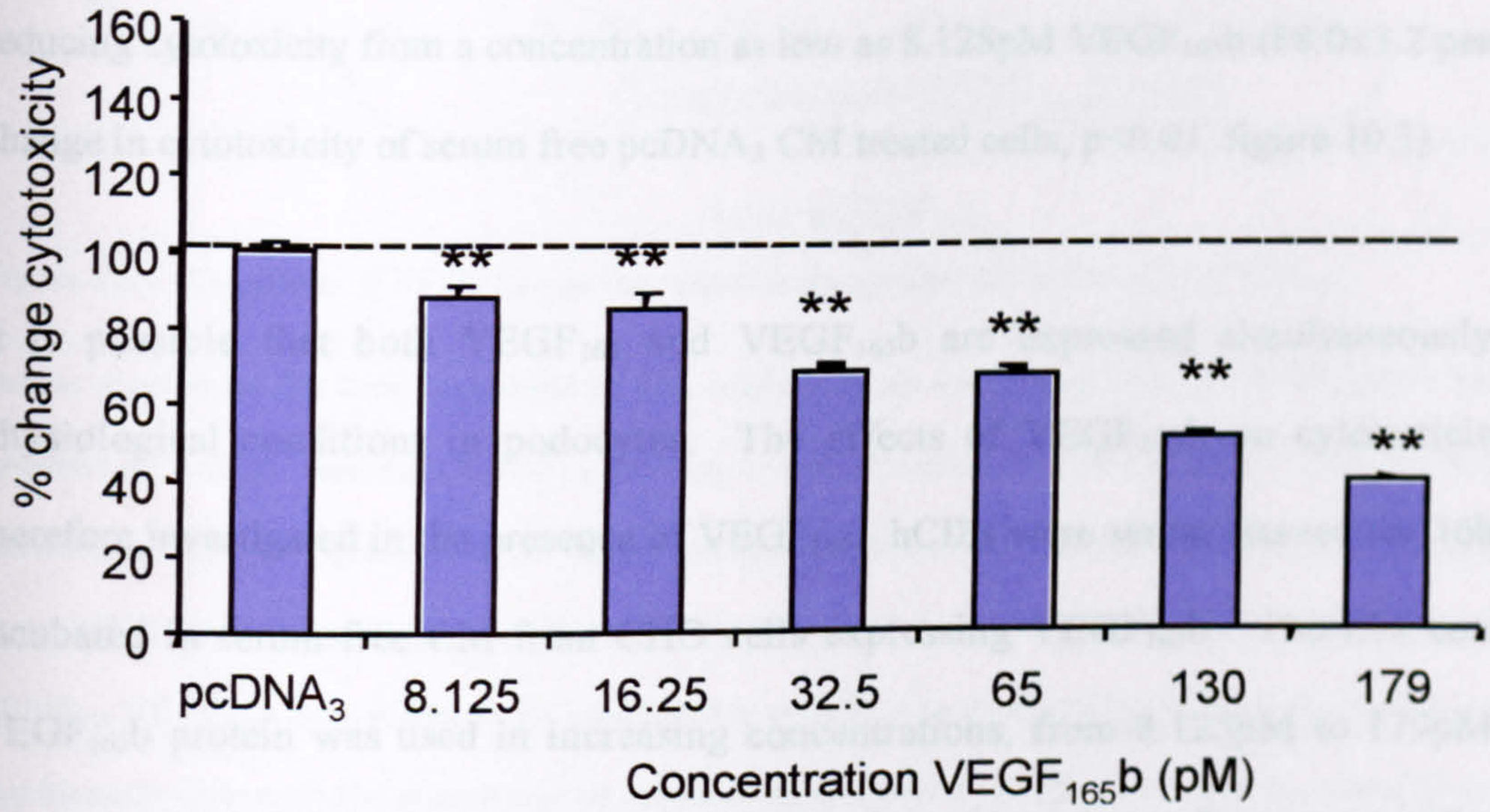

Figure 10.3. The effects of $VEGF_{165}b$ on cytotoxicity in differentiated hCIPs.

Serum starved hCIPs were incubated in conditioned media containing increasing concentrations of $VEGF_{165}b$ for 24hrs and then the amount of LDH release from the cells was quantified. The percentage of cytotoxicity was calculated from this. Data were expressed as mean+SEM percentage change in cytotoxicity, normalised to serum free $pcDNA_3$ CM values. $VEGF_{165}b$ dose-dependently reduced cytotoxicity compared to treatment with pcDNA3 CM in hCIPs. **=$p<0.01$, n= ≤ 8, ANOVA with Bartletts post Hoc test.

hCIPs were serum starved for 16hrs and the media was replaced with a mixture of serum free CM from CHO cells that were transfected with a $pcDNA_3$ vector containing $VEGF_{165}b$ protein or left empty, mixed to give an increasing concentration of $VEGF_{165}b$ and left for 24hrs. The amount of LDH released into the media for the low, experimental and high controls was quantified using a colourimetric assay and these values were then used to calculate the percentage of cytotoxicity, as described in the methods. Unexpectedly, $VEGF_{165}b$ dose dependently decreased cytotoxicity in hCIPs (p.0.01, ANOVA, figure 10.3). The maximum concentration of $VEGF_{165}b$ used was limited by the efficiency of the transfected CHO cells to produce the $VEGF_{165}b$ protein. Therefore, the $VEGF_{165}b$ concentrations were very low compared to those used for $VEGF_{165}$. Nevertheless, $VEGF_{165}b$ was effective at significantly reducing cytotoxicity from a concentration as low as 8.125pM $VEGF_{165}b$ (88.0±3.2 percentage change in cytotoxicity of serum free $pcDNA_3$ CM treated cells, $p<0.01$, figure 10.3).

It is possible that both $VEGF_{165}$ and $VEGF_{165}b$ are expressed simultaneously under physiological conditions in podocytes. The effects of $VEGF_{165}b$ on cytotoxicity were therefore investigated in the presence of $VEGF_{165}$. hCIPs were serum starved for 16hrs then incubated in serum free CM from CHO cells expressing $VEGF_{165}b$. The CM containing $VEGF_{165}b$ protein was used in increasing concentrations, from 8.125pM to 179pM in the presence of 1nM $VEGF_{165}$. The amount of LDH released into the media was quantified using a colourimetric assay and the percentage of cytotoxicity was calculated from this. Surprisingly, in the presence of 1nM $VEGF_{165}$ $VEGF_{165}b$ dose dependently increased cytotoxicity (figure 10.4). At a concentration of 32.5pM, $VEGF_{165}b$ blocked the reduction in cytotoxicity induced by 1nM $VEGF_{165}$ to the same cytotoxicity levels as cells incubated in serum free CM (109±9 percentage increase in cytotoxicity of that in serum free $pcDNA_3$ CM treated cells, figure 10.4). At a concentration of 65pM of $VEGF_{165}b$ protein, there was a

significant increase in cytotoxicity compared to the other concentrations of $VEGF_{165}b$ protein (151±9.4 percentage increase in cytotoxicity of that in serum free $pcDNA_3$ CM treated cells, $p<0.001$, ANOVA, figure 10.4).

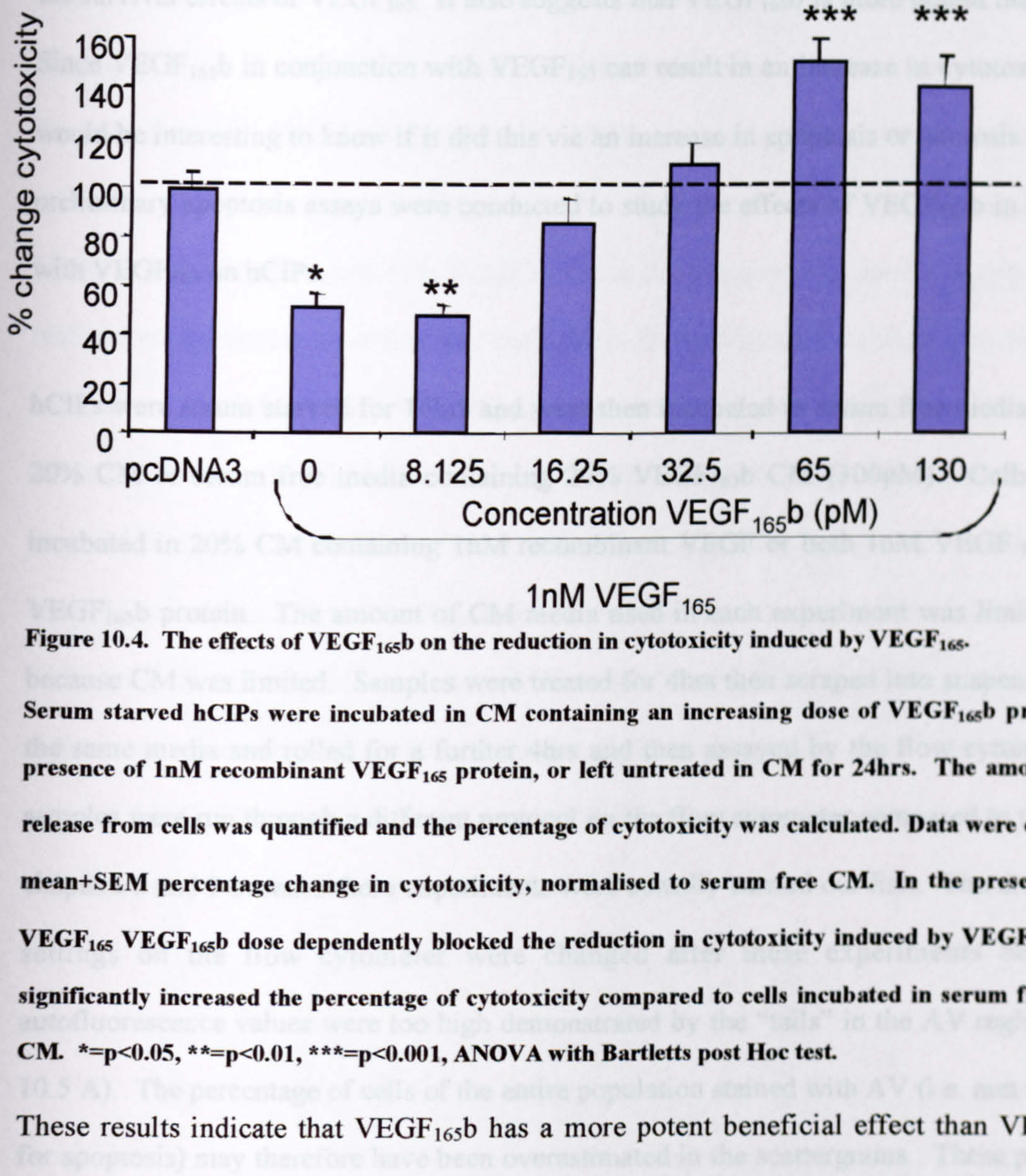

Figure 10.4. The effects of $VEGF_{165}b$ on the reduction in cytotoxicity induced by $VEGF_{165}$.

Serum starved hCIPs were incubated in CM containing an increasing dose of $VEGF_{165}b$ protein in the presence of 1nM recombinant $VEGF_{165}$ protein, or left untreated in CM for 24hrs. The amount of LDH release from cells was quantified and the percentage of cytotoxicity was calculated. Data were expressed as mean+SEM percentage change in cytotoxicity, normalised to serum free CM. In the presence of 1nM $VEGF_{165}$ $VEGF_{165}b$ dose dependently blocked the reduction in cytotoxicity induced by $VEGF_{165}$ and also significantly increased the percentage of cytotoxicity compared to cells incubated in serum free $pcDNA_3$ CM. *=p<0.05, **=p<0.01, ***=p<0.001, ANOVA with Bartletts post Hoc test.

These results indicate that $VEGF_{165}b$ has a more potent beneficial effect than $VEGF_{165}$ on cytotoxicity in podocytes because the concentration required for $VEGF_{165}b$ (100pM) to reduce cytotoxicity to the same extent as that of $VEGF_{165}$ (1nM) was significantly lower. $VEGF_{165}b$ reduced cytotoxicity to 39.2±1.03 percent of that in serum free CM treated cells ($p<0.01$, ANOVA, figure 10.3) at a concentration of 179pM. This demonstrated that $VEGF_{165}b$ was

also more efficacious than $VEGF_{165}$, since a concentration as high as 1nM $VEGF_{165}$ did not reduce cytotoxicity to the same extent (52.1±4.9 percent of that in serum free $pcDNA_3$ CM treated cells, $p<0.05$, ANOVA, figure 10.4). These results suggest that $VEGF_{165}b$ antagonises the survival effects of $VEGF_{165}$. It also suggests that $VEGF_{165}b$ is more potent than $VEGF_{165}$. Since $VEGF_{165}b$ in conjunction with $VEGF_{165}$ can result in an increase in cytotoxicity then it would be interesting to know if it did this via an increase in apoptosis or necrosis. Therefore, preliminary apoptosis assays were conducted to study the effects of $VEGF_{165}b$ in conjunction with $VEGF_{165}$ on hCIPs.

hCIPs were serum starved for 16hrs and were then incubated in serum free media containing 20% CM or serum free media containing 20% $VEGF_{165}b$ CM (300pM). Cells were also incubated in 20% CM containing 1nM recombinant VEGF or both 1nM VEGF and 300pM $VEGF_{165}b$ protein. The amount of CM media used in each experiment was limited to 20% because CM was limited. Samples were treated for 4hrs then scraped into suspension within the same media and rolled for a further 4hrs and then assayed by the flow cytometer. The samples were run through a different protocol on the flow cytometer compared to that used in chapters 6 and 9 because these experiments were actually carried out first. The discriminator settings on the flow cytometer were changed after these experiments because the autofluorescence values were too high demonstrated by the "tails" in the AV regions (figure 10.5 A). The percentage of cells of the entire population stained with AV (i.e. met the criteria for apoptosis) may therefore have been overestimated in the scattergrams. These preliminary results however clearly demonstrated a difference in sub-populations between hCIPs serum starved in 20% CM and those treated with $VEGF_{165}b$, $VEGF_{165}$, and a combination of both at least in this one experiment. Interestingly, cells incubated with both $VEGF_{165}$/CM and $VEGF_{165}b$/CM appeared to have a lower percentage of cells that stained with AV alone (i.e.

met the criteria for apoptosis) than those incubated in serum free CM: Of the total cell population, 51.7% of cells stained with AV alone when treated with serum free CM, 0.4% stained with AV alone when treated with serum free CM containing $VEGF_{165}$, and 0% stained with AV alone when cells were incubated with serum free CM containing 300pM $VEGF_{165}b$ (figure 10.5, C). A combination of both isoforms resulted in a greater amount of cells staining for AV alone than either isoform by itself: Of the total cell population 10.8% of cells stained with AV alone when treated with serum free CM containing 1nM $VEGF_{165}$ plus 300pM $VEGF_{165}b$. In all treatments with VEGF isoforms there was an increase in the cell populations that picked up neither stain (i.e. met the criteria for viable cells) compared to cells that had been serum starved: Of the total cell population 36.5% of cells picked up neither stain when treated with serum free CM, 93.2% of cells picked up neither stain when treated with serum free CM containing $VEGF_{165}$, 84.9% of cells picked up neither stain when treated with serum free CM containing 300pM $VEGF_{165}b$ and 81.9% of cells picked up neither stain when treated with serum free CM containing 1nM $VEGF_{165}$ plus 300pM $VEGF_{165}b$. There was no obvious difference between the populations stained with PI alone or both PI and AV. These results suggest that $VEGF_{165}$ and $VEGF_{165}b$ can individually reduce apoptosis, although together act to reduce apoptosis to a lesser extent than individually.

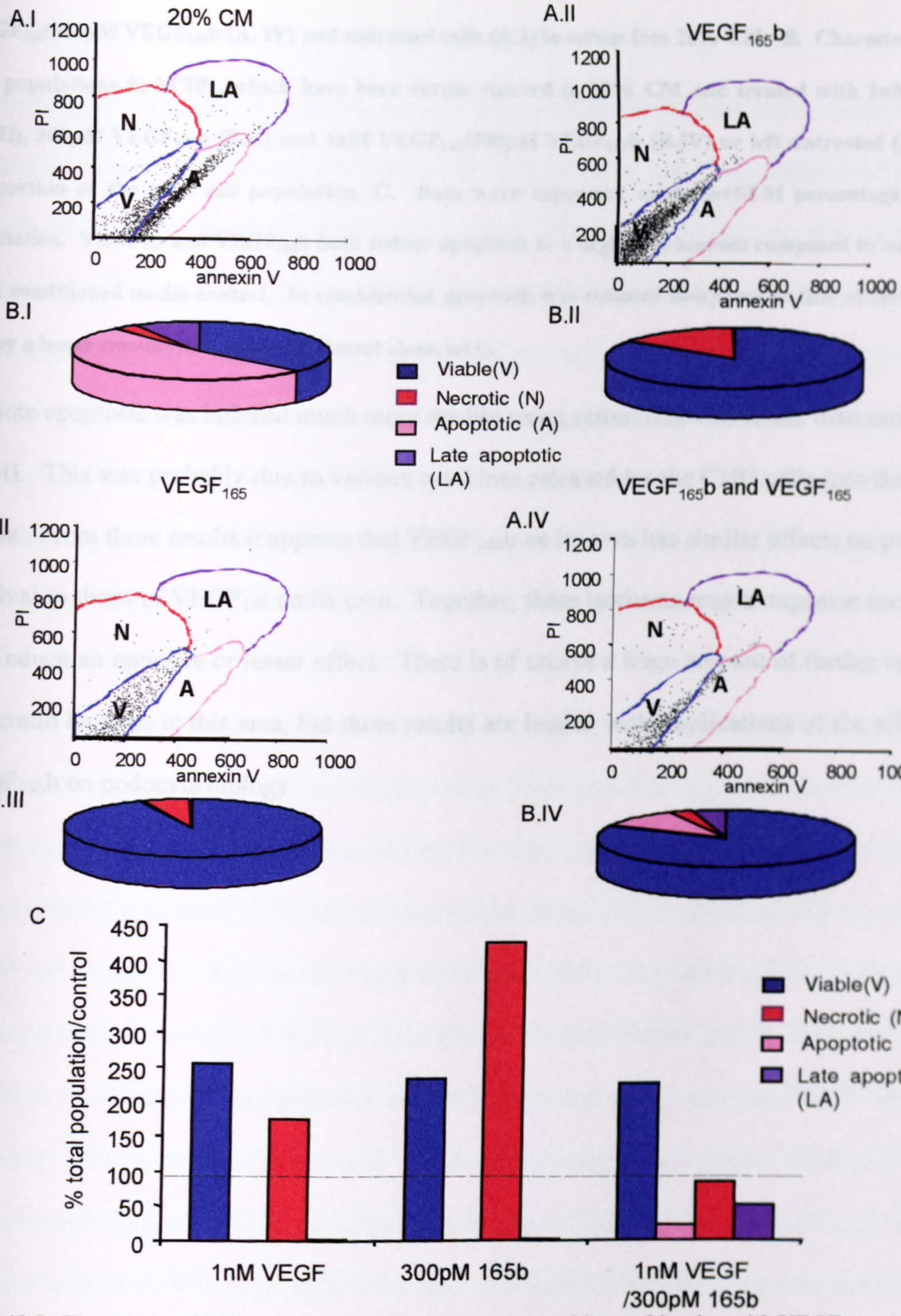

Figure 10.5. The effects of $VEGF_{165}b$ on apoptosis compared to and in combination with $VEGF_{165}$.

Differentiated hCIPs were serum starved for 16hrs and incubated in CM containing $VEGF_{165}b$ protein, CM containing recombinant $VEGF_{165}$ protein or CM with an empty $pcDNA_3$ vector for 4hrs. Cells were then scraped into suspension and rolled for a further 4 hrs before being assayed. A. Comparison of differences in sub-populations in hCIPs incubated in of 1nM VEGF (A.III), 300pM $VEGF_{165}b$ (A.II), 1nM

$VEGF_{165}$/300pM $VEGF_{165}$b (A. IV) and untreated cells (A.I) in serum free 20% CM. B. Characteristics of cell populations in hCIPs, which have been serum starved in 20% CM and treated with 1nM VEGF (B.III), 300pM $VEGF_{165}$b (B.II) and 1nM $VEGF_{165}$/300pM $VEGF_{165}$b (B.IV) or left untreated (B.I) as a proportion of the total cell population. C. Data were expressed as mean+SEM percentage of total population. $VEGF_{165}$ and $VEGF_{165}$b both reduce apoptosis to a negligible amount compared to serum free 20% conditioned media control. In combination apoptosis was reduced compared to that of the control, but by a lesser amount than either treatment alone, n=1).

Of note apoptosis was induced much more readily using serum free CM rather than serum free RPMI. This was probably due to various cytokines released by the CHO cells into the RPMI media. From these results it appears that $VEGF_{165}$b on its own has similar effects on podocyte survival to those of $VEGF_{165}$ on its own. Together, these isoforms may antagonise each other and induce an opposite or lesser effect. There is of course a huge amount of further research that could be done in this area, but these results are loaded with implications of the effects of $VEGF_{165}$b on podocyte biology.

10.4 Discussion

The effects of $VEGF_{165}$ on podocyte biology were previously studied in this thesis because podocytes express high levels of VEGF under physiological conditions (figure 1.5) despite little overt angiogenesis in the mature glomerulus. It had previously been thought that this VEGF expression was conventional $VEGF_{121}$, $VEGF_{165}$ and $VEGF_{189}$. The discovery that podocytes expressed a potentially anti-angiogenic isoform of VEGF - $VEGF_{165}b$ (Bates et al., 2002) possibly more abundantly than $VEGF_{165}$ has significant potential in so far as podocyte biology and function were concerned. Hence, the basic effects of $VEGF_{165}b$ on podocyte survival were determined and, more importantly, the effects of the two isoforms combined, in an attempt to decipher the role of VEGF production on podocyte biology.

$VEGF_{165}b$ protein production by podocytes had previously been shown by quantification using a pan-VEGF ELISA on media from differentiated podocytes that had been transfected with a $VEGF_{165}b$ siRNA match or mismatch siRNA (Cui et al., 2003). The expression of total VEGF was visualised compared to $VEGF_{165}b$ expression using western blotting with an anti-pan VEGF and an anti-$VEGF_{165}b$ specific antibody (figure 10.2). The $VEGF_{165}b$ blot shows bands of greater intensity than the $VEGF_{165}$ blot, despite the fact that the anti-$VEGF_{165}b$ antibody was used at a lower concentration (0.4µg/ml) compared to the anti pan-VEGF antibody (1µg/ml). This indicates that the anti-$VEGF_{165}b$ antibody has a greater binding affinity, therefore unfortunately $VEGF_{165}b$ cannot be expressed as a proportion of total VEGF. Multiple bands were seen in serum starved cell lysate isolated from two separate tissue culture flasks. This suggests the possibility that, apart from glycosylated products, monomers and dimers, the extra bands correspond to different length isoforms from full length $VEGF_{206}$ to $VEGF_{121}$. Bands of the same molecular weight were seen in the blots probed with anti-$VEGF_{165}b$ antibody, which, because the anti-$VEGF_{165}b$ antibody is specific to any VEGF

isoform with an amino acid sequence corresponding to exon 8b, suggests that for each VEGF isoform there is a sister $VEGF_{xxx}b$ isoform. This hypothesis was first postulated by Cui et al (Cui et al., 2003), but this is the first time it has been supported by experimental evidence. Densitometry analysis was carried out on these Western blots and was expressed as a percentage of intensity of band e in each lysate as an internal control. Interestingly, some bands had proportionately different intensities in the anti $VEGF_{xxx}b$ blot compared to the anti pan-VEGF blot. For example the intensity of bands a, b and c were much lower in the pan anti-VEGF blot whereas in the anti-$VEGF_{xxx}b$ blot the intensity of these bands were similar to that of band e. By corresponding the molecular weight of these bands to those in table 10.1, it appears that bands a, b and c are the VEGF monomers-$VEGF_{121}$ and $VEGF_{121}b$, $VEGF_{145}$ and $VEGF_{145}b$, and $VEGF_{165}$ and $VEGF_{165}b$. This suggests that $VEGF_{121}b$, $VEGF_{145}b$ and $VEGF_{165}b$ monomers are present in greater proportions compared to band e in cultured podocytes than their sister isoforms. The scope of VEGF research in podocytes is therefore far greater than just $VEGF_{165}$ and $VEGF_{165}b$ and these implications may stretch beyond podocytes to the rest of the VEGF expressing tissues in the human body.

Published work shows that $VEGF_{165}b$ inhibits the effects of $VEGF_{165}$ induced proliferation, migration and vasodilatation in endothelial cells, yet by itself induces no significant effect from serum starved cells (Bates et al., 2002). It was therefore surprising to see that $VEGF_{165}b$ could induce a dose dependent reduction in cytotoxicity in cultured podocytes. Firstly, because it was not known that $VEGF_{165}b$ was able to induce its own signalling effects and secondly because, if anything, it was expected that $VEGF_{165}b$ would have the opposite effect to that of $VEGF_{165}$. The effects of $VEGF_{165}b$ were surprisingly potent for the low concentrations used. It was yet more surprising to see that $VEGF_{165}b$ dose dependently inhibited the 1nM $VEGF_{165}$ induced reduction in cytotoxicity and, from a concentration of just

65pM, actually increased cytotoxicity in cultured podocytes (figure 10.4). When $VEGF_{165}b$ and $VEGF_{165}$ were used in combination in experiments, they were mixed prior to adding to the cells to avoid one isoform binding to the receptors more dominantly than the other. In endothelial cells $VEGF_{165}b$ competitively binds VEGF-R2, yet it does not initiate the normal signalling pathways that $VEGF_{165}$ does (Woolard et al, Cancer Research, in press). The effects of $VEGF_{165}b$ on VEGF-R1 and VEGF-R3 signalling have not yet been studied in endothelial cells, but the effects may well be different to VEGF-R2. It is not surprising then, that $VEGF_{165}b$ had a different effect on signalling in podocytes than on endothelial cells. It is not known whether $VEGF_{165}b$ binds VEGF-R1 homodimers, or VEGF-R1/VEGF-R3 heterodimers in podocytes. In theory, $VEGF_{165}b$ signalling should be enhanced by Np-1 in podocytes, because VEGF isoforms that contain an amino acid sequence corresponding to exon 7, including $VEGF_{165}b$, are able to bind Np-1 (Soker et al., 1997). The dynamics of VEGF-R3 and Np-2 on functional $VEGF_{165}b$ signalling cannot be predicted at this point but may be involved in podocyte signalling. In endothelial cells $VEGF_{165}b$ homodimers competitively bind to VEGF-R2 (Woolard et al, Cancer Research, submitted). They may also competitively bind to VEGF-R1 or VEGF-R1/VEGF-R3 complexes in podocytes, which would inhibit the effects of $VEGF_{165}$. $VEGF_{165}b$, however, induces a reduction in cytotoxicity in podocytes, which suggests that it may be the receptor to which $VEGF_{165}b$ binds that determines whether $VEGF_{165}b$ has any signalling effects and not the protein itself. Indeed $VEGF_{165}b$ may be the ligand for VEGF-R1. It is interesting to note that VEGF-R1 binds $VEGF_{165}$ with a much greater binding affinity than VEGF-R2 (Neufeld et al., 1999) and if $VEGF_{165}b$ is signalling mainly through VEGF-R1 in podocytes then this may explain the differences seen in response to $VEGF_{165}b$ in endothelial cells. In general VEGF biology it could be postulated that $VEGF_{165}b$ binds VEGF-R1, but that $VEGF_{165}$ competes for the same receptor just as $VEGF_{165}$ binds VEGF-R2, but $VEGF_{165}b$ also competes for the same receptor.

The amino acid sequence corresponding to exon 8 has a proline bond, resulting in a putative kink, which the amino acid sequence corresponding to exon 8b lacks and this may effect protein stability and also conformation of the $VEGF_{165}b$ protein (Bates et al., 2002) (see figure 10.1B). This amino acid "kink" may be utilised in different ways in different receptor binding. The antagonistic effect of $VEGF_{165}b$ on $VEGF_{165}$ in podocytes cannot be due to competitive inhibition as in endothelial cells, otherwise the same effects would be seen as $VEGF_{165}b$ binding alone. The results point to an interaction between the two proteins. In future the purified protein of the two isoforms should be used at the same concentrations to compare the binding affinities. The comparison of effects of $VEGF_{165}b$ protein in CM with purified human recombinant $VEGF_{165}$ protein on podocytes is not ideal. The source of $VEGF_{165}$ protein should have been the same as for $VEGF_{165}b$, and many extraneous variables were probably introduced as a consequence. These experiments should therefore be repeated with purified, recombinant $VEGF_{165}b$, which has become available within the last few weeks, to confirm that the results are the same.

Preliminary apoptosis assay data shows a similar trend of effects of $VEGF_{165}b$ on apoptosis. $VEGF_{165}b$ massively reduced the serum free CM induced apoptosis in hCIPs as did $VEGF_{165}$, together however, although apoptosis was still reduced compared to control it was increased compared to $VEGF_{165}b$ alone (figure 10.5). These results demonstrate that on its own $VEGF_{165}b$ has a similar effect to $VEGF_{165}$ on survival in podocytes, but together $VEGF_{165}b$ may antagonise the effects of $VEGF_{165}$ on apoptosis. The likelihood is that, *in vivo* both isoforms are expressed simultaneously but not in equal proportions. The effects of the isoforms may well depend on the balance between the two. It would be interesting to see the effect of purified human recombinant $VEGF_{165}b$ protein in the same assay, but in RPMI media not CM, which contains many extraneous variables that cannot be controlled. $VEGF_{165}$

protein was used at a higher concentration than $VEGF_{165}b$ protein because $VEGF_{165}b$ appears to be more potent than $VEGF_{165}$ protein, and $VEGF_{165}b$ protein could not be produced at a concentration of 1nM.

It is hard to draw conclusions from these results to reflect physiological effects because there is not yet enough known about $VEGF_{165}$ or $VEGF_{165}b$ protein production in differentiated podocytes. This data is vital as the ratio of the two isoforms will probably determine the actual effect. These results do give a glimpse of the complexity of interactions involved in VEGF signalling in podocytes and opens up a new area of research. The Results shown in figure 10.1 were published in paper 4 of the list of papers arising from this work.

Chapter 11

Discussion

11.1 Discussion

The purpose of this investigation was to test the hypothesis that VEGF can act in an autocrine manner in cultured podocytes promoting survival through phosphorylation of nephrin and a reduction in apoptosis. The interaction of VEGF and nephrin could have been hypothesised because, even though nephrin expression is limited outside of the kidney, it is co-localised with VEGF in more than one organ. For example; VEGF is expressed by the endocrine cells of the Islets of Langerhans, within the pancreas, and VEGF-R1 and VEGF-R2 are expressed by the endothelial-like β-cells (Christofori et al., 1995). Nephrin is also expressed by the β-cells of the Islets of Langerhans, on which VEGF is known to act (Palmen et al., 2001). The role of nephrin in the pancreas is not yet known, although it has been speculated that it is involved in β-cell-cell junctions (Palmen et al., 2001), hence it is not known if VEGF induces nephrin mediated signalling in the pancreas. VEGF, VEGF-R1 and VEGF-R2 are expressed in Leydig cell and Sertoli cells in the testis (Ergun et al., 1997). Nephrin is also expressed by the Sertoli cells, which form a parallel array of tight junctions, of which nephrin is thought to form a part and constitute the blood-testis barrier (Liu et al., 2001). It is unknown whether VEGF can induce nephrin mediated signalling in these cells either, but VEGF induced nephrin mediated signalling in podocytes outlines a role for VEGF-nephrin interactions in other organs.

The evidence from this investigation suggests that $VEGF_{165}$ and VEGF-C promote the survival of cultured podocytes. $VEGF_{165}$ (and presumably $VEGF_{165}b$) are likely to interact with VEGF-R1. There is also the possibly that VEGF receptor complexes form at the plasma membrane of cultured podocytes involving VEGF-R3 and/or Np-1 and/or Np-2. VEGF-C is thought to interact with VEGF-R3, again possibly complexed with Np-2 and/or VEGF-R1 and/or Np-1. VEGF receptor auto-phosphorylation by $VEGF_{165}$ induced the phosphorylation

of nephrin either directly or indirectly. The extent of involvement of PI3-Kinase in VEGF mediated survival signalling is not yet known, although the evidence is contrary to the involvement of AKT phosphorylation. It is possible that the time course chosen for VEGF treatment in the AKT phosphorylation assay was not optimal and that an increase in AKT phosphorylation may have been missed. It would be interesting to investigate levels of basal AKT phosphorylation in unstarved cultured podocytes because these may be significantly greater than those seen in serum starved cultured podocytes. These experiments will be carried out at a future date. The signalling cascade induced by $VEGF_{165}$ resulted in a reduction in cytotoxicity due to a reduction in apoptosis. The auto-phosphorylation of VEGF receptors by VEGF-C (most likely VEGF-R3) stimulated a signalling cascade, which induced a reduction in MAPK phosphorylation and the phosphorylation of nephrin. VEGF-C treatment also resulted in a reduction in cytotoxicity. It would also be interesting to investigate levels of basal MAPK phosphorylation in unstarved cultured podocytes because these may be significantly greater than those seen in serum starved cultured podocytes and may explain the unpredicted response to VEGF-C. In summary $VEGF_{165}$ and VEGF-C therefore seem to promote survival via different signalling pathways in podocytes.

There is still a large amount of research though that could be done to clarify the precise signalling pathways involved. The concept of VEGF signalling in podocytes is very complex, especially when *all isoforms of VEGF*, VEGF receptors and VEGF-C function are considered. It is important to form a concept that considers all of these components, and apply it to the entire glomerulus.

11.1.1 Physiological Relevance

Terminally differentiated podocytes in healthy, mature glomeruli must be maintained because their turnover is so low and risk factors associated with podocyte loss are so high. The findings of this investigation suggest the possibility, *in vivo*, for VEGF to promote podocyte survival. VEGF is expressed throughout glomerulogenesis and in the mature glomerulus by podocytes (Simon et al., 1995). It is generally accepted that VEGF plays a paracrine role in vascularisation during glomerulogenesis (Simon et al., 1995) (Saxen and Sariola, 1987) and is also known that VEGF plays a paracrine role in the mature glomerulus (Eremina et al., 2003). The role of VEGF though is different during development than in maturity *in vivo*. During development (glomerulogenesis) VEGF effects follow an established route for VEGF signalling, such as inducing proliferation, migration and angiogenesis of endothelial cells (Wu et al., 2000), (Ilan et al., 1998). At maturity, however, VEGF is thought to maintain the entire filtration barrier (Simon et al., 1995), (Eremina et al., 2003) including, as suggested by evidence from work in this investigation, podocytes. The change in the role of VEGF *in vivo* appears to be clarified by the discovery that differentiated, cultured podocytes express $VEGF_{165}b$ (Cui et al., 2003)- an anti-angiogenic isoform of VEGF in endothelial cells (Bates et al., 2002) and de-differentiated cultured podocytes do not (Cui et al., 2003). It is possible that there is a splicing switch between $VEGF_{165}$, the isoform that is able to mediate all of the VEGF induced events observed during glomerulogenesis, and $VEGF_{165}b$, the isoform expressed in differentiated cultured podocytes, at podocyte differentiation in maturing glomeruli (*in vivo*). The results from chapter 10 showing the effects of $VEGF_{165}b$ on cultured podocytes (figures 10.3-10.5) supported this hypothesis. On its own $VEGF_{165}b$ appeared to have the same effects as $VEGF_{165}$ on podocyte survival. Assuming that $VEGF_{165}b$ has the same effect on glomerular endothelial cells, *in vivo* as it does on other vascular endothelial cells (Bates et al., 2002) this would have no significant consequence on signalling in

glomerular endothelial cells. If $VEGF_{165}b$ were not expressed during glomerulogenesis then the effects of $VEGF_{165}$ would not be hindered. Complications arise, however, with the simultaneous expression of $VEGF_{165}$ and $VEGF_{165}b$ *in vivo*. According to Cui et al, $VEGF_{165}b$ mRNA is not expressed by proliferating, de-differentiated PCPs (with characteristics relating to immature podocytes *in vivo*), but it is possible that $VEGF_{165}$ is expressed in low levels by differentiated podocytes (with characteristics relating to mature podocytes *in vivo*) (Cui et al., 2003). According to the results describing the effects of $VEGF_{165}b$ with $VEGF_{165}$ on podocytes (chapter 10, figures 10.3-10.4) this would induce an increase in cytotoxicity due to an unknown interaction of the two isoforms. If this were the case *in vivo* then podocytes would die under normal conditions, which is not the case. This suggests that of the two VEGF isoforms $VEGF_{165}b$ expression dominates at maturity. If the splicing switch of the isoforms were at the time of podocyte differentiation this would explain a massive amount of podocyte death seen in culture when podocytes are thermo-switched to induce differentiation. This may also be applicable *in vivo* when podocytes begin to differentiate because there would probably be an overproduction of immature podocytes, whilst they were still proliferative. When podocytes differentiate *in vivo* they take up a lot more capillary surface area and hence there may not be enough space for all of the podocytes to differentiate. An increase in apoptosis, due to the temporary presence of both VEGF isoforms, would therefore decrease podocyte number surplus to requirement. It is vital to investigate whether $VEGF_{165}b$ is solely expressed *in vivo* at maturity, post-differentiation, to fully understand the effects of physiological effects of $VEGF_{165}b$.

The VEGF family of proteins in the mature glomerulus are undoubtedly part of a complex feedback system of growth factors and natural inhibitors controlling angiogenesis, permeability, survival and maintenance of the glomerular filtration barrier. Without knowing

the physiological expression levels of all of these proteins and how they relate to each other it is very hard to predict the effect of individual growth factors, but it seems likely that imbalance in this system may contribute to the progression of glomerular disease.

11.1.2 Pathological relevance

VEGF has been implicated in many types of renal disease. In the past authors have tried to generalise glomerular VEGF expression to renal disease, but there have been many conflicting reports. This is probably because VEGF can induce an effect in glomerular endothelial cells, mesangial cells and podocytes, therefore a change in VEGF expression may have a different effect depending on which cell type is being studied. The type of renal disease may also affect VEGF expression and of course the effect of VEGF will change depending on whether $VEGF_{165}$ or $VEGF_{165}b$ is being investigated. The key to protection of the glomerulus from many glomerular diseases may be to protect the mature state of the glomerulus. $VEGF_{165}b$ expression is switched to that of $VEGF_{165}$ in renal carcinomas (Bates et al., 2002), making it a more exaggerated, developmental environment. The expression of podocyte VEGF receptors in disease states has not yet been considered in detail in the literature, but this is another variable that would affect VEGF signalling in the glomerulus. The state of the cells in pathology also needs to be considered. They may lose their function under sclerotic conditions, therefore levels of VEGF expression may change during the course of some diseases. Finally, the effects of VEGF need to be considered as part of an entire system within the glomerulus, particularly with expression of angiopoietins and their receptors.

11.1.3 Future work

11.1.3.1 $VEGF_{165}b$ expression in the glomerulus

Future considerations as a result of this investigation should be channelled into confirming $VEGF_{165}b$ expression and function in mature podocytes. Firstly, confirmation of sole expression of *$VEGF_{165}b$ at maturity* would ensure that investigations could concentrate on the effects of $VEGF_{165}b$ on podocyte biology, rather than a combination of *$VEGF_{165}$ and* $VEGF_{165}b$ isoforms. This would be carried out using a primer designed specifically towards VEGF exon 8b, together with a primer designed towards VEGF exon 8a against cDNA reverse transcribed from mRNA extracted from both hCIPs and human isolated glomeruli. The splicing switch from $VEGF_{165}$ to $VEGF_{165}b$ at differentiation could also be confirmed by investigating the semi-quantitative expression of both isoforms throughout hCIP differentiation, from 33°C to 14 days at 37°C by PCR. It would be interesting to examine whether in diseased glomerular tissue the same splicing switch is seen as with renal carcinomas..

11.1.3.2 Interaction of VEGF with its receptors on podocytes

A lot of the assumptions made on VEGF signalling in podocytes is based on speculation of VEGF-VEGF receptor interaction and receptor hetero- and homo-dimerization. These interactions need to be clarified, and may be best studied in cells that do not normally express VEGF or its receptors, such as CHO cells. Each receptor could be transfected by itself and the interactions with $VEGF_{165}$ and $VEGF_{165}b$ studied using immunoprecipitation techniques. The receptors could then be double transfected under different combinations and their interactions re-evaluated. Once preliminary data has been collected using an artificial system then interactions could be examined in cultured podocytes. This could be done, again, using

immunoprecipitation studies. When it has been established which receptors are involved in VEGF binding to podocytes, then the signalling pathways could be clarified further.

11.1.3.3 VEGF-C and $VEGF_{165}b$ function in podocytes

Examination of the effects of VEGF-C and $VEGF_{165}b$ in cultured podocytes has only just begun. The signalling pathways should be studied in full, along the same lines as with the $VEGF_{165}$ studies. Once these studies have been carried out then their function within the glomerular system should then be considered.

11.1.3.4 Application of hypothesis in vivo

There has been a lot of speculation made from the results of this investigation in application to physiology and pathology yet the results were obtained from an *in vitro* culture system. Therefore, experiments should be carried out to confirm that the same happens *in vivo* as *in vitro*. The simplest way of approaching this initially would be using an *ex vivo* system, namely isolated human glomeruli. Immunoprecipitation studies examining VEGF effects on nephrin phosphorylation would go a long way in confirming that VEGF promotes survival in podocytes *in vivo* via a nephrin mediated reduction in apoptosis. Various apoptosis methods could also be applied to glomeruli as a whole, including DNA fragmentation (ladder) detection and examination of cleaved caspase proteins using confocal microscopy in conjunction with an antibody towards a podocyte specific protein or Western Blotting.

Bibliography

(2001). DoH Mortality Statistics HMSO.

AIELLO, L. P. and WONG, J. S. (2000). Role of vascular endothelial growth factor in diabetic vascular complications. *Kidney Int Suppl.* **77,** S113-9.

ANTONETTI, D. A.,BARBER, A. J.,HOLLINGER, L. A.,WOLPERT, E. B. and GARDNER, T. W. (1999). Vascular endothelial growth factor induces rapid phosphorylation of tight junction proteins occludin and zonula occluden 1. A potential mechanism for vascular permeability in diabetic retinopathy and tumors. *J Biol Chem.* **274,** 23463-7.

ASANUMA, K.,SHIRATO, I.,ISHIDOH, K.,KOMINAMI, E. and TOMINO, Y. (2002). Selective modulation of the secretion of proteinases and their inhibitors by growth factors in cultured differentiated podocytes. *Kidney Int.* **62,** 822-31.

BACHELDER, R. E.,CRAGO, A.,CHUNG, J.,WENDT, M. A.,SHAW, L. M.,ROBINSON, G. and MERCURIO, A. M. (2001). Vascular endothelial growth factor is an autocrine survival factor for neuropilin-expressing breast carcinoma cells. *Cancer Res.* **61,** 5736-40.

BAILEY, E.,HARPER, S. J.,PRINGLE, J. H.,BAKER, F.,FURNESS, P. N.,SALANT, D. J. and FEEHALLY, J. (1998). Visceral glomerular epithelial cell DNA synthesis in experimental and human membranous disease. *Exp Nephrol.* **6,** 352-8.

BAILEY, E.,BOTTOMLEY, M. J.,WESTWELL, S.,PRINGLE, J. H.,FURNESS, P. N.,FEEHALLY, J.,BRENCHLEY, P. E. and HARPER, S. J. (1999). Vascular endothelial growth factor mRNA expression in minimal change, membranous, and diabetic nephropathy demonstrated by non-isotopic in situ hybridisation. *J Clin Pathol.* **52,** 735-8.

BARISONI, L.,MOKRZYCKI, M.,SABLAY, L.,NAGATA, M.,YAMASE, H. and MUNDEL, P. (2000). Podocyte cell cycle regulation and proliferation in collapsing glomerulopathies. *Kidney Int.* **58,** 137-43.

BARLEON, B.,SOZZANI, S.,ZHOU, D.,WEICH, H. A.,MANTOVANI, A. and MARME, D. (1996). Migration of human monocytes in response to vascular endothelial growth factor (VEGF) is mediated via the VEGF receptor flt-1. *Blood.* **87,** 3336-43.

BARLETTA, G. M.,KOVARI, I. A.,VERMA, R. K.,KERJASCHKI, D. and HOLZMAN, L. B. (2003). Nephrin and Neph1 co-localize at the podocyte foot process intercellular junction and form cis hetero-oligomers. *J Biol Chem.* **278,** 19266-71. Epub 2003 Mar 19.

BATES, D. O. and CURRY, F. E. (1997). Vascular endothelial growth factor increases microvascular permeability via a Ca(2+)-dependent pathway. *Am J Physiol.* **273,** H687-94.

BATES, D. O.,LODWICK, D. and WILLIAMS, B. (1999). Vascular endothelial growth factor and microvascular permeability. *Microcirculation.* **6,** 83-96.

BATES, D. O.,CUI, T. G.,DOUGHTY, J. M.,WINKLER, M.,SUGIONO, M.,SHIELDS, J. D.,PEAT, D.,GILLATT, D. and HARPER, S. J. (2002). VEGF165b, an inhibitory splice variant of vascular endothelial growth factor, is down-regulated in renal cell carcinoma. *Cancer Res.* **62,** 4123-31.

BENIGNI, A.,TOMASONI, S.,GAGLIARDINI, E.,ZOJA, C.,GRUNKEMEYER, J. A.,KALLURI, R. and REMUZZI, G. (2001). Blocking angiotensin II synthesis/activity preserves glomerular nephrin in rats with severe nephrosis. *J Am Soc Nephrol.* **12,** 941-8.

BONNI, A.,BRUNET, A.,WEST, A. E.,DATTA, S. R.,TAKASU, M. A. and GREENBERG, M. E. (1999). Cell survival promoted by the Ras-MAPK signaling pathway by transcription-dependent and -independent mechanisms. *Science.* **286,** 1358-62.

BORTNER, C. D. and CIDLOWSKI, J. A. (2002). Cellular mechanisms for the repression of apoptosis. *Annu Rev Pharmacol Toxicol.* **42,** 259-81.

BOUTE, N.,GRIBOUVAL, O.,ROSELLI, S.,BENESSY, F.,LEE, H.,FUCHSHUBER, A.,DAHAN, K.,GUBLER, M. C.,NIAUDET, P. and ANTIGNAC, C. (2000). NPHS2, encoding the

glomerular protein podocin, is mutated in autosomal recessive steroid-resistant nephrotic syndrome. *Nat Genet.* **24,** 349-54.

BROCK, T. A.,DVORAK, H. F. and SENGER, D. R. (1991). Tumor-secreted vascular permeability factor increases cytosolic Ca2+ and von Willebrand factor release in human endothelial cells. *Am J Pathol.* **138,** 213-21.

BUNIATIAN, G.,GEBHARDT, R.,TRAUB, P.,MECKE, D. and OSSWALD, H. (1999). Dynamics of glial fibrillary acidic protein distribution in cultured glomerular podocytes and mesangial cells of the rat kidney. *Biol Cell.* **91,** 675-84.

CANDIANO, G.,MUSANTE, L.,CARRARO, M.,FACCINI, L.,CAMPANACCI, L.,ZENNARO, C.,ARTERO, M.,GINEVRI, F.,PERFUMO, F.,GUSMANO, R. and GHIGGERI, G. M. (2001). Apolipoproteins prevent glomerular albumin permeability induced in vitro by serum from patients with focal segmental glomerulosclerosis. *J Am Soc Nephrol.* **12,** 143-50.

CAULFIELD, J. P.,REID, J. J. and FARQUHAR, M. G. (1976). Alterations of the glomerular epithelium in acute aminonucleoside nephrosis. Evidence for formation of occluding junctions and epithelial cell detachment. *Lab Invest.* **34,** 43-59.

CHOU, M. T.,WANG, J. and FUJITA, D. J. (2002). Src kinase becomes preferentially associated with the VEGFR, KDR/Flk-1, following VEGF stimulation of vascular endothelial cells. *BMC Biochem.* **3,** 32.

CHRISTOFORI, G.,NAIK, P. and HANAHAN, D. (1995). Vascular endothelial growth factor and its receptors, flt-1 and flk-1, are expressed in normal pancreatic islets and throughout islet cell tumorigenesis. *Mol Endocrinol.* **9,** 1760-70.

CRISCUOLO, G. R. and BALLEDUX, J. P. (1996). Clinical neurosciences in the decade of the brain: hypotheses in neuro-oncology. VEG/PF acts upon the actin cytoskeleton and is inhibited by dexamethasone: relevance to tumor angiogenesis and vasogenic edema. *Yale J Biol Med.* **69,** 337-55.

CRISCUOLO, G. R.,LELKES, P. I.,ROTROSEN, D. and OLDFIELD, E. H. (1989). Cytosolic calcium changes in endothelial cells induced by a protein product of human gliomas containing vascular permeability factor activity. *J Neurosurg.* **71,** 884-91.

CUI, T. G.,FOSTER, R. R.,SALEEM, M. A.,MATHIESON, P. W.,GILLATT, D. A.,BATES, D. O. and HARPER, S. J. (2003). Differentiated human podocytes endogenously express an inhibitory isoform of vascular endothelial growth factor (VEGF165b) mRNA and protein. *Am J Physiol Renal Physiol.* **25,** 25

DEEN, W. M.,LAZZARA, M. J. and MYERS, B. D. (2001). Structural determinants of glomerular permeability. *Am J Physiol Renal Physiol.* **281,** F579-96.

DIXELIUS, J.,MAKINEN, T.,WIRZENIUS, M.,KARKKAINEN, M. J.,WERNSTEDT, C.,ALITALO, K. and CLAESSON-WELSH, L. (2003). Ligand-induced vascular endothelial growth factor receptor-3 (VEGFR-3) heterodimerization with VEGFR-2 in primary lymphatic endothelial cells regulates tyrosine phosphorylation sites. *J Biol Chem.* **278,** 40973-9. Epub 2003 Jul 24.

DONOVIEL, D. B.,FREED, D. D.,VOGEL, H.,POTTER, D. G.,HAWKINS, E.,BARRISII, J. P.,MATHUR, B. N.,TURNER, C. A.,GESKE, R.,MONTGOMERY, C. A.,STARBUCK, M.,BRANDT, M.,GUPTA, A.,RAMIREZ-SOLIS, R.,ZAMBROWICZ, B. P. and POWELL, D. R. (2001). Proteinuria and perinatal lethality in mice lacking NEPH1, a novel protein with homology to NEPHRIN. *Mol Cell Biol.* **21,** 4829-36.

DOUBLIER, S.,SALVIDIO, G.,LUPIA, E.,RUOTSALAINEN, V.,VERZOLA, D.,DEFERRARI, G. and CAMUSSI, G. (2003). Nephrin expression is reduced in human diabetic nephropathy: evidence for a distinct role for glycated albumin and angiotensin II. *Diabetes.* **52,** 1023-30.

DOUBLIER, S.,RUOTSALAINEN, V.,SALVIDIO, G.,LUPIA, E.,BIANCONE, L.,CONALDI, P. G.,REPONEN, P.,TRYGGVASON, K. and CAMUSSI, G. (2001). Nephrin redistribution on

podocytes is a potential mechanism for proteinuria in patients with primary acquired nephrotic syndrome. *Am J Pathol.* **158,** 1723-31.

DRENCKHAHN, D. and FRANKE, R. P. (1988). Ultrastructural organization of contractile and cytoskeletal proteins in glomerular podocytes of chicken, rat, and man. *Lab Invest.* **59,** 673-82.

DURVASULA, R. V.,PETERMANN, A. T.,HIROMURA, K.,BLONSKI, M.,PIPPIN, J.,MUNDEL, P.,PICHLER, R.,GRIFFIN, S.,COUSER, W. G. and SHANKLAND, S. J. (2004). Activation of a local tissue angiotensin system in podocytes by mechanical strain. *Kidney Int.* **65,** 30-9.

DUSTIN, M. L.,OLSZOWY, M. W.,HOLDORF, A. D.,LI, J.,BROMLEY, S.,DESAI, N.,WIDDER, P.,ROSENBERGER, F.,VAN DER MERWE, P. A.,ALLEN, P. M. and SHAW, A. S. (1998). A novel adaptor protein orchestrates receptor patterning and cytoskeletal polarity in T-cell contacts. *Cell.* **94,** 667-77.

EFERL, R. and WAGNER, E. F. (2003). AP-1: a double-edged sword in tumorigenesis. *Nat Rev Cancer.* **3,** 859-68.

EREMINA, V.,SOOD, M.,HAIGH, J.,NAGY, A.,LAJOIE, G.,FERRARA, N.,GERBER, H. P.,KIKKAWA, Y.,MINER, J. H. and QUAGGIN, S. E. (2003). Glomerular-specific alterations of VEGF-A expression lead to distinct congenital and acquired renal diseases. *J Clin Invest.* **111,** 707-16.

ERGUN, S.,KILIC, N.,FIEDLER, W. and MUKHOPADHYAY, A. K. (1997). Vascular endothelial growth factor and its receptors in normal human testicular tissue. *Mol Cell Endocrinol.* **131,** 9-20.

FAKHARI, M.,PULLIRSCH, D.,ABRAHAM, D.,PAYA, K.,HOFBAUER, R.,HOLZFEIND, P.,HOFMANN, M. and AHARINEJAD, S. (2002). Selective upregulation of vascular

endothelial growth factor receptors neuropilin-1 and -2 in human neuroblastoma. *Cancer.* **94,** 258-63.

FEEST, T. G.,RIAD, H. N.,COLLINS, C. H.,GOLBY, M. G.,NICHOLLS, A. J. and HAMAD, S. N. (1990). Protocol for increasing organ donation after cerebrovascular deaths in a district general hospital. *Lancet.* **335,** 1133-5.

FENG, Y.,VENEMA, V. J.,VENEMA, R. C.,TSAI, N. and CALDWELL, R. B. (1999). VEGF induces nuclear translocation of Flk-1/KDR, endothelial nitric oxide synthase, and caveolin-1 in vascular endothelial cells. *Biochem Biophys Res Commun.* **256,** 192-7.

FERRARA, N. (2001). Role of vascular endothelial growth factor in regulation of physiological angiogenesis. *Am J Physiol Cell Physiol.* **280,** C1358-66.

FERRARA, N.,CARVER-MOORE, K.,CHEN, H.,DOWD, M.,LU, L.,O'SHEA, K. S.,POWELL-BRAXTON, L.,*HILLAN, K. J. and* MOORE, M. W. (1996). Heterozygous embryonic lethality induced by targeted inactivation of the VEGF gene. *Nature. 380, 439-42.*

FLOEGE, J.,JOHNSON, R. J.,ALPERS, C. E.,FATEMI-NAINIE, S.,RICHARDSON, C. A.,GORDON, K. and COUSER, W. G. (1993). Visceral glomerular epithelial cells can proliferate in vivo and synthesize platelet-derived growth factor B-chain. *Am J Pathol.* **142,** 637-50.

FORNONI, A.,LI, H.,FOSCHI, A.,STRIKER, G. E. and STRIKER, L. J. (2001). Hepatocyte growth factor, but not insulin-like growth factor I, protects podocytes against cyclosporin A-induced apoptosis. *Am J Pathol.* **158,** 275-80.

FORSTREUTER, F.,LUCIUS, R. and MENTLEIN, R. (2002). Vascular endothelial growth factor induces chemotaxis and proliferation of microglial cells. *J Neuroimmunol.* **132,** 93-8.

FUJIO, Y.,GUO, K.,MANO, T.,MITSUUCHI, Y.,TESTA, J. R. and WALSH, K. (1999). Cell cycle withdrawal promotes myogenic induction of Akt, a positive modulator of myocyte survival. *Mol Cell Biol.* **19,** 5073-82.

GASSLER, N.,ELGER, M.,KRANZLIN, B.,KRIZ, W.,GRETZ, N.,HAIINEL, B.,HOSSER, H. and HARTMANN, I. (2001). Podocyte injury underlies the progression of focal segmental glomerulosclerosis in the fa/fa Zucker rat. *Kidney Int.* **60,** 106-16.

GERBER, H. P.,DIXIT, V. and FERRARA, N. (1998a). Vascular endothelial growth factor induces expression of the antiapoptotic proteins Bcl-2 and A1 in vascular endothelial cells. *J Biol Chem.* **273,** 13313-6.

GERBER, H. P.,MCMURTREY, A.,KOWALSKI, J.,YAN, M.,KEYT, B. A.,DIXIT, V. and FERRARA, N. (1998b). Vascular endothelial growth factor regulates endothelial cell survival through the phosphatidylinositol 3'-kinase/Akt signal transduction pathway. Requirement for Flk-1/KDR activation. *J Biol Chem.* **273,** 30336-43.

GERBER, H. P.,MALIK, A. K.,SOLAR, G. P.,SHERMAN, D.,LIANG, X. H.,MENG, G.,HONG, K.,MARSTERS, J. C. and FERRARA, N. (2002). VEGF regulates haematopoietic stem cell survival by an internal autocrine loop mechanism. *Nature.* **417,** 954-8.

GERKE, P.,HUBER, T. B.,SELLIN, L.,BENZING, T. and WALZ, G. (2003). Homodimerization and Heterodimerization of the Glomerular Podocyte Proteins Nephrin and NEPH1. *J Am Soc Nephrol.* **14,** 918-26.

GIGER, R. J.,URQUHART, E. R.,GILLESPIE, S. K.,LEVENGOOD, D. V.,GINTY, D. D. and KOLODKIN, A. L. (1998). Neuropilin-2 is a receptor for semaphorin IV: insight into the structural basis of receptor function and specificity. *Neuron.* **21,** 1079-92.

GILLE, H.,KOWALSKI, J.,LI, B.,LECOUTER, J.,MOFFAT, B.,ZIONCHECK, T. F.,PELLETIER, N. and FERRARA, N. (2001). Analysis of biological effects and signaling properties of Flt-1 (VEGFR-1) and KDR (VEGFR-2). A reassessment using novel receptor-specific vascular endothelial growth factor mutants. *J Biol Chem.* **276,** 3222-30. Epub 2000 Oct 31.

GLUZMAN-POLTORAK, Z.,COHEN, T.,SHIBUYA, M. and NEUFELD, G. (2001). Vascular endothelial growth factor receptor-1 and neuropilin-2 form complexes. *J Biol Chem.* **276,** 18688-94. Epub 2001 Mar 14.

GOGVADZE, V.,ROBERTSON, J. D.,ZHIVOTOVSKY, B. and ORRENIUS, S. (2001). Cytochrome c release occurs via Ca2+-dependent and Ca2+-independent mechanisms that are regulated by Bax. *J Biol Chem.* **276,** 19066-71. Epub 2001 Mar 22.

GRATTON, J. P.,MORALES-RUIZ, M.,KUREISHI, Y.,FULTON, D.,WALSH, K. and SESSA, W. C. (2001). Akt down-regulation of p38 signaling provides a novel mechanism of vascular endothelial growth factor-mediated cytoprotection in endothelial cells. *J Biol Chem.* **276,** 30359-65. Epub 2001 May 31.

GRIFFIN, S. V.,PETERMANN, A. T.,DURVASULA, R. V. and SHANKLAND, S. J. (2003). Podocyte proliferation and differentiation in glomerular disease: role of cell-cycle regulatory proteins. *Nephrol Dial Transplant.* **18,** vi8-13.

GROSS, A.,MCDONNELL, J. M. and KORSMEYER, S. J. (1999). BCL-2 family members and the mitochondria in apoptosis. *Genes Dev.* **13,** 1899-911.

HARPER, S. J.,XING, C. Y.,WHITTLE, C.,PARRY, R.,GILLATT, D.,PEAT, D. and MATHIESON, P. W. (2001). Expression of neuropilin-1 by human glomerular epithelial cells in vitro and in vivo. *Clin Sci (Lond).* **101,** 439-46.

HOLZMAN, L. B.,ST JOHN, P. L.,KOVARI, I. A.,VERMA, R.,HOLTHOFER, H. and ABRAHAMSON, D. R. (1999). Nephrin localizes to the slit pore of the glomerular epithelial cell. *Kidney Int.* **56,** 1481-91.

HUBER, T. B.,KOTTGEN, M.,SCHILLING, B.,WALZ, G. and BENZING, T. (2001). Interaction with podocin facilitates nephrin signaling. *J Biol Chem.* **276,** 41543-6.

HUBER, T. B.,SCHMIDTS, M.,GERKE, P.,SCHERMER, B.,ZAHN, A.,HARTLEBEN, B.,SELLIN, L.,WALZ, G. and BENZING, T. (2003a). The carboxyl terminus of Neph family

members binds to the PDZ domain protein zonula occludens-1. *J Biol Chem.* **278,** 13417-21. Epub 2003 Feb 10.

HUBER, T. B.,SIMONS, M.,HARTLEBEN, B.,SERNETZ, L.,SCHMIDTS, M.,GUNDLACH, E.,SALEEM, M. A.,WALZ, G. and BENZING, T. (2003b). Molecular basis of the functionalpodocin-nephrin complex: mutations in the NPHS2 gene disrupt nephrin targeting to lipid raft microdomains. *Hum Mol Genet.* **12,** 3397-405. Epub 2003 Oct 21.

HUBER, T. B.,HARTLEBEN, B.,KIM, J.,SCHMIDTS, M.,SCHERMER, B.,KEIL, A.,EGGER, L.,LECHA, R. L.,BORNER, C.,PAVENSTADT, H.,SHAW, A. S.,WALZ, G. and BENZING, T. (2003c). Nephrin and CD2AP associate with phosphoinositide 3-OH kinase and stimulate AKT-dependent signaling. *Mol Cell Biol.* **23,** 4917-28.

HUEZ, I.,BORNES, S.,BRESSON, D.,CREANCIER, L. and PRATS, H. (2001). New vascular endothelial growth factor isoform generated by internal ribosome entry site-driven CUG translation initiation. *Mol Endocrinol.* **15,** 2197-210.

HUH, W.,KIM, D. J.,KIM, M. K.,KIM, Y. G.,OH, H. Y.,RUOTSALAINEN, V. and TRYGGVASON, K. (2002). Expression of nephrin in acquired human glomerular disease. *Nephrol Dial Transplant.* **17,** 478-84.

ICHIMURA, K.,KURIHARA, H. and SAKAI, T. (2003). Actin filament organization of foot processes in rat podocytes. *J Histochem Cytochem.* **51,** 1589-600.

ILAN, N.,MAHOOTI, S. and MADRI, J. A. (1998). Distinct signal transduction pathways are utilized during the tube formation and survival phases of in vitro angiogenesis. *J Cell Sci.* **111,** 3621-31.

JIA, Y.,RANSOM, R. F.,SHIBANUMA, M.,LIU, C.,WELSH, M. J. and SMOYER, W. E. (2001). Identification and characterization of hic-5/ARA55 as an hsp27 binding protein. *J Biol Chem.* **276,** 39911-8.

JOUKOV, V.,SORSA, T.,KUMAR, V.,JELTSCH, M.,CLAESSON-WELSH, L.,CAO, Y.,SAKSELA, O.,KALKKINEN, N. and ALITALO, K. (1997). Proteolytic processing regulates receptor specificity and activity of VEGF-C. *Embo J.* **16,** 3898-911.

JUSSILA, L. and ALITALO, K. (2002). Vascular growth factors and lymphangiogenesis. *Physiol Rev.* **82,** 673-700.

KANEMOTO, K.,TAKAHASHI, S.,SHU, Y.,USUI, J.,TOMARI, S.,YAN, K.,HAMAZAKI, Y. and NAGATA, M. (2003). Variable expression of podocyte-related markers in the glomeruloid bodies in Wilms tumor. *Pathol Int.* **53,** 596-601.

KAPLAN, J. M.,KIM, S. H.,NORTH, K. N.,RENNKE, H.,CORREIA, L. A.,TONG, H. Q.,MATIIS, B. J.,RODRIGUEZ-PEREZ, J. C.,ALLEN, P. G.,BEGGS, A. H. and POLLAK, M. R. (2000). Mutations in ACTN4, encoding alpha-actinin-4, cause familial focal segmental glomerulosclerosis. *Nat Genet.* **24,** 251-6.

KERR, J. F.,WYLLIE, A. H. and CURRIE, A. R. (1972). Apoptosis: a basic biological phenomenon with wide-ranging implications in tissue kinetics. *Br J Cancer.* **26,** 239-57.

KESTILA, M.,LENKKERI, U.,MANNIKKO, M.,LAMERDIN, J.,MCCREADY, P.,PUTAALA, H.,RUOTSALAINEN, V.,MORITA, T.,NISSINEN, M.,HERVA, R.,KASIITAN, C. E.,PELTONEN, L.,HOLMBERG, C.,OLSEN, A. and TRYGGVASON, K. (1998). Positionally cloned gene for a novel glomerular protein--nephrin--is mutated in congenital nephrotic syndrome. *Mol Cell.* **1,** 575-82.

KEYT, B. A.,BERLEAU, L. T.,NGUYEN, H. V.,CHEN, H.,HEINSOIIN, H.,VANDLEN, R. and FERRARA, N. (1996). The carboxyl-terminal domain (111-165) of vascular endothelial growth factor is critical for its mitogenic potency. *J Biol Chem.* **271,** 7788-95.

KHOSHNOODI, J.,SIGMUNDSSON, K.,OFVERSTEDT, L. G.,SKOGLUND, U.,OBRINK, B.,WARTIOVAARA, J. and TRYGGVASON, K. (2003). Nephrin promotes cell-cell adhesion through homophilic interactions. *Am J Pathol.* **163,** 2337-46.

KIM, Y. H.,GOYAL, M.,KURNIT, D.,WHARRAM, B.,WIGGINS, J.,HOLZMAN, L.,KERSHAW, D. and WIGGINS, R. (2001). Podocyte depletion and glomerulosclerosis have a direct relationship in the PAN-treated rat. *Kidney Int.* **60,** 957-68.

KOZIELL, A.,GRECH, V.,HUSSAIN, S.,LEE, G.,LENKKERI, U.,TRYGGVASON, K. and SCAMBLER, P. (2002). Genotype/phenotype correlations of NPHS1 and NPHS2 mutations in nephrotic syndrome advocate a functional inter-relationship in glomerular filtration. *Hum Mol Genet.* **11,** 379-88.

KRETZLER, M.,SCHROPPEL, B.,MERKLE, M.,HUBER, S.,MUNDEL, P.,HORSTER, M. and SCHLONDORFF, D. (1998). Detection of multiple vascular endothelial growth factor splice isoforms in single glomerular podocytes. *Kidney Int Suppl.* **67,** S159-61.

KRUM, J. M. and KHAIBULLINA, A. (2003). Inhibition of endogenous VEGF impedes revascularization and astroglial proliferation: roles for VEGF in brain repair. *Exp Neurol.* **181,** 241-57.

KU, D. D.,ZALESKI, J. K.,LIU, S. and BROCK, T. A. (1993). Vascular endothelial growth factor induces EDRF-dependent relaxation in coronary arteries. *Am J Physiol.* **265,** H586-92.

KURIHARA, H.,ANDERSON, J. M. and FARQUHAR, M. G. (1995). Increased Tyr phosphorylation of ZO-1 during modification of tight junctions between glomerular foot processes. *Am J Physiol.* **268,** F514-24.

LABRECQUE, L.,ROYAL, I.,SURPRENANT, D. S.,PATTERSON, C.,GINGRAS, D. and BELIVEAU, R. (2003). Regulation of vascular endothelial growth factor receptor-2 activity by caveolin-1 and plasma membrane cholesterol. *Mol Biol Cell.* **14,** 334-47.

LAHDENPERA, J.,KILPELAINEN, P.,LIU, X. L.,PIKKARAINEN, T.,REPONEN, P.,RUOTSALAINEN, V. and TRYGGVASON, K. (2003). Clustering-induced tyrosine phosphorylation of nephrin by Src family kinases. *Kidney Int.* **64,** 404-13.

LECOUTER, J.,LIN, R.,FRANTZ, G.,ZHANG, Z.,HILLAN, K.,FERRARA, N.,MORITZ, D. R.,LI, B.,PHILLIPS, G. L.,LIANG, X. H.,GERBER, H. P. and HILLAN, K. J. (2003). Mouse endocrine gland-derived vascular endothelial growth factor: a distinct expression pattern from its human ortholog suggests different roles as a regulator of organ-specific angiogenesis

Angiogenesis-independent endothelial protection of liver: role of VEGFR-1. *Endocrinology.* **144,** 2606-16.

LI, C.,RUOTSALAINEN, V.,TRYGGVASON, K.,SHAW, A. S. and MINER, J. H. (2000). CD2AP is expressed with nephrin in developing podocytes and is found widely in mature kidney and elsewhere. *Am J Physiol Renal Physiol.* **279,** F785-92.

LI, W. and KELLER, G. (2000). VEGF nuclear accumulation correlates with phenotypical changes in endothelial cells. *J Cell Sci.* **113,** 1525-34.

LIN, B.,PODAR, K.,GUPTA, D.,TAI, Y. T.,LI, S.,WELLER, E.,HIDESHIMA, T.,LENTZSCH, S.,DAVIES, F.,LI, C.,WEISBERG, E.,SCHLOSSMAN, R. L.,RICHARDSON, P. G.,GRIFFIN, J. D.,WOOD, J.,MUNSHI, N. C. and ANDERSON, K. C. (2002). The vascular endothelial growth factor receptor tyrosine kinase inhibitor PTK787/ZK222584 inhibits growth and migration of multiple myeloma cells in the bone marrow microenvironment. *Cancer Res.* **62,** 5019-26.

LIU, G.,KAW, B.,KURFIS, J.,RAHMANUDDIN, S.,KANWAR, Y. S. and CHUGH, S. S. (2003). Neph1 and nephrin interaction in the slit diaphragm is an important determinant of glomerular permeability. *J Clin Invest.* **112,** 209-21.

LIU, J.,TIAN, Z.,GAO, B. and KUNOS, G. (2002). Dose-dependent activation of antiapoptotic and proapoptotic pathways by ethanol treatment in human vascular endothelial cells: differential involvement of adenosine. *J Biol Chem.* **277,** 20927-33. Epub 2002 Mar 27.

LIU, L.,AYA, K.,TANAKA, H.,SHIMIZU, J.,ITO, S. and SEINO, Y. (2001). Nephrin is an important component of the barrier system in the testis. *Acta Med Okayama.* **55,** 161-5.

LYNCH, D. K.,WINATA, S. C.,LYONS, R. J.,HUGHES, W. E.,LEHRBACH, G. M.,WASINGER, V.,CORTHALS, G.,CORDWELL, S. and DALY, R. J. (2003). A Cortactin-CD2-associated protein (CD2AP) complex provides a novel link between epidermal growth factor receptor endocytosis and the actin cytoskeleton. *J Biol Chem.* **278,** 21805-13.

LYTTON, J.,WESTLIN, M. and HANLEY, M. R. (1991). Thapsigargin inhibits the sarcoplasmic or endoplasmic reticulum Ca-ATPase family of calcium pumps. *J Biol Chem.* **266,** 17067-71.

MAKINEN, T.,VEIKKOLA, T.,MUSTJOKI, S.,KARPANEN, T.,CATIMEL, B.,NICE, E. C.,WISE, L.,MERCER, A.,KOWALSKI, H.,KERJASCHKI, D.,STACKER, S. A.,ACHEN, M. G. and ALITALO, K. (2001). Isolated lymphatic endothelial cells transduce growth, survival and migratory signals via the VEGF-C/D receptor VEGFR-3. *Embo J.* **20,** 4762-73.

MATHIS, B. J.,KIM, S. H.,CALABRESE, K.,HAAS, M.,SEIDMAN, J. G.,SEIDMAN, C. E. and POLLAK, M. R. (1998). A locus for inherited focal segmental glomerulosclerosis maps to chromosome 19q13. *Kidney Int.* **53,** 282-6.

MATSUMURA, K.,HIRASHIMA, M.,OGAWA, M.,KUBO, H.,HISATSUNE, H.,KONDO, N.,NISHIKAWA, S. and CHIBA, T. (2003). Modulation of VEGFR-2-mediated endothelial-cell activity by VEGF-C/VEGFR-3. *Blood.* **101,** 1367-74.

McMullen, M.,Keller, R.,Sussman, M. and Pumiglia, K. (2004). Vascular endothelial growth factor-mediated activation of p38 is dependent upon Src and RAFTK/Pyk2. *Oncogene.* **23,** 1275-82.

Miao, H. Q.,Lee, P.,Lin, H.,Soker, S. and Klagsbrun, M. (2000). Neuropilin-1 expression by tumor cells promotes tumor angiogenesis and progression. *Faseb J.* **14,** 2532-9.

Michaud, J. L.,Lemieux, L. I.,Dube, M.,Vanderhyden, B. C.,Robertson, S. J. and Kennedy, C. R. (2003). Focal and segmental glomerulosclerosis in mice with podocyte-specific expression of mutant alpha-actinin-4. *J Am Soc Nephrol.* **14,** 1200-11.

Mundel, P.,Reiser, J. and Kriz, W. (1997a). Induction of differentiation in cultured rat and human podocytes. *J Am Soc Nephrol.* **8,** 697-705.

Mundel, P.,Reiser, J.,Zuniga Mejia Borja, A.,Pavenstadt, H.,Davidson, G. R.,Kriz, W. and Zeller, R. (1997b). Rearrangements of the cytoskeleton and cell contacts induce process formation during differentiation of conditionally immortalized mouse podocyte cell lines. *Exp Cell Res.* **236,** 248-58.

Nagata, M.,Nakayama, K.,Terada, Y.,Hoshii, S. and Watanabe, T. (1998). Cell cycle regulation and differentiation in the human podocyte lineage. *Am J Pathol.* **153,** 1511-20.

Nagata, M.,Tomari, S.,Kanemoto, K.,Usui, J. and Lemley, K. V. (2003a). Podocytes, parietal cells, and glomerular pathology: the role of cell cycle proteins. *Pediatr Nephrol.* **18,** 3-8.

Nagata, S.,Nagase, H.,Kawane, K.,Mukae, N. and Fukuyama, H. (2003b). Degradation of chromosomal DNA during apoptosis. *Cell Death Differ.* **10,** 108-16.

NAKAGAWA, H.,SASAHARA, M.,HANEDA, M.,KOYA, D.,HAZAMA, F. and KIKKAWA, R. (2000). Immunohistochemical characterization of glomerular PDGF B-chain and PDGF beta-receptor expression in diabetic rats. *Diabetes Res Clin Pract.* **48,** 87-98.

NEUFELD, G.,COHEN, T.,GENGRINOVITCH, S. and POLTORAK, Z. (1999). Vascular endothelial growth factor (VEGF) and its receptors. *Faseb J.* **13,** 9-22.

NEUFELD, G.,COHEN, T.,SHRAGA, N.,LANGE, T.,KESSLER, O. and HERZOG, Y. (2002). The neuropilins: multifunctional semaphorin and VEGF receptors that modulate axon guidance and angiogenesis. *Trends Cardiovasc Med.* **12,** 13-9.

NITSCHKE, R.,HENGER, A.,RICKEN, S.,GLOY, J.,MULLER, V.,GREGER, R. and PAVENSTADT, H. (2000). Angiotensin II increases the intracellular calcium activity in podocytes of the *intact glomerulus. Kidney Int.* **57,** 41-9.

OLTVAI, Z. N.,MILLIMAN, C. L. and KORSMEYER, S. J. (1993). *Bcl-2 heterodimerizes in vivo* with a conserved homolog, Bax, that accelerates programmed cell death. *Cell.* **74,** 609-19.

ORLANDO, R. A.,TAKEDA, T.,ZAK, B.,SCHMIEDER, S.,BENOIT, V. M.,MCQUISTAN, T.,FURTHMAYR, H. and FARQUHAR, M. G. (2001). The glomerular epithelial cell anti-adhesin podocalyxin associates with the actin cytoskeleton through interactions with ezrin. *J Am Soc Nephrol.* **12,** 1589-98.

PAJUSOLA, K.,APRELIKOVA, O.,KORHONEN, J.,KAIPAINEN, A.,PERTOVAARA, L.,ALITALO, R. and ALITALO, K. (1992). FLT4 receptor tyrosine kinase contains seven immunoglobulin-like loops and is expressed in multiple human tissues and cell lines. *Cancer Res.* **52,** 5738-43.

PALMEN, T.,AHOLA, H.,PALGI, J.,AALTONEN, P.,LUIMULA, P.,WANG, S.,JAAKKOLA, I.,KNIP, M.,OTONKOSKI, T. and HOLTHOFER, H. (2001). Nephrin is expressed in the pancreatic beta cells. *Diabetologia.* **44,** 1274-80.

PARRY, G. A. M. (2000). The effects of type 2 cytokines on GECs.

PATRAKKA, J.,KESTILA, M.,WARTIOVAARA, J.,RUOTSALAINEN, V.,TISSARI, P.,LENKKERI, U.,MANNIKKO, M.,VISAPAA, I.,HOLMBERG, C.,RAPOLA, J.,TRYGGVASON, K. and JALANKO, H. (2000). Congenital nephrotic syndrome (NPHS1): features resulting from different mutations in Finnish patients. *Kidney Int.* **58,** 972-80.

PAVENSTADT, H. (2000). Roles of the podocyte in glomerular function. *Am J Physiol Renal Physiol.* **278,** F173-9.

PETERMANN, A. T.,HIROMURA, K.,BLONSKI, M.,PIPPIN, J.,MONKAWA, T.,DURVASULA, R.,COUSER, W. G. and SHANKLAND, S. J. (2002). Mechanical stress reduces podocyte proliferation in vitro. *Kidney Int.* **61,** 40-50.

PIPAS, J. M. and LEVINE, A. J. (2001). Role of T antigen interactions with p53 in tumorigenesis. *Semin Cancer Biol.* **11,** 23-30.

POCOCK, T. M.,FOSTER, R. R. and BATES, D. O. (2004). Evidence of a role for TRPC channels in VEGF-mediated increased vascular permeability in vivo. *Am J Physiol Heart Circ Physiol.* **286,** H1015-26. Epub 2003 Oct 9.

POCOCK, T. M.,WILLIAMS, B.,CURRY, F. E. and BATES, D. O. (2000). VEGF and ATP act by different mechanisms to increase microvascular permeability and endothelial [Ca(2+)](i). *Am J Physiol Heart Circ Physiol.* **279,** H1625-34.

POENIE, M. (1990). Alteration of intracellular Fura-2 fluorescence by viscosity: a simple correction. *Cell Calcium.* **11,** 85-91.

PUTNEY, J. W., JR. and MCKAY, R. R. (1999). Capacitative calcium entry channels. *Bioessays.* **21,** 38-46.

REGELE, H. M.,FILLIPOVIC, E.,LANGER, B.,POCZEWKI, H.,KRAXBERGER, I.,BITTNER, R. E. and KERJASCHKI, D. (2000). Glomerular expression of dystroglycans is reduced in minimal

change nephrosis but not in focal segmental glomerulosclerosis. *J Am Soc Nephrol.* **11,** 403-12.

REISER, J.,KRIZ, W.,KRETZLER, M. and MUNDEL, P. (2000a). The glomerular slit diaphragm is a modified adherens junction. *J Am Soc Nephrol.* **11,** 1-8.

REISER, J.,PIXLEY, F. J.,HUG, A.,KRIZ, W.,SMOYER, W. E.,STANLEY, E. R. and MUNDEL, P. (2000b). Regulation of mouse podocyte process dynamics by protein tyrosine phosphatases rapid communication. *Kidney Int.* **57,** 2035-42.

RIZZUTO, R.,PINTON, P.,FERRARI, D.,CHAMI, M.,SZABADKAI, G.,MAGALHAES, P. J.,DI VIRGILIO, F. and POZZAN, T. (2003). Calcium and apoptosis: facts and hypotheses. *Oncogene.* **22,** 8619-27.

ROBERT, B.,ZHAO, X. and ABRAHAMSON, D. R. (2000). Coexpression of neuropilin-1, Flk1, and VEGF(164) in developing and mature mouse kidney glomeruli. *Am J Physiol Renal Physiol.* **279,** F275-82.

ROSA SANTOS, S. C. and DIAS, S. (2004). Internal and external autocrine VEGF/KDR loops regulate the survival of subsets of acute leukemia through distinct signaling pathways. *Blood.* **15,** 15

ROUSSEAU, S.,HOULE, F. and HUOT, J. (2000). Integrating the VEGF signals leading to actin-based motility in vascular endothelial cells. *Trends Cardiovasc Med.* **10,** 321-7.

RUHRBERG, C. (2003). Growing and shaping the vascular tree: multiple roles for VEGF. *Bioessays.* **25,** 1052-60.

RUOTSALAINEN, V.,LJUNGBERG, P.,WARTIOVAARA, J.,LENKKERI, U.,KESTILA, M.,JALANKO, H.,HOLMBERG, C. and TRYGGVASON, K. (1999). Nephrin is specifically located at the slit diaphragm of glomerular podocytes. *Proc Natl Acad Sci U S A.* **96,** 7962-7.

SALEEM, M. A.,O'HARE, M. J.,REISER, J.,COWARD, R. J.,INWARD, C. D.,FARREN, T.,XING, C. Y.,NI, L.,MATHIESON, P. W. and MUNDEL, P. (2002). A conditionally immortalized

human podocyte cell line demonstrating nephrin and podocin expression. *J Am Soc Nephrol.* **13,** 630-8.

SAXEN, L. and SARIOLA, H. (1987). Early organogenesis of the kidney. *Pediatr Nephrol.* **1,** 385-92.

SCHNABEL, E.,ANDERSON, J. M. and FARQUHAR, M. G. (1990). The tight junction protein ZO-1 is concentrated along slit diaphragms of the glomerular epithelium. *J Cell Biol.* **111,** 1255-63.

SCHWARTZ, M. M. (2000). The role of podocyte injury in the pathogenesis of focal segmental glomerulosclerosis. *Ren Fail.* **22,** 663-84.

SCHWARZ, K.,SIMONS, M.,REISER, J.,SALEEM, M. A.,FAUL, C.,KRIZ, W.,SIHAW, A. S.,HOLZMAN, L. B. and MUNDEL, P. (2001). Podocin, a raft-associated component of the glomerular slit diaphragm, interacts with CD2AP and nephrin. *J Clin Invest.* **108,** 1621-9.

SCOTT, M. P. and MILLER, W. T. (2000). A peptide model system for processive phosphorylation by Src family kinases. *Biochemistry.* **39,** 14531-7.

SEDOVA, M. and BLATTER, L. A. (1999). Dynamic regulation of [Ca2+]i by plasma membrane Ca(2+)-ATPase and Na+/Ca2+ exchange during capacitative Ca2+ entry in bovine vascular endothelial cells. *Cell Calcium.* **25,** 333-43.

SELLIN, L.,HUBER, T. B.,GERKE, P.,QUACK, I.,PAVENSTADT, H. and WALZ, G. (2003). NEPH1 defines a novel family of podocin interacting proteins. *Faseb J.* **17,** 115-7. Epub 2002 Nov 1.

SHANKLAND, S. J.,EITNER, F.,HUDKINS, K. L.,GOODPASTER, T.,D'AGATI, V. and ALPERS, C. E. (2000). Differential expression of cyclin-dependent kinase inhibitors in human glomerular disease: role in podocyte proliferation and maturation. *Kidney Int.* **58,** 674-83.

SHIBUYA, M. (2001). Structure and dual function of vascular endothelial growth factor receptor-1 (Flt-1). *Int J Biochem Cell Biol.* **33,** 409-20.

SHIH, N. Y.,LI, J.,KARPITSKII, V.,NGUYEN, A.,DUSTIN, M. L.,KANAGAWA, O.,MINER, J. H. and SHAW, A. S. (1999). Congenital nephrotic syndrome in mice lacking CD2-associated protein. *Science.* **286,** 312-5.

SHUSHANOV, S.,BRONSTEIN, M.,ADELAIDE, J.,JUSSILA, L.,TCHIPYSHEVA, T.,JACQUEMIER, J.,STAVROVSKAYA, A.,BIRNBAUM, D. and KARAMYSHEVA, A. (2000). VEGFc and VEGFR3 expression in human thyroid pathologies. *Int J Cancer.* **86,** 47-52.

SIMON, M.,GRONE, H. J.,JOHREN, O.,KULLMER, J.,PLATE, K. H.,RISAU, W. and FUCHS, E. (1995). Expression of vascular endothelial growth factor and its receptors in human renal ontogenesis and in adult kidney. *Am J Physiol.* **268,** F240-50.

SIMONS, M.,SCHWARZ, K.,KRIZ, W.,MIETTINEN, A.,REISER, J.,MUNDEL, P. and HOLTHOFER, H. (2001). Involvement of lipid rafts in nephrin phosphorylation and organization of the glomerular slit diaphragm. *Am J Pathol.* **159,** 1069-77.

SMITH, C. I.,ISLAM, T. C.,MATTSSON, P. T.,MOHAMED, A. J.,NORE, B. F. and VIHINEN, M. (2001). The Tec family of cytoplasmic tyrosine kinases: mammalian Btk, Bmx, Itk, Tec, Txk and homologs in other species. *Bioessays.* **23,** 436-46.

SMOYER, W. E. and RANSOM, R. F. (2002). Hsp27 regulates podocyte cytoskeletal changes in an in vitro model of podocyte process retraction. *Faseb J.* **16,** 315-26.

SOKER, S.,ROBERT, B.,ZHAO, X. and ABRAHAMSON, D. R. (2001). Neuropilin in the midst of cell migration and retraction. *Int J Biochem Cell Biol.* **33,** 433-7.

SOKER, S.,GOLLAMUDI-PAYNE, S.,FIDDER, H.,CHARMAHELLI, H. and KLAGSBRUN, M. (1997). Inhibition of vascular endothelial growth factor (VEGF)-induced endothelial cell proliferation by a peptide corresponding to the exon 7-encoded domain of VEGF165. *J Biol Chem.* **272,** 31582-8.

SOKER, S.,TAKASHIMA, S.,MIAO, H. Q.,NEUFELD, G. and KLAGSBRUN, M. (1998). Neuropilin-1 is expressed by endothelial and tumor cells as an isoform-specific receptor for vascular endothelial growth factor. *Cell.* **92,** 735-45.

SOMPAYRAC, L. and DANNA, K. J. (1983). A simian virus 40 dl884/tsA58 double mutant is temperature sensitive for abortive transformation. *J Virol.* **46,** 620-5.

SORENSSON, J.,FIERLBECK, W.,HEIDER, T.,SCHWARZ, K.,PARK, D. S.,MUNDEL, P.,LISANTI, M. and BALLERMANN, B. J. (2002). Glomerular endothelial fenestrae in vivo are not formed from caveolae. *J Am Soc Nephrol.* **13,** 2639-47.

TAKAHASHI, M.,MATSUI, A.,INAO, M.,MOCHIDA, S. and FUJIWARA, K. (2003). ERK/MAPK-dependent PI3K/Akt phosphorylation through VEGFR-1 after VEGF stimulation in activated hepatic stellate cells. *Hepatol Res.* **26,** 232-236.

TAKASHIMA, S.,KITAKAZE, M.,ASAKURA, M.,ASANUMA, H.,SANADA, S.,TASHIRO, F.,NIWA, H.,MIYAZAKI JI, J.,HIROTA, S.,KITAMURA, Y.,KITSUKAWA, T.,FUJISAWA, H.,KLAGSBRUN, M. and HORI, M. (2002). Targeting of both mouse neuropilin-1 and neuropilin-2 genes severely impairs developmental yolk sac and embryonic angiogenesis. *Proc Natl Acad Sci U S A.* **99,** 3657-62.

TAKEDA, T.,GO, W. Y.,ORLANDO, R. A. and FARQUHAR, M. G. (2000). Expression of podocalyxin inhibits cell-cell adhesion and modifies junctional properties in Madin-Darby canine kidney cells. *Mol Biol Cell.* **11,** 3219-32.

THOMAS, S. M. and BRUGGE, J. S. (1997). Cellular functions regulated by Src family kinases. *Annu Rev Cell Dev Biol.* **13,** 513-609.

TRAXLER, P.,BOLD, G.,BUCHDUNGER, E.,CARAVATTI, G.,FURET, P.,MANLEY, P.,O'REILLY, T.,WOOD, J. and ZIMMERMANN, J. (2001). Tyrosine kinase inhibitors: from rational design to clinical trials. *Med Res Rev.* **21,** 499-512.

TSUKITA, S. and YONEMURA, S. (1997). ERM proteins: head-to-tail regulation of actin-plasma membrane interaction. *Trends Biochem Sci.* **22,** 53-8.

UTHAISANG, W.,NUTT, L. K.,ORRENIUS, S. and FADEEL, B. (2003). Phosphatidylserine exposure in Fas type I cells is mitochondria-dependent. *FEBS Lett.* **545,** 110-4.

VASMANT, D.,MAURICE, M. and FELDMANN, G. (1984). Cytoskeleton ultrastructure of podocytes and glomerular endothelial cells in man and in the rat. *Anat Rec.* **210,** 17-24.

VERMA, R.,WHARRAM, B.,KOVARI, I.,KUNKEL, R.,NIHALANI, D.,WARY, K. K.,WIGGINS, R. C.,KILLEN, P. and HOLZMAN, L. B. (2003). Fyn binds to and phosphorylates the kidney slit diaphragm component Nephrin. *J Biol Chem.* **278,** 20716-23.

VILLEGAS, G. and TUFRO, A. (2002). Ontogeny of semaphorins 3A and 3F and their receptors neuropilins 1 and 2 in the kidney. *Mech Dev.* **119,** S149-53.

WANG, L.,ZENG, H.,WANG, P.,SOKER, S. and MUKHOPADHYAY, D. (2003). Neuropilin-1-mediated vascular permeability factor/vascular endothelial growth factor-dependent endothelial cell migration. *J Biol Chem.* **278,** 48848-60.

WANG, S. X.,MENE, P. and HOLTHOFER, H. (2001). Nephrin mRNA regulation by protein kinase C. *J Nephrol.* **14,** 98-103.

WELSCH, T.,ENDLICH, N.,KRIZ, W. and ENDLICH, K. (2001). CD2AP and p130Cas localize to different F-actin structures in podocytes. *Am J Physiol Renal Physiol.* **281,** F769-77.

WEN, Y.,EDELMAN, J. L.,KANG, T. and SACHS, G. (1999). Lipocortin V may function as a signaling protein for vascular endothelial growth factor receptor-2/Flk-1. *Biochem Biophys Res Commun.* **258,** 713-21.

WHITTLE, C.,GILLESPIE, K.,HARRISON, R.,MATHIESON, P. W. and HARPER, S. J. (1999). Heterogeneous vascular endothelial growth factor (VEGF) isoform mRNA and receptor mRNA expression in human glomeruli, and the identification of VEGF148 mRNA, a novel truncated splice variant. *Clin Sci (Lond).* **97,** 303-12.

WOOD, J. M.,BOLD, G.,BUCHDUNGER, E.,COZENS, R.,FERRARI, S.,FREI, J.,HOFMANN, F.,MESTAN, J.,METT, H.,O'REILLY, T.,PERSOHN, E.,ROSEL, J.,SCHNELL, C.,STOVER, D.,THEUER, A.,TOWBIN, H.,WENGER, F.,WOODS-COOK, K.,MENRAD, A.,SIEMEISTER, G.,SCHIRNER, M.,THIERAUCH, K. H.,SCHNEIDER, M. R.,DREVS, J.,MARTINY-BARON, G. and TOTZKE, F. (2000). PTK787/ZK 222584, a novel and potent inhibitor of vascular endothelial growth factor receptor tyrosine kinases, impairs vascular endothelial growth factor-induced responses and tumor growth after oral administration. *Cancer Res.* **60,** 2178-89.

WU, L. W.,MAYO, L. D.,DUNBAR, J. D.,KESSLER, K. M.,BAERWALD, M. R.,JAFFE, E. A.,WANG, D.,WARREN, R. S. and DONNER, D. B. (2000). Utilization of distinct signaling pathways by receptors for vascular endothelial cell growth factor and other mitogens in the induction of endothelial cell proliferation. *J Biol Chem.* **275,** 5096-103.

WYMANN, M. P.,BULGARELLI-LEVA, G.,ZVELEBIL, M. J.,PIROLA, L.,VANHAESEBROECK, B.,WATERFIELD, M. D. and PANAYOTOU, G. (1996). Wortmannin inactivates phosphoinositide 3-kinase by covalent modification of Lys-802, a residue involved in the phosphate transfer reaction. *Mol Cell Biol.* **16,** 1722-33.

YAOITA, E.,YAMAMOTO, T.,SAITO, M.,KAWASAKI, K. and KIHARA, I. (1991). Desmin-positive epithelial cells outgrowing from rat encapsulated glomeruli. *Eur J Cell Biol.* **54,** 140-9.

YAOITA, E.,KURIHARA, H.,SAKAI, T.,OHSHIRO, K. and YAMAMOTO, T. (2001). Phenotypic modulation of parietal epithelial cells of Bowman's capsule in culture. *Cell Tissue Res.* **304,** 339-49.

YU, C. C.,YEN, T. S.,LOWELL, C. A. and DEFRANCO, A. L. (2001a). Lupus-like kidney disease in mice deficient in the Src family tyrosine kinases Lyn and Fyn. *Curr Biol.* **11,** 34-8.

YU, Y.,HULMES, J. D.,HERLEY, M. T.,WHITNEY, R. G.,CRABB, J. W. and SATO, J. D. (2001b). Direct identification of a major autophosphorylation site on vascular endothelial

growth factor receptor Flt-1 that mediates phosphatidylinositol 3'-kinase binding. *Biochem J.* **358,** 465-72.

YUAN, L.,MOYON, D.,PARDANAUD, L.,BREANT, C.,KARKKAINEN, M. J.,ALITALO, K. and EICHMANN, A. (2002). Abnormal lymphatic vessel development in neuropilin 2 mutant mice. *Development.* **129,** 4797-806.

ZACHARY, I. and GLIKI, G. (2001). Signaling transduction mechanisms mediating biological actions of the vascular endothelial growth factor family. *Cardiovasc Res.* **49,** 568-81.

Publications arising from this work

Papers

1. **Foster RR**, Hole R, Anderson K, Satchell SC, Coward RJ, Mathieson PW, Gillatt DA, Saleem MA, Bates DO, Harper SJ. Functional evidence that vascular endothelial growth factor may act as an autocrine factor on human conditionally immortalised podocytes. Am J Physiol. 2003 Jun; 284 (6):F1263-73.

2. Cui TG, **Foster RR**, Saleem MA, Mathieson PW, Gillatt DA, Bates DO, Harper SJ. Differentiated human podocytes endogenously express an inhibitory isoform of vascular endothelial growth factor (VEGF 165b) mRNA and protein. Am J Physiol. Renal Physiol. 2004 April;286(4):F767-73.

3. **R.R. Foster**, M.A. Saleem, P.W. Mathieson, D.O. Bates, S.J. Harper Vascular endothelial growth factor acts through nephrin to reduce apoptosis in human podocytes. American Journal of Physiology: Renal Physiology 2004. Accepted.

4. Woolard J, Wang W, Qiu Y, Bevan HS, Cui T, Sugiono M, Waine E, Perrin R, Glass CA, **Foster RR**, Whittles CE, Mushens R, Morbidelli L, Gillat DA, Ziche M, Harper SJ, Bates DO. Vascular endothelial growth factor splice variant $VEGF_{165}b$ is an endogenous, inhibitory, anti-angiogenic circulating protein. Cancer Research, 2004, accepted.

Abstracts

1. Vascular endothelial growth factor may act as an autocrine factor in human visceral glomerular epithelial cells. **R.R Foster,** D.O Bates, S.J. Harper, YPS, Southampton 2001. Unpublished. POSTER

2. Vascular endothelial growth factor causes a decrease in intracellular calcium changes in visceral glomerular epithelial cells. **R.R., Foster** D.O. Bates, M. Saleem, S. Harper, Proceedings of the 7th International Congress of Microcirculation. POSTER

3. Vascular endothelial growth factor acts as an autocrine factor in podocytes. **R. Foster,** S.J. Harper, R.J. Coward, P.W.Mathieson, D.O. Bates and M.A.Saleem. YPS, Bristol 2001. Unpublished. POSTER

4. Vascular Endothelial Growth Factor (VEGF) increases intracellular calcium concentrations through VEGF-R2 activated TRPC6 channels. **R.R Foster,** T.P Pocock,. D.O Bates. J Vasc Res (2002) 39: 552. POSTER

5. Vascular Endothelial Growth Factor (VEGF) reduces cytosolic calcium in human visceral glomerular epithelial cells and promotes survival - functional evidence for an autocrine loop. **R. Foster,** K.Anderson, S. Satchell, M.A.Saleem, P.W.Mathieson, D.O. Bates and S.J. Harper. Abstract 17, York, April 2002, Renal Association online. TALK.

6. Vascular Endothelial Growth Factor (VEGF) induces a decrease in intracellular calcium concentration $[Ca^{2+}]_i$ in visceral Glomerular Endothelial Cells (vGECs). **R.R Foster,** D.O. Bates, M. Saleem, S. Harper. FASEB J (2002) 16:(5) 868.4. POSTER

7. Vascular Endothelial Growth Factor (VEGF) is a podocyte autocrine factor for $[Ca^{2+}]_i$ and survival **R. Foster,** M. Saleem K. Anderson, S. Satchell , P.W. Mathieson, D.O.Bates and S.J.Harper. J. Vasc. Res. 2002; 39: suppl 1, POM.05.

8. Ultrastructural and molecular evidence that vascular endothelial growth factor may be a podocyte autocrine factor. R.Hole, **R.Foster,** M.Saleem, D.O.Bates and S.J.Harper. Paper 14, London, Autumn 2002. Renal Association online. PLENARY TALK

9. Vascular endothelial growth factor (VEGF) is an endogenous autocrine factor for primary cultured podocytes. **R.Foster,** K. Anderson, S. Satchell, P.W. Mathieson, D.O.Bates and S.J.Harper. FASEB J (2003) 17:(5) 801.1. POSTER

10. Vascular endothelial growth factor-A_{165} (VEGF) acts as an autocrine survival factor for human podocytes via a PI3–kinase dependent pathway. **R. Foster,** D.O.Bates, PW Mathieson, M. Saleem, and S.J.Harper. J Vasc Res 2003; 40:285-316. POSTER

11. $VEGF_{165}$ and $VEGF_{165}b$ inhibit apoptosis in human conditionally immortalised podocyte cells (hCIPs). **R.Foster,** J Yem, A Nishikawa PW Mathieson, M. Saleem, D.O.Bates and S.J.Harper. J Vasc Res 2003; 40:285-316. POSTER

12. Vascular endothelial growth factor (VEGF) signals through nephrin and AKT in human conditionally immortalised podocytes (hCIPs). **R.Foster,** P.W.Mathieson, M.A.Saleem, D.O.Bates, S.J.Harper. (2003) 555P PC46, Physiology online. POSTER

Appendix

Ethical consent form

North Bristol NHS

NHS Trust

Clinical Governance Directorate
Beaufort House
Southmead Hospital
Westbury-on-Trym
Bristol BS10 5NB
Tel: 0117 959 5207
Fax: 0117 959 5589
Email: bowman_sue@hotmail.com

20 March 2001

Dr D J Harper
Richard Bright Renal Unit
SMH

Dear Dr Harper

PROJECT 007/01: MOLECULAR STUDIES IN ISOLATED GLOMERULI

I am pleased to inform you that the Southmead Local Research Ethics Committee, at its meeting on 14 March 2001, approved your application in respect of the above project.

Approval is given on the understanding that:-

a) Any ethical problems arising in the course of the project will be reported to the Ethics Committee;

b) Any change in protocol will be reported to the Ethics Committee;

c) An annual progress report will be submitted and a brief final report on completion.

Yours sincerely

Sue Bowman

Mrs S B Bowman
Administrator
Southmead Local Research Ethics Committee